

CRANFIELD INSTITUTE OF TECHNOLOGY

DEPARTMENT OF MATERIALS

Ph.D THESIS

J.M.F. MOTA

CHEVRON CRACKING IN STEEL WELD METALS

Supervisor:

Professor R.L. Apps

May, 1979.

BEST COPY

AVAILABLE

Variable print quality

ABSTRACT

A less well known form of transverse cracking in carbon manganese and low alloy steel weld metals, generally referred to as chevron cracking, has been found in a large number of industrial welds. These cracks are characterized by their macroscopic orientation, which is approximately transverse to the welding direction and at 45° with the plane of the plates (in a butt joint), and by the staircase morphology, which is easily recognized under microscopical examination. A special test was designed to reproduce these cracks under laboratory controlled conditions and a large number of welds was carried out. Chevron cracks were found in the tests with medium strength weld metals deposited by submerged arc with a basic agglomerated flux and by manual metal arc with basic and cellulosic electrodes. No chevron cracks were observed in the welds with rutile electrodes. High temperature baking of the submerged arc flux and the basic electrodes eliminated or reduced markedly the incidence of cracking in all cases indicating that hydrogen was the main factor controlling the cracking occurrence.

The fracture surface of a chevron crack consisted generally of a series of staggered microcracks exhibiting quasi-cleavage linked by ductile failure. A close similarity was found amongst the features observed on the fracture surface of chevron cracks, microfissures, hydrogen induced cracks in Y groove Tekken tests and hydrogen charged tensile specimens.

A two stage mechanism for the formation of chevron cracks has been suggested, based on recently proposed theories for hydrogen assisted cracking. The mechanism is based on the transport of hydrogen by dislocations along slip bands at 45° with the welding direction and nucleation of staggered microcracks within the slip bands; subsequently these microcracks are linked by ductile failure.

The increase in the strength of the weld metal produced first an increase in the incidence of chevron cracking and, above a certain level, a change in the orientation of the cracks from 45° to perpendicular to the welding direction. This change was believed to be due to an alteration in the cracking mechanism rather than a change in the nature of the cracks.

ACKNOWLEDGEMENTS

The author wishes to express his gratitude to his supervisor, Professor R.L. Apps for the help, guidance and encouragement during this research project and to Mr. J.E.M. Jubb for the supervision in the beginning of the work and comments during the later stages.

The financial support from Calouste Gulbenkian Foundation (Lisbon) is acknowledged with gratitude as well as the help and assistance of Miss da Silva (from the U.K. and Commonwealth Branch).

Thanks are due to BOC Murex for having manufactured the special batches of manual metal arc welding electrodes used during the experimental work.

During this project, discussions were held with a large number of persons who gave useful information on industrial experience and commented on various aspects of the work; from these, the author wishes to refer in particular to Dr. G. Saunders, Dr. R.A. Farrar, Dr. B. Chew, Mr. P. Rogers, Dr. W.I. Pumphrey, Dr. R. John, Dr. J. Garland and Mr. V. Wright.

Part of the ultrasonic inspection referred herein was carried out by Mr. Charles J. Abrahams who made a very useful contribution and showed great interest.

Thanks are also due to the laboratory and workshop staff of the Department of Materials for their willing assistance.

CONTENTS

	Page
I - INTRODUCTION	1
II - LITERATURE SURVEY	4
1. Chevron Cracking	5
1.1 Historical Review	5
1.2 Recent Research	7
1.3 Published Work Related with the Present Project	9
1.4 Summary and Discussion	11
2. Weld Metal Cracking in C-Mn and Low Alloy Steels	13
2.1 Hot Cracking	13
2.1.1 Thermal etching	13
2.1.2 Ductility dip	14
2.1.3 Ductility dip and cracking of metals and alloys	17
2.1.4 Summary and discussion	18
2.2 Hydrogen Embrittlement and Hydrogen Induced Cold Cracking	20
2.2.1 Hydrogen in steel weld metal	21
2.2.1.1 Sources of hydrogen	21
2.2.1.2 Weld metal hydrogen level	22
2.2.1.3 Solubility of hydrogen in steel	24
2.2.1.4 Entrapment and diffusion of hydrogen	25
2.2.2 Effect of composition and microstructure on susceptibility to hydrogen embrittlement	27
2.2.3 Stresses and strains in weldments	29
2.2.4 The effect of temperature and strain rate	31
2.2.5 Morphology of hydrogen induced cold cracks	32
2.2.6 Special types of hydrogen induced cold cracks	33
2.2.6.1 Microcracks in mild and low alloy steel weld metal	33
2.2.6.2 Fish-eyes in mild and low alloy steel weld metals	35
2.2.7 Theories of hydrogen embrittlement	36
2.2.8 Summary and discussion	40
III - MATERIALS AND EQUIPMENT	45
1. Materials	46
1.1 Parent Materials	46

1.2	Welding Consumables	46
1.3	Weld Metal Chemical Composition	46
2.	Equipment	46
2.1	Welding	46
2.2	Ultrasonic Inspection	47
2.3	Magnetic Particle Inspection	47
2.4	Acoustic Emission	47
2.5	Temperature Measurement	47
2.6	Cathodic Charging of Tensile Specimens with Hydrogen	47
2.7	Mechanical Testing	48
2.8	Metallography	48
2.9	Fractography	48
IV -	EXPERIMENTAL PROCEDURES	49
1.	Weld Metal Cracking Tests	50
1.1	Tuliani Test	50
1.2	Continuous Water Cooling Test	50
2.	Baking and Moisturizing Procedures for Welding Consumables	51
3.	Non Destructive Testing	52
3.1	Ultrasonic Inspection	52
3.2	Magnetic Particle Inspection	52
3.3	Detection of Cracks by Acoustic Emission	52
4.	Measurement of Weld Metal Cooling Rates During the Tests with Continuous Water Cooling	53
5.	Procedure to Reheat Chevron Cracks	53
6.	Preparation and Testing of Hydrogen Charged Tensile Specimens	54
7.	Preparation of Specimens for Metallographic Examination	55

8. Hardness Testing	55
9. Preparation of Fracture Surfaces to be Observed in the Scanning Electron Microscope	55
10. Preparation of Carbon Extraction Replicas from Fracture Surfaces to be Observed in the Transmission Electron Microscope	55
11. Chemical Analysis	56
12. Weld Metal Hydrogen and Flux Moisture Determinations	56
 V - RESULTS	 57
1. Chevron Cracks on Longitudinal Sections of Industrial Samples	58
2. Weld Metal Cracks in Laboratory Tests	58
3. Ultrasonic Inspection and Detection of Cracks by Acoustic Emission	59
4. Hydrogen Levels in the Weld Metals	60
5. Influence of Continuous Water Cooling on the Weld Metal Cooling Rate During the Cracking Tests	60
6. Metallographic Examination	61
6.1 Weld Metal Microstructures and Microhardnesses	61
6.2 Metallographic Study of the Transverse Cracks in the Weld Metals	61
6.3 Morphology of Hydrogen Induced Cracks Observed in Y Groove Tekken Tests	63
7. Fractographic Examination	63
7.1 Scanning Electron Microscopy	63
7.1.1 Chevron cracks from industrial samples	63
7.1.2 Chevron cracks produced under laboratory controlled conditions	63
7.1.3 Cracks produced through the Y groove Tekken test	65
7.1.4 Fracture surfaces of hydrogen charged tensile specimens	65
7.1.5 Reheated chevron cracks	66
7.2 Transmission Electron Microscopy	66
8. Summary of Relevant Results	67

VI - DISCUSSION	69
1. Introduction	70
2. Experimental Procedure to Produce Chevron Cracks	71
3. Weld Metal Cracking Experiments	71
3.1 Submerged Arc Welds	71
3.2 Manual Metal Arc Welds	72
3.3 MIG Weld	77
4. Cracking Morphology : Metallographic and Fractographic Studies	77
5. Subsidiary Work	81
6. Summary	84
7. A Mechanism for Chevron Cracking	86
VII - CONCLUSIONS	89
REFERENCES	92
DIAGRAM	109
TABLES	111
FIGURES	132
APPENDIX	210

LIST OF TABLES

1.	Storage and Reconditioning Temperatures for Welding Consumables (after Graville (96)).	112
2.	Chemical Composition of the Submerged Arc Welding Wires Used in the Cracking Tests (wt. %).	113
3.	Constitution of the Commercial Submerged Arc Welding Flux OP41TT According to the Manufacturer (wt. %).	113
4.	Chemical Composition and Hardness of Industrial Weld Metal Samples Containing Chevron Cracks.	114
5.	Chemical Composition and Hardness of Submerged Arc Welds.	115
6.	Chemical Composition and Hardness of Manual Metal Arc Welds Deposited with Commercially Available Electrodes.	116
7.	Chemical Composition and Hardness of Manual Metal Arc Welds Deposited with Specially Manufactured Electrodes.	117
8.	Chemical Composition and Hardness of Manual Metal Arc Welds Deposited with Specially Manufactured Nickel Bearing Electrodes.	118
9.	Welding Procedures for Tuliani Cracking Tests; Submerged Arc Welds.	119
10.	Welding Procedures for Continuous Water Cooling Cracking Tests; Submerged Arc Welds.	120
11.	Welding Procedures for Continuous Water Cooling Cracking Tests; Manual Metal Arc Welds.	121
12.	Welding Procedures for Continuous Water Cooling Cracking Tests; MIG Weld.	122
13.	Incidence of Cracking Identified by Magnetic Particle Inspection (Tuliani Tests TP1-4).	123
14.	Incidence of Cracking Identified by Magnetic Particle Inspection (Continuous Water Cooling Tests TP5 - 27).	124
15.	Incidence of Cracking Identified by Magnetic Particle Inspection (Continuous Water Cooling Tests, TP28 - 39).	125
16.	Incidence of Cracking Identified by Magnetic Particle Inspection (Continuous Water Cooling Tests, TP40 - 56).	126
17.	Incidence of Cracking Identified by Magnetic Particle Inspection (Continuous Water Cooling Tests, TP57 - 60, 62 and 63).	127
18.	Incidence of Cracking Identified by Magnetic Particle Inspection (Continuous Water Cooling Test, TP65).	128
19.	Diffusible Hydrogen Levels for Weld Deposits with Manual Metal Arc Electrodes.	129

- | | | |
|-----|---|-----|
| 20. | Moisture in the Submerged Arc Welding Flux and Corresponding Weld Metal Diffusible Hydrogen Levels. | 130 |
| 21. | Mechanical Properties of Hydrogen Charged Tensile Specimens Machined with the Axis at 45° with the Welding Direction. | 131 |
| 22. | Mechanical Properties of Hydrogen Charged Tensile Specimens Machined with the Axis Parallel to the Welding Direction. | 131 |

LIST OF FIGURES

1.	Typical example of chevron cracking in a longitudinal section of an industrial sample. 1x.	133
2.	Details of a chevron crack. (a) Longitudinal section observed in the light microscope. 200x. (b) Fracture surface observed in the scanning electron microscope (from a direction perpendicular to the horizontal components). 80x.	133
3.	Hypothetical hot ductility curve along with individual contributions which combine to make the curve. (After Yeniscavich).	134
4.	Typical potential hydrogen levels (moisture levels in coatings and fluxes). (After Coe).	135
5.	Typical hydrogen levels in weld metals deposited with different types of consumables. (After Coe).	135
6.	Solubility of hydrogen in steel as a function of temperature. (After Graville).	136
7.	Variation of overall hydrogen diffusivity coefficient, D_H , with temperature, for different steels. (After Coe).	136
8.	Distribution of residual stresses owing to shrinkage in a butt weld. (After Macherauch).	137
9.	Effect of hydrogen on the ductility of a SAE 1020 steel as a function of temperature and strain rate. (a) Uncharged specimens. (b) Hydrogen charged specimens. (After Toh and Baldwin).	138
10.	Schematic representation of failure characteristics of a hydrogenated high strength steel. (After Troiano).	138
11.	Common positions and orientations of hydrogen induced cold cracks in butt and Fillet welds. (After Graville).	139
12.	Weld preparation for the Tuliani test.	140
13.	Cross section of the joint after completing the weld. Tuliani test, 1x.	140
14.	Preparation of a channel in a plate for the continuous water cooling test.	141
15.	Set of plates used for the continuous water cooling test.	142
16.	Weld preparation used for the continuous water cooling test.	142

17.	(a) Welding sequence adopted for the series of submerged arc welds.	143
	(b) Cross section of the weld metal and backing bar. 1x.	143
18.	(a) Welding sequence adopted for the series of manual metal arc welds.	143
	(b) Cross section of the weld metal and backing bar. 1x.	143
19.	Test plates with acoustic emission transducers to detect the occurrence of cracks in the deposited weld metal.	144
20.	Equipment used for the acoustic emission monitoring.	144
21.	Type and location of the tensile specimens in the stripe of weld metal.	145
22.	(a) Dimensions of the non-standard weld metal tensile specimen.	145
	(b) Detail of the notch used in one specimen.	145
23.	Sectioning of weld metal specimens to prepare fracture surfaces to be examined in the scanning electron microscope.	146
	(a) Chevron crack. (b) Vertical crack.	
24.	Chevron cracks in the industrial sample A.	147
	(a) Cross section of the joint where the cracks were found. 1x.	
	(b) Longitudinal section showing cracks of typical size. 1x.	
	(c) Longitudinal section showing the longest cracks found. 1x.	
25.	Chevron cracks in the industrial sample B.	148
	(a) Cross section of the joint where the cracks were found. 1x.	
	(b) Longitudinal section corresponding to the plane Π_1 . 1x.	
	(c) Longitudinal section corresponding to the plane Π_2 . 1x.	
26.	Chevron cracks in the industrial sample B.	149
	(a) Cross section of the joint where the cracks were found. 1x.	
	(b) Longitudinal-horizontal section (corresponding to the plane Π_3). 1x.	
27.	Chevron cracks in a longitudinal horizontal section (parallel to the plane of the plates). Submerged arc weld with the wire-flux combination SD2/3Ni + OP41TT. TP17. 1x.	150

28.	Chevron cracks in submerged arc welds.	150
	(a) Deposited with the wire-flux combination S4 + OP41TT. TP9. 1x.	
	(b) Deposited with the wire-flux combination SD3/Mo + OP41TT. TP21. 1x.	
29.	Chevron cracks in a submerged arc weld deposited with the wire -flux combination SD2/3Ni + OP41TT. TP17. 1x.	151
30.	(a) Chevron cracks in a submerged arc weld deposited with the wire flux combination SD2/3Ni + OP41TT. High heat input weld made by Crouch (7).	151
	(b) Cross section of the weld metal and backing bar.	151
31.	Vertical cracks in high strength submerged arc welds.	152
	(a) Deposited with the wire-flux combination SD3/1Ni $\frac{1}{2}$ Mo + OP41TT (damp). TP24. 1x.	
	(b) Deposited with the wire-flux combination SD2/1Cr1Ni $\frac{1}{2}$ Mo + OP41TT (as received). TP26. 1x.	
	(c) Deposited with the wire-flux combination SD2/1Cr1Ni $\frac{1}{2}$ Mo + OP41TT (damp). TP27. 1x.	
32.	Chevron cracks, fissures and porosity in manual metal arc welds deposited with E8018C1 electrodes.	153
	(a) Weld with electrodes from manufacturer A TP32. 1x.	
	(b) Weld with electrodes from manufacturer B (batch 1). TP35. 1x.	
	(c) Weld with electrodes from manufacturer B (batch 2). TP38. 1x.	
33.	Chevron cracks in manual metal arc welds.	154
	(a) Deposited with electrodes B1. TP40. 1x.	
	(b) and (c) Deposited with electrodes B2. TP42. 1x.	
34.	Chevron cracks in manual metal arc welds.	155
	(a) Deposited with electrodes C1. TP47. 1x.	
	(b) Deposited with electrodes C2. TP48. 1x.	
	(c) Deposited with electrodes C3. TP49. 1x.	
35.	Vertical cracks in a manual metal arc weld with electrodes C5. TP51. 1x.	156
36.	Porosity in a manual metal arc weld with rutile electrodes R1. TP52. 1x.	156
37.	Vertical cracks in manual metal arc welds with electrodes B5Ni.	157
	(a) Weld with electrodes in the as received condition. TP62. 1x.	
	(b) Weld with electrodes baked at 400°C. TP63. 1x.	
38.	Weld metal cooling curves between 1400° and 300°C observed during the continuous water cooling test. (Heat input 2.4 kJ/mm, except for d which was 1.6 kJ/mm).	158

39.	Weld metal cooling curves below 350°C observed during the continuous water cooling test. (Heat input 2.4 kJ/mm).	159
40.	Weld metal microstructure of the industrial sample A. (a) 50x. (b) 500x (reduced 30% on reproduction).	160
41.	Weld metal microstructure of the industrial sample B. (a) 50x. (b) 500x (reduced 30% on reproduction).	160
42.	Microstructure of a submerged arc weld deposited with the wire-flux combination. SD3 + OP41TT. TP6. (a) 50x. (b) 500x (reduced 30% on reproduction).	161
43.	Microstructure of a submerged arc weld deposited with the wire-flux combination S4 + OP41TT. TP9. (a) 50x. (b) 500x (reduced 30% on reproduction).	161
44.	Microstructure of a submerged arc weld deposited with the wire-flux combination SD3/1Ni + OP41TT. TP11. (a) 50x. (b) 500x (reduced 30% on reproduction).	161
45.	Microstructure of a submerged arc weld deposited with the wire-flux combination SD2/3Ni + OP41TT. TP16. (a) 50x. (b) 500x (reduced 30% on reproduction).	162
46.	Microstructure of a submerged arc weld deposited with the wire-flux combination SD2/3Ni + OP41TT. High heat input weld by Crouch (7). (a) Detail showing very large grains, 25x. (c) 50x. (c) 500x (reduced 30% on reproduction).	162
47.	Microstructure of a submerged arc weld deposited with the wire-flux combination SD3/1Mo + OP41TT. TP20. (a) 50x. (b) 500x (reduced 30% on reproduction).	163
48.	Microstructure of a submerged arc weld deposited with the wire-flux combination SD3/1Ni1/2Mo. TP24. (a) 50x. (b) 500x (reduced 30% on reproduction).	163
49.	Microstructure of a submerged arc weld deposited with the wire-flux combination SD2/1Cr1Ni1/2Mo + OP41TT. TP26. (a) 50x (b) 500x (reduced 30% on reproduction).	163
50.	Microstructure of a manual metal arc weld deposited with E8018C1 electrodes (from manufacturer A). TP30. (a) 50x. (b) 500x (reduced 30% on reproduction).	164
51.	Microstructure of a manual metal arc weld deposited with E8018C1 electrodes (from manufacturer B, batch 1). TP35. (a) 50x. (b) 500x (reduced 30% on reproduction).	164

52.	Microstructure of a manual metal arc weld deposited with E8018C1 electrodes (from manufacturer B, batch 2). TP37. (a) 50x. (b) 500x (reduced 30% on reproduction).	164
53.	Microstructure of a manual metal arc weld deposited with electrodes B1. TP40. (a) 50x. (b) 500x (reduced 30% on reproduction).	165
54.	Microstructure of a manual metal arc weld deposited with electrodes B2. TP42. (a) 50x. (b) 500x (reduced 30% on reproduction).	165
55.	Microstructure of a manual metal arc weld deposited with electrodes B3. TP43. (a) 50x. (b) 500x (reduced 30% on reproduction).	165
56.	Microstructure of a manual metal arc weld deposited with electrodes B4. TP44. (a) 50x. (b) 500x (reduced 30% on reproduction).	166
57.	Microstructure of a manual metal arc weld deposited with electrodes B5. TP46. (a) 50x. (b) 500x (reduced 30% on reproduction).	166
58.	Microstructure of a manual metal arc weld deposited with electrodes B0Ni. TP57. (a) 50x. (b) 500x (reduced 30% on reproduction).	166
59.	Microstructure of a manual metal arc weld deposited with electrodes B2Ni. TP58. (a) 50x. (b) 500x (reduced 30% on reproduction).	167
60.	Microstructure of a manual metal arc weld deposited with electrodes B3Ni. TP59. (a) 50x. (b) 500x (reduced 30% on reproduction).	167
61.	Microstructure of a manual metal arc weld deposited with electrodes B4Ni. TP60. (a) 50x. (b) 500x (reduced 30% on reproduction).	167
62.	Microstructure of a manual metal arc weld deposited with electrodes B5Ni. TP62. (a) 50x. (b) 500x (reduced 30% on reproduction).	168
63.	Microstructure of a manual metal arc weld deposited with electrodes C1. TP47. (a) 50x. (b) 500x (reduced 30% on reproduction).	168
64.	Microstructure of a manual metal arc weld deposited with electrodes C2. TP48. (a) 50x. (b) 500x (reduced 30% on reproduction).	168

65.	Microstructure of a manual metal arc weld deposited with electrodes C3. TP49.	169
	(a) 50x. (b) 500x (reduced 30% on reproduction).	
66.	Microstructure of a manual metal arc weld deposited with electrodes C4. TP50.	169
	(a) 50x. (b) 500x (reduced 30% on reproduction).	
67.	Microstructure of a manual metal arc weld deposited with electrodes C5. TP51.	169
	(a) 50x. (b) 500x (reduced 30% on reproduction).	
68.	Microstructure of a manual metal arc weld deposited with commercially available E6013 electrodes. TP39.	170
	(a) 50x. (b) 500x (reduced 30% on reproduction).	
69.	Microstructure of a manual metal arc weld deposited with electrodes R1. TP52.	170
	(a) 50x. (b) 500x (reduced 30% on reproduction).	
70.	Microstructure of a manual metal arc weld deposited with electrodes R2. TP53.	170
	(a) 50x. (b) 500x (reduced 30% on reproduction).	
71.	Microstructure of a manual metal arc weld deposited with electrodes R3. TP54.	171
	(a) 50x. (b) 500x (reduced 30% on reproduction).	
72.	Microstructure of a manual metal arc weld deposited with electrodes R4. TP55.	171
	(a) 50x. (b) 500x (reduced 30% on reproduction).	
73.	Microstructure of a manual metal arc weld deposited with electrodes R5. TP56.	171
	(a) 50x. (b) 500x (reduced 30% on reproduction).	
74.	Chevron crack in the industrial sample A.	172
	(a) 40x. (b) Detail, 200x.	
75.	Chevron crack associated with a pore. Industrial sample A.	172
	(a) 20x. (b) Detail, 200x.	
76.	Chevron cracks in the industrial sample B.	173
	(a) and (b) 20x.	
77.	Chevron crack in a submerged arc weld with the wire-flux combination SD3/1Ni + OP41TT. TP12.	174
	(a) 40x. (b), (c) and (d) details from (a). 400x.	

78.	Chevron crack in a submerged arc weld with the wire-flux combination SD2/3Ni + OP41TT. TP17. 120x.	175
79.	Chevron crack in a submerged arc weld with the wire-flux combination SD3/Mo + OP41TT. TP21. (a) 60x. (b) Detail, 400x.	176
80.	Chevron crack in a submerged arc weld with the wire-flux combination SD3/Mo + OP41TT showing incomplete linking between vertical components. TP21. (a) 60x. (b) Detail, 400x.	176
81.	Chevron crack in a submerged arc weld with the wire-flux combination SD3/Mo + OP41TT. TP21. (Same crack as in Figure 79). Saspanansa etch. (a) 40x. (b) Detail, 200x.	177
82.	Chevron crack in a submerged arc weld with the wire-flux combination SD3/Mo + OP41TT. TP21. (Same crack as in Figure 80). Saspanansa etch. (a) 40x. (b) Detail, 200x.	177
83.	Detail of a chevron crack in a manual metal arc weld with electrodes E8018C1. TP29. 200x.	178
84.	Chevron crack in a manual metal arc weld with electrodes E8018C1 as observed in the longitudinal horizontal plane (parallel to the plane of the plates). TP29. (a) 40x. (b) Detail, 200x.	178
85.	Chevron crack in a manual metal arc weld with electrodes B1. TP40. (a) 40x. (b) Detail, 200x.	179
86.	Chevron crack in a manual metal arc weld with electrodes C1. TP47. (a) 40x. (b) Detail, 200x.	179
87.	Wide open chevron crack in a manual metal arc weld with electrodes C1. TP47. (a) 40x. (b) Detail, 200x.	180
88.	Chevron crack in a manual metal arc weld with electrodes C4. TP50. (a) 60x. (b) Detail, 400x.	180
89.	Chevron cracks with different orientations in the same run. Manual metal arc weld with electrodes E8018C1. TP35. 20x.	181
90.	Chevron crack in the refined region of a manual metal arc weld with electrodes B2. TP42. (a) 40x. (b) Detail, 200x.	181

91.	Staggered, non-linked microcracks.	182
	(a) Manual metal arc weld deposited with electrodes E8018C1. TP29. 60x.	
	(b) Submerged arc weld deposited with the wire-flux combination SD3/Mo + OP41TT. TP21. 200x.	
92.	Staggered microcracks at an intermediate stage of linking. Submerged arc weld deposited with the wire-flux combination SD3/Mo + OP41TT. TP21.	182
	(a) 60x. (b) Detail, 200x.	
93.	Vertical crack with a morphology reminiscent of a chevron crack. Submerged arc weld deposited with the wire-flux combination SD3/1Ni $\frac{1}{2}$ Mo + OP41TT. TP24.	183
	(a) 40x. (b) Detail, 200x.	
94.	Vertical cracks without typical cracking path. Submerged arc weld deposited with the wire-flux combination SD3/1Ni $\frac{1}{2}$ Mo + OP41TT. TP24.	183
	(a) and (b) 80x.	
95.	Vertical cracks in a manual metal arc weld deposited with electrodes B5Ni. TP62.	184
	(a) 40x. (b) and (c) Details, 200x.	
96.	Microfissures in manual metal arc welds.	185
	(a) Deposited with electrodes E8018C1. TP29. 400x.	
	(b) Deposited with electrodes C3. TP49. 20x.	
97.	Microfissures in manual metal arc welds.	185
	(a) Deposited with electrodes E6013. TP39. 80x.	
	(b) Deposited with electrodes R4. TP55. 80x.	
98.	Longitudinal crack with a staircase morphology produced in a Y groove Tekken test. Weld metal deposited with electrodes C1. Cross section of the joint. 5x.	186
99.	Fracture surface of a chevron crack in the industrial sample B.	187
	(a) General aspect. (b) Detail of vertical and horizontal components. (c) Detail of a horizontal component.	
100.	Vertical components of a chevron crack in the industrial sample B.	188
	(a) General aspect. (b) Detail from (a).	
	(c) Detail from (b). (d) Detail from (c).	
101.	Vertical components of a chevron crack observed in the industrial sample A.	189
	(a) General aspect. (b) Detail from (a).	
	(c) Another detail from (a). (d) Detail from (c).	

102.	Vertical component of a chevron crack which was exposed to high temperatures. Industrial sample B.	190
	(a) General aspect. (b) Detail from (a). (c) Detail from (b).	
103.	Fracture surface of a chevron crack in a submerged arc weld. TP17.	191
	(a) General aspect.	
	(b) Detail from a horizontal component showing mainly dimples.	
	(c) Detail of a horizontal component showing dimples and quasi-cleavage.	
104.	Vertical components of a chevron crack in a submerged arc weld. TP17.	192
	(a) General aspect. (b) Detail from (a). (c) Detail from (b).	
105.	Vertical component of a chevron crack in a submerged arc weld. TP21.	193
	(a) General aspect. (b) Detail from (a)	
	(c) Another detail from (a).	
106.	Vertical component of a chevron crack showing inter and transgranular failure. Submerged arc weld. TP21.	193
	(a) General aspect. (b) Detail from (a). (c) Detail from (b).	
107.	Vertical components of a chevron crack in a manual metal arc weld. TP42.	194
	(a) General aspect. (b) Detail from (a). (c) Detail from (b).	
	(d) Detail of a component nucleated at an inclusion.	
	(e) Detail of a component showing inter and transgranular failure.	
	(f) Detail of the centre of a component without clear origin.	
108.	Vertical components of a chevron crack in a manual metal arc weld. TP47.	195
	(a) General aspect. (b) Detail from a component.	
	(c) Detail from (b).	
	(d) Detail of striations in the centre of a component.	
	(e) Detail of a component exposed to high temperatures.	
	(f) Detail from (e).	
109.	Vertical component of a chevron crack in a submerged arc weld showing signs of high temperature exposure. TP17.	196
	(a) General aspect. (b) Detail from (a). (c) Detail from (b).	
	(d) Detail of quasi-cleavage in the outer regions of the component.	
110.	Propagation of a chevron crack which was broken open after precooling in liquid nitrogen.	196
	(a) General view. (b) Detail from (a).	
111.	Fracture surface of a vertical crack in a submerged arc weld. TP24.	197
	(a) General aspect. (b) Detail from (a). (c) Detail from (b).	
	(d) Detail of transgranular failure by quasi-cleavage.	

112. Detail of areas of ductile failure linking brittle fracture regions in a vertical crack. Submerged arc weld. TP24. (Crack also shown in Figure 93). 197
(a) General aspect. (b) Detail from (a) showing the aspect of the dimples.
113. Vertical crack in a submerged arc weld associated with phosphorous segregation. TP27. 198
(a) General aspect of the crack.
(b) Detail of segregation.
(c) Detail of segregation and chemical analysis.
114. Vertical crack in a manual metal arc weld deposited with electrodes B5Ni. TP62. 199
(a) General aspect. (b) Detail from (a). (c) Detail from (b).
(d) Detail of inter and transgranular failure.
(e) and (f) Detail of less common features.
115. Fissure in a submerged arc weld deposited with the wire-flux combination SD2/3Ni + OP41TT. High heat input weld by Crouch (7). 200
(a) General aspect. (b) Detail from (a). (c) Detail from (b).
116. Fissures in a manual metal arc weld deposited with electrodes E6013. TP39. 200
(a) General aspect. (b) Detail of fissure. (c) Detail from (b).
117. Fracture surface of a longitudinal crack produced by the Y Groove test. Weld deposited with electrodes E8018C1. 201
(a) Detail of the staircase morphology (observed from an angle perpendicular to the ductile failure components).
(b) Detail similar to the vertical components of chevron cracks (observed from a direction parallel to the ductile failure components).
(c) Detail from (b). (d) Detail from (c). (e) Detail from (b).
118. Fracture surface of a longitudinal crack produced by the Y Groove test. Weld deposited with electrodes C2. 202
(a) Detail similar to the vertical components of the chevron cracks.
(b) Detail from (a). (c) Detail from (b).
(d) Detail of another component. (e) Detail from (d).
(f) Detail from (e).
119. Fracture surface of a hydrogen charged tensile specimen. (Specimen 4, Table 21). 203
(a) General aspect. (b) Detail from (a). (c) Detail from (b).
(d) Detail of the fracture surface in the columnar region.
(e) Detail from (d). (f) Detail from (d).
120. Fish-eye in a hydrogen charged tensile specimen. (Specimen 3, Table 21). 204
(a) General aspect. (b) Detail from (a). (c) Detail from (b).

121. Hydrogen charged tensile specimens after being tested.
(Specimens referred to in Table 22). 1x. 204
(6) Non charged specimen. (7) Specimen charged for 4 hrs.
(8) Specimen charged for 24 hrs.
(9) Specimen charged for 48 hrs.
122. Details from the fracture surface of hydrogen charged tensile specimens reminiscent of the staircase morphology of chevron cracks. 205
(a) Specimen 7 (Table 22). (b) Detail from (a).
(c) Specimen 9 (Table 22). (d) Detail from (c).
(e) Detail from (d).
123. Chevron crack in a submerged arc weld, which was reheated on purpose. TP21. 206
(a) Horizontal components. (b) Detail from (a) showing the effect of reheating. (c) Vertical components.
(d) Detail from (c) showing the effect of reheating.
(e) Detail from (d). (f) Detail from (d).
124. Thermal facets on the fracture surface of a chevron crack reheated on purpose (same crack as in Figure 123). Single stage carbon extraction replica examined in the transmission electron microscope. TP21. 207
(a) General aspect, 5000x. (b) Detail, 18000x.
125. (a) and (b) Thermal facets on the fracture surface of a chevron crack (same crack as in Figure 108). TP47. 15000x. 207
126. Details from the fracture surfaces of chevron cracks. Single stage carbon extraction replicas examined in the transmission electron microscope. 208
(a) and (b) TP20, 7500x. (c) TP21, 5000x. (d) TP47, 5000 x.
(e) Dimples corresponding to the horizontal components. TP47. 7500x.
127. Variation in the type and incidence of cracking with the hydrogen level in medium strength weld metals deposited with basic electrodes. 209

I - INTRODUCTION

I - INTRODUCTION

During the late sixties and early seventies the problem of hydrogen induced cold cracking in the heat affected zone of welded joints decreased, due to a better understanding of this phenomenon and due to the introduction of better quality steels with lower carbon content. Over the same period weld metal cracking increased, some forms were undoubtedly due to hydrogen whilst in other cases the mechanism was less certain. One apparently new type of cracking was identified in the weld metals deposited with the, then newly developed, agglomerated basic fluxes for submerged arc welding (1), (2); due to the parallel pattern of the defects it was called 'chevron cracking', 'transverse 45° cracking' or 'staircase cracking', but the first name is still the most used.

For a better understanding of the phenomenon an extensive literature survey was carried out to highlight the relevant background information, to put the problem into perspective and relate it with other known forms of cracking. A long bibliography is presented in an appendix to assist further studies.

Chevron cracking is not peculiar to submerged arc welding with basic agglomerated fluxes : similar cracks have been identified in manual metal arc welding with basic electrodes (3), (4). The problem has been found to occur with a wide range of consumables; stringent ultrasonic inspection has revealed the existence of chevron cracks in components such as heavy module structures for the North Sea oil production platforms, circumferential seams in pressure vessels and restrained box sections weldments in heavy engineering fabrications (3). Chevron cracking has not been limited to the United Kingdom : similar cracks have been observed in many other countries around the world as confirmed by several private communications. However, in spite of the importance of this subject, very little has been reported in the published literature.

These cracks, which can occur in medium strength weld metals of the carbon manganese and low alloy type, are characterized by their orientation, which is approximately transverse to the welding direction and at 45° with the plane of the plates in a butt welded joint. The cracks are more easily identified in longitudinal sections of the weld metal cut perpendicularly to the plane of the plates; in these sections some cracks intersect at 90° producing typical chevrons, observable at low magnifications, Figure 1. In the optical or scanning electron microscopes, the stepped characteristic is readily apparent with two sets of components observed with the outline of a staircase, Figure 2.

The unusual orientation and morphology of the cracks, not readily related to other known forms of weld metal cracking, created some speculation about the causes and the mechanisms. Their occurrence with 'low hydrogen' consumables, in conditions supposed to produce low weld metal hydrogen levels, tended to exclude this element as a possible cause of cracking. However, hydrogen was eventually assumed to be the most likely cause of cracking by excluding all the other poss-

ibilities on the basis of the available evidence. In fact, the problems tended to disappear when it was treated as hydrogen induced, with careful control of the moisture level in the consumables and with increased preheat, although it still persisted in a few situations in which anti-hydrogen measures were reported to have been used.

Before this present research was initiated, two opposing theories on the mechanism of chevron cracking were being argued. The first (3) postulated that cracking would occur in two stages, the critical event being the appearance of the 'vertical components', microcracks perpendicular to the welding direction, at high temperatures, followed by linking of these components assisted by hydrogen cracking. The second theory (5) simply considered that cracks would occur due to the combined effect of stresses and hydrogen in the weld metal. Both theories were argued for some time without a consensus opinion being reached due to the lack of more convincing evidence to support one or the other approach.

This was the starting point for this research programme; it began with the study of industrial cases, followed by tests to determine the parameters which control the occurrence of cracking. A special test was designed to reproduce chevron cracks under laboratory controlled conditions and a considerable number of welds were deposited by the submerged arc welding process, with a basic agglomerated flux, and by the manual metal arc welding process with basic, cellulosic and rutile electrodes. These welds were examined by ultrasonics and by magnetic particle inspection on longitudinal sections to determine the orientation, size and number of cracks for each test, which were related with the type, composition and condition of the welding consumables. Metallographic and fractographic examinations were carried out for a representative number of specimens containing cracks. The intention of this examination was to confirm that cracks observed in industrial samples and in laboratory tests were of the same nature, to obtain further information on the cracking type and fracture mode and to relate these to the microstructure.

Tensile tests of weld metal specimens, charged with hydrogen, were carried out to produce fracture surfaces which could be compared with chevron cracks to assist in fractographic interpretation. With a similar aim an independent project was carried out (6) using the Y groove Tekken test and hot tensile tests on weld metals similar to the ones tested previously. This work was extended in this research programme and is reported subsequently.

In another independent project (7), the effect of submerged arc welding parameters which affect the heat input was studied, briefly, in relation to chevron cracking. This work was also extended in this research programme to investigate possible variations of the cracking mode and nature of cracks for welds made in extreme conditions.

Two other forms of weld metal cracking were found in the laboratory programme : these were microcracking, of a very high density in some cases, and transverse cracking perpendicular to the welding direction. These were also studied in so far as their nature is related to that of chevron cracking.

In conclusion, this research has been related to previous work and current hydrogen cracking theories to develop an explanation for the occurrence of chevron cracking.

The programme of studies on chevron cracking is summarized in diagram 1.

II - LITERATURE SURVEY

II - LITERATURE SURVEY

A literature survey was carried out with the aim of finding information on chevron cracking, which is the main issue studied in this thesis, and on the phenomena which were referred to as being probably involved in this type of cracking, i.e. hot cracking and hydrogen embrittlement.

1. Chevron Cracking

1.1 Historical review

Chevron cracking was mentioned for the first time in public in 1968 by Thomas (1) and Cotton (2), who referred to its occurrence in the girth welds of large storage tanks, when certain combinations of submerged arc welding wires and fluxes were used. The cracks were found to be confined to the weld metal, were typically at 45° with the plate surface and could occupy up to 80° of the metal thickness. No comments were made by Thomas (1) on the causes or mechanism of the phenomenon but an investigation on the effect the cracks might have had on the service performance was mentioned. The assessment was based on a wide series of tests of defective welds including cross joint tensile specimens, Charpy-V specimens, large longitudinal tensile specimens, longitudinal specimens tested in cyclic tension and a wide plate test. The defective welds were considered *'to behave satisfactorily in all respects in the cracked condition'* (1).

Further information on the case referred to above was presented in a historical review of industrial experience by Woodend (8) and by Rogers (9). It was stated that the first cracks were discovered during examination of a 1.3" (33mm) test plate welded in laboratory as part of a series to establish conditions under which transverse cracks could occur in repairs of submerged arc welds by manual metal arc welding. The existence of these cracks in the girth welds of the storage tanks was confirmed by ultrasonic inspection. The cracking was apparently restricted to plates thicker than 20mm and seemed to increase with the increase in thickness.

One of the peculiarities of this form of cracking was its occurrence exclusively with basic agglomerated fluxes in submerged arc welding, irrespective of manufacturer. Cracks were consistently absent in welds made with fused fluxes and the wire type and origin made no difference. However, it was discovered that cracks could be eliminated in the welds with agglomerated fluxes provided that a 150°C pre-heat/interpass temperature was used, instead of the $30 - 50^\circ\text{C}$ for fissured welds (8).

Amongst the parameters investigated to determine the mechanism of this type of cracking, Woodend (8) and Rogers (9) referred to the hot tensile properties. Hot tensile tests, of weld metal specimens of the Hounsfield type, carried out in the range 20 to 1100°C , revealed that all the weld metals tend to show a similar behaviour. The elongation increased gradually up to a temperature of about 700°C where it reached values as high as 60%. At

950°C a sharp drop in elongation occurred, generally to around 20 - 25%, with the exception of a particular wire flux combination which exhibited a fall to 12%. Above 950°C and up to 1100°C the elongations increased gradually to 60%. It is interesting to note that the results for the fused fluxes and for the agglomerated fluxes fell into two separate scatter bands, irrespective of the weld metal composition, with the fused fluxes giving higher values of ductility throughout the testing range. However, as pointed out by Rogers (9), many of these agglomerated fluxes did contain deliberate metal alloy additions and therefore, if the comparison was made with the neutral fluxes which are generally adopted today, a completely different picture might have emerged.

In spite of the extensive research carried out, no satisfactory correlation with the parameters investigated was found and, thus, no explanation for the mechanism was provided.

Chevron cracking was mentioned again in 1972 by Hamilton (10), who referred to the occurrence of '*staircase cracks*' in 3" (76mm) thick welds in pressure vessels deposited by submerged arc welding with an agglomerated flux. The cracks were typically 3 - 10mm long and consisted of a series of intercolumnar cracks linked by transgranular failure of the columnar grains. The fractures appeared to have propagated from an initially smooth fracture along prior austenitic grain boundaries. No films or inclusions on the surfaces of the intercolumnar cracks were found, although small amorphous precipitates were occasionally detected. The chemical analyses of the weld metals were not such as to suggest solidification cracking and microprobe scans also failed to give any indication that this form of cracking was a significant factor. The cracks were linked by two mechanisms, principally by deformation fracture and to a minor extent by brittle fracture. According to the same author (10), the cracks did not show '*characteristics typical of hydrogen induced cracks*', but hydrogen was assumed to be the most likely cause of cracking. In fact, the problem was overcome by increasing the pre-heating from 100 to 150°C minimum with post weld heat treatment following immediately on completion of welding.

Chitty and Brown (11), in work published in 1972, reported the occurrence of chevron cracking in 33mm thick submerged arc and basic low hydrogen manual metal arc deposits in the as-welded condition. It was confirmed that the problem in the case of submerged arc welding was restricted to basic agglomerated fluxes, and was aggravated by increase in the joint thickness. According to the same authors (11), the cracks occurred, predominantly, in the as-deposited weld metal and could be both inter and transgranular. Fractography gave no evidence of solidification or other high temperature cracking and it appeared that the fracture occurred with low energy involvement. Again the cracking was attributed to hydrogen because it tended to be eliminated with well known anti hydrogen measures such as careful drying of electrodes and increasing the level of pre-heat. The occurrence of the phenomenon with 'low hydrogen' consumables in thick sections was interpreted in terms of hydrogen build up and restraint caus-

ing delayed cracking along the weakest path in the weld metal, such as the boundaries of the columnar crystals.

At least in the early years, chevron cracking seemed to be more prevalent in submerged arc welds, with basic agglomerated fluxes. One of the causes of its occurrence was supposed to be the relatively high moisture content and reabsorption characteristics of these fluxes. This fact has been emphasized by the history of the occurrence of chevron cracking with the basic flux GP41TT (3), (12). From 1969 to 1971, the flux received a final bake at 500°C and was packed in bags; the flux moisture level was typically 0.14%, various fabricators found chevron cracks in submerged arc welds deposited with this flux. The cracking was considered by the flux manufacturer to be hydrogen induced and, in fact, the problem was overcome by baking the flux at 800°C and supplying it in vacuum sealed steel drums. The moisture level was reduced to about 0.05% and the re-absorption characteristics very much improved by the initial high baking temperature. This produced a dramatic decrease in the incidence of cracking during the following three years, but in mid 1974 a new spate of cracking was observed which was attributed by the manufacturer to an inadvertent increase in moisture content of some batches of flux to 0.07 - 0.09%. This problem was overcome in late 1974 and the moisture level was again restored to the 0.04 - 0.05% level. Tight control of the weld metal hydrogen level seemed to have solved most of the industrial problems caused by this flux.

1.2 Recent research

After some serious problems, particular attention has been paid to chevron cracking over the last 3 or 4 years. In fact, most of the published works appeared during this period.

One of the most controversial papers was presented by Tuliani (3), who reproduced chevron cracks in laboratory using a test, designed at Southampton University (13) which proved, accidentally, to produce this type of cracking, when very low interpass temperatures were adopted. This author (3) found a good similarity between the laboratory produced cracks and the ones encountered in practice and proposed an explanatory theory for the occurrence of chevron cracking based on the metallographic and fractographic study. Tuliani (3) considered that an individual chevron crack resulted from the combination of two separate cracking components. Firstly, microcracks oriented perpendicularly to the plane of the plates occurred due to decohesion of columnar (prior austenite) grain boundaries at high temperature, under ductility dip and favourable stress conditions; this was followed by subsequent linkage, at low temperatures, resulting from the combined effects of residual stresses and hydrogen embrittlement.

The same author (3) recognized that the impurity content of the flux, in submerged arc welding, can be of some importance in so far as minute quantities of impurities might segregate, at high temperatures, along the austenite boundaries. Therefore, the initiation of the high temperature component could be elimin-

ated by careful control over the flux impurity content. The secondary linkage of the intercolumnar cracks, being an hydrogen assisted phenomenon, could be eliminated by well established anti-hydrogen measures, such as increasing the pre-heat and interpass temperature, which could also help to suppress the high temperature component by restraint relaxation.

One of the most controversial issues of this work (3) is the existence of a high temperature component of the cracks, which is assumed on the evidence of features such as thermal facets and thermal grooving on the fracture surfaces, generally indicative of a free surface exposed to high temperature. However, in a multi run weld they could have been caused by reheating during the deposition of a subsequent run.

In order to eliminate the possibility that a reheating cycle could affect the results, Farrar and Taylor (14), (15), concentrated their examination on the features of the cracks occurring on the top run. In the scanning electron microscope, these authors found the 'vertical components' dominated by the presence of large smooth facets which appeared to be featureless at low magnification, with some ductile dimple tearing. At higher magnification they could find small deoxidation products in some smooth areas. Carbon replicas from the same fracture surfaces observed in the TEM revealed the presence of thermal facets and thermal grooving at the grain boundaries, as reported by Tuliani (3).

Farrar (15) proposed also a two stage mechanism similar to the one advanced by Tuliani (3). The critical event would be the occurrence of the vertical components, which would occur at high temperature in the proeutectoid grain boundary resulting from solidification micropores and segregation of impurities which could produce low ductility in these regions in the temperature range 900 ~ 1000°C. The secondary interlinking cracks appeared to be initiated from the high temperature ones, at low temperatures, as they crossed transformation products which were formed below 550°C, by a ductile shearing mechanism. Their nature suggested that they were assisted in their propagation by hydrogen.

A very different theory was proposed by Keville (5), who reproduced chevron cracks in laboratory using the same test as Tuliani (3), though with different consumables: wire flux combinations SD3/Mo+BX300 and SD3/Mo+OP41TT instead of SD3/1Ni+OP41TT. In a series of welds interrupted at different stages, the above author (5) found that no cracks or microfissures were observed until a minimum of 3 runs were deposited, when they began to form in the second run. The subsequent welds, with an increasing number of runs, showed that these microfissures were extending with the number of runs. On no occasion were cracks or microfissures found in the uppermost run. In another experiment, instead of quenching the joint some time after each run, it was allowed to cool in air to room temperature, *'as a means of increasing the time for hydrogen to diffuse'*. The resulting weld presented no evidence of chevron cracks or microfissures which was considered to result from a 50% reduction in hydrogen retained by air cooling, as compared with water quenching.

From the evidence referred to above and the similarity between the features of fracture surfaces of chevron cracks and weld metal hydrogen induced cracks, Keville (5) concluded that the factors controlling the formation and propagation of chevron cracks in a weld are a combination of stress and hydrogen. Her work presented no evidence to suggest that a high temperature mechanism was, even partially, involved in the occurrence of chevron cracks.

Reflecting the deep concern of fabricators and consumable manufacturers caused by the spate of chevron cracking, a Workshop was organised by the Marchwood Engineering Laboratories of the C.E.G.B. in March 1977, during which relevant industrial experience concerning the occurrence of this type of cracking was presented, as well as the research being carried out on the subject. Unfortunately, no proceedings were published to cover either the work presented or the subsequent discussions (4), (5), (12), (16-25).

The problem of chevron cracking has been overcome, in general, through anti-hydrogen measures which were adopted on the basis of empirical evidence. In fact, no systematic work to correlate the phenomenon with hydrogen in the weld metal was published until recently (26), (27), (28).

The work by Wright and Davison (28) concentrated on the influence of the submerged arc welding fluxes on the cracking phenomenon, considering, in particular, the type of flux, i.e. fused or agglomerated, its basicity and the moisture level relative to weld metal hydrogen level. For this purpose, the Tuliani test was selected and a S3 1% Ni wire was used. Based on the experimental evidence, the above authors (28) concluded that :

'Weld metal hydrogen resulting from the flux moisture forms the major factor in promoting chevron cracking in submerged arc weld metals produced from S3 1% Ni wire; chevron cracking is readily produced by the higher basicity agglomerated fluxes, but with sufficient moisture being present, can also occur with lower basicity and/or fused fluxes.'

It is particularly interesting that Wright and Davison (28) have produced cracking by moisturising a flux, after an unsuccessful attempt with the flux in the 'as received' condition. In fact, they found a clear boundary between cracking no-cracking, corresponding to a certain weld metal hydrogen level, which was observed with very few exceptions.

High strain side bend tests, carried out on the uncracked longitudinal weld sections from the tests referred to above, revealed no undetected defects; this suggested that the theory of crack propagation from pre-existing cracks, resulting from ductility dip, was unlikely in this case (28).

1.3 Published work related with the present project

Two MSc projects were carried out within the scope of the present research programme on chevron cracking with the aim of

studying some particular aspects : 'Relation of hydrogen cracking and high temperature ductility dip to chevron cracking in steel weld metal' (6) and 'The influence of heat input on weld metal transverse cracking' (7).

Bihari (6), using defect free weld metals, which were deposited under the same conditions as other welds containing chevron cracks, with the exception that the submerged arc welding flux was baked 1h at 450°C before welding, found no ductility dip in the hot tensile tests carried out in the temperature range 500 - 1320°C. The elongation and reduction of area were found to increase with the temperature and their values were always above 25% and 70% respectively. The fracture surfaces of the hot tensile specimens observed in the scanning electron microscope showed exclusively dimples. However, this work was not taken as absolute proof that ductility dip did not exist for weld metals being considered. The phenomenon is very complex, depending on several variables such as strain rate, thermal cycle (in particular the peak temperature) and chemical composition of the material, therefore negative results must be considered with great care; but the evidence raised some scepticism on the theories which explained the cracking phenomenon based on the existence of a ductility dip.

The second part of Bihari's project (6), concerned the relation between the features of hydrogen induced cold cracks and those of chevron cracks. This work was based on the metallographic and fractographic study of hydrogen cracks produced by the Y Tekken groove test, using the same welding consumables which were previously submitted to chevron cracking tests. A very good correlation was found : many of the features characteristic of the chevron cracks such as the 'staircase' appearance could be easily recognised. This subject was investigated in greater depth by the present author and is reported later.

The work by Crouch (7) was intended to study the influence of the welding parameters and in particular the heat input on the occurrence and severity of chevron cracking, using the test developed by the writer. It was found that, in the case of submerged arc welding, the cracking severity was greatly increased when the heat input was increased in the range 1.2 to 9.6 kJ/mm by varying the welding speed. For the lowest heat inputs the cracking tended to assume the form of fissuring, i.e. microcracks oriented perpendicularly to the plane of the plates, but, as the heat input was increased, chevron cracking became predominant. A similar study was made in which the heat input was increased by varying the welding current; a similar trend, in terms of cracking, was found, but in this case the heat input was limited to about 2.8 kJ/mm due to operational difficulties. Crouch (7) attributed the variations in cracking to the general deterioration of weld metal properties due to microstructural changes, because of the increase in heat input, and to possible variations of the hydrogen level in the weld metal.

Further investigation on the fractographic characteristics of the cracks produced during the series of experiments just mentioned

was carried out by the present author and will be reported later.

Three papers were published dealing with different aspects of the present work (25), (27) (29) but these are dealt with in detail in the main body of this thesis.

1.4 Summary and discussion

The chevron cracking phenomenon is known to have caused serious problems in industrial welding since the late sixties, apparently coinciding with the introduction of basic agglomerated fluxes for submerged arc welding. Later on, this type of cracking was also found in manual metal arc welds deposited with basic coated electrodes. The problem has been overcome, in general, by anti-hydrogen measures such as careful control of the moisture level in the submerged arc welding fluxes and in the coating of manual metal arc welding electrodes and by increasing the preheat/interpass temperature levels. However, this solution was based on the assumption that the problem was likely to be induced by hydrogen rather than on systematic work. In some cases, however, good low hydrogen practice did not always appear to work and sometimes cracking occurred in pre-existing sound weld metal after the deposition of subsequent runs during repairs (4) (30).

Two main theories were presented to explain the phenomenon. Tuliani (3) considered that the cracking occurred in two stages, firstly microcracks oriented perpendicularly to the plane of the plates, occurred from the decohesion of columnar (prior austenite) grain boundaries, at high temperature, followed by the linkage of these components by further cracking, at relatively low temperatures, this latter stage to be considered to be hydrogen assisted. Keville (5) attributed the cracking to be a combination of stresses and hydrogen and her work presented no evidence to indicate that a high temperature mechanism could be, even partially, involved in the formation of chevron cracks.

One of the most controversial issues of Tuliani's theory is the significance of the high temperature component of the chevron cracks, based on the interpretation of features observed in carbon extraction replicas examined in the transmission electron microscope, such as thermal facets and thermal grooving, typical of free surfaces exposed to high temperatures. It can be argued that such features could have been produced on the fracture surface of a pre-existing crack by reheating during a subsequent run. However, Farrar and Taylor (14) (15) supported this theory claiming that similar features could have been observed in cracks occurring in the last run of a weld, which was not reheated.

Tuliani (3) recognized the difficulty in explaining how anti-hydrogen measures could have reduced the incidence of chevron cracking, which he considered to be mainly due to lack of high temperature ductility. The explanation he considered was that the increase in pre-heat and interpass temperature would relax the restraint in the weld metal which, in turn, reduced the straining in the ductility dip temperature range. However, the elimination

of chevron cracking resulting only from the control of the moisture content of the welding consumables has yet to be explained.

In the majority of the welding trials, Tuliani (3) dried the submerged arc welding flux 16h at 150°C, but this procedure was not correlated with the actual moisture level in the flux or hydrogen level in the weld metal. In fact, 150°C must be regarded as a high storage temperature, see Table 1, rather than a baking temperature to eliminate moisture in the flux. If this point was intended to be unambiguous, a 450°C baking temperature for 1 hour should have been adopted, which would probably have eliminated cracking even in the severe test conditions. As it will be seen later, minor variations in the flux moisture level can be critical in terms of hydrogen in the weld metal and cracking.

Two independent projects were carried out within the scope of the present research project on chevron cracking. The first (6) produced a negative correlation between ductility dip and chevron cracking though it left the field still open to some controversy. However, it also showed that most of the features of chevron cracking could be reproduced by the Y Tekken Groove Test. The second work (7), a brief study of the influence of the welding parameters on cracking severity, showed that cracking increased with the heat input (by varying the welding speed and current). This was attributed to a general deterioration of weld metal properties and to a possible variation in the weld metal hydrogen level.

Recent work on the effect of hydrogen on chevron cracking by the writer (26) (27), and by Wright and Davison (28), established that hydrogen is the single major factor promoting chevron cracking in several weld metals. The work by Wright and Davison (28) indicated a clear boundary, in terms of hydrogen level in the weld metal, between cracked and non-cracked welds. However, one must not attach too much significance to the particular hydrogen level corresponding to the boundary situation, because it must, obviously, depend on testing conditions.

2. Weld Metal Cracking in C-Mn and Low Alloy Steels

The conditions in which chevron cracking generally occurs, together with the works reported in the previous section, suggested that this type of cracking resulted from a hot cracking and/or a hydrogen induced cold cracking type of mechanism. However, neither the type of welding consumables nor the first examinations of the cracks produced clear evidence in favour of one or another. A literature survey was carried out on these specific types of cracking with the aim of finding evidence and theories which could explain the industrial cases as well as the results of the experiments carried out.

2.1 Hot cracking

The intergranular welding cracks occurring at high temperature, can be subdivided in two main types according to Hemsworth et al (31) :

- (1) Type 1 - Segregation cracking - associated with micro-segregation leading to intergranular films.
- (2) Type 2 - Ductility dip cracking - occurring at newly migrated grain boundaries free from films. The crack may occur in the heat affected zone, in the primary weld metal or in the reheated weld metal.

According to the above authors, the type 1 cracking will be unambiguously recognized by the presence of films while type 2 will show relatively clean crack surfaces decorated by slip bands, thermal etching or both.

It is commonly agreed, and confirmed by the experimental work reported herein, that there are no visible films associated with chevron cracks. Thus, if these cracks do occur at high temperature, they must be associated with a ductility dip cracking mechanism. Therefore the literature survey on hot cracking was mainly concentrated on this type.

2.1.1 Thermal etching

One of the features which contributes to the identification of a 'hot crack' is thermal etching, which occurs in free surfaces exposed to high temperatures at near vacuum. It shows as grain boundary grooving or thermal faceting (32)(33).

Some authors (34), (35), (36), have explained thermal etching by the vaporization and surface migration of metal atoms to expose surface facets with minimum energy, i.e. low index planes. Others (37), (38), considered the adsorption of impurity elements such as oxygen and sulphur to be an important factor in the surface energy minimization. Gjostein (39) suggested that thermal faceting may be produced by either of the two mechanisms.

In work by Henry et al (40), quoted by Boniszewski and

Brown (33), it is suggested that the formation of terrace like facets occurred on grain boundaries in nickel, i.e. on interfaces as opposed to free surfaces. They assumed that the grain boundary striations were analogous to the free surface striations, i.e. both were due to the adsorption of impurities, a process accompanied by lowering of the surface energy by the exposure of low index crystallographic planes. Because of the possibility of formation of striations in the grain boundaries, Boniszewski and Brown (33) stated that these could not be regarded as an unambiguous indication of the presence of a free surface exposed to high temperature.

2.1.2 Ductility dip

Relatively low ductilities in the high temperature range (800 - 1200°C for steels), seem to be a general property of ferrous weld metals such as mild steels deposited with rutile and low hydrogen electrodes (41), (42), (43), carbon steels (44), (45), (46), (47), high strength steels like HY80 (48) and high alloy steels (49), (50), (51). Other alloys and metals like austenitic Fe-Ni alloys (52), Ni-Cr-Fe alloys (53), binary Cu-Ni alloys (54), copper (55) and aluminium bronze (56), (57), show similar ductility troughs in the high temperature range.

The hot ductility of metals and alloys is generally assessed by the elongation and/or reduction of area after tensile tests carried out at high temperature. The technique of rapidly testing tensile specimens at various temperatures in a simulated thermal cycle was introduced by Nippes et al (58) using an apparatus usually referred to as Gleeble (59), (60). The test was received with enthusiasm since it was believed that the ductility response in the high temperature range would correlate with weld hot cracking. Many tests have been carried out but the interpretation of results and its correlation with the practical situations is not as straightforward as had been anticipated. No unambiguous characteristic, such as zero ductility over a large temperature range, was found to differentiate between crack sensitive and crack resistance material (53).

One of the most elaborate interpretations of the hot ductility curves was presented by Yeniscavich (53), (61), who studied the behaviour of the Ni-Cr-Fe alloy weld metal. According to this author a typical hot ductility curve, Figure 3, can be explained through the positive and negative contributions of temperature dependent phenomena. He assumed an intrinsic ductility for the alloy, independent of temperature, and equivalent to 50% reduction of area. A positive contribution to ductility arises at high temperature because of recrystallization: as the temperature is increased above a critical level, the deformed grains will be replaced by new, undeformed ones, thus, the metal can undergo further deformation without rupturing and the specimens can eventually rupture only when 100% reduction of area is reached. However, recrystallization is time, temperature and strain dependent

and other phenomena, which produce their own contributions to the ductility may occur simultaneously.

In the mid temperature range a negative contribution to the ductility is due to precipitation hardening caused, for example, by metallic carbides. A second negative contribution occurs at higher temperatures due to grain boundary liquation. As the temperature increases, the film thickness grows and so does the fraction of grain boundary area containing the liquid film. When a certain fraction of the grain boundary has liquated the ductility of the specimen will be reduced to zero because of the notch effect caused by liquid films. However, the tensile strength will not be reduced to zero until the film extends completely through the grain boundary volumes and reaches a thickness in excess of 2000 Å (53).

The precipitation of secondary phase particles has been considered to be the most likely cause of ductility dip by most of the authors who have studied this phenomenon. In the case of stainless steel type AISI 347 (18.12.1Nb) the ductility trough at about 850°C was attributed to the precipitation of NbC, which results in strengthening the matrix compared with the grain boundaries and causes most of the straining to occur in boundary regions with resultant intergranular failure at low overall elongations (51). Precipitation of NbC was confirmed by other authors (50), (62), (63).

A different view was expressed by Haddrill and Baker (64), who studied the tendency towards microcracking in fully austenitic 25 Cr/20 Ni weld metals, in multi run welds, which they related to ductility dip. These authors considered that the phenomenon cannot be due to a loss in ductility by precipitation hardening because an increase in carbon, which would be expected to enhance it, resulted in a lower degree of microcracking. However, they admitted that the microcrack surfaces showed the presence of carbides and isolated spherical non metallic inclusions and amongst the factors which might have affected the hot ductility they considered the morphology and distribution of grain boundary carbides.

In the case of low carbon steels, several precipitates have been mentioned as being responsible for the ductility dip. Lankford (46) found this phenomenon to be dependent on the sulphur and manganese content of the steel and in particular on the Mn/S ratio; he considered that the precipitation of liquid droplets of FeS could occur in planar arrays in the austenite boundaries producing paths of easy crack propagation. The recovery of ductility for slower cooling rates or isothermal treatment was attributed to the coalescence and growth of precipitates. With a relatively large mean free distance between particles, the crack propagation was hindered because of the increased size of the plastic zone associated with the crack tip. Another cause of recovery was the formation of the more stable MnS. With

high Mn/S ratios, or more specifically higher manganese contents, the steels would not be embrittled at high temperatures because the solubility of MnS is lower and the conditions of precipitation favour the precipitation of MnS in the matrix.

Matsubara (65), quoted by Lankford (46), found that for steels with Mn/S ratios between 0.5 and 24 the precipitation of sulphides took place between 1180 and 1200°C. The embrittlement was attributed to a matrix hardening of the austenite by sulphide precipitation and the lowering of grain boundary cohesion by precipitation of grain boundary sulphides. Wilber et al (47) also considered that the loss of ductility for steels similar to the ones considered above was caused by segregation of sulphur at the austenite grain boundaries and the solid state precipitation of fine (Mn, Fe)S inclusions. Sulphur segregation would tend to lower grain boundary cohesion and increase the ease of grain boundary sliding. The resulting concentration of strain at the grain boundaries would nucleate voids around the intergranular (Mn, Fe)S precipitates leading to further concentration of strain and propagation of grain boundary microcracks. Concentration of strain at the austenite grain boundaries could be increased by matrix hardening caused by fine precipitation of sulphides as suggested by Matsubara (65).

The ductility dip in mild steel weld metals was studied by Jones (43), who carried out a series of high temperature tensile tests in vacuum and in hydrogen and nitrogen atmospheres using a resistance heated furnace. The results showed low ductility in the range 950 - 1100°C which was not appreciably affected by changes in the atmosphere. Similar results were obtained using rapid heating by high frequency in argon atmosphere. Jones attempted to correlate the relatively poor ductility observed at about 1000°C, with the Mn/S ratio of the weld metals (varied between 7.7 and 35.6) : there was no steady variation but a sharp rise in ductility occurred for Mn/S above 14. The most likely cause for the low ductility at around 1000°C he considered to be the *'formation of small quantities of liquid sulphide in the grain boundary'* and the improved ductility of the wrought steel as compared with the weld metal or cast steel was supposed to be due to the break up and alteration of constitution of the sulphide inclusions. The minimum ductility at 1000°C showed very poor correlation with the susceptibility to hot cracking as assessed by the Murex hot cracking test.

Aluminium nitrides have been suggested since the middle fifties as a possible cause for the ductility dip observed in steels tested in the temperature range 800 - 1200°C. Beynon (66) tested several wrought steels at around 970°C and found considerable difference in their performance, which was related with their state of deoxidation. In fact, the semi-killed steels showed almost 100% reduction of area at fracture while the fully killed steels showed a much lower

value. The figures for aluminium nitride content suggest that hot ductility is related to the amount of aluminium nitride present in the steel. The deleterious effect of the aluminium nitrides on the hot ductility of steels was also reported by Desai (67) and Erasmus (68). Recently, Funnell and Davies (45), also considered the loss in ductility of the austenitic phase in carbon steels as being attributable to the presence of aluminium nitride and showed that it depends on the aluminium nitride particle size. According to these authors the phenomenon can probably be explained by the effect of these particles on the austenite grain boundary pinning at lower strain rates and the inter-particle spacing on the austenite recrystallization at higher strain rates.

The phenomenon of 'strain induced hot cracking,' which is also related with the ductility dip, was recently studied by Keville and Cochrane (69). These authors carried out their study using a modified Transvarestraint test, and depositing a series of submerged arc welds on microalloyed plates with different fluxes. The cracking under different fluxes could be correlated with inclusion size and distribution and how this influences the degree of pinning of prior austenite grain boundaries. It was considered that inclusions can act as nucleation sites for cavities as straining proceeds.

A different explanation for the hot ductility behaviour was presented by Evans and Jones (52) who studied austenitic Fe-Ni alloys. According to these authors, the ductility troughs have been observed over a wide range of strain rates and in all cases the cause of failure appears to be the development of grain boundary cracks and cavities which can nucleate at a variety of sites including non-wetting particles, grain corners and the intersection of subgrain boundaries. In all these cases the authors (52) considered that the critical feature for nucleation and subsequent growth is grain boundary sliding. If grain boundaries can be removed from developing cavities their growth ceases and they play no further part in the deformation process, but if the cavities become sufficiently large, they will pin boundaries so that the grain boundary movement which produces good ductility must occur before the critical radius is attained. Thus, the problem is reduced to establish whether the grain boundary movement over a critical distance (of the order of the cavity diameter) can occur within the time required to create cavities of the size of the critical radius.

2.1.3 Ductility dip and cracking of metals and alloys

The loss in ductility in the intermediate to high temperature ranges has been considered as a major cause of fissuring and cracking of metals and alloys when cooling from the molten state or when they are reheated. It has been quoted as a cause of weld and parent metal cracking during

welding (31), cracking during the continuous casting process (46) and cracking during hot work of fully austenitic steels (31).

Hot tensile testing is an obvious way to identify embrittlement at high temperatures through the measurement of reduction of area or elongation of the specimens being tested. However, the correlation with the practical situation is not an easy one. It has been found, in general, that crack sensitive materials exhibit a ductility dip, but no unambiguous characteristic, such as zero ductility over a large temperature range, was found to differentiate between crack sensitive and crack resistant materials. Thus, more or less empiric and arbitrary criteria have been adopted to correlate hot ductility response with weld cracking. The following criteria were mentioned by Yeniscavich (53)

- (i) recovery rate of ductility from some arbitrary peak temperature,
- (ii) recovery rate of ductility along with recovery rate of tensile strength,
- (iii) minimum ductility value (for example, a minimum reduction of area).

The criterion adopted by Yeniscavich (53) to evaluate the hot ductility response of Ni-Cr-Fe alloy weld metal was to assume that if a material exhibited no ductility it would be fissure sensitive, while if it exhibited some measurable ductility (say 1% reduction of area) then it would be fissure resistant. This criterion is based on the consideration of the strains developed during welding which are, usually, a result of thermal contraction. Cooling through a temperature range of 350° , under fully restrained conditions, only causes 0.5% uniform contraction, hence a small amount of ductility is all that is needed to accommodate this contraction.

2.1.4 Summary and Discussion

The ductility dip phenomenon observed in the high temperature range (around the recrystallisation temperature (31)) is generally agreed to be caused by precipitation of second phase particles, such as carbides, aluminium nitrides and sulphides, which can harden the structure and/or reduce the grain boundary cohesion. Strong support to this theory comes from the fact that the ductility can be recovered by isothermal treatment (45), (46), which may produce overaging and that the phenomenon is dependent on the thermomechanical history.

The dependence on the thermomechanical history emphasizes the need to carefully control the main parameters such as the maximum temperature of the thermal cycle (53), the cooling rates (53), (46), holding time at a temperature before testing (46) and the strain rate (52). Disagreements amongst the results reported by different authors may easily be attributed to differences in testing conditions. The peak temperature of the thermal cycle is particularly significant, its importance seems to be related with the solution treatment (or sensitizing) required to produce the right sort of precipitates during cooling and may determine if the phenomenon is going to occur or not; for example, some materials exhibit ductility dip when tested on the cooling cycle, but not on the heating cycle (48).

It was established that fissuring occurring in the temperature range corresponding to the ductility dip can be readily correlated with poor ductilities in the same temperature range, but no criterion which allows prediction of fissuring susceptibility for a certain metal or alloy from hot tensile tests seem to be universally accepted. This results from the fact that no unambiguous characteristic, such as zero ductility over a wide temperature range, was found to differentiate between crack sensitive and crack resistant materials. However, criteria based, for example, on a minimum arbitrary ductility, assessed by the elongation or reduction of area, have been used (53).

Ductility dip cracking is reminiscent, morphologically, of wedge cracking in creep, though the time factors are different (31), (70). In fact, considering the mechanisms proposed to explain the ductility dip, reviewed herein, and the ones for creep rupture (71), a few similarities seem to exist. Of course, a much closer relationship exists between creep rupture and reheat cracking (70) where there is no suggestion of grain boundary weakness but merely a strengthening of the grains.

The subdivision of hot cracks into segregation and ductility dip cracking by Hemsworth et al (31), based on the presence of films on the fracture surfaces in the first case, may not be so unambiguous as the authors claimed, because the segregates may not be immediately recognized, as admitted, in part, by Boniszewski (70). The problem of intergranular cracking due to reduction of cohesion along grain boundaries, caused by residual impurities from groups IVB to VIB of the periodic table, seems to be a more generic one. It was the advent of Auger electron spectroscopy which provided the critical event that led to the understanding of the fundamental processes which underlie these types of cracking (72).

2.2 Hydrogen Embrittlement and Hydrogen Induced Cold Cracking

The hydrogen embrittlement of steels, i.e. fracture for an abnormally low stress and/or ductility was discovered more than one hundred years ago (73), (74), (75). Hydrogen induced cold cracking has been one of the most controversial and least understood types of cracking. The severity of the problems resulted in extensive research and, according to Bernstein (76), in 1970 there was already more than 3,000 research papers dealing with the problem of hydrogen embrittlement in metals. This fact, by itself, confirms the importance of the phenomenon and its complexity. But so far, neither the mechanism nor a preventive course of action have been firmly established and the best prescription has been to avoid the introduction of hydrogen in the metal whenever it is likely to cause problems.

According to Louthan et al (77), hydrogen embrittlement of metals can be divided into several different categories which are listed below.

- (i) Embrittlement resulting from hydride formation. This can occur, for example, in zirconium (78), (79), titanium (80), and uranium (81).
- (ii) Embrittlement resulting from reaction between hydrogen and some impurity or alloy addition in the metal, as for example



and



- (iii) Embrittlement resulting from hydrogen which is adsorbed on or absorbed in the metal, causing, for example, surface cracking of 304L when tested in hydrogen (85), and reversible embrittlement of steel (86).
- (iv) Other investigators (86) list, as a fourth category, hydrogen blistering or cracking that is caused by the sudden decrease in solubility during cooling of hydrogen-saturated specimens (82), by prolonged cathodic charging (87), and by other techniques which produce high pressure gas bubbles. This form of embrittlement is clearly due to gas pressure build up at microcracks and voids (82).

It seems to be generally agreed that there are four fundamental factors governing the hydrogen embrittlement of steels :

- (i) the hydrogen content;
- (ii) susceptibility of the metal to hydrogen embrittlement which is primarily related to composition and microstructure;

(iii) stress level at the point of crack initiation;

(iv) the temperature and strain rate.

All these factors are equally important but depending on the situation one of them may be dominant. They will be considered herein and discussed from the viewpoint of steel welding.

2.2.1 Hydrogen in steel weld metal

2.2.1.1 Sources of hydrogen

Hydrogen can be introduced in steel in a number of ways. In welding it may exist in the arc atmosphere to be dissolved in the molten steel and retained on cooling; it may be introduced when the steel is at high temperature in a hydrogen atmosphere; at low temperature it may be introduced by electrolytic action or chemical action (e.g. action of acids during pickling) or the action of hydrogen sulphide; or at very high pressure at room temperature (88).

In the weld metal hydrogen can come, generally, from several sources:

- (i) breakdown of water (water may be absorbed on electrode coatings, fluxes or wires, or be chemically combined);
- (ii) from the breakdown of organic materials such as cellulose in coated electrodes and, in this case, hydrogen forms an important part of the shielding gas;
- (iii) wire drawing compounds; in the case of copper coated submerged arc welding wire there is a possibility that hydrogen containing compounds may be present, in uncontrolled amounts, either on the coated surfaces or trapped at the interface of the copper and the welding wire making the wire an important source of potential hydrogen (10) (89);
- (iv) from moisture accumulated on the parent material;
- (v) hydrated oxide, e.g. rust, on the surface of welding wires;
- (vi) oil, grease, dirt, paint, etc. on the surfaces and adjacent to the weld preparation can breakdown to produce hydrogen in the arc atmosphere;
- (vii) degreasing fluids used to clean surfaces before

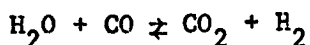
welding may likewise breakdown to produce hydrogen.

In the industrial practice most of the problems caused by the presence of hydrogen in the weld metal seem to result from the breakdown of water which can be retained in a flux after manufacture in three basic forms (90) (91) :

- (i) hygroscopic-water absorbed from the atmosphere by a compound over a period of time;
- (ii) water of crystallization - water chemically bounded into a salt after precipitation from an aqueous solution;
- (iii) Zeolitic - water chemically bounded under pressure.

2.2.1.2 Weld metal hydrogen level

A good correlation exists between weld metal hydrogen and moisture level in the coating of basic manual metal arc welding electrodes (92) or in basic agglomerated submerged arc welding fluxes (93) (94). It is possible, therefore, to specify the hydrogen producing tendency of a basic electrode by referring to its moisture content. However, no general correlation exists between the potential and actual hydrogen content. It was shown by Chew (95) that two electrodes having the same moisture content could, in principle, generate different hydrogen contents in the weld metal depending on the quantity of shielding gas produced by the metal carbonates in the flux coating. In fact, under conditions of equilibrium, the concentration of hydrogen dissolved in the liquid weld pool will depend on the partial pressure of hydrogen in the arc atmosphere (96). In a rather simplistic manner one can consider the effect of the atmosphere illustrated by the water gas reaction:



an increase in the water vapour content would move the action to the right while an increase in the CO_2 would move it to the left. Basic electrodes, containing CaCO_3 in their coatings, can supply CO_2 to the arc atmosphere and this may be one of the reasons why these electrodes can achieve very low hydrogen levels (96). The same theory seems to be applicable to submerged arc welding basic agglomerated fluxes (97).

In the case of manual metal arc welding electrodes of the rutile and cellulosic type, the effect of an addition of water vapour to the arc atmosphere may not result in an increased hydrogen content of the weld metal.

Considering the conditions controlled by the water gas equilibrium Van den Blink (98) and Christensen (99), concluded that, in this case, the effect of water vapour additions will mainly have the effect of a diluent, thereby reducing the partial pressure of hydrogen.

The potential hydrogen of basic manual metal arc welding electrodes is very much dependent on the formulation of the electrode, especially on the binder employed, which influences the amount of water retained after baking and the rate of water adsorption during storage (92)(94). Silicates are generally used as binders, in particular sodium silicate, which may be the main source from which hydrogen comes (92). Thus, if cracking is to be avoided, some form of drying or baking the electrodes is generally required to remove the moisture and reduce the weld metal hydrogen level.

It was shown by Bradstreet (100) and Chew (92) that manual metal arc basic electrodes may regain a significant amount of moisture, at room temperature, in a matter of hours rather than days, though wide variation may occur from one brand to another. This demonstrates the need for proper storage, at a temperature which may be as high as 150°C, if moisture re-absorption is to be kept at an acceptable level.

Typical baking and storage conditions for a wide range of welding consumables are shown in Table 1, according to Graville (96).

High temperature baking of basic electrodes (450 - 550°C), can be beneficial in reducing substantially the rate of moisture absorption (100); but may not produce a significant reduction in the weld metal hydrogen level below the one obtained according to the recommended practice, where the electrodes are used shortly after baking (101). However, these procedures may be very detrimental to the characteristics of the electrodes, they may cause an important loss of manganese and silicon deoxidants, as well as breakdown of calcium carbonates, which affect the operating characteristics and the ease of deslagging due to incomplete deoxidation (101). The electrode coatings are very much embrittled by high temperature baking.

In the case of submerged arc welding basic agglomerated fluxes, baking above 500 - 600°C is sufficient to remove the bulk of the moisture used in the manufacturing process and little improvement takes place by increasing the baking temperature. However, a flux baked at higher temperature shows much lower propensity to absorb water from the surrounding air than those baked at lower temperatures; it was found that a

temperature of 800°C can reduce this effect to a minimum (91) (102). The problem with the high baking temperatures is that they do not allow the presence in the fluxes of such constituents as alloying elements and deoxidation agents, therefore it is necessary to resort to wire flux combinations in which the alloying and deoxidising elements are transferred from the wire or the parent material (102).

In the case of fused fluxes for submerged arc welding, the manufacturing process eliminates any moisture and due to its glassy nature it is not reabsorbed, as opposed to the basic agglomerated type in which the presence of mineral constituents such as CaO and MgO makes them more or less hygroscopic (97).

Submerged arc welding fluxes generally have lower potential hydrogen than basic coated electrodes, but the fluxes produce much more hydrogen in the weld, at an equivalent moisture level, than basic electrodes. Therefore the presence of moisture is extremely critical; the reason seems to be that, in contrast with the electrodes, the readily absorbed water is not driven off but remains in the vicinity of the weld to be subsequently dissociated in the arc (94).

As mentioned previously, no general correlation exists between potential and actual hydrogen content in the weld metal and, in consequence, it is the latter which has to be controlled. Hydrogen levels are classified according to the IIW (103) (104) into

- (i) very low (0 - 5 ml/100g deposited weld metal),
- (ii) low (5 - 10 ml/100g deposited weld metal),
- (iii) medium (10 - 15 ml/100g deposited weld metal),
- (iv) high (>15 ml/100g deposited weld metal).

Typical potential hydrogen levels (related to the moisture levels in coatings and fluxes) and typical hydrogen levels for different processes are shown in Figures 4 and 5.

2.2.1.3 Solubility of hydrogen in steel

The solubility of hydrogen in liquid iron and steel is relatively high, approximately 38 ml/100g at 1 atm. pressure at 1600°C (96), but it decreases very rapidly with the temperature, as illustrated in Figure 6. A sharp diminution in solubility occurs as soon as the molten metal solidifies, only increasing slightly with the transformation from δ ferrite to austenite. This is followed by a steady decrease with the temperature

and finally the transformation from austenite to ferrite produces another sharp diminution, followed by a steady decrease till the room temperature is reached.

Austenitic steels present a higher solubility and and lower diffusivity for hydrogen than the ferritic ones; these characteristics have been considered by some authors to account for the higher resistance of austenitic steels to hydrogen embrittlement and for the beneficial effects of using austenitic electrodes on weld cracking (89) (105) (106).

2.2.1.4 Entrapment and diffusion of hydrogen

The presence of hydrogen in steels is potentially dangerous, due to the embrittlement effects. Thus, in the case of welding, one must initially prevent the introduction of this element in the joint; however, this is not always possible under practical circumstances. Therefore, in critical situations, one has to create the conditions for a sufficient amount of hydrogen to be removed from the joint before the temperature decreases below the levels at which the embrittlement mechanism becomes effective; this can be achieved through pre and post heating treatments (89) (107) (108). The type and duration of treatment required, if any, is dependent on the mobility of hydrogen in the metal which can be assessed through the diffusivity coefficient.

The diffusivity of hydrogen in ferritic steels does not follow a simple law as one would expect from theoretical considerations; experimental results show that there are two regimes of behaviour depending on the temperature. At high temperatures (approximately 200 - 1000°C) hydrogen appears to diffuse in a 'classical' manner, with the atoms moving freely through the metal lattice under the influence only of concentration or temperature gradients; when the temperature falls below about 200°C, an anomalous behaviour starts to be displayed, hydrogen diffuses more slowly than would be expected. The variation of the diffusivity coefficient of hydrogen with temperature is illustrated in Figure 7, according to Coe (109), who recently made a review of the subject.

The reason for the anomalous behaviour of the hydrogen diffusivity with the temperature is regarded as being due to the trapping or delaying of hydrogen, which is retained, for example, in microvoids, as it moves through the lattice. Evans and Rollason (110) found that the apparent diffusivity of hydrogen could vary within wide limits depending on the extent to which the microvoid volume was influenced by the inclusion content, the types of inclusions present and the thermo-

mechanical history. This confirmed the work by Boniszewski and Moreton (111) who had found that microvoids in ferrous materials retarded the evolution rate of hydrogen, though the ones they investigated did not retain the gas permanently. Other factors which may influence the diffusivity are : the chemical composition, the microstructure, though often with small effect, and dislocations which can be regarded as ultimate microvoids but these do not appear to correlate as directly with the diffusivity as larger voids produced by plastic deformation (109).

In summary, it can be said that, though the hydrogen embrittlement mechanism is not fully explained, the knowledge of the diffusion coefficient has a practical importance in determining the procedure to be followed to avoid cold cracking.

The control of diffusivity can also be used as a means to reduce hydrogen embrittlement. Bernstein et al (112) considered that improved hydrogen performance is possible if hydrogen is prevented from reaching noxious locations in sufficient quantities. This can be achieved by providing innocuous trapping centers, by reducing hydrogen diffusivity, or by affecting the slip mode (when hydrogen is being transported via dislocations). Pressouyre and Bernstein (113) claimed that this is a highly practical means of developing alloys resistant to hydrogen embrittlement.

In the case of welding, Fikkers and Muller (114) also considered that the diffusivity coefficient may serve as an indication on the susceptibility to cracking of different types of weld metal.

A different interpretation of the hydrogen induced cracking problem as related with inclusions/voids was recently presented by Hart (115), who studied the problem for the heat affected zone of carbon manganese steels with varying sulphur contents. This author confirmed that low sulphur steels are more prone to that form of cracking than higher sulphur steels, but his explanation is primarily associated with an enhanced hardenability of low sulphur steels and not with a change in hydrogen diffusivity. Hart (115) considered that sulphides, as well as silicates, are able to nucleate ferrite, which effectively raises the transformation start temperature and lowers the hardenability. This contradicts, in part, the suggestions presented above and other studies (116)(117) relating the susceptibility to hydrogen cracking with the void volume, which was supposed to vary with the sulphur content. Voids, in particular the ones associated with MnS inclusions, were believed to act as sinks and traps for hydrogen (111).

2.2.2 Effect of composition and microstructure on susceptibility to hydrogen embrittlement.

In the case of welding, hydrogen induced cracking may occur either in the weld or in the parent material. In general, for carbon manganese and low alloy steels, the harder the microstructure the greater is the risk of cracking. Soft microstructures can tolerate more hydrogen than hard before cracking occurs. Based on empirical data, critical hardness levels have been established below which a low risk of cracking exists. An upper limit of 350 Hv has been suggested very often for practical applications, though higher values can be accepted provided that stringent anti hydrogen measures are taken.

As the hardenability is governed primarily by the chemical composition of the steel, empirical formulas were established which take into account the effect of the important elements on hardenability. One of the most well known is the IIW Carbon equivalent (CE) formula (89) (107):

$$CE = C + \frac{Mn}{6} + \frac{Cr + Mo + V}{5} + \frac{Ni + Cu}{15}$$

The other parameter governing the hardenability is the cooling rate, which is dependent on the initial temperature of the parent material, joint thickness and heat input.

Selection of pre-heating/interpass temperature levels for carbon, carbon manganese and carbon manganese micro-alloyed steels have been greatly aided in recent years by development of monograms such as those in BS 5135 : 1974 (107). However, as pointed out by Dolby (118), there is increasing evidence that the monograms are not accurate for low carbon levels (about 0.10% or less) and the heart of the matter is the IIW carbon equivalent formula. In fact, it appears inadequate for low carbon steels in view of the higher carbon steel compositions used for its original derivation. The formula describes the hardenability of the heat affected zone and correlates with cracking susceptibility within a limited range of compositions; outside this range, where hardenability and susceptibility are not related in the same way, new formulae are required.

Several other carbon equivalent formulae and cracking parameters were developed (119) and of these the Ito-Bessyo formula (120) (121) :

$$P_{cm} = C + \frac{Mn}{20} + \frac{Si}{30} + \frac{Ni}{60} + \frac{Cu}{20} + \frac{Cr}{20} + \frac{Mo}{15} + \frac{V}{10} + 5B$$

is regarded with increasing interest, because it appears the best approach to assess the low carbon steels. This formula was specifically developed for carbon manganese and low alloy steels with carbon contents in the range 0.07 - 0.22% and weights carbon much more strongly than other

elements. Ito and Bessyo used a small slit type test for a wide range of steel compositions and varied the restraint, hydrogen level and pre-heat. They found that cracking occurred when the cooling time between 300 - 100° (or between welding and 100°C) was less than a critical value dependent on the composition, restraint and hydrogen content. These three factors could be expressed in a linear parameter (96) :

$$P_w = P_{cm} + \frac{H}{60} + \frac{k}{40 \times 10^3}$$

where H is the diffusible hydrogen, as determined by the glicerine test method, k = 66t (for butt joints) and t is the thickness of the plates.

The importance of carbon as being the most important factor governing the cold cracking susceptibility has been realised at least since the sixties and steel manufacturers have been reducing carbon to the lowest possible levels; the strength of the steels has been obtained by other means such as precipitation hardening and grain refining rather than solid solution strengthening from macroalloys. As the carbon content of the steels decreases towards 0.10% or less they tend to be free from the heat affected zone cracking problem and the welding procedure will be controlled by the need to avoid cracking in the weld metal.

As the susceptibility to hydrogen induced cracking is related to the hardness and carbon content, in most situations a low susceptibility would be expected from the deposited weld metals. However, cracking does often occur in the weld metal rather than in the heat affected zone, but this results mainly from the higher hydrogen level and residual stresses, not from a higher susceptibility to hydrogen induced cracking.

A great amount of research has been carried out to improve the toughness of the weld metals and a good deal of information exists on the influence of microstructure on the toughness, although this subject is beyond the scope of this literature survey some brief comments are worth mentioning since structure toughness and cold cracking susceptibility are closely related (122).

In most weld metals of the carbon manganese and low alloy type, used with structural steels, the major transformation products are : proeutectoid ferrite, ferrite side plates and acicular ferrite (123). Generally proeutectoid ferrite can be found at the prior austenite grain boundaries, sometimes with ferrite side plates (or upper bainite) growing inwards into the columnar grains, and acicular ferrite in the interior of the grains.

The proeutectoid ferrite is not inherently brittle, but in weld metals it is often present as thin veins surrounding

areas of harder transformation products which form at lower temperatures, such as acicular ferrite. Strain is thus concentrated in the proeutectoid ferrite and it is there that cleavage cracks often initiate. Proeutectoid ferrite is generally considered to have a damaging effect on cleavage resistance.

The ferrite side plates also have a deleterious effect on the cleavage resistance of the weld metal (123), this may be due to the possible retention of thin sheets of austenite amongst the plates of ferrite which may subsequently precipitate carbides which can act as cleavage crack initiators. Moreover, since there are no high angle boundaries between the plates, cleavage cracks can readily propagate across a colony of side plates and this is the place where brittle fractures are often found to originate. This structure is also usually regarded as undesirable in weld metals.

Acicular ferrite, on the contrary, shows inherent strength and toughness, the reasons for this are the very small grain size and the high angle boundaries across individual crystals (124).

The tendency for hydrogen induced cracks occurring in the proeutectoid ferrite was confirmed by Watkinson (125), who used a constant load rupture technique for cathodically and thermally charged specimens. He found that the initiation of cracking in the as deposited single run weld metals was associated with the proeutectoid ferrite at the boundaries between the prior austenite grains, while the detailed microstructure of the transformed austenite grains appeared to be of secondary importance, possibly affecting the amount of strain imposed on the proeutectoid ferrite.

A microstructure showing, in general, low susceptibility to hydrogen cracking may be offset to some extent by factors that do not affect hardness, such as decoration of grain boundaries (solidification and austenite grain boundaries) (114).

2.2.3 Stresses and strains in weldments

The stresses acting upon a weld are a function of weld size, joint geometry, fit up, external restraint and the yield strength of the weld and parent metals. The presence of hydrogen appears to lower the stress level at which cracking will occur (89).

According to Granjon (126), the stresses to be considered when studying cold cracking fall into three categories: direct, indirect and external which may be defined as follows:

Direct stresses - appear locally in the vicinity of the joint due to a non-uniform distribution of temperatures to which are added the effects of transforma-

tions (i.e. short range stresses due to volume changes during phase transformations);

Indirect or restrained stresses - result from the welding process due to external restraint connections, these can be controlled to some extent at the design stage;

External stresses - are those arising from various circumstances of fabrication, which may act upon a welded joint during and after its execution and independently of its execution, for example, the parts' own weight, elastic reactions in the parts, shrinkage of other weld beads, clamping of parts and lifting after welding.

Notches may cause stress concentration in particular zones and increase the cracking susceptibility in conditions which would be safe otherwise.

Probably the most important source of residual stresses is that resulting from the difference in shrinkage of differently heated and cooled areas of a welded joint. The weld metal originally subjected to the highest temperature tends to contract more than the other areas but this contraction is hindered by the cooler parts of the joint. Thus, the weld metal is subjected to tensile stresses in the longitudinal direction, as soon as its temperature has fallen enough to allow a marked yield strength. As the yield strength increases with a further decrease in the temperature, the tensile stresses in the continuously contracting weld increase as well. The resultant tensile stresses parallel to the seam can become as high as the yield point. As a consequence of the shrinkage stresses parallel to the seam, residual stresses must also arise in the direction perpendicular to it, these may be increased by the effect of restraint caused by previous runs or externally.

It is important to note that for most steels a temperature rise of 150°C would cause the formation of residual stresses and a rise of 300°C would cause yield magnitude stresses(127).

Another source of residual stresses is the phase transformations. On cooling, steel transforms from austenite to ferrite, bainite or martensite; this transformation is associated with an increase in the specific volume of the material in the seam and in the heat affected zone it tends to expand but it is hindered, at least in the direction parallel to the seam, by the cooler material not being transformed. Thus, the area being transformed is subject to compression, if the transformation temperature is sufficiently low so that the material already has a marked yield strength after the transformation. The magnitude of these stresses increases as the transformation temperature decreases as for bainite and martensite.

A typical distribution of residual stresses for a butt joint is shown in Figure 8 (128). The distribution of residual stresses varies with the length of the plates and for the same plates throughout the length and thickness of the joint (129).

2.2.4 The effect of temperature and strain rate

The existing experimental evidence shows that hydrogen embrittlement of steels is strongly dependent on the temperature and strain rate. This fact has been related with an alteration in the rate of supply of hydrogen to possible crack nucleation sites and crack tips which are controlled by diffusion and/or by the transport of hydrogen by dislocations (130).

Hydrogen embrittlement/cracking normally occurs in the temperature range - 100° to + 200°C and it is maximum approximately at room temperature (76) (131). At very low temperatures the hydrogen cannot diffuse at a rate sufficiently rapid to build up the critical concentration for cracking, while an increase in temperature increases the diffusion rate of hydrogen and gives it opportunity to escape from the lattice by effusion at the surface of the section (131).

Embrittlement is also affected by strain rate. According to Linnert (131), if the strain rate exceeds about 10 in/in/min (10 mm/mm/min) the embrittling mechanism becomes inoperative because the hydrogen cannot diffuse sufficiently fast to exert its adverse effect. This explains why impact tests frequently do not reveal the presence of a hydrogen content capable of producing embrittlement.

Temperature and strain rate are mutually dependent variables when considering hydrogen embrittlement; their effect was studied by Toh and Baldwin (132) for a SAE 1020 steel both before and after cathodic charging, the results of this work are shown on Figure 9.

When loading statically a series of notched tensile specimens and waiting for failure, under conditions of very slow strain rate and constant hydrogen level, the results show a typical pattern of behaviour - the 'static fatigue curve', Figure 10. The effect of hydrogen is reflected in the following facts (133) :

- (i) the notch tensile strength is lowered (corresponding to a loss in ductility);
- (ii) the delayed failure may occur over a wide range of applied stresses causing just a slight variation in the time to failure;
- (iii) there is a minimum period for crack initiation - 'incubation period', strongly dependent on the hydrogen level and a minimum critical stress below which cracking does not occur.

Decreasing the hydrogen level displaces the curves to the right and upwards, i.e. the upper and lower critical stresses are raised and the incubation time increased. The increase in the lower critical stress with decreasing hydrogen concentration to initiate the delayed failure suggests that crack initiation is controlled by a combination of hydrogen and stress. This is also confirmed by the increase in the static fatigue limit with the notch severity (133). Another important characteristic shown by slowly strained hydrogen charged specimens is the discontinuous growth of the cracks which can be revealed by resistivity/time curves (133) or by acoustic emission (134).

2.2.5 Morphology of hydrogen induced cold cracks

Hydrogen induced cold cracks can be classified on the macroscopic level in terms of the region where they appear (heat affected zone or weld metal), their orientation in relation to the weld joint (transverse or longitudinal) and their position in the joint (root, toe, underbead, etc.). Typical orientations of hydrogen cracks are shown in Figure 11, after Graville(96).

Hydrogen induced cracks in a welded joint, which may occur either in the weld metal or in the heat affected zone, can be inter or transgranular, or both, and present wide variation in size. They may have microscopic dimensions - 'microcracks' or 'microfissures', or be big enough to be immediately recognized without any aids. However, these cracks do not have a specific morphology; according to Boniszewski and Watkinson (122), hydrogen exploits the crack nucleation mechanism which is the easiest in a given microstructure, i.e. that which requires the least amount of overall plastic deformation. In these conditions, identification of hydrogen embrittlement by fractography is at best not completely unambiguous (135). For example, if the processing history of the part is not completely known, it will be difficult to conclude quickly that fracture along the prior austenite grain boundary was due to hydrogen cracking, rather than temper embrittlement, stress corrosion cracking or quench cracks. Pelloux (135), considered that a simple hydrogen embrittlement fracture test, followed by careful metallography and fractography, would help in characterizing the exact mode of fracture due to hydrogen, for a specific grade of steel, and the information would provide a reference basis for the complete failure analysis.

One of the possible explanations for the variation in the cracking mode of the hydrogen induced cracks in the same material has been proposed by Beacham (136), who showed that the fracture crack propagation, in the presence of gaseous hydrogen, in a high strength low alloy steel, depends strongly upon the stress intensity factor (K). At high K levels fracture proceeds by the initiation and coalescence of microvoids, at intermediate K fracture is by quasi cleavage, while at low

K the fracture is intergranular along the prior austenite grain boundaries. The above author (136) considered that this transition is caused by competition between the energetically favourable, but kinetically slow, intergranular fracture and the kinetically favourable, at high K's, microvoid coalescence and quasi cleavage processes.

2.2.6 Special types of hydrogen induced cold cracks

2.2.6.1 Microcracks in mild and low alloy steel weld metal

Microcracks or microfissures in weld metals deposited with mild steel covered electrodes seem to have been reported for the first time by Flanigan (137) in 1947. This author found that fine scale fissuring in the deposited weld metals may be produced by rapid cooling (quenching) in the low temperature range, i.e. below the transformation temperatures of the austenite, due to a mechanism in which hydrogen plays a dominant role (138).

Similar observations were made by Bland (139) who produced microfissures in weld metals by very different means such as quenching the weld bead some time after welding, precooling the plates to -45°C and depositing the bead over a hole drilled in the plate, in line with the weld bead, through which water at about 15°C was flowing. The results of this work showed that increasing the quench time, i.e. the interval between completion of weld and quenching, decreases the extent of microfissure formation, regardless of subsequent rapid cooling of the weld deposit. Bland (139) explained this fact through the reduction in the amount of retained hydrogen when the quench time was increased and emphasized that quenching, in itself, does not produce fissures in a weld metal deposit from which an apparently significant amount of original dissolved hydrogen had been evolved.

Several factors affect the occurrence of microfissures, hydrogen seems to be the most important but it is not the only one. Nitrogen has been considered by several authors as having a significant influence on the microfissure formation (140) (141). The welding current and arc length were also reported to affect the phenomenon (142).

The occurrence of microfissuring in multi run mild steel weld metals was studied, amongst others, by Evans and Christensen (143). These authors found that the tendency to microfissuring is more pronounced in multi run deposits than in single beads welded under similar conditions, the fissure density increases from one layer to the next, existing fissures propagate further on re-

heating by subsequent runs and small adjacent fissures join to form large continuous cracks. They considered that at least part of the disparity between the multi and single layer results was due to the build up of hydrogen, i.e. supplementary hydrogen being introduced into one bead due to the pick up from previously deposited beads. Thermal and straining effects of subsequent beads might also have been important (142).

Evans and Christensen (143) investigated the additive effect of hydrogen by degassing between runs and comparing the relative crack densities. It was observed that the density of microfissures was considerably decreased when degassing at 650°C but some increase from one layer to another still persisted, the authors concluded that other additional factors may be involved, one of which probably being nitrogen.

Non-metallic inclusions are often observed in the path of fissures and this has usually been taken as indicating that the fissures can nucleate at non-metallic inclusions. Winterton (144) has suggested that large spherical inclusions, as well as hot microcracks, may nucleate fissures, and explained the incidence of microcracking in terms of accumulation of hydrogen in pre-existing flaws and superimposed residual stresses. In these conditions, the alterations in the weld metal cooling rate may be particularly important due to the influence on the amount of retained hydrogen. The above author illustrated this fact with the example of a pronounced increase in microcracking with a change in the initial plate temperature (before welding) from 20° to 0°C.

The types of microcracks reviewed so far were essentially due to a cold cracking mechanism, but this has not always been the case. Boniszewski and Brown (33) found a form of fissuring in the refined regions of multi-run mild steel weld metal, deposited from titania covered electrodes, which they considered to be akin to the hot tearing caused by low melting point sulphides. According to the above authors, the critical event in the formation of this particular type of microfissure is the occurrence of low melting point particles of manganese silicates, densely spaced, playing a role similar to the non-metallic films.

Microcracks in mild and low alloy steel weld metals have been indiscriminately referred to as 'fissures' or microfissures'. However, some important differences may exist and their types must be carefully defined. Boniszewski and Brown (33) distinguish the following types of microcracking in as-deposited mild and low alloy steel weld metals:

- (i) Transcrystalline fissures which are the result of cleavage cracking induced in alpha iron by a combination of high hydrogen and internal stresses. These fissures form probably below 200°C.
- (ii) Intercolumnar fissures which are also caused by hydrogen and internal stresses but which appear to be associated with non-metallic particles laying between the columnar crystals. At their tips these cracks become transcrystalline, which suggests that cracking occurs in alpha ferrite range also below 200°C.
- (iii) Hot cracking which shows wide separation of solidification crystals, occurs when impurity segregation has led to the extensive formation of liquid or semi liquid non metallic deposits between the columnar crystals. The hot cracks delineate the contours of the crystals and their path is smooth in contrast to the serrated path of the intercolumnar fissures. When the hydrogen content and restraint are high enough these cracks may propagate as cold cracks.

Although it is not considered in the classification above, it seems possible that, for the weld metals with higher alloy content, intercolumnar (or intergranular) microcracks may also occur, only due to the presence of hydrogen and stresses without the need for non-metallic inclusions. This matter will be discussed later.

The microcracks occurring in the refined regions of mild and low alloy weld metals may be induced either by a hot cracking mechanism, as referred to above, or a hydrogen cracking mechanism. The distinction by fractography is complicated by the fact that some of the hydrogen induced microcracks may be reheated by a subsequent run, which gives to the fracture surface a smooth appearance typical of hot cracks, though without the presence of non-metallic particles or films.

2.2.6.2 Fish-eyes in mild and low alloy steel weld metals

Fish-eyes are another manifestation of the presence of hydrogen in steel. They may be observed on the fracture surface of weld metal specimens submitted to tensile or bend tests carried out at slow strain rate, about ambient temperature, when they contain a sufficient amount of hydrogen to cause embrittlement. They may also be induced in other steel tensile specimens when pre-charged with hydrogen (88).

Fish-eyes generally show a central region or 'pupil' consisting of a pore, an inclusion or other small flaw

which nucleates the crack, surrounded by an 'iris', generally exhibiting a quasi-cleavage appearance in a pattern radiating from the 'pupil', which is believed to result from hydrogen embrittlement. It is generally considered that the iris is due to cracking propagating from the largest defects present, when the tensile strain exceeds the elastic limit of the steel embrittled by hydrogen. The iris stops growing later on due to fast local strain rates, when necking occurs, as well as due to self heating during plastic deformation, which may stop the embrittlement mechanism due to hydrogen (145). It may also happen that outside the halo sufficient plastic deformation occurs to blunt the crack and change the mode of fracture to ductile (33). Fish-eyes are generally surrounded by an area of ductile failure resulting from microvoid coalescence.

Fish-eyes may be eliminated if hydrogen is allowed or forced to diffuse from the weld metal before testing.

2.2.7 Theories of hydrogen embrittlement

Most of the proposed theories on hydrogen embrittlement of ferrous materials are based on one or more of the following factors (76) :

- (i) pressure,
- (ii) surface adsorption,
- (iii) binding energy,
- (iv) dislocation mobility.

Until recently, three main theories were being considered to explain the phenomenon (146), which are summarised below. The present trends will be drawn subsequently.

Zappfe's 'planar pressure theory' (147) is the oldest and until recently the most popular. The author envisaged that atomic hydrogen dissolved in the lattice structure would precipitate into internal voids and combine to form molecular hydrogen. Due to the square-root relationship between the pressure of the dissolved atomic hydrogen and the pressure of the precipitated molecular hydrogen, very high pressures were believed to build up in these voids causing premature failure. This theory was refined by de Kazinczy (148) who introduced some formalism, suggesting that hydrogen diffusion to pre-existing voids or cracks is necessary to maintain the internal stress as the crack propagates; this would explain the time and temperature dependence of hydrogen embrittlement. Further refinements in the theory were introduced by Garofalo et al (149) and by Bilby and Hewitt (150) who applied dislocation concepts. More recently, the theory was reviewed by Tetelman (151) (152), who was quoted as having produced the most complete and most believable treatment of the pressure theory (76).

Petch's surface adsorption theory (153) (154) proposed that fracture arises from the formation of a crack ahead of an array of dislocations piled up against a grain boundary. Because of adsorption of hydrogen on the surface of the crack the metal surface energy is lowered and the propagation became easier, i.e. the stress required for fracture is lower. According to the above author the phenomenon is dependent on the diffusion of hydrogen to the crack edge; this would explain the variation in embrittlement with temperature and strain rate.

Troiano's 'lattice interaction theory' (133) (155), postulated that hydrogen diffuses to the highly stressed regions (stress-induced diffusion) and a concentration gradient is created in conformity with the stress gradient. The magnitude of the concentration gradient created in the tri-axiality stressed region depends primarily on three factors (155)

- (i) the initial hydrogen concentration,
- (ii) the hydrogen diffusion rate,
- (iii) the time during which hydrogen may diffuse.

The two latter factors would account for the temperature and strain rate dependence of hydrogen embrittlement. If the stress is increased or if the hydrogen is allowed to diffuse at constant load, the critical combination of hydrogen concentration and stress state may be attained and a crack open in the lattice at the point of maximum tri-axiality. According to Troiano (133), the explanation for the phenomenon would be that the fracture strength or the cohesive strength of the lattice is lowered in the places where hydrogen is concentrated, i.e. in maximum tri-axiality zones. The decrease in the cohesive strength of the lattice would result from the increase in the repulsive forces between the metallic cores due to hydrogen, as explained subsequently. The interatomic distances of the transition metals, such as iron, cobalt and nickel, are determined by the repulsive forces due to the overlapping of their d bands; the electrons of the hydrogen atoms in solution would enter the d bands of the metallic cores, increasing the concentration of these bands, this would produce an increase in the repulsive forces between the metallic cores, or, in other words, a decrease in the cohesive strength of the lattice.

The above theory was modified by Oriani (156) (157) (158), who postulated, in his 'decohesion theory' for hydrogen induced crack propagation, that regions exist at crack fronts where non-Hookean elastic stresses attain significant fractions of the elastic modulus. In such regions the chemical potential of dissolved hydrogen is lowered sufficiently, so that dissolved hydrogen attains

concentrations that are several orders of magnitude larger than the normal concentration in equilibrium with the given environing hydrogen fugacity. The abnormally large hydrogen accumulation lowers the maximum resistive cohesive force between the atoms. The crack grows when the local tensile elastic stress, normal to the plane of the crack, equals the local maximum cohesive force per unit area. The velocity of crack growth is governed by the rate of transport of hydrogen.

In summary, the Troiano-Oriani theory postulated that hydrogen would decrease the cohesion energy between iron atoms at places where the hydrogen atoms concentrated, i.e. in maximum triaxiality zones for Troiano and for Oriani at the crack tip, in the zone where the deformation does not obey Hooke's law (146).

A 'new model for hydrogen assisted cracking' was proposed by Beachem (136) who noted that all the failure modes existed in the presence of hydrogen and could be found also in its absence. In short, the mode of failure is not typical of the presence of hydrogen; microvoid coalescence, quasi-cleavage or intergranular fracture may occur. Beacham (136) found evidence of microscopic plasticity on fracture surfaces of specimens cracked by hydrogen 'embrittlement', which varied from relatively large degrees, when the mode of failure was microvoid coalescence, to small degrees when quasi-cleavage or intergranular failure occurred. In the case of cracks propagating along prior austenite grain boundaries, he believed that they were caused by severe localised crack tip deformation and were not a result of cessation, restriction or exhaustion of ductility. In these circumstances he considered that the designation 'hydrogen-assisted' cracking would be more appropriate than 'hydrogen embrittlement' cracking. These observations led to the formulation of a new model according to which it is suggested that hydrogen diffuses into the lattice, just ahead of the crack tip, and aids whatever deformation process the matrix will allow. Microvoid coalescence, quasi-cleavage or intergranular fracture are postulated to occur as a result of this deformation process, apparently depending upon the chemistry of the steel, its heat treatment, the stress intensity at the crack tip and the rate of supply of hydrogen to the crack tip, which determines the concentration of hydrogen there. Beachem (136) also suggested that hydrogen instead of locking dislocations unlocks them and allows them to multiply or move at reduced stresses. In this context the new model does not accommodate the 'embrittlement' theories. However, the author (136) considers that the new model fits well with the planar pressure model at low stress intensities, with the theory that hydrogen concentrates in volumes of material under triaxial tensile stress and the theory that hydrogen lowers the true fracture strength of the lattice, if this

is extended to mean that dislocation multiplication and motion are made easier.

The hydrogen-dislocation interaction was foreshadowed by Bastien and Azou (159) in 1951, and has been supported by other authors (77) (160) (161). Hydrogen has been associated with dislocations either to restrict dislocation mobility or to provide localised hydrogen accumulations and thereby embrittle the lattice (162). Though the dislocation transport of hydrogen is not an embrittlement mechanism, per se, it may be involved in whatever mechanism is valid (162). It was considered in the most recent model to explain hydrogen assisted cracking in weldments proposed by Savage et al (161), who advanced the following seven points argument.

1. *It is first necessary to introduce hydrogen at, or above, some critical concentration. This critical concentration is a function of the ratio of the local stress at the crack initiation site (or crack tip) to the yield stress of the material, and will also depend upon the microstructure. In general, hydrogen tends to segregate at grain and cell boundaries and to form Cottrell atmospheres at dislocations; thus the critical level may be exceeded locally with extremely low nominal concentrations of hydrogen.*
2. *The critical stress level for the particular combination of microstructure and local hydrogen content must be exceeded at the crack initiation site (or the tip of a propagating crack). The magnitude of the local stress will depend upon the residual stresses, the externally applied stress, and the type and location of geometric or metallographic features which act as stress concentrators.*
3. *Localized plastic flow occurs at stress concentration sites and continues until dislocation pile ups at barriers such as inclusions, grain boundaries or martensite platelets deactivate the sources. Since hydrogen atmospheres can accompany the moving dislocations, this plastic flow can transport hydrogen to the vicinity of the barrier at rates in excess of those possible by diffusion alone.*
4. *Hydrogen transported to the pile ups by the dislocations can readily diffuse to the barrier interface until the critical concentration required to initiate microcracking at the level of stress present at the location is reached. This critical hydrogen concentration is probably lowest at inclusions which intersect the active slip planes, but if sufficient hydrogen is present, microcrack initiation can also occur at grain boundaries or other barriers.*

5. Once formed, the microcrack can 'absorb' the dislocation pile-up, thus reducing the back pressure on the dislocation sources. The reactivated sources then generate new dislocations which propagate along the slip plane. Many of these acquire hydrogen atmospheres in the process and transport additional hydrogen to the microcrack. The stress concentration near the crack tip can also act to cause additional localized dislocation motion (and further transport of hydrogen in this area).
6. Thus, by a combination of transport by both dislocation motion and diffusion, the hydrogen content at the crack tip is increased more rapidly than would be possible by bulk diffusion alone. Once the critical level of hydrogen is reached in the region of stress concentration, at the tip of the crack, the crack propagates until it enters a region where the hydrogen content again falls below the critical level.
7. The stress concentration present at the crack tip, however, causes additional plastic flow until either dislocation pile ups deactivate the sources or the amount of hydrogen transported to the region reaches the critical level for further crack propagation. In the event that the former is the case, the argument reverts to item 4 above and the succeeding steps are repeated.

The process by which hydrogen embrittles the steel is not clear from the above argument. However, it is understood from the work being quoted (161) that the hydrogen transported by dislocations and by diffusion to a barrier interface, such as a grain boundary or a martensite plate which intersects the active slip plane, reduces the 'bonding energy' at the interface, and aids the nucleation and propagation of a crack. It is important to note that if the hydrogen concentration is high enough near the stress raiser to lower the 'bonding energy' to the point where a crack can form without the aid of a dislocation pile up, no plastic deformation is necessary for crack formation.

2.2.8 Summary and discussion

The problem of hydrogen embrittlement of steels has been known since the last century, its importance and the controversy about the mechanism are clear from the very high number of publications dealing with this subject. However, it is well established that this phenomenon is controlled by the hydrogen content of the steel, the microstructure, the stress level and the temperature and strain rate. All these parameters are equally important but any one may be dominant in

specific cases.

Hydrogen embrittlement is particularly significant in the case of steel welding because this element is present in most of the welds carried out under practical circumstances. The problem used to be more prevalent in the hard heat affected zones and to overcome it the welding specifications have limited the maximum value of hardness for each case. A better knowledge of the phenomenon resulted, in particular during the last decade, in a dramatic decrease in the carbon content of the steels towards 0.10% or less. These new steels tend to be free from the heat affected zone, cold cracking problem and the welding procedure is governed by the need to avoid cracking in the weld metal.

The hydrogen level in the weld metal depends on the welding process itself and in particular on the consumables and their condition. For each process and consumable a good correlation exists between the potential and actual hydrogen level, although no universal relation has been found. The presence of absorbed moisture is extremely critical in the case of submerged arc welding with basic agglomerated fluxes, because, in contrast with the electrodes, the readily absorbed water does not tend to be driven off but remains in the vicinity of the weld to be dissociated in the arc. These facts point to the need to carefully control the moisture content of the welding consumables and to (re)bake, if necessary, the basic electrodes and fluxes.

The ideal solution to prevent hydrogen induced cracking would be to avoid hydrogen introduction into the weld, but, as this is impossible under practical circumstances, its noxious action has to be counteracted by allowing it to escape before the temperature decreases to a level below which it becomes potentially dangerous. This can be achieved by pre and post heating. The effect of this treatment may also be beneficial in terms of transformation of the deposited weld metal to less susceptible microstructures. The type and duration of the treatment required, if any, is dependent on the mobility of the hydrogen in the metal which can be assessed through the diffusivity coefficient. This coefficient may also be related with the rate of supply of hydrogen to a crack initiator or to a crack tip, and may be critical in terms of crack initiation and propagation. This was emphasized by Fikkers and Muller (114) who considered that the diffusivity coefficient may serve as an indication of susceptibility to cracking of different types of weld metal.

The diffusivity coefficient of hydrogen shows an anomalous behaviour in the low temperature range (below approximately 200°C), which is supposed to be due to trapping of hydrogen in microvoids such as porosity, inclusion cavities, etc. Some authors (116) (117), who studied hydrogen induced cracking in the heat affected zone of welds, consid-

ered that the cracking susceptibility may be associated with the void volume which, in turn, varies with the sulphur content or the number of manganese sulphide inclusions; these were supposed to act as sinks and traps for hydrogen. A different view, however, was expressed by Hart (113), who considered that the higher susceptibility of the low sulphur steels is primarily associated with their higher hardenability resulting from lack of sulphides which may nucleate ferrite and raise the transformation start temperature.

There is no typical hydrogen induced fracture mode. Hydrogen exploits the crack nucleation mechanism which is the easiest in a given microstructure. Intergranular quasi-cleavage or microvoid coalescence fracture modes may operate, apparently depending upon the chemistry of the steel, its microstructure, the stress intensity at the crack tip and the rate of supply of hydrogen to the crack tip (136). Therefore the identification of hydrogen induced or assisted cracks, based exclusively on the fractographic evidence may be ambiguous due to the lack of features which are exclusively typical of hydrogen cracking. The fact that a crack may have propagated from a pre-existing 'hot crack', or may be reheated by a subsequent weld run, complicates the interpretation even further.

'Fissuring' or 'microfissuring' is a common designation for a form of microcracking observed in mild and low alloy steel weld metals which has been known since the late forties (33), (137), (139), (143). It has been usually related with the hydrogen retained in the weld metal. These microcracks have been reproduced under laboratory controlled conditions by increasing the weld metal cooling rate in the low temperature range, i.e. below the austenite transformation temperature. This was achieved, in general, by quenching the weld and parent metal (137) (138), by cooling the parent material, continuously, with water (139), or by pre-cooling the parent material (144) (139). These procedures were considered to produce a marked increase in the amount of retained hydrogen and probably in the internal stresses (especially when quenching), resulting in the occurrence of microfissures. Several other factors were considered to enhance the phenomenon, particularly the nitrogen (140), (141), (143). In some cases, microfissures appeared to result from a hot cracking mechanism similar to hot tearing caused by sulphides in the heat affected zone of the welded joint (33). Due to the indiscriminate use of the designation, some care must be taken relatively to the type to which they refer.

Fish eyes are another manifestation of hydrogen embrittlement in steel and in particular in steel weld metals, which is generally revealed during tensile and bend tests at slow strain rates. The fish-eyes show, in general, a 'pupil', i.e. a central region consisting of a pore, an inclusion or other small flaw, which nucleated the crack, surrounded by an 'ir-

is', generally exhibiting quasi-cleavage, which is believed to result from hydrogen embrittlement. This type of crack is unlikely to be observed in a welded joint not submitted to destructive testing, because it occurs after straining the material beyond yield which will rarely occur in practice. Its practical significance may be associated with a reduction in ductility observed in the mechanical tests and in showing that the initial level of hydrogen in the weld metal may have been dangerously high.

Until recently three main theories were being considered to explain the embrittlement of steels by hydrogen. The first, initially proposed by Zapffe (147), known as the 'planar pressure theory' postulated that atomic hydrogen dissolved in the lattice precipitates into internal voids and combines to form molecular hydrogen and therein build up pressure to cause premature failure. This theory has the capacity to explain most of the observations related with hydrogen embrittlement and was adopted by many authors who introduced some formalism and refinements (149) (150) (152). However, it was considered by others to have only a restricted application (136) (146). Petch's 'surface adsorption theory' (153) proposed that the fracture stress is lowered due to a reduction in the surface energy of the material by adsorption of hydrogen at surfaces of internal cracks or voids. This theory was considered by Oriani and Josephic (158) as a necessary condition but not sufficient by itself. The third theory, initially proposed by Troiano (133), postulated that hydrogen diffuses under the influence of a stress gradient, to regions of high tensile stresses within the lattice and there interacts with the metal to lower the cohesive strength of the lattice. This theory was modified by Oriani (156) and has gained wide acceptance.

The fact that hydrogen is not associated with a particular mode of failure served as the basis for Beachem (136) to propose a new model according to which it is suggested that hydrogen would diffuse in the lattice, just ahead of the crack tip, aiding whatever deformation process the structure will allow; the mode of failure would result accordingly. The model suggested that hydrogen, instead of locking dislocations, unlocks them and allows them to multiply or move at reduced stresses.

The hydrogen-dislocation interaction, initially proposed by Bastien and Azou (159) has been considered by several authors (77) (160) (161). Although the transport of hydrogen by dislocations is not an embrittlement mechanism by itself, it may be involved in whatever mechanism is valid (162). Savage et al (161) proposed, recently, a mechanism relying partially on this type of transport.

Each of the proposed theories was developed to explain experimental observations and/or industrial experience. Thus,

each one is consistent with some portion of relevant data. However, none of the proposed mechanisms as now formulated, taken singly, explains all the observations accompanying hydrogen embrittlement, as discussed by Louthan (162). Therefore, either there is no universal embrittlement mechanism, or yet a new theory must be developed (162). In spite of the lack of universal agreement it seems that in the last few years Troiano's theory, modified by Oriani, and the interaction between hydrogen and plastic deformation, have gained more credibility (146). However, the 'planar pressure theory' is still being considered, in particular to explain cases such as blistering (163) or, more generally, cases of low stress intensities where the pressure serves as a source of stress and driving energy (136). Pressure may also act in cases of high fugacity (146).

III - MATERIALS AND EQUIPMENT

III - MATERIALS AND EQUIPMENT

1. MATERIALS

1.1 Parent Materials

The material of the plates and backing bars used in the cracking tests was mild steel, conforming to BS 4360 grade 43A, 25mm thick in the case of the Tuliani test and 38mm thick in the case of the continuous water cooling test; the backing bars were 12mm thick.

1.2 Welding Consumables

The submerged arc welds carried out during the cracking tests were deposited with a series of 3.2mm dia. wires, with chemical compositions shown in Table 2, and with the flux OP41TT supplied by Oerlikon Ltd. This is a fully basic agglomerated flux, with chemical constituents shown in Table 3, suitable for welding with direct current, electrode positive, at currents up to 800A.

The series of manual metal arc welds were carried out, initially, with commercially available electrodes conforming to AWS E8018 C1, supplied by the manufacturers designated herein as A and B, and with rutile electrodes, conforming to AWS E 6013. Twenty small batches of electrodes with basic, cellulosic and rutile coatings, produced especially for this project by BOC Murex, were also tested. The diameter of all the electrodes tested was 5mm except for those supplied by manufacturer B, which was 6mm.

1.3 Weld Metal Chemical Composition

The industrial weld metal samples containing chevron cracks were submerged arc welding deposits with chemical compositions presented in Table 4.

The chemical analyses for the weld metals used in the cracking tests are presented in Tables 5 to 8.

2. EQUIPMENT

2.1 Welding

The submerged arc welds were carried out with a Hagglunds type LSIT 1200 transformer rectifier rated at 84 KVA corresponding to 1200A, 44V DC output. This unit has a drooping static power characteristic and was used with a Hagglunds HSA 150, voltage controlled wire feed system and head. The welding head was mounted on horizontal and vertical slides with the workpiece placed beneath it on a moving table.

The manual metal arc welds were made with an English Electric Co. LWAD 600 power source. A voltmeter and an ammeter

were incorporated in the welding circuit for arc voltage and welding current measurement.

The MIG weld was carried out with a Union Carbide power supply type SUI 500, with a Linde welding control type SCC-9 and a Linde wire feeder type - SEH3. The welding head was mounted on horizontal and vertical slides with the workpiece placed beneath it on a moving table.

2.2 Ultrasonic Inspection

The ultrasonic inspection was performed with an Ultrasonoscope model Mk4 using a 40° probe operating at 5MHz in the pulse echo mode. Calibration of the equipment was attained using an IIW standard calibration block. Oil or grease were used as couplants.

2.3 Magnetic Particle Inspection

The magnetic particle inspection was carried out with a Magnaflux k-12 portable unit by means of a coil, approximately 120mm in diameter, formed by 3 turns of heavy duty cable 4/0, 9m long. The cracks were revealed by a Magnaflux prepared bath type No. 7AHF - black.

2.4 Acoustic Emission

The acoustic emission equipment used to monitor the continuous water cooling cracking test, was of the 3000 series manufactured by Dunegan/Endevco.

2.5 Temperature Measurement

The weld metal temperature measurements were made using 6% Rhodium-Platinum 30% Rhodium-Platinum thermocouples sheathed in 4mm diameter twin bore recrystallized alumina insulators. In the low temperature range, i.e. below 350°C, the weld metal temperature was measured using Chromium Alumel thermocouples.

A multi channel UV recorder, manufactured by S.E. Laboratories Ltd., type 3006, was used to record simultaneously the thermocouple voltage output and its derivative trace, from which the weld metal cooling curve and the austenite transformation temperatures were obtained. This equipment was developed by Rodrigues (164) in conjunction with the Instrumentation Department at the Cranfield Institute of Technology.

A multipurpose digital voltmeter and a power source were used for calibration purposes.

2.6 Cathodic Charging of Tensile Specimens with Hydrogen

The weld metal specimens were cathodically charged with hydrogen using a Farnell stabilized power supply model L30E, an electrolyte consisting of an aqueous solution of 5% H₂SO₄.

and 0.05g/l of As_2O_3 as a poison and a 50mm diameter cylindrical anode made of 2mm thick mild steel sheet.

2.7 Mechanical Testing

An Instron model TT-C tensile test machine was used for testing the hydrogen charged tensile specimens.

The Vickers hardness measurements were carried out on a tester made by Zwick & Co. KG., model 3202.

2.8 Metallography

A Reichert model 'Me F' projection microscope was used for all optical microscopy.

2.9 Fractography

The majority of fractographic studies were carried out using a Stereoscan 600 scanning electron microscope made by Cambridge Instruments Ltd. However, this microscope failed to give the resolution required and other scanning microscopes were used at the Universities of Cambridge and Southampton, towards the end of the project, an ISI model 100 and a Cambridge Instruments model S150 respectively.

A small amount of work with carbon replicas was done using a JEOL 200 KV transmission electron microscope, model 200 B.

IV - EXPERIMENTAL PROCEDURES

IV - EXPERIMENTAL PROCEDURES

1. Weld Metal Cracking Tests

1.1 Tuliani Test

This test was adopted in a form very similar to the one proposed by Tuliani (3). The plates were flame cut and the cut surfaces and backing bar were dressed smooth by hand grinding. The dimensions of the joint, set up and welding sequence are shown in Figures 12 and 13. No external restraint was applied. The welding consumables and procedure are specified in Table 9.

After completing each run the joint was allowed to cool naturally, for 5 minutes in the lower third of thickness, 10 minutes in the middle third and 15 minutes in the upper third. After this period the excess flux and slag were removed, the joint was quenched into water, dried and then transferred to a cooling bath consisting of acetone and liquid nitrogen. Liquid nitrogen was added until the required temperature was attained, a few degrees below the nominal in order to account for heat gain during setting up. The temperature was controlled by a thermocouple placed in the plate, near the joint. Due to the very low temperatures, water tended to condensate and freeze on the surface of the joint, but this was removed before the flux was manually added. Generally each test required about 14 runs to be completed.

During one test of the series, TP4, Table 13, the joint was quenched about 20 to 25 seconds after finishing each run, having removed the excess flux but with the slag still left on, in order to increase the severity of the test.

At least 72 hours elapsed before the weld metal was sectionned through the planes shown in Figure 13.

1.2 Continuous Water Cooling Test

This test is based on the cooling of the joint by water passing continuously through a channel in each plate. As it would be difficult to drill the channels, due to the length of the plates, welded construction was used as illustrated in Figures 14 and 15. This design allows control of the weld metal cooling rate through the separation of cooling water from the weld preparation (t in Figure 14) and through the rate of water flow. The effect of continuous water cooling on weld metal cooling rate, as compared with the non-water cooled joint, is presented in Chapter V.

Before welding, the base plates were flame cut and hand ground to remove scale and oxides. Backing bars were also hand ground in order to allow good electrical contact and to prevent the introduction of dirt into the weld joint; furthermore, the backing bar was shaped as shown in Figure 16, to allow good fit up and reduce the likelihood of longitudinal cracking in the root. With both base plates and backing bar correctly profiled, they were assembled with the aid of a template to the desired weld

joint preparation, Figure 16. No external restraint was applied and the preset of the weld preparation was planned to ensure that the edges of the joint became parallel when it was completed, Figures 17 and 18. After setting up the joint, tack welds at least 50mm long were deposited with manual metal arc welding electrodes conforming to AWS E7018. For good electrical pick-up, tags were welded onto the base plates for clamping the flying earth lead. The welding consumables and procedures are specified in Tables 10, 11 and 12.

The welding sequence generally adopted in these tests is shown in Figure 17 for the submerged arc welds and MIG weld and in Figure 18 for the manual metal arc welds. In this case three runs were deposited per layer in order to avoid the use of a weaving technique.

After completing each run about two minutes were allowed before removing the excess flux and/or slag. The weld metal cooled to the water temperature of 18 - 25°C shortly afterwards. The period between runs was kept constant, at about 7 to 10 minutes, but in some cases this was impossible and one or two breaks of half to one hour occurred during a test.

After completing each weld at least 72 hours elapsed before sectioning the weld metal to allow for any delayed cracking. Sectioning was carried out with a vertical band saw through the planes shown in Figures 17 and 18. The parent plates could then be used for subsequent testing after being dressed to the desired profile by hand grinding. To increase the test production three sets of plates were used.

2. Baking and Moisturizing Procedures for Welding Consumables

The submerged arc welding flux was used 'as received', 'damp' and 'baked at 450°C'. To moisturize the flux, i.e. to produce 'damp' flux, it was exposed to the workshop atmosphere for about 10 days in shallow trays not deeper than 40 to 50mm and periodically raked to expose fresh flux. To bake the flux at 450°C it was also spread in shallow trays, in layers not deeper than 40 to 50mm, and introduced into an oven with a convection fan. The temperature was allowed to stabilize at 450°C and kept for about 1 hour. The temperature of the atmosphere inside the oven was checked by means of a thermocouple and was found to be within 10°C of the nominal value. After baking, the flux was transferred from the trays to small steel drums and kept at about 120°C during all the welding operation.

All the manual metal arc welding electrodes were used in the 'as received' condition. Some batches of basic electrodes were also used 'damp', and baked at 300°C and at 400°C. The 'as received' electrodes were used straight from a box without special precautions to avoid moisture pick up during the test. To produce 'damp' electrodes, electrodes were simply spread on a table and exposed to the workshop atmosphere for about 10 days before welding. Baking was carried out in an oven with a convection fan, for about 50 electrodes each time. The temperature was allowed to stabilize around the required level, 300 or 400°C, and kept for 1 hour. The temperature inside the oven was

checked by means of a thermocouple and found to be, in general, up to 10°C higher than the nominal temperature for which the furnace was set. The baked electrodes were transferred from the oven to a hot quiver where they were kept at about 100°C during all the welding operation. The temperature inside the quiver was checked several times by means of a thermocouple welded to the core of an electrode.

3. Non Destructive Testing

3.1 Ultrasonic Inspection

After sectioning the strip of weld metal and backing bar through the planes shown in Figures 17 and 18, ultrasonic inspection was carried out with a 40° probe, operating at 5 MHz in the pulse echo mode. Ultrasonic inspection gave an indication of the number and distribution of cracks for each test. If an abnormal distribution occurred this information was taken into account in further sectioning of the specimen.

During one test in the manual metal arc welding series, TP31, Table 15, ultrasonic inspection of the weld metal was carried out while the test was in progress, immediately after each run, in order to find where and at which stage the cracks occurred.

3.2 Magnetic Particle Inspection

In order to allow a more exact macroscopic examination, both cut surfaces of each weld metal strip were ground smooth with a surface finisher and surface or near surface cracks were detected by magnetic particle inspection. Specimens were magnetized in a coil, approximately 120mm in diameter, formed by 3 turns of heavy duty cable, with the power source set to maximum current, approximately 1100A, DC. The cracks were exposed by magnetic ink sprayed on the surface of the specimen. A significant number of specimens containing cracks was photographed. In some cases the surface was previously etched before spraying the ink, this procedure allowed association of cracks with particular weld runs and made photography easier by reducing the light reflection. However, etching was avoided when the fracture surfaces of the cracks were to be examined.

Further sectioning was generally carried out as shown in Figures 17 and 18. The new cut surfaces were also ground smooth with a surface finisher and submitted to magnetic particle inspection according to the procedure mentioned above.

3.3 Detection of Cracks by Acoustic Emission

During the welding of TP18, Table 14, an acoustic emission apparatus was used to detect precisely when the cracks initiated and/or propagated. The technique is based on the detection of stress waves, resulting from the extension of a crack, by piezoelectric transducers attached to the surface of the plates. The equipment and the location of the transducers on the side of the joint are shown in Figures 19 and 20.

4. Measurement of Weld Metal Cooling Rates During the Tests with Continuous Water Cooling

For comparison purposes, weld metal cooling curves were determined for several welding and cooling conditions. The manual metal arc welding process was selected and 5mm diameter electrodes conforming to AWS E8018 C1 were used. The welding current was 235 A and the voltage 24V whilst the welding speed was varied according to the heat input required. The temperature measurements were carried out in weld runs deposited in the middle and upper third of the joint.

For temperature measurements in the range 1400°C down to 300°C, 6% rhodium-platinum and 30% rhodium-platinum thermocouples, sheathed in twin-bore recrystallized alumina insulators, were used. For each measurement, the full length of an electrode was deposited and the thermocouple was manually introduced, in the middle region of the run, in the molten weld pool, immediately behind the arc. The positioning of the thermocouple was found to be critical; if it was placed too close to the arc the thermocouple would melt and no signal was obtained.

The thermocouple output voltage, corresponding to the weld metal cooling curve and its derivative were recorded, whilst welding was in progress, on a UV recorder previously calibrated with a multi purpose digital voltmeter. The weld metal cooling curve was obtained from the UV recorder chart by measuring accurately the thermocouple output voltage and converting these values into temperatures, using the calibration chart supplied by the thermocouple manufacturer, J.J. Matthews. The method and equipment used have been developed by Rodrigues (164). The weld metal cooling curves were plotted on a temperature-time graph, with indication of the approximate austenite transformation temperatures obtained from the sharp change in slope of the weld metal cooling curve shown by the first derivative (164).

The cooling curves between 350°C and room temperature, during the above tests, were determined using chromel -alumel thermocouples. For this purpose, the thermocouples were implanted in the previously deposited weld metal and parent plates in positions calculated to be about 3mm from the fusion boundary of the weld run to be deposited. The output from the thermocouples was recorded with a multi-channel UV recorder previously calibrated for this purpose with a digital voltmeter and a power source. The cooling curve was obtained directly from the UV recorder chart. It was assumed and verified by comparison with the previous cooling curves for the weld metal, that below the 350°C temperature range there was no significant difference between the temperature at the centerline of the weld run and at a point in the heat affected zone 3mm from the fusion boundary.

5. Procedure to Reheat Chevron Cracks

A specimen containing chevron cracks buried internally, as revealed by ultrasonic inspection, was sectioned just above the level where the cracks were found, through a plane slightly inclined with the longitudinal axis. A weld run was deposited on the cut surface by manual metal arc welding, in order to reheat the chevron cracks in a way similar to what could have occurred in practice. As the position

of the fusion boundary relative to the cracks could not be precisely determined in advance, the use of an inclined section was found to be a useful means to reheat the series of cracks to different temperatures, according to the distance from the fusion boundary. The specimen was subsequently sectioned longitudinally, submitted to magnetic particle inspection and the cracks supposed to have been reheated to the adequate temperature were selected to be observed in the scanning and transmission electron microscopes.

6. Preparation and Testing of Hydrogen Charged Tensile Specimens

Tensile specimens were machined from the weld metal of TP14, Table 14, deposited with the wire flux combination SD2/3Ni + OP41TT, which had been considered crack free as far as could be detected by ultrasonic and magnetic particle inspection. The location of the tensile specimens in the weld metal is shown in Figure 21 and the dimensions of the non standard specimens in Figure 22. Friction welded extension pieces were necessary for the shanks of the specimens in order to obtain the desired orientation.

Several techniques to charge specimens with hydrogen have been described in the literature (88), (161), (165 - 170). Cathodic charging was preferred because it is easy to carry out and does not involve reheating the specimens. The surface of the specimens was polished to produce a smooth finish and carefully degreased prior to charging. The specimens worked as the cathode of a cell, surrounded by a steel anode, approximately 50mm in diameter, immersed in the electrolyte specified in Chapter III, 2.6. The charging current was supplied by a power source and was rated at 80 mA/cm². The charging time was varied in order to produce a higher or lower hydrogen concentration, as specified in Tables 21 and 22 for each test.

This charging method is likely to produce a concentration gradient of hydrogen : the hydrogen level is relatively high in the outer regions of the specimen while the inside remains relatively free. To overcome this problem some authors refer to the use of plating, for example with zinc, to avoid the loss of hydrogen, and reheating to produce homogenization (161). However, preliminary tests showed that satisfactory results could be obtained without homogenization and this procedure was not followed.

The tensile tests were carried out in an Instron tensile testing machine within a few minutes of hydrogen charging. The selected cross head speed produced an extension rate of 2% per minute for the Hounsfield No. 14 specimens and 3% per minute for the longer, non-standard specimens; the tests took only a few minutes to be completed.

Preliminary tests had shown that the specimens tended to fail in the region of the shoulder and to avoid this problem the heads and shoulders were coated with vinyl to concentrate the hydrogen in the gauge length of the specimen.

7. Preparation of Specimens for Metallographic Examination

A representative number of weld metal sections were prepared for metallographic examination. The longitudinal sections, intended to show the relation between the crack path and microstructure, were selected according to previous magnetic particle inspection. Relatively small specimens mounted in bakelite were wet ground and polished on rotating cloth pads using 6, 1 and $\frac{1}{2}$ micron diamond dust paste. The etchants used were 2% nital and Saspa Nansa (171). Cross sections were prepared in the same manner to study weld metal microstructures.

8. Hardness Testing

A hardness survey was carried out on cross sections of weld specimens corresponding to each batch of manual metal arc electrodes and to each wire-flux combination used in the submerged arc welds. At least three indentations were made for each of the regions selected: non-refined weld metal in the last run, non-refined weld metal in the middle runs and refined regions.

9. Preparation of Fracture Surfaces to be Observed in the Scanning Electron Microscope

The weld metal longitudinal strips were initially polished and submitted to magnetic particle inspection. If chevron or vertically oriented cracks were found, two or three representative cracks were selected and the specimen sectioned as shown in Figure 23. Subsequently the specimen was cooled in liquid nitrogen, placed in a vice and broken through the crack and notch by the impact of a hammer. Specimens containing only fissures were deeply notched and loaded in tension until rupture in a tensile test machine. These specimens normally included the top run, i.e. the last weld metal run deposited, in order that non-reheated fissures could also be observed.

For reference purposes all specimens were marked with an arrow indicating the vertical orientation and a series number, Figure 23. Before being examined the specimens were demagnetized and placed on a stub. In the scanning electron microscope the specimens were observed from several angles, but generally photographed from a direction approximately perpendicular to the fracture surface or, in the case of chevron cracks, from directions perpendicular to the vertical and horizontal components, respectively. In order to avoid oxidation of the fracture surfaces these specimens were not previously etched unless otherwise stated.

10. Preparation of Carbon Extraction Replicas from Fracture Surfaces to be Observed in the Transmission Electron Microscope

Carbon extraction replicas were prepared from a representative number of fracture surfaces matching those previously observed in the scanning electron microscope. Carbon was evaporated on the fracture surface according to the standard procedure after masking the non-relevant areas. Subsequently the replica was sectioned in small rectangles, 2 to 3mm², and the specimen placed in 5% nital until the under-

lying metal was dissolved by chemical etching and the replica could be freed. Then the replica was washed in distilled water, placed in a replica grid and allowed to dry before being examined in the transmission electron microscope.

11. Chemical Analysis

Chemical analyses of all the weld metals tested during this project were carried out by Quantivac for non gaseous elements; oxygen and nitrogen were not determined.

12. Weld Metal Hydrogen and Flux Moisture Determinations

The diffusible hydrogen analysis of the weld metals deposited with manual metal arc electrodes was carried out according to the BS 639 method. Moisture determinations on the submerged arc welding fluxes was carried out according to the Gayley Wooding method.

V - RESULTS

V - RESULTS

1. Chevron Cracks on Longitudinal Sections of Industrial Samples.

Typical examples of chevron cracks occurring in industrial practice are shown in Figures 24, 25 and 26. In the longitudinal sections of the weld metal, perpendicular to the plane of the plates, the cracks were inclined at $45 - 50^\circ$ with the longitudinal direction and tended to be concentrated in a few preferential layers. The cracks, in general, were only a few millimetres long, but in exceptional cases they could traverse through several runs for 25mm or longer. In longitudinal sections parallel to the plane of the plates the cracks were inclined at $80 - 90^\circ$ to the welding direction, i.e. they were almost transverse, Figure 26. Chevron cracks were more prevalent in the middle third of the welded joint.

2. Weld Metal Cracks in Laboratory Tests.

In order to show the variation in weld metal cracking for the different testing conditions, weld metal longitudinal sections were submitted to magnetic particle inspection and the following parameters were recorded for each test :

- (i) orientation of the cracks relative to the welding direction;
- (ii) maximum number of cracks longer than 1mm in any longitudinal section 100mm long;
- (iii) the average crack length of the cracks referred to in (ii);
- (iv) the length of the longest crack observed in any section;
- (v) an estimate of the amount of fissures less than 1mm long.

The results of the weld metal cracking tests are presented in Tables 13 to 18. It is apparent that the first factor controlling the occurrence of cracking, in weld metals deposited by submerged arc and by manual metal arc with basic electrodes, was the condition of the consumables, which could be related to the hydrogen level in the joint. The severity of cracking, for the welds deposited with consumables in the 'damp' or 'as received' condition, was found to increase with the alloying/strength of the weld metals. This factor also seemed to control the orientation of the cracks in the sense that for medium strength weld metals the cracks were oriented at 45° with the welding direction and for higher strength weld metals cracks tended to be vertically oriented.

The welds deposited with cellulosic electrodes were found to be exceptionally prone to transverse cracking, either at 45° or vertical, depending on the alloying/strength of the metal, see Table 16. The welds deposited with rutile electrodes produced mostly small fissures (less than 1mm long).

A representative number of specimens containing cracks was photographed in order to show the typical size, distribution and orientation of the cracks detected by magnetic particle inspection, Figures 27 to 37. In the longitudinal horizontal sections (parallel to the plane of

the plates) the cracks were inclined about 80° to 90° with the welding direction, i.e. they were approximately transverse, Figure 27. In longitudinal vertical sections (perpendicular to the plane of the plates) the cracks were inclined about 45 to 50° with the welding direction for the medium strength weld metals, Figures 28, 29, 32, 33 and 34, and were approximately vertical, i.e. perpendicular to the welding direction, for the high strength weld metals, Figures 31, 35 and 37. In specimens etched with nital prior to magnetic particle inspection, it could be seen clearly that each row of chevron cracks tended to be associated with a particular run or refined region of weld metal. These cracks occurred in general in the middle third of the joint and with the exception of one weld deposited with cellulosic electrodes, Figure 34, no cracks were found in the uppermost weld run.

Vertically oriented fissures, less than 1mm, were found in all tests with the exception of the submerged arc welds with flux baked at 450°C . Some fissures could be observed when the consumables were used in the 'as received' condition, but their number was very much increased when the consumables were 'damp'. In general, the weld runs containing chevron cracks presented a lower density of fissures compared with the others.

3. Ultrasonic Inspection and Detection of Cracks by Acoustic Emission

Ultrasonic inspection was carried out on all the longitudinal sections of weld metal, to provide information on transverse cracking, in particular on buried cracks not detected by magnetic particle inspection. No important discrepancies were observed between the results from the two sources, thus the information obtained from magnetic particle inspection was preferred.

During one test, TP31, Table 15, ultrasonic inspection was carried out immediately after each run, by a very experienced ultrasonic inspector, in order to investigate when and how the chevron cracks grew as the joint was built up. It was found that until the twelfth run (fourth layer) was deposited, no cracks were detected. After the thirteenth run, three small cracks were found in a zone at the level of the third or fourth layers. The next two runs produced two more cracks at the same depth. With the three subsequent runs small cracks were found in the fifth layer and the previous ones were found to have increased in size. This was typical of what happened until the end of the welding operation.

Essentially, the ultrasonic inspection during the intermediate stages of welding revealed that a certain number of runs was required before cracking could be detected; after that stage chevron cracks were found to occur and grow in the lower runs as the weld progressed. In some cases cracks were detected in the vicinity of a run shortly after cooling to room temperature and although their positions could not be exactly defined, careful examination suggested that they occurred in a lower layer relative to the last run deposited or, eventually, in the refined region between the two top layers. Final ultrasonic inspection showed the chevron cracks, in this test, to be mainly concentrated in a few preferential layers (or runs) in the middle to lower third of the joint.

The attempt to use acoustic emission, Figure 19 , during the welding of TP18, Table 14, to provide more precise information about the moment of initiation of chevron cracks, proved to be unsuccessful. The noise caused by the arc during welding made it impossible to detect any cracks being formed during this period, after welding the slag started to crack and detach from the weld bead, also producing noises for some time after extinguishing the arc. A further source of noise was the water circulating in the holes on each side of the joint. Thus, the information which could be obtained by this process started a few minutes after extinguishing the arc and was of limited interest. It was decided that the work required to improve the process would take too long and it was abandoned.

4. Hydrogen Levels in the Weld Metals

The results of diffusible hydrogen determinations for welds deposited with a representative number of manual metal arc electrodes, in the same conditions in which they were used, are shown in Table 19. The welds deposited with the electrodes E8018 C1 from batch 1, manufacturer B, produced relatively high hydrogen levels. This may have resulted from the fact that the analysis was carried out for the remaining electrodes from a box used during a test and they may have been exposed for some time to the workshop atmosphere. Unfortunately no more electrodes were available from this batch and the result could not be verified. The hydrogen analysis for the electrodes from manufacturer A, in the 'as received' condition, was carried out for electrodes from a sealed box.

The effect of the condition of the submerged arc welding fluxes on its moisture content and on the diffusible hydrogen in the weld metal is shown in Table 20. Although the moisture levels were relatively low there was a significant variation in the hydrogen levels which will be related with the cracking occurrence.

5. Influence of Continuous Water Cooling on the Weld Metal Cooling Rate During the Cracking Tests.

In order to establish precisely the influence of the continuous water cooling on the weld metal cooling rates, a comparative study was made for several welding/cooling conditions. The results of this work, are shown in Figures 38 and 39. Essentially it was observed that the water cooling did not produce very significant alterations in the cooling rate above the transformation temperatures, but in the low temperature range, in particular below 300°C, the cooling rate increased dramatically. For the manual metal arc welds carried out in accordance with the procedure described in Chapter IV, Section 4 , it was found that the water cooled run took about 32 seconds to reach 200°C and 1.5 minutes to 50°C when cooling from 1400°C, against 45 seconds and 15 minutes, respectively, for the non water cooled run.

6. Metallographic examination

6.1 Weld Metal Microstructures and Microhardnesses

In order to compare the characteristics which could have influenced the occurrence and morphology of the weld metal cracks, photographs of the microstructures observed in cross sections of the different weld metals studied herein are presented in Figures 40 to 73. With the exception of welds deposited with rutile and high nickel content basic electrodes, the main microstructural constituents of these weld metals were proeutectoid ferrite, acicular ferrite and ferrite side plates. The increase in the proportion of alloying elements produced, essentially, a decrease in the amount of proeutectoid ferrite and a refinement in the microstructure. The influence of the type of microstructure on the cracking occurrence, path and morphology will be discussed later.

Hardness measurements were carried out for all the different microstructures as a complement of the study above and to compensate for the lack of information on the strength of some weld metals. The results of the measurements are shown in the Tables 4 to 8, for weld metals in the as deposited condition (in the uppermost run), in the refined regions and in the non-refined middle runs.

6.2 Metallographic Study of the Transverse Cracks in the Weld Metals

Longitudinal sections, from all the specimens containing chevron cracks were observed in the light microscope with the objective of establishing a relation between the morphology of the cracks and the weld metal microstructure. A large number of these cracks was photographed; a selected group, intended to show the types and relevant features, is shown in Figures 74 to 92. As there were no major differences between the cracks observed in the industrial samples and those in the laboratory tests the results and comments below refer to both except where otherwise stated.

Chevron cracks were found to occur in both the as deposited and refined weld metal. However, in the tests, the cracks in the submerged arc welds tended to occur predominantly in the as deposited metal and to be contained in a single run, while those in the manual metal arc welds often occurred in the refined metal.

Chevron cracks always presented a characteristic staircase appearance with vertical and horizontal components. Although it is not possible to appreciate from a two dimensional representation the size of a three-dimensional defect, it is clear that there were variations in the size of individual components of the cracks; in particular in the refined regions the steps were found to be much smaller. The vertical components of the cracks in the as deposited weld metal tended to occur predominantly in the proeutectoid ferrite (at the prior austenite grain

boundaries), but often they propagated away from it, Figure 77c, or followed a different path, Figure 77d. The vertical components tended to be wider (more open) than the horizontal ones, Figure 79, but in many cases the cracks were very narrow all along their path, Figure 86, which reflects the differences in weld metal straining after cracking. In a weld run most of the chevron cracks tended to be inclined in the welding direction, however a few were found to be inclined at 90° to the main group, which could not always be associated with any apparent alteration in the microstructure, Figure 89.

Many examples were found of non-linked microcracks with a spacial arrangement very similar to the vertical components of the chevron cracks, Figure 91. In some cases there was an indication that these microcracks started to link but the process was not completed, Figure 92. These staggered microcracks were generally found alongside other fully developed chevron cracks.

The industrial samples showed a few examples of chevron cracks associated with voids (probably pores), Figure 75. This could suggest, at first sight, that the pores resulted from the deposition of a weld run on the top of the cracks, however similar voids could be found on the same runs which were not associated with any crack.

In the longitudinal horizontal plane, i.e. in an orientation parallel to the plane of the plates, chevron cracks were found to be almost transverse to the welding direction and had a typical morphology illustrated in Figure 84.

Vertical cracks, i.e. cracks oriented perpendicularly to the plane of the plates or just slightly inclined, were typical of the higher strength weld metals used in the laboratory tests. In some cases the cracks presented a staircase morphology reminiscent of the 45° cracks, Figure 93, but this was unusual. In general the cracks did not follow a typical path, they could be both inter and transgranular, continuous or intermittent and sometimes branched, Figures 94 and 95.

Microcracks or microfissures, Figures 96 and 97, could be easily found in all the weld metal cracking tests, with the exception of submerged arc welds with the flux baked for 1 hour at 450°C . The microfissures were randomly distributed throughout the longitudinal sections, but their density was reduced in the top run(s) and in the runs containing a high number of macrocracks. Microfissuring was the typical form of cracking in weld metals deposited with rutile electrodes, Figure 97; in some cases they were found to be nucleated at a void, Figure 97b. In general these weld metals did not develop longer cracks except for the most highly alloyed.

Some specimens were etched with saspanansa, but the crack paths did not show any significant relation with the solidification structure, Figures 81 and 82.

6.3 Morphology of Hydrogen Induced Cracks Observed in Y Groove Tekken Tests

A series of Y groove tests was carried out with the objective of producing hydrogen induced cracks in the weld metal which could be used in a comparative study. This work was part of another project already referred to in the literature survey (6); however, due to its relevance, an example of a cross section of a joint showing a longitudinal crack was examined further, Figure 98. This crack had a staircase appearance similar to the chevron cracks and occurred in a similar microstructure (see also Section 7.1.3).

7. Fractographic Examination

7.1 Scanning Electron Microscopy

7.1.1 Chevron cracks from industrial samples

Chevron cracks from two industrial samples, already referred to as A and B, were observed in the scanning electron microscope in order to establish the typical features of this type of cracking and to serve as a reference in further studies. At low magnifications, the staircase appearance of the cracks was easily recognized, Figure 99. Increasing the magnification it was readily apparent that there were two distinct sets of components which could be observed in planes approximately perpendicular to each other. The vertical components presented mainly quasi-cleavage, Figures 100 and 101, but some showed relatively smooth areas, Figure 102, the significance of which will be discussed later. The origin of each vertical component was not always clear, however very often they seemed to radiate from the central region. The horizontal components showed essentially dimples, Figure 99.

7.1.2 Chevron cracks produced under laboratory controlled conditions

Chevron cracks were observed in a wide range of medium strength weld metals deposited with different types of consumables, Tables 13 to 17. Variations in the fracture morphology were anticipated from the differences in microstructure, however, these differences did not affect the characteristic features, i.e. the staircase morphology with mainly quasi-cleavage in one set of components and dimples in the other, Figures 103 to 108, as already described for the industrial samples.

As for the industrial samples, many vertical components of the chevron cracks did not present a clear origin, while others showed a pattern radiating from the centre where a void (probably an inclusion hole) could be found sometimes, Figure 104. Some vertical components in the higher strength weld metals which still presented this form of cracking, such

as TP17 and TP21 (Table 14), showed manifestations of intergranular failure surrounded by areas of quasi cleavage, Figure 106. Areas with a relatively smooth appearance and almost featureless at high magnification in the scanning electron microscope could also be observed in some vertical components, Figures 108 and 109. In general, these areas were surrounded by well defined quasi-cleavage failure and in some cases there was a clear boundary between the two regions.

The horizontal components of the chevron cracks presented mainly dimples, which could vary in size and shape, Figure 103. In some cases quasi-cleavage facets were blended with the dimples, Figure 103c.

The typical features of the fracture surface corresponding to the propagation of a chevron crack, when it was broken-open after pre-cooling in liquid nitrogen, are illustrated in Figure 110; in this case the mode of failure was by cleavage.

In order to study possible alterations on the fracture surface of chevron cracks identified in a weld made by Crouch (7), at high heat input (9.4 kJ/mm), two cracks were broken open and examined by the writer. Although these cracks were much bigger than others previously observed in a test in which the same consumables were used with a relatively low heat input (2.4 kJ/mm), TP17 (Table 14), the characteristics of the individual components of the cracks were very similar in both cases.

The fracture surfaces of the vertical cracks observed in the higher strength weld metals, such as in TP24 and TP27 (Table 14) and TP46 and TP51 (Table 16), presented a morphology different from the one of the chevron cracks. At low magnifications they did not show a staircase appearance; increasing the magnification they were found to be formed by a succession of clearly defined inter and transgranular components, Figure 111. The mode of failure through the grains was mainly by quasi-cleavage. Regions of dimples could be found linking areas of brittle failure, this produced, in some cases, a morphology resembling the chevron cracks, Figure 112, but was not typical. In the case of TP27 (Table 14), phosphorus segregation was observed in one crack, Figure 113; however this seemed to be unusual.

The tests carried out with the nickel bearing electrodes B4Ni and B5Ni, TP60 and TP62 (Table 17), also presented vertical cracks, the typical features are illustrated in Figure 114.

Microfissures were observed in all the weld metal compositions; the ones found in the medium strength weld metals, Figure 115, presented a mode of failure similar to the vertical components of chevron cracks, but tended to be

bigger in size. In the case of welds deposited with rutile electrodes the fissures showed larger cleavage facets and a higher density of inclusions, Figure 116. Fissures occurring in the runs below the top one very often presented smooth regions, resembling those found on the vertical components of the chevron cracks.

7.1.3 Cracks produced through the Y groove Tekken test

The fractographic study of the longitudinal cracks which occurred in Y groove Tekken tests confirmed the existence of extensive regions with a staircase morphology, similar to the one described in the previous section for the chevron cracks. Close examination, at higher magnifications, showed a very good correlation with the features observed on the vertical and horizontal components of the chevron cracks in similar weld metals, Figures 117 and 118.

7.1.4 Fracture surfaces of hydrogen charged tensile specimens

In order to provide more background information about the characteristic features of hydrogen induced cracks in the weld metals being studied, a series of tests was carried out using tensile specimens charged with hydrogen. These specimens were machined from the weld metal of TP14 (Table 14).

The first series of tests was carried out with specimens machined with their axis at 45° with the welding direction; the conditions and results for each particular test are shown in Table 21. The fracture surfaces of the specimens 1 and 4 showed extensive areas of quasi-cleavage and some smooth regions probably corresponding to grain boundaries, Figure 119. The specimen 5 had been notched prior to being charged with hydrogen in order that the plane of failure could not have been determined by pre-existing defects; a complex fracture was produced in this case, with multiple origins, but at high magnifications the characteristic features of the areas of brittle failure were entirely similar to the ones found on specimens 1 and 4. The specimen 3, which was improperly charged, presented only a few fish-eyes surrounded by large areas of ductile failure, Figure 120. For comparison purposes the specimen 2 was tested without being charged with hydrogen; the fracture surface showed exclusively dimples in this case.

A second series of tests was carried out, intended to study the effect of the hydrogen level, produced by different charging times, on the degree of embrittlement and on the characteristics of the fracture surfaces; the relevant results are shown in Table 22 and Figures 121 and 122. The examination of the fracture surfaces revealed ductile failure by microvoid coalescence for the non-charged specimen, fish-eyes and microfissure like spots, for the moderately charged specimens, and large brittle failure areas showing

mainly quasi-cleavage for the long charging periods. The brittle fracture areas were always surrounded by dimples. In the specimens 7 and 9 some regions could be observed with a staircase morphology closely resembling the chevron cracks, Figure 122.

7.1.5 Reheated chevron cracks

Chevron cracks which were reheated on purpose by a weld metal run, according to the procedure described in Chapter IV, Section 5, were observed in the scanning electron microscope to study the modifications caused on the fracture surface by exposure to high temperatures; the results are illustrated in Figure 123. At low magnifications the morphology of the crack was not much changed but at high magnifications it could be immediately recognised that the sharp edges, corresponding to the quasi-cleavage facets, were smoothed and river pattern like marks had disappeared to produce a relatively smooth fracture surface.

7.2 Transmission Electron Microscopy

Carbon extraction replicas from the fracture surface of chevron cracks were observed in the transmission electron microscope after having examined the corresponding surfaces on the scanning electron microscope. This work was intended to investigate the existence of very small features, such as thermal facets and thermal grooving, associated with a free surface exposed to high temperatures, which in general cannot be resolved by the scanning microscope. These features could be easily observed on replicas from the reheated chevron cracks mentioned in the previous section, Figure 124, or on replicas from fracture surfaces containing similar smooth areas, Figure 125. In other cases, for which the scanning microscope revealed only quasi-cleavage failure in the vertical components of the chevron cracks, no thermal facets or thermal grooving could be identified on the carbon replicas in spite of extensive search. Essentially it was confirmed that areas of dimples alternated with areas of quasi-cleavage, Figure 126. In a few cases thermal facets and grooving were found in very small, circular shaped areas, which were identified as voids (micropores or inclusion holes).

8. Summary of Relevant Results

The cracks found during the experimental work were divided into three groups : chevron or 45° cracks; vertical cracks and fissures less than 1mm long (microcracks or microfissures).

Chevron cracks were easily reproduced on medium strength weld metals deposited by submerged arc or manual metal arc welding using a weld metal cracking test with increased cooling rates in the low temperature range. Baking the consumables at the maximum temperature recommended by the manufacturer eliminated chevron cracking in the submerged arc welds and reduced markedly their incidence in the manual metal arc welds in spite of the very severe testing conditions. The welds deposited with cellulosic electrodes proved to be exceptionally prone to chevron cracking, while the welds with lower strength rutile electrodes produced only microfissures.

In order to compare the laboratory experiments with situations closer to the industrial practice, the increasing cooling rates due to water cooling were measured and compared with the ones in welds without water cooling. It was found that the effect of water cooling is only significant below the transformation temperatures.

During one test of the series, ultrasonic inspection was carried out immediately after each run in order to determine the moment of initiation and propagation of chevron cracks. It was found that no cracks were detected until a certain number of runs was deposited; as the weld progressed cracks occurred and/or propagated in the lower runs. No cracks were positively identified in a run shortly after cooling to room temperature, but in some cases cracks were found immediately below the last run during the intermediate stages of welding and inspection.

Metallographic examination on longitudinal sections revealed that chevron cracks presented a typical staircase appearance, with vertical and horizontal components, which was maintained in spite of the variations in the microstructure or the crack occurring in the as deposited or refined weld metal. The vertical components, in the as deposited weld metal, occurred predominantly in the proeutectoid ferrite though some were found to deviate or follow a different path; the horizontal components often traversed the acicular ferrite. Saspanansa etching did not reveal any significant relation with the solidification microstructure.

The increase in the alloying content/strength of the weld metals produced first an increase in the number of chevron cracks and, above a certain level, a change in the orientation of the cracks from 45° to perpendicular to the welding direction (vertical cracks). The amount of proeutectoid ferrite, around the prior austenite grain boundaries, decreased markedly with the increase in the alloying content and was very much reduced, in some cases virtually non-existent, in the materials exhibiting vertical cracks. These cracks were found to be transgranular and intergranular with a crack path following well defined grain boundaries.

Fractographic examination confirmed the similarity between the chevron cracks found in the industrial samples and those reproduced under laboratory controlled conditions. Essentially each crack consisted of two distinct sets of components. The vertical components exhibited typically quasi-cleavage, in many cases without a clear origin, others presented a pattern radiating from the centre where a void (probably an inclusion hole) could be found sometimes. Some vertical components presented relatively smooth regions, almost featureless at high magnifications in the scanning electron microscope, generally surrounded by larger areas of quasi-cleavage. The horizontal components exhibited mainly dimples.

Microfissures were observed in all the weld metal cracking tests with the exception of the submerged arc welds carried out with baked flux. The fracture surfaces of the microfissures were found to be very similar to the vertical components of the chevron cracks in similar materials.

The vertical cracks which occurred in the high strength weld metals were inter and transgranular. The transgranular components presented a quasi-cleavage mode of failure. Regions of ductile failure, exhibiting dimples, were found linking brittle areas which could eventually create a morphology reminiscent of the chevron cracks, but this was not typical.

In order to provide a reference for the fractographic interpretation, hydrogen induced cracks were produced using the Y groove Tekken test. The fracture surfaces of these cracks showed extensive regions with a staircase morphology resembling very closely that of chevron cracks in similar weld metals. With the same purpose tests were carried out with hydrogen charged tensile specimens; the areas of brittle failure on the fracture surfaces of these specimens also presented features very similar to the vertical components of chevron cracks.

To study the effect of exposure to high temperatures, several chevron cracks were reheated on purpose. It was found that reheating did not produce significant changes on the fracture surfaces, when these were observed at low magnifications; increasing the magnification it was clear that sharp features were smoothed such as in the case of other vertical components mentioned above.

Transmission electron microscopy confirmed the findings of prior work in the scanning microscope. Cracks with vertical components presenting smooth areas, which were supposed to have been reheated, presented, in fact, thermal facets and thermal grooving; the others presented only a succession of areas of quasi cleavage and dimples without signs of having been exposed to high temperatures.

VI - DISCUSSION

VI - DISCUSSION

1. Introduction

When this research programme on chevron cracking was initiated, two different explanatory theories had just appeared. Insufficient evidence did not allow the controlling parameters of the phenomenon to be firmly established, which left the field open to controversy over the causes and mechanism. Keville's theory (5), which suggested that cracking resulted from a combination of hydrogen and stresses, seemed to be supported by industrial experience. However, the alternative presented by Tuliani (3), based on the existence of a high temperature component, could not simply be dismissed on the grounds that the features identified on the fracture surfaces, typical of exposure to high temperatures, were caused by reheating on the deposition of subsequent runs of weld metal (14).

Although the existing evidence pointed towards hydrogen as being the main factor controlling the occurrence of chevron cracking, there was a distinct possibility that some form of hot cracking could be involved. The problem was studied by using a wide range of chemical compositions and consumables and carrying out hot tensile tests on weld metals already studied for cracking susceptibility. The influence of hydrogen on the cracking incidence was studied by using the submerged arc basic flux and basic manual metal arc electrodes with different moisture contents, producing different hydrogen levels in the weld metal. In brief, it was intended to support the metallographic and fractographic interpretation with extensive experimental evidence.

The results of the cracking tests have been presented herein in a quantitative form, indicating the maximum number, size and orientation of cracks longer than about 1mm. It can be argued that these figures may be strongly dependent on the sectioning plane for each specimen; however, the significance of this problem was reduced by using ultrasonic inspection, which gave a prior indication of the number and size of cracks and by the capacity of the magnetic particle inspection to indicate the existence of cracks at some distance below the surface (172). In these circumstances it is believed that no significant number of cracks could have passed undetected in a specimen. The quantitative presentation of the results shows important trends, as for example the variation in incidence and type of cracking with the type and condition of the consumables, which would have passed unnoticed if a 'crack/no-crack' criterium had been adopted. A second problem concerns the reproducibility of the cracking test, because these types of test are likely to present a large scatter in the results. However, it is interesting to note that for the cases where duplicates were carried out the results were reasonably similar: submerged arc welds TP13/14/15 and TP 17/18 (Table 14) and manual metal arc welds TP29/30 and TP31/32 (Table 15).

Three types of weld metal transverse cracks were identified on longitudinal sections. According to their size and orientation relative to the plane of the plates they were designated '45° cracks' or 'chevron cracks', 'vertical cracks' and 'microcracks' or 'micro-fissures'. Although these three types of cracks might not be intrinsically different in nature, variations in the cracking mechanism

were expected as well as changes in the fracture mode due to the different microstructures and/or hydrogen levels for which they occur; in these circumstances the different designations were sustained for this research programme.

2. Experimental Procedure to Produce Chevron Cracks

The test ascribed to Tulliani (3) was initially adopted, but the number of cracks produced was low and their size small (Table 13), thus it was considered that the test would not be severe enough. Furthermore, it was felt that some water could remain entrapped after the quenching operation, or condense during the low temperature tests, making it possible for hydrogen to be artificially introduced in the joint in uncontrolled amounts.

To overcome the above problems a new, more severe test was designed, which was intended to discriminate different degrees of weld metal cracking susceptibility and to clearly define the principal parameters that cause chevron cracking. The use of continuous water cooling had the advantage of an easier control of the weld metal cooling rates and allowed the welding to proceed almost continuously without intermediate quenching operations. In spite of the larger number of runs required to fill the joint, as compared with the Tulliani test, the time required to complete the test was reduced. The major disadvantage was the time required for the preparation of the parent plates but, as the same plates are used throughout the series of tests, this problem was minimized.

The weld metal cooling rates were measured in order to relate the tests to naturally cooled welds. For the testing conditions selected, it was found that no significant alterations were produced on the cooling curves above the transformation temperatures; therefore no significant changes were expected in the microstructure. However, the cooling rate was very much increased in the low temperature range and this must certainly have had a major effect on the amount of retained hydrogen.

The principles used in these cracking tests were not entirely new. Both Flanigan (138) and Bland (139) used pre-cooling, water quenching and continuous water cooling to enhance the incidence of microfissuring. These authors attributed the increased incidence of microfissuring to increased amounts of retained hydrogen and residual stresses. It is also interesting to note that Ito and Bessyo (121) found that cracking occurred when the cooling time between 300 - 100°C (or between welding and 100°C) was less than a critical value dependent on the composition, restraint and hydrogen content.

3. Weld Metal Cracking Experiments

3.1 Submerged Arc Welds

The series of submerged arc welds were intended to study the variation in cracking susceptibility and morphology with the weld metal alloying/strength, keeping the hydrogen level constant through the careful control of the moisture level in the flux.

The basic agglomerated flux OP41TT was selected because it was known from industrial experience to have produced chevron cracking in the past and because it would allow a straightforward comparison with work by other authors. The probable variation of cracking morphology and characteristic features, associated with variations in microstructure, was expected to highlight some of the factors controlling the cracking mechanism. The variation in the incidence of cracking with hydrogen levels, resulting from the use of the flux in three conditions, was expected to give more precise information about the influence of this factor on the occurrence of cracks for each case.

The initial work using the Tuliani test, Table 13, produced a relatively low number of cracks, but a trend existed showing that their number increased with the moisture level in the flux. During the welding of TP4, the joint was quenched almost immediately after completing each run, which produced a noticeable increase in the number of cracks, in particular towards the ends of the joint, which were quenched from higher temperatures. The higher density of cracks is believed to be associated with the increase in retained hydrogen and residual stresses, because the phase transformations should be completed before quenching, as confirmed by metallography.

The tests using continuous water cooling produced a large variation in the number, size and type of cracks. It is readily apparent from the results shown in Table 14 that the first factor controlling the incidence of cracking is the condition of the flux, which is related to the weld metal hydrogen level (Table 20). All forms of cracking were eliminated by baking the flux at 450°C and keeping it hot. Conversely the number and size of cracks were very much increased in welds with the flux in a damp condition. Although the exact mechanism of cracking can still be disputed, it was established that the weld metal hydrogen level, dependent on the condition of the flux, was the primary cause of chevron cracking in welds deposited with OP41TT and the series of wires SD3, S4, SD3/1Ni, SD2/3Ni and SD3/1Mo. This is in accordance with the work by Wright and Davison (28), reviewed in Chapter II and with recent work by Chew (173), who found a correlation between the incidence of cracking and the weld metal hydrogen level in submerged arc welds.

The second factor controlling the occurrence of chevron cracking was the weld metal alloying content which determined its microstructure, strength and hardness. In welds with damp flux there was a trend for the number and size of chevron cracks to increase with the weld metal alloying/strength. In the tests carried out with the wires SD3, S4 and SD3/1Ni, the number of cracks was markedly lower and the cracks slightly smaller than in the welds with the wires SD2/3Ni and SD3/Mo. This is considered to be related to the increase in cracking susceptibility with the weld metal alloying/strength and will be discussed later, in section 4 of this chapter. No previous direct evidence

of the importance of weld metal composition had been reported although the preference of two workers (3) (28) for alloyed wires was an indication that this factor may be significant.

When the weld metal alloying/strength was increased above a certain level, the cracks were oriented vertically to the welding direction. This happened for the welds deposited with SD3/1Ni $\frac{1}{2}$ Mo and SD2/1Cr 1Ni $\frac{1}{2}$ Mo wires. The variation in the orientation of the cracks and in cracking severity with the alloying content will also be discussed later in terms of the alterations in microstructure.

3.2 Manual Metal Arc Welds

Manual metal arc welds were also reported to be prone to chevron cracking (3) (4) but very little investigational work had been carried out (8) (18). Therefore it was decided to include the study of manual metal arc welds in the present research programme using, initially, commercially available E8018 Cl electrodes. After verifying that chevron cracks could be produced with these electrodes when used in the 'as received' condition, a more extensive programme was devised to include a series of specially manufactured experimental electrodes with basic, cellulosic and rutile coatings. This series of tests was intended to produce further evidence on the influence of weld metal composition, microstructure, hydrogen level and inclusion content on the occurrence of chevron cracking. In order to make comparisons easier these electrodes were designed to produce weld metal deposits matching the chemical compositions of the submerged arc welds, Table 5. This objective proved to be very difficult to achieve and many of the proposed compositions were far from being reached, Table 7. However, the special batches of electrodes did produce some useful information in terms of cracking susceptibility.

The manual metal arc welds presented the same trends as those deposited by submerged arc welding : the incidence of cracking was controlled by the hydrogen level (depending on the condition of the consumables) and the cracking orientation was controlled by the alloying/strength. However, some differences were observed; for example, it is apparent from Table 15 that there is no simple relation between the number of chevron cracks and the hydrogen level in the weld metals which were prone to this form of cracking. Although it had been well established that high temperature baking of the electrodes reduced or even eliminated the occurrence of both chevron cracks and microfissures, the results from TP28 to TP38 (Table 15) show that there is no steady increase in the number of chevron cracks with the weld metal hydrogen level. Rather, the number of cracks reached a maximum for a medium to low weld metal hydrogen level, i.e. 5 - 15 ml H₂/100g of deposited weld metal, but above this level microfissuring became the preferred form of cracking, eventually associated with porosity for the very high hydrogen contents.

The results indicate that cracks did not occur until a

critical hydrogen level was reached, which is consistent with previous work on hydrogen induced cold cracking (133). Above this level cracks started to occur and either microfissures or small chevron cracks were detected; their number depended on the hydrogen available at the possible nucleation sites. However, if the hydrogen level was too high, fissuring was the preferred form of cracking, because microcracks may nucleate very easily and the chevron cracking mechanism did not develop, see later. For the highest levels of hydrogen, porosity could also be observed; this may be explained through the formation of bubbles due to the diminution of hydrogen solubility at the solidification point (174). The variation in the type and incidence of weld defects with the hydrogen level is illustrated in Figure 127.

The series of welds with commercially available E8018C1 electrodes confirmed hydrogen as being the factor controlling the occurrence of chevron cracking, but the susceptibility seemed to depend on other factors which were not entirely clear from the experimental work. In fact, the batches of electrodes 1 and 2 from manufacturer B, Tables 6 and 15, were offered for testing with the indication, based on cracking history in industrial experience, that the batch 1 would probably be crack prone while batch 2 would not. Although the batches were produced by different plants of the same manufacturer, they produced weld deposits with similar chemical compositions, Table 6, and microstructures, Figures 51 and 52, but the results confirmed that batch 1 showed much higher cracking susceptibility. The difference in number and size of the cracks observed in TP35 and TP37 were beyond what could be expected from the scatter of results in the cracking test. Admitting, on the basis of the evidence already presented, that both chevron cracking and microfissuring in these weld metals were hydrogen induced, it is possible that other factors could have influenced the cracking incidence. For example, the rate of supply of hydrogen to crack nucleation sites and crack tips, which depends on the diffusion coefficient and on the transport of hydrogen by dislocation, may have been changed. In particular, the diffusion coefficient may have been modified by hydrogen trapping mechanisms associated with the inclusion population producing different cracking susceptibilities. This possibility, already referred to by Fikkers and Muller (114) and by Pressouyre and Bernstein (113), deserves further attention in future work.

The case of the weld TP43 deposited with the electrodes B3, (Table 16), was also surprising because of the low number of chevron cracks. The reason for this is not apparent: weld metal alloying, hardness, microstructure and hydrogen level were within the range for chevron cracking. Comparing the results with those for the welds with the electrodes B1 and B2, which produced a larger number of chevron cracks, it was noted that the weld metal deposited with the electrodes B3 presented some improved characteristics, such as lower carbon content and a larger proportion of acicular ferrite, Figure 55. However, it is unlikely that this improvement has rendered the material more crack resistant than welds deposited with the electrodes E8018 C1. This was

another case for which, after verifying the reproducibility of the test, further investigation would be required to find out other factors likely to be responsible for the chevron cracking susceptibility, as referred to above.

In line with the submerged arc welding results, where the alloying content of the welds deposited with basic electrodes was increased above a certain level, the cracks were vertically oriented. The reasons for the change in orientation of the cracks and possible variation in the cracking morphology will be discussed later. Although baking the electrodes B5 for 1 hour at 400°C did not eliminate the vertical cracks in TP45, this procedure produced a marked decrease in the number of cracks which indicates the critical importance of hydrogen in this case.

The results for both the manual metal arc and submerged arc welds showed that weld metal transverse cracking could occur with low weld metal hydrogen levels (within the range 5 - 10 ml/100g of deposited weld metal) for severe conditions of restraint and cooling rate. This emphasizes the critical importance of controlling the moisture content in consumables of the basic type. As recently shown by Boniszewski (175), the temperatures of electrodes being baked in an oven may be considerably lower than the atmosphere inside the oven, especially for those electrodes in the centre of a large pack. This fact, allied to the capacity of some electrodes to reabsorb significant amounts of moisture when stored at temperatures below 100 - 150°C (92), may be a cause of considerable errors in predicting the moisture levels of the consumables and might have accounted for the occurrence of cracking in cases in which 'stringent anti-hydrogen measures' were apparently taken.

The series of welds with cellulosic electrodes produced extremely severe chevron cracking which was not surprising on the consideration of the very high weld metal hydrogen levels (Table 19). However, as opposed to the welds with basic electrodes containing very high hydrogen levels, they did not produce porosity and fissuring as preferential form of cracking. Apparently the cellulosic welds allow a higher hydrogen level than basic welds. The reason for this is not clear but a probable explanation is that hydrogen trapping mechanisms have operated in cellulosic welds, reducing the amount of hydrogen available to cause cracking and porosity. In these circumstances, fissuring as a preferential form of cracking would only occur if the hydrogen level was exceedingly high such as in the case of TP49 with the electrodes C3. No attempt was made to reduce the hydrogen level of the welds deposited with cellulosic electrodes because these were inherently high hydrogen consumables.

The welds with the series of rutile electrodes failed to produce chemical compositions comparable with the ones for the previous tests and, in spite of their smooth running characteristics, commonly produced slag inclusions. In the cracking tests all the welds deposited with the special batches of rutile electrodes presented a very high density of fissures less than 1mm long, porosity and slag inclusions; only the ones deposited with

the electrodes R4 and R5 produced longer cracks. Due to the high weld metal hydrogen level it is possible that microcracks might have nucleated very easily and precluded the occurrence of chevron cracking as already discussed. The only correlation with results from other tests was a trend to increase the incidence of cracking with the alloying/hardness. The fact that no chevron cracks were observed in this series of tests does not mean that this type of cracking cannot be reproduced with rutile electrodes; it is believed that, if the appropriate conditions were provided, in particular if the hydrogen level was lower, chevron cracks would have occurred. This suggestion is strongly supported by the observation of a weld metal longitudinal crack, with a stair-case morphology reminiscent of a chevron crack, produced in a Y groove test using a rutile electrode R2 (6).

Nickel has been regarded as a hot cracking promoter; Stout and Doty (174) stated that for a given sulphur content in weld metal, nickel in amounts as low as 0.5% may increase the amount of grain boundary sulphide and consequent cracking. Edwards et al (176) showed that nickel segregation to the austenite grain boundaries may cause embrittlement and low ductility in low alloy steels as well as tin, phosphorous and nitrogen. For the cases studied by these authors, hydrogen was found to alter the strain to fracture but not the mode of fracture. Farrar and Taylor (14), inferred that due to the nickel segregation in these steels there is a distinct possibility that nickel rich inter-metallic compounds can be produced in the boundary regions thus enhancing cracking.

Considering the possibility that nickel could promote the occurrence of a high temperature component in the chevron cracks, a series of tests was carried out with nickel bearing electrodes with nominal compositions varying between 0 and 5% nickel (see Table 8). The welds deposited with the electrodes B2Ni and B3Ni presented a significant number of chevron cracks (see Table 17) as expected from other tests with similar weld metals. The non-existence of chevron cracks in the weld deposited with the electrodes B0Ni (TP57), probably resulted from the very low amount of alloying elements, which produced a very low carbon equivalent and therefore a low cracking susceptibility. The welds deposited with the electrodes B4Ni and B5Ni, which contained 4.8 and 5.7% nickel, respectively, produced only vertically oriented cracks which were not eliminated by anti-hydrogen measures, such as baking the electrodes at 400°C and a 120°C interpass temperature, Table 17. It is interesting to note that baking the electrodes markedly reduced the number of cracks, but their length, in the weld with the electrodes B5Ni, was increased, Table 17 and Figure 37. In this case the weld metal hardness was very high (see Table 7) and these materials were likely to be highly susceptible to hydrogen cracking. The fact that cracking could not be entirely eliminated does not necessarily mean that most cracks were not hydrogen induced; it is possible that the critical hydrogen level is extremely low in this case and that the above anti-hydrogen measures were insufficient. However, due to the high nickel con-

tent , hot cracking and segregation of impurities to the grain boundaries were likely to occur and these may have enhanced the nucleation and propagation of hydrogen induced cracks. The reduction in the number of cracks for the lower hydrogen levels, TP63, as compared with TP62 (Table 17), may be associated with the ease with which cracks were nucleated. For lower hydrogen levels the cracks are more difficult to nucleate but as there are fewer present they grow longer to release the strain.

Thus, it was concluded from the welds with nickel bearing electrodes that nickel, in amounts up to 3.2%, did not produce any dramatic changes in the occurrence of chevron cracking and its influence may be interpreted in terms of the general effect of alloying elements. Nickel in relatively high levels, 4.8 and 5.7%, probably enhanced the occurrence of hot cracks which propagated at low temperature due to hydrogen, but there was no correlation with chevron cracking.

3.3 MIG Weld

It was intended to extend this research programme to MIG welding in an attempt to produce chevron cracking simply by changing the moisture or hydrogen content in the shielding gas and eliminating other factors which could be eventually associated with electrode coatings. However, the test proved to be too sensitive to the welding conditions and some runs contained large amounts of porosity. As these problems could not be overcome within the time available during the later stages of the programme, this series of tests was abandoned.

4. Cracking Morphology : Metallographic and Fractographic Studies

When observed in the light microscope, the main characteristic of the chevron cracks was the staircase appearance, Figures 74 to 90. This resulted from the intersection of two sets of components which were designated as 'vertical' and 'horizontal' due to their orientation approximately perpendicular and parallel to the welding direction. This characteristic was observed irrespective of the weld metal microstructure.

In the submerged arc welds the chevron cracks were found to occur predominantly in the as deposited weld metal and tended to be contained in a single run, apparently being arrested by the upper and lower refined regions. This was in contrast to the manual metal arc welds for which a large number of chevron cracks occurred in the refined or intercritical regions, Figures 89 and 90. The reason for this was not entirely clear, but a possible explanation is that the different welding sequences adopted for each process, Figures 17 and 18, produced a larger amount of refined weld metal in the manual metal arc welds and enhanced the occurrence of cracks in the refined and intercritical regions. The argument that these cracks might have occurred in the initial as deposited weld metal, before it was reheated and refined by the subsequent run, was rejected because the fracture surfaces did not show, in the majority of cases, signs of having been reheated. The individual components of the cracks which occurred in the refined regions, Figure 90, were, in general, smaller and more regular than

those observed in the as deposited weld metal, Figures 74 to 88; this relation with the microstructure also indicates that they occurred after the weld metal was refined.

The chevron cracks observed in the as deposited weld metal had the vertical components generally associated with the proeutectoid ferrite veins, though in many cases these vertical components were found either to deviate or to follow a different path, Figure 77. The proeutectoid ferrite is not inherently brittle but in these weld metals it is often present as thin veins surrounding areas of harder transformation products, such as acicular ferrite, which form at lower temperatures. In these circumstances, the proeutectoid ferrite becomes the weakest microstructural link, which explains why it is a preferential site for nucleation and propagation of hydrogen induced cracks or, in particular, vertical components of chevron cracks. This fact has been confirmed by work on the effect of the weld microstructure on hydrogen induced cracking (122) (125). The increase in cracking susceptibility with the alloying and strength of the weld metals, which was particularly evident in the submerged arc welding series might be interpreted in the context of the explanation given above. Increasing the hardness of the transformed acicular microstructure increased the strain transferred to the prior austenite grain boundaries, where nucleation generally occurred, and this caused a higher cracking susceptibility (122).

Saspa-nansa etching was used in some cases in order to correlate the path of the chevron cracks with the solidification structure, Figures 81 and 82. This would have suggested induction by a hot cracking mechanism, but no significant correlation was found. This possibility will be discussed later in terms of the fractographic study.

The existence of staggered, non-linked, vertical components, Figure 91, and others at an intermediate stage of linking, Figure 92, alongside with fully developed chevron cracks, strongly suggested that the formation of the vertical components was the first stage in the occurrence of a chevron crack. The non-existence of isolated horizontal microcracks suggested that the horizontal components were determined by the vertical ones during the linking stage. Under these conditions, the path of the horizontal components, was dependent on the position of the crack tips of adjacent vertical components.

The path and dimensions of the randomly distributed microfissures were found to be similar to the vertical components of the chevron cracks when examined in the light microscope, Figure 96. This suggests that they were probably of the same nature in spite of the difference in distribution.

When the alloying content of the weld metals was increased, the macroscopic orientation of the cracks changed from inclined at 45° to vertical and a greater tendency for the cracks to propagate along the prior austenite grain boundaries was observed, Figures 93, 94 and 95. The embrittlement of the grain boundaries was considered to be a direct consequence of the changes caused by the increase in the alloying content. In fact, for the most highly alloyed weld metals

(with higher strength), the amount of proeutectoid ferrite was very much reduced, or even suppressed, and the matrix was hardened. This resulted in the transference of higher strains to the prior austenite grain boundaries and in the relative weakening of these regions (114) (122). The adverse balance of strength between the matrix and the grain boundary could create, per se, the conditions for intergranular failure without the need for impurity segregation at the grain boundaries. However, if impurities were present in the steel, the amount of boundary segregation could increase with the alloying/strength, enhancing even further the possibility of intergranular failure (177) (178). Although some resemblance could be found with the staircase morphology of the chevron cracks in a few cases, Figure 93, in general the vertical cracks presented an irregular path, not following a pattern; there was no indication that they resulted mainly from a two stage mechanism. The reasons for the change in the morphology and orientation of the cracks with the increase in the alloying/strength of the weld metals will be discussed later in terms of a variation in the chevron cracking mechanism.

The fractographic study in the scanning electron microscope proved that the morphology and features observed on the fracture surfaces of the chevron cracks in the industrial samples were entirely similar to those observed in the laboratory tests. Therefore, the subsequent observations and discussion apply equally to both.

At low magnifications the staircase characteristic of chevron cracks, already identified in the light microscope, was immediately recognised, Figure 99. Increasing the magnification it became apparent that the vertical components presented mainly quasi-cleavage while the inter-linking horizontal components showed dimples. Many vertical components of the chevron cracks were found to radiate from a centre where a microvoid could be seen occasionally, Figure 104, while others presented no obvious origin, Figure 107. Other variations denoted changes in microstructure and not a change in the mode of failure. In the case of the most highly alloyed weld metals for which chevron cracking could still be observed, some vertical components were found to exhibit manifestations of intergranular failure, Figure 106. This was probably a consequence of the relative weakening of the grain boundaries with the increase in alloying referred to above. The shape of the dimples in the horizontal components was also found to vary from almost equiaxed to elongated, in some cases mixed with a quasi-cleavage mode of failure, Figure 103, indicating, in this case, that the failure was probably assisted by hydrogen.

Although the above description does not provide, by itself, any element which permits immediate identification of the nature of the cracks, it is coherent with the experimental evidence which suggested that the cracks were hydrogen induced. In fact, the observation of the vertical components, which were found to govern the formation of chevron cracks, showed that most of their area could not have been exposed to high temperatures, otherwise the edges of the sharply defined quasi-cleavage facets would have become rounded. However, the fractographic interpretation was complicated by the presence of some vertical components with areas of smooth appearance, almost featureless at high magnifications, Figures 108 and 109, in a few cases with striations.

The interpretation of these areas is potentially controversial; although the evidence indicated that most of them were exposed to high temperatures, it was not clear if they resulted from a hot cracking mechanism, or if they were simply reheated by a subsequent run. These possibilities will be explored later and discussed in the light of further evidence.

The vertical cracks in the most highly alloyed weld metals had both intergranular and transgranular (quasi-cleavage) components. In this case the cracks did not follow a staircase pattern; adjacent cracks could be linked by ductile failure, reminiscent of chevron cracking, Figure 112, but this was not a necessary part of the growth process as for the chevron cracks. Generally the vertical cracks seemed to have grown continuously through the material, though the process may have been intermittent in time. Their morphology was also consistent with other experimental evidence which suggested that they were hydrogen induced. Although there was a similarity between some features observed on the fracture surfaces of the 45° cracks and on vertical cracks, it is clear that the microstructure produced a major alteration in the cracking mechanism.

Evidence of phosphorous segregation was found in one crack observed in a high strength weld metal, Figure 113, which probably enhanced the occurrence of this particular crack, but it was not a common feature. Phosphorous segregation is interpreted here as a result of an increased tendency for segregation of impurities with the increase in alloying and strength (177) (178).

The fracture surfaces corresponding to the microfissures observed in the tests were found to be very similar to the vertical components of the chevron cracks in the same weld metals; the only difference related to the dimensions as the microfissures may be slightly bigger. Although the tests with rutile electrodes did not produce chevron cracks, the fracture mode of the microfissures was also of a similar nature to the vertical components of other chevron cracks, being quasi cleavage or cleavage; the main difference was that the cleavage planes were much better defined.

The fracture surface of microfissures occurring in the lower runs of weld metals containing high hydrogen levels presented, quite often, a smooth surface, similar to that of some vertical components of chevron cracks, which was probably caused by high temperature exposure. As this type of fracture surface was observed on microfissures occurring in the lower runs but not in those found in the uppermost run, points to the cause of thermal damage by reheating from subsequent runs, rather than exposure to high temperatures as a result of a hot cracking mechanism. The probable explanation is that for high hydrogen levels microfissures are easily nucleated shortly after a weld run is deposited and these are inevitably reheated by the next runs. Considering the close similarity between the fracture surfaces of microfissures and the vertical components of chevron cracks, this evidence is an important indication that the smooth areas in some vertical components of chevron cracks also resulted from reheating by subsequent runs.

In order to resolve the fine details which could exist on some

of the smooth areas of the vertical components of the chevron cracks, carbon extraction replicas were prepared from a representative number of fracture surfaces for examination in the transmission electron microscope. However, this work only confirmed the scanning microscope observations : chevron cracks which showed vertical components with smooth surfaces had thermal facets and thermal grooving typical of high temperature exposure, Figures 124 and 125; the others presented mainly quasi-cleavage and dimples, without any signs of high temperature damage, Figure 126. In a few cases, thermal facets and grooving were observed in small circular shaped regions, which were identified as micropores or inclusion holes and these should not be confused as hot microcrack initiators of the vertical components. This study confirmed that a large number of vertical components of chevron cracks did not present signs typical of high temperature exposure, therefore it is unlikely that they might have resulted from a hot cracking mechanism.

Although the fundamental importance of hydrogen in controlling the occurrence of chevron cracks, vertical cracks and microfissures in carbon-manganese and low alloy steel weld metals has been established on the basis of the results already discussed, some questions remain unanswered:

- (i) when do chevron cracks occur?
- (ii) how does the fracture surface of chevron cracks compare with the ones of hydrogen induced (or assisted) cracks in similar weld metals?
- (iii) what is the effect of reheating on the fracture surface of a chevron crack?
- (iv) what is the effect of the welding parameters (in particular those which control the heat input) on the occurrence of chevron cracking?

To answer the above questions further testing was carried out, the results have already been reported and will be discussed subsequently.

5. Subsidiary Work

One of the most important issues concerning the occurrence of chevron cracking is the moment of initiation and propagation, i.e. when do the cracks occur? The ideal way to solve this problem would be to use continuous monitoring by an acoustic emission technique (179) (180), which has the capability to indicate the exact moment of initiation and/or propagation of a crack and to locate it. However, this task proved to be impossible due to parasite noises accompanying welding.

To overcome the problems inherent to the acoustic emission monitoring, a conventional ultrasonic inspection was carried out after each run during one test of the series with manual metal arc electrodes, TP31 (Table 15). Although this inspection could

not establish the exact moment of initiation and propagation of the crack, it could at least indicate at what stage they occurred. The results indicated that no cracks were detectable until a certain number of runs was deposited and that no cracks could be identified on a weld run shortly after it cooled to room temperature, during the intermediate stages of welding and inspection. Cracks were found to occur and/or propagate in the lower runs as the weld progressed. This evidence also suggests that cracks must occur at low temperatures and be associated with a delayed cracking mechanism. Apparently a certain number of runs was required to build up the stresses and probably the hydrogen concentration to a critical level (143). It is possible that in some cases vertical components occurred immediately after a run was deposited and the subsequent runs just provided the extra residual stresses required to extend and join them. However, there is evidence showing that the short vertical cracks, corresponding to the vertical components, produce ultrasonic signals similar to the ones for fine porosity (9) and should be detectable. Thus, on the basis of careful inspection, it is unlikely that this occurred in most cases. These facts have great implications with regard to the consideration for repairs. The repair of a joint containing a layer susceptible to chevron cracking can be particularly troublesome, because cracks can occur, or propagate, in regions below the repair, which previously were considered as sound; this has been supported by industrial experience (4) (30).

In order to find out how the vertical components of the chevron cracks compare with the hydrogen induced (or assisted) cracks in similar weld metals, tests were carried out with hydrogen charged tensile specimens. The ones of the initial series (Table 21), had their axis at 45° with the welding direction, in order that the load could be applied perpendicularly to the orientation in which chevron cracks were likely to occur. However, it was apparent that the plane of failure was not simply determined by the direction of maximum tensile stress; instead other factors seemed to be more important, such as the directions of maximum shear stress and grain growth. Thus, in the second series (Table 22), the specimens were machined with their axis parallel to the welding direction. The hydrogen charging period had a dramatic influence on ductility, as measured by the elongation or reduction of area of the tensile specimens (Figure 121 and Table 22). This could be immediately related with the observation of the fracture surfaces: the non-charged specimens exhibited exclusively dimples while the charged specimens exhibited regions of dimples surrounding others of brittle failure, the area of which increased with the charging period. Detailed examination of the regions of brittle failure showed a close similarity with the vertical components of chevron cracks. Compare Figures 99 - 107 with Figures 119 - 122. The fact that the brittle failure regions were only observed in the hydrogen charged specimens is indicative that they were hydrogen assisted. The similarity between these and the vertical components of the chevron cracks, though not conclusive, substantiates the suggestion that they must be also hydrogen assisted.

Fish-eyes were found on the fracture surfaces of tensile specimens charged for relatively short periods, specimens 3 and 7 (Tables 21 and 22). Their morphology resembled the fissures found in the cracking tests but they revealed a more clear radiating pattern pointing towards the centre where a void (pore or inclusion hole) could generally be found, Figure 120. In the tests being considered fish-eyes seem to be associated with relatively low hydrogen levels. In these cases embrittlement only occurs if it is possible to concentrate hydrogen above a critical level for the existing stress state; pores, inclusion holes or other flaws may serve this purpose by acting as stress raisers to which hydrogen may diffuse (133), or be transported by dislocations (161). When the hydrogen level was increased, by extending the charging period, nucleation and propagation of cracks became easier and fish-eyes did not occur.

The comparison between the fracture surfaces of chevron and hydrogen induced cracks included also some cracks produced by the Y groove Tekken test in single runs of weld metals, deposited with manual metal arc welding electrodes which were known to be prone to chevron cracking (6). The longitudinal cracks found in these tests often had a 'staircase' morphology with two sets of components intersecting at an angle, resembling the vertical and horizontal components of the chevron cracks, Figures 117 and 118. As the cracks in the Y groove tests could be eliminated by baking the electrodes of the basic type at high temperature, it was concluded that most probably they were hydrogen induced. Considering the similarity with the chevron cracks this evidence substantiates even further the theory that chevron cracks occur by a hydrogen assisted mechanism.

The above finding is particularly important in showing that the staircase pattern is a more general morphology of hydrogen cracking than was realised; it was observed in all the Y groove tests which showed weld metal cracking. The extent of the 'staircase' morphology depended, apparently, on geometric factors which determined their path, such as grain growth and the convexity of the bead; in general, cracks running laterally presented larger areas of staircase than those following the centreline of the weld.

In order to study the possibility that the smooth areas observed on some vertical components of chevron cracks were caused by reheating, a row of chevron cracks was reheated on purpose by depositing a weld run just above the level where they were identified. The alterations on the fracture surface are illustrated in Figure 123. At low magnifications no important changes were observed, but increasing the magnification it became apparent that the sharp features had become smooth in a way similar to some other chevron cracks not reheated on purpose, Figures 102, 108 and 109. This observation substantiates that, in conditions for which microcracks are easily nucleated, they may occur shortly after a weld run is deposited and be reheated by subsequent runs; later they may grow and/or join others to produce chevron cracks. This resulted in the rather confusing effect

created by the existence of sharp and smooth areas, even in the same vertical component, although the boundary was often clear. It is suggested that this effect accounts for most of the 'hot crack' vertical components reported by Tuliani (3).

The effect of the welding parameters on the occurrence of chevron cracking was studied briefly by Crouch (7), who found that, under the testing conditions, the cracking severity increased with the heat input. However, for very low heat inputs fissuring became the preferential form of cracking. In order to study possible alterations on the fracture mode, test specimens produced under extreme heat input conditions (1.2kg/mm and 9.4kg/mm) were examined by the writer. It was found that the fracture surfaces were entirely similar to other fissures and chevron cracks observed in similar material, with no apparent alteration in the nature of the cracks. The variation in the cracking severity was thought to result, simply, from the changes in microstructure and in the weld metal hydrogen content which depended on the cooling rate, bead dimensions and flux consumption. The transition to fissuring as the preferred form of cracking, for the very low heat input welds, was likely to be associated with a higher retention of hydrogen due to very high cooling rates; in this case microcracks might have nucleated very easily, precluding the occurrence of chevron cracks.

6. Summary

The evidence discussed herein showed conclusively that hydrogen was the most important factor controlling the occurrence of chevron cracking and that the phenomenon must be due to a hydrogen induced cold cracking mechanism. Hot microcracks might serve as crack initiators, as might other flaws, but they were not a necessary factor. This conclusion was based on the following observations :

- (i) Chevron cracking was eliminated simply by careful baking of the submerged arc welding flux and conversely cracking was very much increased by increasing the moisture content of the flux. Baking the manual metal arc electrodes at 400°C was not always enough to reduce the hydrogen below the critical level corresponding to the severest testing conditions; however, a marked reduction in the incidence of cracking occurred and it is clear that the trends observed for the submerged arc welds were followed.
- (ii) By fractographic examination it was possible to establish a very good correlation amongst the features observed on the vertical components of the chevron cracks, microfissures and the areas of brittle failure on the fracture surface of hydrogen charged tensile specimens, in similar weld metals.
- (iii) The longitudinal cracks observed in the Y groove tests, which were hydrogen induced, reproduced very closely the staircase morphology of the chevron cracks.
- (iv) Most vertical components of the chevron cracks observed in the scanning and transmission electron microscopes did not show any signs of having been exposed to high temperatures. Others,

containing relatively smooth areas, were believed, in most cases, to have been reheated by subsequent runs.

- (v) Hot tensile tests, carried out in the range 600 - 1320°C, for weld metals known to be prone to chevron cracking, did not show any 'ductility dip' (6).
- (vi) Tensile specimens from weld metal deposited by submerged arc welding with a fully baked flux presented a ductile failure showing exclusively dimples on the fracture surfaces. If the problem was due to hot cracking, it would be expected that some manifestation could be observed independently from the weld metal hydrogen level. This fact is in accordance with similar findings by Keville (5) and by Wright and Davis-on (28).

The increase in weld metal alloying/strength produced first an increase in the severity of chevron cracking and, above a certain level, a change in the orientation of the weld metal transverse cracks from 45° to perpendicular to the welding direction; this was accompanied by an increase in the amount of intergranular cracking. As the cracking occurrence was always determined by the hydrogen level in the weld metal, it was thought that the variation in microstructure, due to the increase in alloying, only caused an alteration in the cracking mechanism and was not associated with a change in the nature of the cracks.

The occurrence and severity of chevron cracking for a certain weld metal composition was found to depend on factors other than the hydrogen level; one of these was believed to be the rate of supply of hydrogen to crack nucleation sites and crack tips which is dependent on the diffusion coefficient and on the transport of hydrogen by dislocations. It is possible that trapping mechanisms were operating in some cases to modify the hydrogen diffusivity and consequently the effectiveness of this element as an embrittlement factor. This may have resulted, for example, from different inclusion/microvoid contents and accounted for the relatively high immunity to chevron cracking of weld metals deposited with some basic electrodes.

7. A Mechanism for Chevron Cracking

Chevron cracks occur in carbon-manganese and low alloy steels by a two stage mechanism. The critical event is the occurrence of the vertical components, i.e. microcracks perpendicular to the welding direction, due to hydrogen embrittlement. The second stage consists in the linking of the vertical components due to the excessive stress between adjacent crack tips, which may be assisted by hydrogen. A two stage mechanism was initially suggested by the different cracking modes and orientation of the vertical and horizontal components when observed in the scanning electron microscope, Figures 99 to 109; further support came from the existence of non-linked staggered vertical microcracks and intermediate stages of linking alongside with fully developed chevron cracks as illustrated in Figures 91 and 92. A possible explanation for the unusual mechanism may be found in the analysis of the residual stresses in the weld and in the hydrogen embrittlement or hydrogen assisted cracking theories.

The occurrence of chevron cracks in a particular weld metal is determined by the hydrogen level, therefore it is first necessary to introduce hydrogen above some critical concentration, which may vary from one material to another, depending on factors such as the chemical composition, microstructure, diffusion coefficient of hydrogen and the stress level. However, as hydrogen tends to segregate at grain and cell boundaries and to form Cottrell atmospheres at dislocations, the critical level may be exceeded locally with extremely low overall concentrations (161).

In the conditions of occurrence of chevron cracking it is reasonable to assume that the transverse and through thickness residual stresses in the weld metal are small compared with the longitudinal stresses, which may be of yield strength magnitude (126) (161). Thus it was expected that cracking would occur predominantly transverse to the welding direction, i.e. perpendicular to the maximum tensile stress, and, in fact, this was confirmed by the preferred orientation of microcracks and vertical cracks in the higher strength weld metals. Chevron cracks, occurring macroscopically at 45° with the welding direction, seem to be an exception, but they follow the rule if one considers the two stage mechanism described above. However, the occurrence of the staggered vertical components along an orientation at approximately 45° with the welding direction has yet to be explained.

Assuming that the weld metal is essentially submitted to an uniaxial load of yield strength magnitude, parallel to the welding direction, the maximum shear stress occurs in a plane at 45° with this direction (5). Thus, the slip bands will have this orientation. Dislocations moving in the slip bands and transporting hydrogen as Cottrell atmospheres may concentrate hydrogen on potential crack nucleation sites, such as preexisting microcracks, inclusions or grain boundaries, at a rate much faster than would be possible by diffusion alone (161). When hydrogen transported by dislocations and by diffusion reaches the critical level for the existing stress state, vertical microcracks propagate from the nucleation sites. This effect may be further enhanced if, as claimed by Beachem (136), hydrogen allows the dislocations to multiply and move at reduced stresses.

Dislocations may also pile up at some barrier, such as a grain boundary which intersects the active slip plane, and form microcracks (122) (161). These may propagate due to the presence of hydrogen as referred to above. Alternatively, if the hydrogen concentration in the vicinity of a stress raiser is above the critical level corresponding to the stress state, a crack may occur without the need for plastic deformation (161).

Based on the experimental results already reported and the above arguments, the following model for the formation of chevron cracks is advanced.

- (1) Hydrogen has to be introduced in the weld metal above some critical concentration depending on the microstructure, the stress level and the diffusion coefficient of hydrogen.
- (2) Due to the longitudinal residual stresses in the weld metal, which are of yield strength magnitude, slip bands occur at approximately 45° with the welding direction. The presence of hydrogen may allow dislocations to multiply and move at reduced stresses in the slip bands.
- (3) Dislocations transport hydrogen along slip bands until they find a barrier such as a grain boundary, a pre-existing crack or an inclusion where they form pile ups and concentrate hydrogen at a rate much faster than would be possible by hydrogen diffusion alone. Once the critical hydrogen concentration for the existing state of stress is reached, a microcrack occurs with an orientation perpendicular to the maximum tensile stress. This process is repeated along the slip band producing a series of staggered microcracks along an orientation at 45° with the welding direction.
- (4) The microcracks are arrested when they enter a region where hydrogen falls below the critical level for the existing state of stress at the crack tip; the growth will not be restarted until hydrogen is built up to the critical level, or an increase in the stress is observed. The crack growth may also be arrested by blunting of the crack tip.
- (5) When a microcrack is arrested, plastic slip at its tip may occur and this develops in slip band formation; further cracks may occur along these slip bands as referred to in (3).
- (6) The existence of high shear stresses between the tips of adjacent microcracks results, in general, in rupture and linking of microcracks during a second stage of the cracking process, which may be assisted by hydrogen.
- (7) If the hydrogen level is too high, the microcracks may nucleate easily and do not depend on the transport of hydrogen by dislocations along slip bands; in these circumstances the microcracks instead of being arranged with a staircase distribution occur randomly. If the hydrogen level is too low nucleation is very difficult, in this case microcracks are

simply eliminated or a few are randomly distributed.

This model is based on the fact that hydrogen present in steel, once concentrated above a critical level, would facilitate the growth of crack nuclei. It does not specify the mechanism by which hydrogen embrittles the steel and is valid regardless of whichever embrittlement theory one cares to accept.

An experimental verification of the model may be done using hydrogen charged tensile specimens with appropriate hydrogen level and loading conditions. The tensile specimen 7 (Table 22) showed evidence of formation of staggered components linked by ductile failure in a way very similar to chevron cracks, Figure 122, though this specimen was strained continuously to rupture. Very recently Iino (163) presented evidence which completely supported the model and its more general application. This author, studying hydrogen assisted cracking in linepipe steels, found, for a hydrogen charged specimen loaded at 95% of the yield stress of the material, that :

'In the presence of an external stress near to the yield strength fracture develops by linking hydrogen embrittlement cracks generated in slip bands formed during testing; therefore the fracture surface is, when viewed macroscopically, slanted with an angle of approximately 45 deg to the stress axis.'

This evidence was obtained by the observation of the fracture surfaces in the scanning electron microscope and, in fact, photographs similar to those from chevron cracks were presented.

In the context of this model the existence of hot microcracks as crack initiators (3), must be interpreted as valid but probably infrequent or a sufficient but not necessary cause for a vertical component of a chevron crack to occur; however, hydrogen would be required for the propagation of such microcracks.

When the weld metal alloying/strength was increased, the orientation of the weld metal transverse cracks changed from approximately 45° to perpendicular to the welding direction. This was associated with a change in the failure mode, in this case the fracture surface showed a relatively small number of regions of dimples linking large areas of brittle fracture, suggesting that there was essentially a single stage cracking mechanism. Compared with the medium strength weld metals, the high strength ones have a higher susceptibility to hydrogen embrittlement, due to metallurgical reasons already reviewed. In this case, cracks may nucleate and/or propagate with lower hydrogen levels, without relying on the transport of this element by dislocations as suggested for the 45° cracks. On the other hand, the dimensions of the plastic zone around the crack tip become smaller and blunting is unlikely; thus, the crack growth can be easily restarted. In these conditions the vertical cracks grow continuously through the material, though the process may be discontinuous in time as is typical of hydrogen cracking.

VII - CONCLUSIONS

VII - CONCLUSIONS

1. Chevron cracks were reproduced under laboratory controlled conditions, in weld metals of the carbon-manganese and low alloy type, using a test which increased substantially the cooling rate in the low temperature range (below the austenitic transformation temperatures). The high cooling rates in the low temperature range were considered to cause mainly an increase in the retained hydrogen and did not invalidate the results for normal cooling.
2. Chevron cracks were typically inclined at 45° with the welding direction, in a section perpendicular to the plane of the plates, and at 80° - 90° in a section parallel to the plane of the plates. In general they were only a few millimetres long and were contained in a single run of weld metal; in exceptional cases they could be 25mm or longer. The cracks tended to be concentrated in the middle third of the weld and, with only one exception, were never found in the uppermost run.
3. Ultrasonic inspection after each run, during a multirun weld, revealed that chevron cracks did not occur until a certain number of runs had been deposited but, as the weld progressed, cracks were formed in the lower layers and pre-existing cracks were found to propagate. This fact indicated that the cracks must occur at low temperatures and that a certain build up of hydrogen and/or stresses was required before cracking occurred.
4. Chevron cracks were found to be typical of medium strength carbon manganese and low alloy weld metals, deposited by the submerged arc process with a basic flux or by manual metal arc with basic and cellulosic electrodes. No chevron cracks were observed in run-tile weld deposits. The increase in alloying and strength produce first an increase in the cracking susceptibility and, above a certain level, a change in the orientation of the cracks from approximately 45° to perpendicular to the welding direction. The change in the orientation of the cracks was believed to be caused by an alteration in the cracking mechanism rather than in the nature of the cracks.
5. The cracking/no-cracking situation was primarily controlled by the hydrogen level in the weld metal. Under test conditions cracking was found to occur for hydrogen levels below 10ml/100g of weld metal; this pointed to the critical importance of controlling the moisture level in consumables of the basic type if cracking was to be avoided.
6. For each particular weld metal it was believed that chevron cracking only occurred if the hydrogen level was within a certain range. Below that range cracking was completely eliminated or a few microfissures were formed; for very high hydrogen levels microfissures were easily nucleated and occurred with a very high density precluding the formation of chevron cracks.
7. For weld metals with the same nominal composition, deposited under similar conditions, the incidence of chevron cracking seemed to depend on factors other than the hydrogen level, such as the diffusion

coefficient and transport of hydrogen by dislocations.

8. In the optical and scanning electron microscopes chevron cracks were found to consist of two sets of components with the outline of a staircase. This characteristic was maintained irrespective of changes in microstructure and of the cracks occurring in the as deposited or refined weld metal.
9. The vertical components of the chevron cracks presented typically a quasi-cleavage mode of failure often with a pattern radiating from the centre where an inclusion hole could be found in many cases. The horizontal components presented generally dimples. Some vertical components, or at least part of their surface, presented clear evidence of having been exposed to high temperatures; detailed examination showed that these areas resulted from reheating by subsequent runs. There was no evidence to support the suggestion that the vertical components were generally nucleated by 'hot microcracks'.
10. Close similarity was found amongst the features observed on the fracture surfaces of vertical components of chevron cracks, microfissures and hydrogen induced or assisted cracks produced under the experimental conditions reported herein. The fracture surface of the fish-eyes found on weld metal tensile specimens was reminiscent of that of microfissures.
11. The staircase morphology was not exclusive of chevron cracks, it was found on hydrogen induced cracks in weld metals submitted to the Y groove Tekken test. The two sets of components observed in the cracks produced by this test resembled very closely the vertical and horizontal components of the chevron cracks in similar materials.
12. The dependence on the hydrogen level, as well as the metallographic and fractographic evidence, indicated that chevron cracks resulted from a two stage cracking mechanism. The critical event was the occurrence of the vertical components along an orientation at 45° with the welding direction induced by hydrogen; this was followed by linking of the vertical components by ductile failure between the crack tips producing a staircase morphology; this second stage might also be assisted by hydrogen.

REFERENCES

REFERENCES

- (1) THOMAS, S.N.G. Colloquium - The Implications of Weld Cracking in Practice. Cracking in Welds. Welding Institute Autumn Meeting, 1968. Metal Construction, 1969, 1, (2), 142.
- (2) COTTON, H.C. Colloquium - The Implications of Weld Cracking in Practice. Cracking in Welds. Welding Institute Autumn Meeting, 1968. Metal Construction, 1969, 1, (2), 144.
- (3) TULIANI, S.S. A Metallographic Study of Chevron Cracks in Submerged Arc Weld Metals. Welding Research International, 1976, 6, (6), 19 - 45.
- (4) MARSHALL, V.G. Chevron Cracking - RDL Industrial Experience. CEGB - Chevron Cracking Workshop. Lyndhurst, March, 1977.
- (5) KEVILLE, B.R. An Investigation to Determine the Mechanism Involved in the Formation and Propagation of Chevron Cracks in Submerged Arc Weldments. Welding Research International, 1976, 6, (6), 47 - 66.
- (6) BIHARI, L.M. Relation of Hydrogen Cracking and High Temperature Ductility to Chevron Cracking in Steel Weld Metal. MSc Thesis, Cranfield Institute of Technology, 1978.
- (7) CROUCH, S.J. The Influence of Heat Input on Weld Metal Transverse Cracking. MSc Thesis, Cranfield Institute of Technology, 1978.
- (8) WOODEND, D. The Influence of Welding Procedure on Chevron Cracking, Review of Whessoe Experience. CEGB - Chevron Cracking Workshop. Lyndhurst, March, 1977.
- (9) ROGERS, P.F. Private communication, 1977.
- (10) HAMILTON, I.G. Trends in User Requirements for Welding Consumables. Proceedings of International Conference on Welding Research, Related to Power Plant. Eds. N.F. Eaton and L.M. Wyatt, CEGB, 1972. Paper 21, 285 - 292.

- (11) CHITTY, A. and BROWN, J.M. Welding Consumables for the Turbine-Generator Industry. Proceedings of International Conference on Welding Research Related to Power Plant. Eds. N.F. Eaton and L.M. Wyatt, CEGB, 1972, Paper 22, 293 - 299.
- (12) GARLAND, J.G. Weld Metal Microcracking with Oerlikon Submerged Arc Basic Fluxes - the Historical Background and Present Position. CEGB - Chevron Cracking Workshop. Lyndhurst, March 1977.
- (13) TAYLOR, L.G. The Effect of Microstructure on the Tensile and Fracture Toughness Properties of Submerged Arc Weld Metal. University of Southampton, Interim Report No. ME 75/1, 1975.
- (14) FARRAR, R.A. and TAYLOR, L.G. A Metallographic Study of Chevron Cracking in Submerged Arc Weld Metals. Welding and Metal Fabrication, Nov. 1977, 45, (9), 575 - 578.
- (15) FARRAR, R.A. The Nature of Chevron Cracking in Submerged Arc Weld Metals. Welding Research International, 1977, 7, (2), 85 - 88.
- (16) TAYLOR, L. G. Chevron Cracking as a Fabrication Problem. CEGB - Chevron Cracking Workshop. Lyndhurst, March, 1977.
- (17) WRIGHT, V.S. Chevron Cracks in Submerged Arc Welds - Fabrication Experience. CEGB - Chevron Cracking Workshop. Lyndhurst, March 1977.
- (18) JOHN, R. Chevron Cracking - Consumable Aspects. CEGB - Chevron Cracking Workshop. Lyndhurst, March 1977.
- (19) WRIGHT, V.S. Chevron Cracking in Submerged Arc Welds - Consumable Aspects. CEGB - Chevron Cracking Workshop. Lyndhurst, March 1977.
- (20) BONISZEWSKI, T. Some Experiments on Chevron Cracking. CEGB - Chevron Cracking Workshop, Lyndhurst, March 1977.
- (21) TULIANI, S.S. Metallographic Study of Chevron Cracks in Submerged Arc Weld Metal. CEGB - Chevron Cracking Workshop. Lyndhurst, March, 1977.

- (22) KEVILLE, B.R. An Investigation to Determine the Mechanism of Formation and Propagation of Chevron Defects.
CEGB - Chevron Cracking Workshop.
Lyndhurst, March, 1977.
- (23) HART, P.H.M. Welding Institute Presentation on Mechanism of Chevron Cracking.
CEGB - Chevron Cracking Workshop.
Lyndhurst, March, 1977.
- (24) MOTA, J.M.F., JUBB, J.E.M., APPS, R.L. The Cranfield Investigation into Chevron Cracking.
CEGB - Chevron Cracking Workshop.
Lyndhurst, March 1977.
- (25) FARRAR, R.A. The Nature of Chevron Cracking in Submerged Arc Weld Metals.
CEGB - Chevron Cracking Workshop.
Lyndhurst, March, 1977.
- (26) MOTA, J.M.F. and APPS, R.L. Transverse, 45° Cracking - Chevron Cracking - in C-Mn and Low Alloy Weld Metals.
IIW DOC. IX-1080.78 for AA.78..
- (27) MOTA, J.M.F., APPS, R.L. and JUBE, J.E.M. Chevron Cracking in Manual Metal Arc Welding.
Conference - Trends in Steels and Consumables for Welding.
Welding Institute Autumn Meeting, London 1978. Paper No. 18.
- (28) WRIGHT, V.S. and DAVISON, I.T. Chevron Cracking in Submerged Arc Welds.
Conference - Trends in Steels and Consumables for Welding.
Welding Institute Autumn Meeting, London 1978, Paper No. 38.
- (29) MOTA, J.M.F., JUBB, J.E.M., and APPS, R.L. Chevron Cracking : Initiation and Propagation.
Welding and Metal Fabrication, 1978, 46, (9), 625 - 627.
- (30) APPS, R.L. Private communication, 1978.
- (31) HEMSWORTH, B., BONISZEWSKI, T. and EATON, N.F. Classification and Definition of High Temperature Welding Cracks in Alloys.
Cracking in Welds; Welding Institute Autumn Meeting, 1968,
Metal Construction, 1969, 1, (2), 5 - 16.
- (32) GLOSSOP, B.A., EATON, N.F. and BONISZEWSKI, T. Reheat Cracking in Cr-Mo-V Steel Weldments.
Welding Institute Autumn Meeting, 1968.
Metal Construction, 1969, 1, (2), 68-73.

- (33) BONISZEWSKI, T. and BROWN, E.D. Fissures in the Refined Region of Multi-Run Weld Metals. British Welding Journal, 1966, 13 (1), 18 - 31.
- (34) CHALMERS, B., KING, R. and SHUTTLEWORD, R. The Thermal Etching of Silver. Proceedings of the Royal Society, Series A, 1948, 193, 465 - 483.
- (35) OLNEY, M.J. and SMITH, G.C. Surface Effects Occurring During the Heating and Cooling of Plain Carbon Steels. Journal of the Iron and Steel Institute, 1959, 193, 107 - 116.
- (36) MOORE, A.J.W. The Influence of Surface Energy on Thermal Etching. Acta Metallurgica, 1958, 6, 293-304.
- (37) MOREAU, J. and BENARD, J. On the Reversible Striation of Iron and Its Alloys. Acta Metallurgica, 1962, 10, 247-251.
- (38) ONDAR, J., BRONTY, F. and BENARD, J. Striation Reversible des Surfaces Metalliques Dans Les Atmospheres Faiblement Sulfurantes. Acta Metallurgica, 1961, 9, 520
- (39) GJOSTEIN, N.A. Adsorption and Surface Energy; (II): Thermal Faceting from Minimization of Surface Energy. Acta Metallurgica, A 1963, 11, 969 - 978.
- (40) HENRY, G. et al Mem. Sc. Rev. Met., 1959, 56, 416
- (41) BALL, J.G. and WINTERTON, K. Tensile Properties of Mild Steel Weld Metal at High Temperatures. Welding Research, 1950, 4, 104r - 124r.
- (42) MERCER, J.F. and TOWERS, R.T. Ductility of Weld Metals with Special Reference to High Temperatures. Report - Murex Welding Processes Ltd. Research Department, June 1961.
- (43) JONES, P.W. Hot Cracking in Mild Steel Welds (Final Report on High Temperature Tensile Tests) British Welding Journal, 1959, 6, 269-281.
- (44) DUPUY, E.L. An Experimental Investigation on the Mechanical Properties of Steels at High Temperatures. Journal of the Iron and Steel Institute, 1921, 104, (2), 91 - 116.
- (45) FUNNEL, G.D. and DAVIES, R.T. Effect of Aluminium Nitride Particles on Hot Ductility of Steel. Metals Technology, 1978, 5, (5), 150-153.

- (46) LANKFORD, Jr. W.T. Some Considerations of Strength and Ductility in the Continuous Casting Process.
The 1972 Howe Memorial Lecture.
Metallurgical Transactions, 1977, 34, (6), 1331 - 1357.
- (47) WILBER, G.A., PATRA, R., The Effects of Thermal History and SAVAGE, W.F. and Composition on the Hot Ductility of CHILDS, W.J. Low C Steels.
Metallurgical Transactions, 1975, 6A, (9), 1727 - 1735.
- (48) WILLIAMS, C.S. Steel Strength and Ductility Response: to Arc Welding Thermal Cycles.
Welding Journal, 1963, 42, (1), 1s-8s.
- (49) BORLAND, J.C. and Some Aspects of Cracking in Welded Cr-Ni YOUNGER, R.N. Austenite Steels. (A Survey of the Literature).
BWRA Report. British Welding Journal, 1960, 7, (1), 22 - 59.
- (50) BARFORD, J. and Structure Related to Hot Ductility of MYERS, J. Three Austenitic Steels.
Journal of the Iron and Steel Institute, 1963, 201, 1025 - 1031.
- (51) TRUMAN, R.J. and Some Ductility Aspects of 18-12-1Nb Steel. KIRKBY, H.V. Journal of the Iron and Steel Institute, 1960, 196, 180 - 188.
- (52) EVANS, R.W. and Hot Ductility of Fe-Ni Alloys. JONES, F.L. Metals Technology, 1976, 3, (11), 494-496.
- (53) YENISCAVICH, W. A Correlation of Ni-Cr-Fe Alloy Weld Metal Fissuring with Hot Ductility Behaviour.
Welding Journal, 1966, 45, (9), 344s - 356s.
- (54) CHUBB, J.P. and Effect of Nickel on Hot Ductility of Binary BILLINGHAM, J. Copper-Nickel Alloys.
Metals Technology, 1978, 5, (3), 100 - 103.
- (55) DAVIES, P.W. et al Fracture Behaviour of Copper During Hot Deformation.
Journal of the Institute of Metals, 1971, 99, 195 - 197.
- (56) CLEWS, K.J. Cracking of Aluminium Bronze Plate During Welding.
British Welding Journal, 1965, 12, (6), 301-309.
- (57) McKEOWN, D. Ductility Dip Cracking in Aluminium Bronze.
Welding Institute Research Bulletin 1974, 15, (3), 59 - 65.

- (58) NIPPES, E.F. et al An Investigation of the Hot Ductility of High Temperature Alloys. Welding Journal, April 1955, 34, (4), 183s - 196s.
- (59) NIPPES, E.F., SAVAGE, W.F. and GROTKÉ, G. Further Studies of the Hot Ductility of High Temperature Alloys. Welding Research Council Bulletin, No. 33, 1957.
- (60) SAVAGE, W.F. Apparatus for Studying the Effects of Rapid Thermal Cycles and High Strain Rates on the Elevated Temperature Behaviour of Materials. Journal of Applied Polymer Science, 1966, 6, (21), 303 - 315.
- (61) YENISCAVICH, W. The Superalloys, Chapter 18 - 'Joining' Book edited by C.T. Sims and W.C. Hagel Published by John Wiley & Sons, 1972. 509 - 532.
- (62) MYERS, J. Hot Ductility of Three Austenitic Steels. British Welding Journal, 1962, 9, (3), 106 - 114.
- (63) IRVINE, K.J. and PICKERING, F.B. The Effect of Heat Treatment and Micro-Structure on the High Temperature Ductility of 18% Cr-12%Ni-1%Nb Steels. Journal of the Iron and Steel Institute. 1960, 196, Part 2, 166 - 179.
- (64) HADDRILL, D.M. and BAKER, R.G. Microcracking in Austenitic Weld Metal. British Welding Journal, 1965, 12, (8), 411 - 419.
- (65) MATSUBARA, K. Transactions Iron Steel Institute, Japan, 1966, 6, 139 - 148.
- (66) BEYNON, W.G. Structural Steels, A Preliminary Investigation on the Relation of Hot Tensile Properties to a) Composition and State of Deoxidation and b) Weldability. Welding and Metal Fabrication, 1957, 25, (7), 262 - 264.
- (67) DESAI, S.C. Longitudinal Panel Cracking in Ingots. Journal of the Iron and Steel Institute, 1959, 191, 250 - 256.
- (68) ERASMUS, L.A. Effect of Aluminium Additions on Forgeability, Austenite Grain Coarsening and Impact Properties of Steel. Journal of the Iron and Steel Institute, 1964, 202, 32 - 41.

- (69) KEVILLE, B.R. and COCHRANE, R.C. Strain-Induced Hot Cracking in Ferritic Weld Metals. Conference - Trends in Steels and Consumables for Welding. Welding Institute Autumn Meeting, London 1978, Paper No. 28.
- (70) BONISZEWSKI, T. Discussion Session 1 - General Characteristics of Weld Cracking, Cracking in Welds. Welding Institute Autumn Meeting, 1968. Metal Construction, 1969, 1, (2s), 106.
- (71) REED-HILL Physical Metallurgy Principles, Chapter 19 - 'Creep'. Book published by Van Nostrand Reinhold Co. New York, London, 1972.
- (72) McMAHON, Jr., C.J. Intergranular Fracture in Steels. Materials Science and Engineering, 1976, 25, (), 233 - 239.
- (73) CAILLETET, M. C.R. Acad. Sc. Paris, 1868, 66, 847 - (Quoted by Thompson, A.W. (75)).
- (74) JOHNSON, W.H. Proc. Roy. Soc., 1875, No. 158, 168 - 179. (Quoted by Thompson, A.W. (75)).
- (75) THOMPSON, A.W. The Mechanism of Hydrogen Participation in Ductile Fracture. Proceedings of a Conference on 'Effect of Hydrogen on Behaviour of Materials'. Jackson Lake Lodge, Moran, Wyoming. Sept. 7-11, 1975, 467 - 477.
- (76) BERNSTEIN, I.M. The Role of Hydrogen in the Embrittlement of Iron and Steel. Materials Science and Engineering, 1970, 6, (1), 1 - 19.
- (77) LOUTHAN, M.R., CASKEY, G.R., DONOVAN, J.A. and RAWL, D.E. Hydrogen Embrittlement of Metals. Materials Science and Engineering, 1972, 10, 357 - 368.
- (78) MARSHAL, R.P. and LOUTHAN, Jr. M.R. Tensile Properties of Zircaloy with Oriented Hydrides. Transactions of the ASM, 1963, 56, 693 -
- (79) NUTTALL, K. et al Metallographic Observations of the Interaction of the Hydride, Stress and Crack Growth at 600°K in a Zr - 2.5% Nb Alloy. Scripta Metallurgica, 1976, 979 - 982.

- (80) JAFFEE, R.I., LENNING, Transactions of the AIME, 1956, 206, G.A. and CRAIGHEAD, C.M. 907 -
- (81) COTTERILL, P. Progr. Mat. Sci. 1961, 9, 201
(Quoted by Louthan (77)).
- (82) FAST, V.D. Interaction of Metals and Gases.
Academic Press, New York, 1965, p54.
- (83) WEINER, L.C. Corrosion, 1961, 17, 109.
(Quoted by Louthan (77)).
- (84) WESTPHAL, D.A. and Hydrogen Attack of Steel.
WORZALA, F.J. Proceedings of Conference 'Hydrogen in
Metals'.
Published by ASM, 1973.
- (85) VENNETT, R.M. and The Effect of High Pressure Hydrogen
ANSELL, G.S. upon the Tensile Properties and Frac-
ture Behaviour of 304L Stainless Steel.
Transactions of the ASM, 1967, 60, (2),
242 - 251.
- (86) BARTH, C.F. and Evaluation of Hydrogen Embrittlement
STEIGERWALD, E.A. Mechanism.
Metallurgical Transactions, 1970, 1,
3451 - 3455.
- (87) HOLZWORTH, M.L. and Jr. Corrosion, 1968, 24, 110
LOUTHAN Jr., M.R. (Quoted by Louthan (77)).
- (88) VIBRANS, G. Fish-Eyes in Rolled Steel Exposed to
Hydrogen at Room Temperature.
Metallurgical Transactions, 1977, 8A,
1318 - 1320.
- (89) COE, F.R. Welding Steels Without Hydrogen Cracking.
Welding Institute Publication, 1973.
- (90) WEBB, W. An Investigation into Basic Type Agglom-
erated Fluxes for Submerged Arc Welding.
MSc Thesis, Materials Department, Cran-
field Institute of Technology, 1969.
- (91) GARLAND, J.G. and Fluxes for Submerged Arc Welding Ferritic
BAILEY, N. Steels.
A Literature Survey. Part I : Manufacture,
Quality Control and Weldability.
Welding Institute Research Report, M/84/
75, 1975.
- (92) CHEW, B. Moisture Loss and Regain by Some Basic
Flux Covered Electrodes.
Welding Journal, 1976, 55, (5), 127s-134s.

- (93) EVANS, G.M. and GARLAND, J.G. Water Absorption and Redrying Characteristics of Two High Basic Agglomerate Fluxes. Oerlikon Ltd., Technical Report.
- (94) EVANS, G.M. and BAACH, H. Hydrogen Content of Welds Deposited by Different Welding Processes. Metals Technology Conference A-E, IIW Annual Assembly, Public Session, 1976.
- (95) CHEW, B. Prediction of Weld Metal Hydrogen Levels Obtained Under Test Conditions. Welding Journal, 1973, 52, (9), 386s-391s.
- (96) GRAVILLE, B.A. The Principles of Cold Cracking Control. Book published by Dominion Bridge Co. Ltd., Montreal, Canada, 1975.
- (97) BAILEY, N. and DAVIS, M.L.E. Fluxes for Submerged Arc Welding Ferritic Steels. A Literature Survey; Part II : Weld Properties and Weld Defects. Welding Institute, Research Report, 10/1976/M, 1976.
- (98) BLINK, W.P. van dan Note on the Influence of the Water Content of an Electrode Coating on the Hydrogen Content of a Weld. Welding Journal, 1947, 26 (6), 369 - 370.
- (99) CHRISTENSEN, N. Metallurgical Aspects of Welding Mild Steel. Welding Journal, 1949, 28, (8), 373s-380s.
- (100) BRADSTREET, B.J. Moisture Absorption in Low Hydrogen Electrode Coatings and Porosity in Welds. Welding Journal, 1964, 43, (1), 43s-48s.
- (101) BOSWARD, I.G. The Effect of Excessive Redrying on Fortrex 35A and Ferex 7018LT. BOC Murex, Research and Development Laboratories, Report No. D498.
- (102) WILLI, A. and BAACH, H. Water Content in S.A.W. Fluxes and its Influence upon Weld Cracking. Proceedings of the First International Symposium on Cracking and Fracture in Welds. Japan Welding Society, Tokyo, Japan, 1971. pp IIB2.1 - IIB2 - 10.
- (103) IIW-DOC-452-74. Weld metal Hydrogen Levels and the Definition of Hydrogen Controlled Electrodes. Welding in the World, 1974, 12, (3/4), 69 - 76.

- (104) IIW-DOC-II-778-75. Recommended Methods of Reporting Weld Metal Hydrogen Contents. Welding in the World, 1977, 15, (3/4).
- (105) BAKER, R.G. Some Aspects of the Practical Control of Weld Cold Cracking. Metals Technology Conference A-B, IIW Annual Assembly. Public Session, 1976.
- (106) BAILEY, N. Hydrogen Cracking and Austenite Electrodes. Metal Construction, 1978, 10, (12), 580 - 583.
- (107) BS 5135 : 1974. Specification for Metal-Arc Welding of Carbon and Carbon Manganese Steels.
- (108) CAPLAN, J.S. and LANDERMAN, J.S. Preventing Hydrogen-Induced Cracking After Welding of Pressure Vessel Steels by Use of Low Temperature Postweld Heat Treatments. WRC Bulletin No. 216, 1976.
- (109) COE, F.R. Hydrogen Diffusion in Welding. An Assessment of Current Knowledge. DOC IIW-491-75 published in Welding in the World, 1976, 14, (1/2), 1 - 10.
- (110) EVANS, G.M. and ROLLASON, E.C. Influence of Non-Metallic Inclusions on the Apparent Diffusion of Hydrogen in Ferrous Materials. Journal of the Iron and Steel Institute 1969, 207, (11), 1484 - 1490.
- (111) BONISZEWSKI, T. and MORETON, J. Effect of Microvoids and MnS Inclusions in Steel on Hydrogen Evolution and Embrittlement. British Welding Journal, 1967, 14, 321 - 336.
- (112) BERNSTEIN, I.M., GARBER, R. and PRESSOUYRE, G.M. Effect of Dissolved Hydrogen on Mechanical Behaviour of Metals. Proceedings of a Conference on 'Effect of Hydrogen on the Behaviour of Metals' Jackson Lake Lodge, Moran, Wyoming, September 1975. 37-58.
- (113) PRESSOUYRE, G.M. and BERNSTEIN, I.M. A Quantitative Analysis of Hydrogen Trapping. Metallurgical Transactions, 1978, 9A, (11) 1571 - 1580.
- (114) FIKKERS, A.T. and MULLER, T. Hydrogen Induced Cracking in Weld Metal. Welding in the World, 1976, 14, 11/12, 238 - 247.

- (115) HART, P.H.M. Low Sulphur in C-Mn Steels and Their Effect on HAZ Hardenability and Hydrogen Cracking. Conference - Trends in Steels and Consumables for Welding; Welding Institute Autumn Meeting, London 1978, Paper No. 20.
- (116) SMITH, N. and BAGNALL, B.I. The Influence of Sulphur on Heat Affected Zone Cracking of Carbon Manganese Steel Welds. Cracking in Welds; Welding Institute Autumn Meeting, 1968. Metal Construction, 1969, 1, (2s), 17 - 23.
- (117) HEWITT, J. and MURRAY, J.D. Effect of Sulphur on the Production and Fabrication of Carbon Manganese Steel Forgings. Cracking in Welds; Welding Institute Autumn Meeting, 1968. Metal Construction, 1969, 1, (2s), 24 - 31.
- (118) DOLBY, R.E. The Weldability of Low Carbon Structural Steels. Welding Institute Research Bulletin, 1977, 18, (8), 209 - 216.
- (119) HRIVNAK, I. The Mutual Relationship and Interdependence of Developments in Steel Metallurgy and Welding Technology. Houdremont Lecture, IIW Annual Assembly, 1978.
- (120) ITO, Y. and BESSYO, K. Cracking Parameter of High Strength Steels Related to Heat Affected Zone Cracking. Journal of the Japan Welding Society, 1968, 37, (9), 983 - 991.
- (121) ITO, Y. and BESSYO, K. A Prediction of Welding Procedure to Avoid Heat Affected Zone Cracking. IIW-DOC-IX-631-69.
- (122) BONISZEWSKI, T. and WATKINSON, F. Effect of Weld Microstructure on Hydrogen Induced Cracking in Transformable Steels. Metals and Materials, 1973, 7. Part 1 : February issue pp 90 - 96. Part 2 : March issue pp 145 - 151.
- (123) WIDGERY, D.J. and SAUNDERS, G.G. Microstructures in Steel Weld Metals. Welding Institute Research Bulletin, 1975, 16 (10), 277 - 281.
- (124) FARRAR, R.A., TULIANI, S.S. and NORMAN, S.R. Relationship between Fracture Toughness and Microstructure of Mild Steel SAW Metal. Welding and Metal Fabrication, 1974, 42 (2), 68 - 73.

- (125) WATKINSON, F. Hydrogen Cracking in High Strength Weld Metals.
Welding Journal, 1969, 48, (9), 417s - 424s.
- (126) GRANJON, H. Cold Cracking in the Welding of Steels.
IIW-DOC.IX-748-71.
Welding in the World, 1971, 9, (11/12), 382-397.
- (127) DAWES, M.G. Residual Stresses and Strains in Weldments.
Welding Institute Research Bulletin, 1974, 15, (9), 264 - 268.
- (128) MACHERAUCH, E. and WOHLFAHRT, H. Different Sources of Residual Stresses as a Result of Welding.
Conference - 'Residual Stresses in Welded Construction and Their Effects';
Welding Institute Autumn Meeting, London, 1978, Paper 11, 267 - 282.
- (129) Residual Stresses and Distortion.
AWS Welding Handbook, 7th Edition, 1976 Vol. 1, Chapter 6.
- (130) LOUTHAN Jr. M.R. Effects of Hydrogen on the Mechanical Properties of Low Carbon and Austenitic Steels.
Conference - 'Hydrogen in Metals', 1973 Proceedings Published by ASM, pp 53-75.
- (131) LINNERT, G.E. Welding Metallurgy.
Vol. 2, 3rd Edition 1967.
Published by AWS.
- (132) TOH, T. and BALDWIN, W.M. Ductility of Steel with Varying Concentrations of Hydrogen.
Stress, Corrosion, Cracking and Embrittlement. John Wiley and Sons, New York 1956 p. 176.
- (133) TROIANO, A.R. The Effect of Hydrogen and Other Interstitials on the Mechanical Behaviour of Metals.
Transactions of the ASM, 1960, 52, (1), 54 - 80.
- (134) SAVAGE, W.F., NIPPES, E.F. and SAWHILL, J.M. Hydrogen Induced Cracking During Implant Testing of Alloy Steels.
Welding Journal, 1976, 55, (12), 400s - 407s.
- (135) PELLOUX, R.M. and AVYLE, J.A. van den Testing and Diagnosis of Hydrogen Susceptibility.
Conference 'Hydrogen in Metals', 1973. Proceedings Published by ASM, 547 - 558.

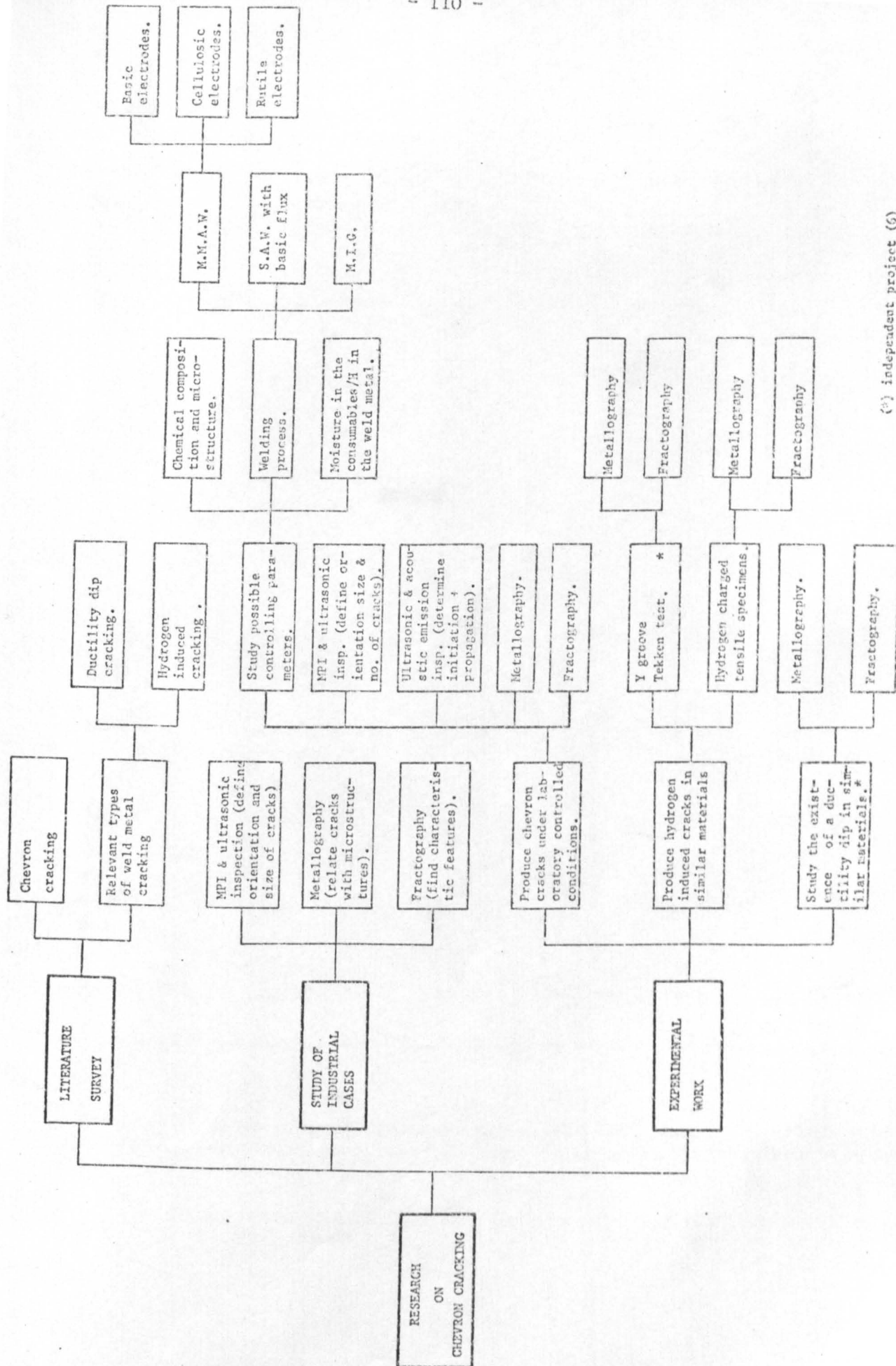
- (136) BEACHEM, C.D. A New Model for Hydrogen Assisted Cracking (Hydrogen 'Embrittlement'). Metallurgical Transactions, 1972, 3, 437 - 451.
- (137) FLANIGAN, A.E. An Investigation of the Influence of Hydrogen on Ductility of Arc Welds in Mild Steel. Welding Journal, 1947, 26, (4), 193s - 214s.
- (138) FLANIGAN, A.E. and KAUFMAN, M. Microcracks and the Low Temperature Cooling Embrittlement of Welds. Welding Journal, 1951, 30, (12), 613s - 622s.
- (139) BLAND, J. Effect of Quench Time on Weld Metals. Welding Journal, 1949, 28, (5), 216s - 226s.
- (140) ROLLASON, E.C. and ROBERTS, R.R. Effect of Cooling Rate and Composition on the Embrittlement of Weld Metal. Journal of the Iron and Steel Institute, 1950, 166, 105 - 112.
- (141) WEGRZYN, J. and APPS, R.L. Effect of Nitrogen on Fissuring in Mild Steel Weld Deposits. British Welding Journal, 1968, 15, (11), 532 - 540.
- (142) Recommended Methods of Testing for the Assessment of the Microfissuring Tendency of Mild and Low Alloy Steel Weld Metal Deposited by Manual Arc Welding Covered Electrodes. IIW DOC II-477-75 Published in Welding in the World, 1975, 13, (5/6), 155-160.
- (143) EVANS, G.M. and CHRISTENSEN, Microfissuring of Multi-Run Mild Steel Weld Metal. British Welding Journal, 1963, 10 (10), 508 - 515.
- (144) WINTERTON, K. Mechanism of Microcracking in Mild Steel Welding. Welding Journal, 1957, 36, (10), 449s - 456s.
- (145) BAILEY, N. Fisheyes, Hydrogen Embrittlement and Removal. Welding Institute Research Bulletin, 1974, 15, (12), 369 - 372.
- (146) CORNET, M. and TALBOT-BESNARD, S. Present Ideas about Mechanisms of Hydrogen Embrittlement of Iron and Ferrous Alloys. Metals Science, 1978, 12, (7), 335 - 339.

- (147) ZAPFFE, C. Transactions of the ASM, 1947, 39, 191.
- (148) KAZINCZY, F. de A Theory of Hydrogen Embrittlement. Journal of the Iron and Steel Institute, 1954, 177, 85 - 92.
- (149) GAROFARO, F., CHOU, T.T. and AMBEGAO-KAR, V. Effect of Hydrogen on Stability of Microcracks in Iron and Steel. Acta Metallurgica, 1960, 8, (3), 504 - 512.
- (150) BILBY, B.A. and HEWITT, J. Hydrogen in Steels - the Stability of Microcracks. Acta Metallurgica, 1962, 10, (6) 587 - 600.
- (151) TETELMAN, A.S. and ROBERTSON, W.D. Direct Observation and Analysis of Crack Propagation in Iron - 3% Silicon Single Crystals. Acta Metallurgica, 1963, 11, 415 - 426.
- (152) TETELMAN, A.S. Recent Developments in Classical (Internal) Hydrogen Embrittlement. Conference - 'Hydrogen in Metals' 1973 Proceedings published by ASM, 17 - 34.
- (153) PETCH, N.J. and STABLES, P. Delayed Fracture of Metals under Static Load. Nature, 1952, 169, 842 - 843.
- (154) PETCH, N.J. The Lowering of Fracture-Stress Due to Surface Adsorption. Philosophical Magazine, 8th Series, 1956, 1, 331 - 337.
- (155) MORLET, J.G., JOHNSON, H.H. and TROIAN, A.R. A New Concept of Hydrogen Embrittlement in Steel. Journal of the Iron and Steel Institute, 1958, 189, 37 - 44.
- (156) ORIANI, R.A. A Mechanistic Theory of Hydrogen Embrittlement of Steels. Ber. Bunsenges, 1972, 76, (8), 848 - 857.
- (157) ORIANI, R.A. and JOSEPHIC, P.H. Testing the Decohesion Theory of Hydrogen Induced Crack Propagation. Scripta Metallurgica, 1972, 6, (8), 681 - 687.
- (158) ORIANI, R.A. and JOSEPHIC, P.H. Equilibrium Aspects of Hydrogen Induced Cracking of Steels. Acta Metallurgica, 1974, 22, 1065 - 1074.

- (159) BASTIEN, F. and AZOU, P. Effect of Hydrogen on the Deformation and Fracture of Iron and Steel in Simple Tension. Proceedings of the 1st World Metallurgical Congress; ASM, 1951, 535 - 552.
- (160) DONOVAN, J. Accelerated Evolution of Hydrogen from Metals During Plastic Deformation. Metallurgical Transactions, 1976, 7A, 1677 - 1683.
- (161) SAVAGE, W.F., NIPPES, E.G. and TOKUNAGA, Y. Hydrogen Induced Cracking in HY-130 Steel Weldments. Welding Journal, 1978, 57, (4), 118s-126s.
- (162) LOUTHAN Jr., M.R. The Role of Test Technique in Evaluating Hydrogen Embrittlement Mechanisms. Conference 'Effect of Hydrogen on Behaviour of Materials', Jackson Lake Lodge, Moran, Wyoming, Sept. 1975, 496 - 506.
- (163) IINO, M. The Extension of Hydrogen Blister-Crack Array in Line Pipe Steels. Metallurgical Transactions, 1978, 9A, (11), 1581 - 1590.
- (164) RODRIGUES, P.E.L.B. The Relationship Between the Welding Thermal Cycles, Microstructure and Toughness of Weld Metal in C-Mn Steels. PhD Thesis, Cranfield Institute of Technology, 1978.
- (165) MALLET, M.W. and RIEPPEL, P.J. Underbead Cracks in Welds Cathodically Charged with Hydrogen. Welding Journal, 1950, 29, (7), 343s - 347s.
- (166) HOESON, J.D. and SYKES, C. Effect of Hydrogen on the Properties of Low Alloy Steel. Journal of the Iron and Steel Institute, 1951, 169, 209 -
- (167) HOESON, J.D. and HEWITT, J. The Effect of Hydrogen on the Tensile Properties of Steel. Journal of the Iron and Steel Institute. 1953, 175 , 131 - 140.
- (168) FARREL, K. and QUARREL, A.G. Hydrogen Embrittlement of an Ultrahigh Tensile Steel. Journal of the Iron and Steel Institute, 1964, 202, 1002 - 1011.
- (169) GIBALA, R. Internal Friction of Hydrogen Charged Iron. Transactions ASM-AIME, 1967, 239, 1574 - 1585.

- (170) GERBERICH, W.W. and CHEN, Y.T. Hydrogen Controlled Cracking - an Approach to Threshold Stress Intensity. Metallurgical Transactions A, 1975, 6A, 271 - 278.
- (171) BONISZEWSKI, T. Etchant for Revealing the Solidification Structure in Mild Steel Weld Metal. British Welding Research Association Bulletin 1965, 6, 12, 304 - 305.
- (172) PATEL, R. and ROGERSON, J.H. Magnetic Particle Inspection - Its Sensitivity When Used on Welded Joints. Metal Construction, 1978, 10, (12), 585 - 587.
- (173) CHEW, B. Private communication. Work to be published.
- (174) STOUT, R.D. and DOTY, W. Weldability of Steels. Edited by S. Epstein and R.E. Somers. Published by Welding Research Council, 2nd edition, 1971.
- (175) BONISZEWSKI, T. and PAVELEY, D.A. Timing at Temperature when Drying Welding Electrodes before Use. Metal Construction, 1978, 10, (11), 530 - 531.
- (176) EDWARDS, B.C., BISHOP, H.E., RIVIERE, J.C. and EYRE, B.L. An AES Study of Temper Embrittlement in Low Alloy Steels. Acta Metallurgica, 1976, 24, 957 - 967.
- (177) VISWANATHAN, R. and HUDAK, S.J. The Effect of Impurities and Strength Level on Hydrogen Induced Cracking in 4340 Steels. Proceedings of a conference on 'Effect of Hydrogen on Behaviour of Materials'. Jackson Lake Lodge, Moran, Wyoming, Sept. 1975, 262 - 272.
- (178) VISWANATHAN, N.R. and HUDAK, S.J. The Effect of Impurities and Strength Level on Hydrogen Induced Cracking in a Low Alloy Turbine Steel. Metallurgical Transactions A, 1977, 8A, 1633 - 1677.
- (179) TETELMAN, A.S. Use of Acoustic Emission Testing to Monitor Hydrogen Embrittlement in Steels. Tewksbury Symposium on Fracture, 3rd; University of Melbourne, Australia. June 4 - 6, 1974, 78 - 97.
- (180) GRANJOH, H. and DEBIEZ Note on Acoustic Emission Associated with Cold Cracking in Welding of Steel. Proceedings, 8th World Conference on Non-Destructive Testing, Cannes 1976, Comité Français d'Etude des Essais Non Destructifs, Paper No. 3k14.

DIAGRAM



(*) independent project (6)

TABLES

TABLE 1 - Storage and Reconditioning Temperatures for Welding Consumables (1) (after Graville (96)).

WELDING PROCESS (2)	TYPE OF CONSUMABLE	AWS CLASSIFICATION	STORAGE TEMPERATURE (°C)	REBAKING TEMPERATURE (°C)
SMAW	cellulosic coated	EXX 10 EXX 11	25 - 50	not recommended
	basic coated	EXXX 5 EXXX 6 EXXX 8	100 - 150	375 - 425
	Other manual mild steel electrodes	EXX 12, EXX 13, EXX 14, EXX 20, EXX 24, EXX 27	25 - 50	125 - 150
	stainless steel	All DC lime All AC-DC tit- ania	100 - 150	250 - 275 200 - 225
	hardsurfac- ing alloys	All	100 - 150	300 - 425
FCAW	mild and low alloy steel	All	50 - 150	not recommended
SAW	fluxes	All	100 - 150	400 - 450
SAW CMAW ESW	wires	All	25 - 50	-
ESW	fluxes	All	100 - 150	not usually necessary

NOTES: (1) These temperatures are typical values; however suppliers should be consulted for exact storage and rebaking conditions.

(2) Standard American Welding Society letter designations.

TABLE 2 - Chemical Composition of the Submerged Arc Welding Wires Used in the Cracking Tests (wt. %)

WIRE (1)	C	Mn	Si	S	P	Ni	Cr	Mo	Cu
SD3	.11	1.51	.23	.015	.011				
S ₄ (2)	.10	2.0	.10	.01	.01				
SD3/1Ni	.13	1.64	.30	.012	.018	1.50			
SD2/3Ni	.11	1.13	.16	.013	.009	2.77	.07	.14	.06
SD3/Mo	.11	1.50	.21	.017	.013			.48	
SD3/1Ni/1Mo	.13	1.61	.29	.009	.008	1.31		.62	
SD2/1Cr/1Ni/1Mo	.11	1.07	.28	.019	.015	.98	.90	.48	

NOTES : (1) Designation according to IIW recommendation.
(2) Typical analysis, real analysis not available.

TABLE 3 - Constitution of the Commercial Submerged Arc Welding Flux GP411T According to the Manufacturer (wt. %)

SiO ₂	CeO + MgO	Al ₂ O ₃ + MnO	CaF ₂
10	35	20	30

TABLE 4 - Chemical Composition and Hardness of Industrial
Weld Metal Samples Containing Chevron Cracks

CONSUMABLES	SPECIMEN IDENTIFICATION	CHEMICAL COMPOSITION (wt %)										CARBON EQUIVALENT			HARDNESS HV5		
		C	Mn	Si	S	P	Fe	Cr	Mo	Cu	CE (1)	Last Run	Middle Runs	Refined Regions			
(2)	A	.08	1.06	.41	.015	.022	.10	.05	<.01	.17	.29	220	211	197			
(2)	B	.08	1.07	.39	.014	.024	.02	.01	<.01	.07	.27	214	202	197			

NOTE - (1) Carbon equivalent according to the ITW formula : $CE = C + \frac{Mn}{6} + \frac{Cr + Mo + V}{5} + \frac{Ni + Cu}{15}$

(2) Not specified.

TABLE 5 - Chemical Composition and Hardness of Submerged Arc Welds

CONSUMABLES (wire + flux)	TEST PLATES (TP)	CHEMICAL COMPOSITION (wt. %)										CARBON EQUIVALENT		HARDNESS HV5			MECHANICAL PROPERTIES (2)	
		C	Mn	Si	S	P	Ni	Cr	Mo	Cu	CE (1)	Last Run	Middle Run	Refined Regions	Y.S. N/mm ²	U.T.S. K/mm ²		
SD3 + OP41TT	1,5,6,7	.11	1.24	.15	.018	.021	.07	.03	.03	.16	.34	222	203	186	>420 (>370)	580 - 630 (520 - 560)		
S4 + OP41TT	8,9	.050	1.37	.18	.010	.022	.03	.03	.02	.23	.31	221	207	190	- (3)	- (3)		
SD3/INI+OP41TT	2,3,4,10,11	.14	1.40	.18	.017	.019	1.50	.07	.04	.23	.51	245	225	216	450 - 500 (390 - 440)	560 - 630 (520 - 570)		
SD2/3Ni+OP41TT	13,14,15,16, 17,18	.060	1.05	.20	.010	.017	2.94	.08	.13	.16	.49	249	226	210	- (3)	- (3)		
SD3/Mo+OP41TT	19,20,21	.055	1.13	.18	.010	.016	.09	.06	.51	.16	.37	251	223	217	500 - 540 (450 - 500)	630 - 680 (570 - 630)		
SD3/INI+Mo + OP41TT	22,23,24	.059	1.33	.24	.05	.009	1.26	.05	.63	.24	.51	266	257	232	- (3)	- (3)		
SD2/1Cr1Ni1Mo + OP41TT	25,26,27	.08	.85	.19	.018	.022	1.01	.84	.50	.22	.57	277	270	254	(500 - 560)	(600 - 680)		
															650 - 700 (690 - 730)	750 - 800 (850 - 850)		

NOTES : (1) See note (1) Table 4.

(2) Mechanical properties according to Oerlikon for weld metals in the as welded condition, equivalent values for weld metals in the stress relieved condition are presented in brackets.

(3) Not available.

TABLE 6 - Chemical Composition and Hardness of Manual Metal Arc Welds Deposited with Commercially Available Electrodes

CONSUMABLES (Electrodes)	TEST PLATES (TP)	CHEMICAL COMPOSITION (wt.%)							CARBON EQUIVALENT	HARDNESS HV5			MECHANICAL PROPERTIES (2)	
		C	Mn	Si	S	P	Ni	Cr	Mo				Y.S. N/mm ²	U.T.S. N/mm ²
E8018C1 Manufacturer A 28 to 34		.045	.98	.23	.009	.014	1.92	.02	.01	.35	241	218	202	590
Manufacturer B Batch 1	35	.067	1.00	.30	.008	.017	2.56	.04	.03	.42	254	232	214	600 (570)
Batch 2	36,37,38	.069	.82	.19	.010	.011	2.81	.04	.01	.40	254	223	201	600 (570)
E6013	39	.044	.51	.16	.017	.017	.04	.05	.01	.14	198	188	182	510

NOTES : (1) See note (1), Table 4.

(2) Typical all weld metal mechanical properties according to the electrode manufacturers; the figures in brackets correspond to the mechanical properties for the weld metals stress relieved at 600°C.

TABLE 7 - Chemical Composition and Hardness of Manual Metal Arc Welds
Deposited with Specially Manufactured Electrodes

CONSUMABLES (Electrodes)	TEST PLATES (TP)	CHEMICAL COMPOSITION (wt. %)										CARBON EQUIVALENT CE(1)	HARDNESS HV5		
		C	Mn	Si	S	P	Ni	Cr	Mo	Last Run	Middle Runs		Refined Regions		
BASIC															
B1	40	.13	1.26	.18.	.013	.015	.04	.03	.01			.33	245	214	201
B2	41,42	.13	1.29	.22	.013	.014	.67	.03	.01			.40	261	241	223
B3	43	.054	1.03	.18	.013	.012	.04	.05	.70			.37	251	232	225
B4	44	.052	1.04	.17	.014	.012	.69	.03	.31			.34	250	223	218
B5	45,46	.051	1.00	.19	.013	.012	.59	.70	.30			.46	271	242	235
CELLULOSIC															
C1	47	.13	.68	.16	.017	.011	.03	.02	.09			.24	238	219	210
C2	48	.13	.69	.18	.016	.012	.55	.02	.10			.31	241	224	204
C3	49	.12	.38	.11	.016	.010	.03	.02	.35			.25	253	235	210
C4	50	.13	.72	.17	.014	.011	.58	.02	.20			.33	244	237	216
C5	51	.13	.65	.15	.017	.011	.53	.39	.19			.39	317	280	260
ROUTLE															
R1	52	.062	.18	.19	.019	.015	.03	.03	.01			.092	212	188	174
R2	53	.057	.15	.15	.020	.016	.61	.02	.02			.12	214	193	175
R3	54	.039	.19	.16	.018	.014	.03	.02	.64			.20	225	214	188
R4	55	.039	.20	.14	.019	.014	.53	.02	.30			.17	230	207	192
R5	56	.041	.20	.12	.022	.016	.62	.37	.32			.25	241	229	206

NOTE : (1) See note (1), Table 4.

TABLE 8 - Chemical Composition and Hardness of Manual Metal Arc
Welds Deposited with Specially Manufactured Nickel
Bearing Electrodes

CONSUMABLES (Electrodes)	TEST PLATES (TP)	CHEMICAL COMPOSITION (wt %)									CARBON EQUIVALENT CE (1)	HARDNESS HV5		
		C	Mn	Si	S	P	Ni	Cr	Mo	Last Run		Middle Runs	Refined Regions	
B0Ni	57	.043	.85	.11	.009	.011	.04	.03	.01	.20	211	198	186	
B2Ni	58	.037	.65	.10	.009	.009	2.06	.03	.01	.29	239	221	212	
B3Ni	59	.036	.65	.10	.009	.008	3.24	.03	.01	.37	273	241	228	
B4Ni	60,61	.031	.82	.13	.010	.009	4.76	.03	.01	.49 (2)	532	290	250	
B5Ni	62,63 64	.029	.79	.14	.011	.009	5.70	.03	.01	.55 (2)	360	310	282	

NOTE : (1) See Note (1) Table 4.

(2) For the welds with the electrodes B4Ni and B5Ni the figures for CE may be unrealistic; due to the high nickel content the composition is outside the range for which these formulae were developed.

TABLE 9 - Welding Procedures for Tuliani Cracking Tests; Submerged Arc Welds.

WELDING CONDITIONS	TULIANI TEST
- Welding process	Submerged arc welding
- Flux	OP41TT
- Condition of the flux	Baked 16 hours at 150°C, 'as received' and 'damp' (1)
- Wire	SD3 and SD3/1Ni (1) (2)
- Wire diameter	3.2mm
- Electrode extension	38mm
- Type of current and polarity	DC + (electrode positive)
- Current	500 A
- Voltage	30 V
- Welding speed	6.3mm/s (380 mm/min)
- Heat input	2.4 kJ/mm
- Interpass temperature	- 10 and + 20°C (1)
- Cooling medium	Water quenching (3)
- Welding preparation and welding sequence	See figures 12 and 13.
- Welding direction	Reversed after each layer (2 runs)

NOTES : (1) See Table 13 for each particular test.

(2) Wire designations conforming to IIW recommendation.

(3) The exact procedure is specified in Chapter IV, Section 1.1.

TABLE 10 - Welding Procedures for Continuous Water Cooling Cracking Tests; Submerged Arc Welds.

WELDING CONDITIONS	CONTINUOUS WATER COOLING TEST
- Welding process	Submerged arc welding
- Flux	OP41TT
- Condition of the flux	Baked 1 hour at 450°C, 'as received' and 'damp' (1)
- Wire	SD3, S4, SD3/1Ni, SD2/3Ni, SD3/Mo, SD3/1Ni $\frac{1}{2}$ Mo and SD2/1Cr1Ni $\frac{1}{2}$ Mo (1) (2)
- Wire diameter	3.2mm (3)
- Electrode extension	38mm (4)
- Type of current and polarity	DC + (electrode positive)
- Current	500 A
- Voltage	30 V
- Welding speed	6.3mm/s (380 mm/min)
- Heat input	2.4 kJ/mm
- Interpass temperature	18 - 25°C (5)
- Cooling medium	Continuous water cooling
- Cooling water flow rate	15 l/min (in each channel)
- Weld preparation and welding sequence	See figures 16 and 17
- Welding direction	reversed after each layer (2 runs) (6)

NOTES : (1) See Table 14 for each particular test.

(2) Wire designations conforming to IIW recommendation.

(3) In the case of the wire SD2/1Cr1Ni $\frac{1}{2}$ Mo the diameter was 2.5mm.

(4) In the case of the wire SD2/1Cr1Ni $\frac{1}{2}$ Mo the electrode extension was 22 - 25mm.

(5) The interpass temperature was dependent on the cooling water temperature.

(6) In the case of TP18 all runs were deposited in the same direction.

TABLE 11 - Welding Procedures for Continuous Water Cooling Cracking Tests; Manual Metal Arc Welds.

WELDING CONDITIONS	CONTINUOUS WATER COOLING TEST
- Welding process	Manual metal arc welding
- Electrodes	Basic, cellulosic and rutile (1)
- Condition of the electrodes	Baked at 400°C, baked at 300°C, 'as received' and 'damp' (1)(2)
- Electrode diameter	5mm 6mm (3)
- Type of current	AC (4)
- Current	230 - 240 A (5) 280 A (3)
- Voltage	22 - 30 V (6)
- Welding speed	2.3 mm/s (5) (7)
- Heat input	2.4 kJ/mm (7)
- Interpass temperature	18 - 25°C (8)
- Cooling medium	Continuous water cooling
- Cooling water flow rate	15 l/min (in each channel)
- Weld preparation and welding sequence	See figures 16 and 18
- Welding direction	Reversed after each layer (3 runs)

NOTES : (1) See tables 15, 16 and 17 for each particular test.

(2) Baking and moisturizing procedures are specified in Chapter IV, 2.

(3) In the case of the Electrodes E8018C1 from manufacturer B.

(4) Attempts to use DC+ during these tests were unsuccessful due to severe arc blow.

(5) Current and welding speed could be slightly varied, according to the voltage, in order to keep a constant heat input.

(6) The voltage was dependent on the electrode type.

(7) In the case of TP31 the welding speed was 3.5mm/s and the heat input was reduced to 1.6 kJ/mm.

(8) The interpass temperature was dependent on the cooling water temperature.

TABLE 12 - Welding Procedures for Continuous
Water Cooling Cracking Tests; MIG Weld

WELDING CONDITIONS	CONTINUOUS WATER COOLING TEST
- Welding process	MIG welding
- Shielding gas	Argon
- Gas flow rate	20 l/min
- Condition of the gas	Bubbled through a column of water 200mm high (the water was about 20°C)
- Wire	SD3/Mo (1)
- Wire diameter	1.6mm
- Electrode extension	15 - 18mm
- Type of current and polarity	DC + (electrode positive)
- Current	300 A
- Voltage	30 V
- Welding speed	3.8 mm/sec
- Heat input	2.4 kJ/mm
- Interpass temperature	18 - 25°C (2)
- Cooling medium	Continuous water cooling
- Cooling water flow rate	15 l/min (in each channel)
- Weld preparation and welding sequence	See figures 16 and 17
- Welding direction	Reversed after each layer (2 runs)

NOTES : (1) Designation according to IIW recommendation

(2) The interpass temperature was dependent on the cooling water temperature.

TABLE 13 - Incidence of Cracking Identified by Magnetic Particle Inspection (Tuliani Tests TP1-4)

TEST PLATE	CONSUMABLES (Wire + Flux)	Condition of the Flux	Inter- pass Temper- ature	Max. No. of Cracks > 1mm in a Longitudinal Section 100mm Long		Longest Crack (mm)	Average Crack Length (mm)	NOTES
				45°	Vertical			
TP1	SD3 + OP41TT	AR (1)	- 10°C	-	-	-	-	
TP2	SD3/INI + OP41TT	B150°C (2)	- 10°C	2	-	1.5	1	Some fissures <1mm were found
TP3	SD3/INI + OP41TT	D (3)	- 10°C	4	-	1.5	1	Some fissures <1mm (the number was higher than for TP2).
TP4	SD4/INI + OP41TT	D	+ 25°C (4)	7	-	2.0	1	The number of cracks increased towards the ends of the joint where the cooling rate from higher temperatures was faster.

NOTES : (1) AR - 'as received'

(2) B150°C flux baked 16h at 150°C before being used.

(3) D - 'damp' - i.e. flux exposed to the workshop atmosphere for 10 days, with increased moisture content.

(4) This temperature was reached by quenching the joint in water about 20 - 25 seconds after completing each run.

TABLE 14 - Incidence of Cracking Identified by Magnetic Particle Inspection (Continuous Water Cooling Tests TP5 - 27)

TEST PLATE	CONSUMABLES (wire + flux)	Conditions of the Flux	Max. No. of Cracks > 1mm in a Longitudinal Section 100mm Long		Longest Crack (mm)	Average Crack Length (mm)	NOTES
			45°	Vertical			
TP5	SD3 + OP41TT	B450°C (1)	-	-	-	-	Some fissures < 1mm were found As above
TP6	SD3 + OP41TT	AR (2)	2	-	2	2	
TP7	SD3 + OP41TT	D (3)	10	-	4.5	3	
TP8	S4 + OP41TT	B450°C	-	-	-	-	As above
TP9	S4 + OP41TT	D	13	-	3.5	2.5	
TP10	SD3/INI + OP41TT	B450°C	-	-	-	-	As above
TP11	SD3/INI + OP41TT	AR	4	-	1	1	
TP12	SD3/INI + OP41TT	D	16	-	4.5	2.5	Tensile test specimens were machined from this weld metal As above Some fissures < 1mm
TP13	SD2/3NI + OP41TT	B450°C	-	-	-	-	
TP14	SD2/3NI + OP41TT	B450°C	-	-	-	-	
TP15	SD2/3NI + OP41TT	B450°C	-	-	-	-	As above
TP16	SD2/3NI + OP41TT	AR	10	-	2.5	1	
TP17	SD2/3NI + OP41TT	D	45	-	4.5	3	All runs were deposited in the same direction. Test monitored by acoustic emission.
TP18	SD2/3NI + OP41TT	D	25	-	6	3.5	
TP19	SD3/No + OP41TT	B450°C	-	-	-	-	Some fissures < 1mm As above
TP20	SD3/No + OP41TT	AR	6	-	3.5	2	
TP21	SD3/No + OP41TT	D	27	-	7	3.5	As above
TP22	SD3/INI/No + OP41TT	B450°C	-	-	-	-	
TP23	SD3/INI/No + OP41TT	AR	-	12	2	1	As above
TP24	SD3/INI/No + OP41TT	D	-	25	3	2	
TP25	SD2/ICr1Ni1/2Mo + OP41TT	B450°C	-	-	-	-	As above
TP26	SD2/ICr1Ni1/2Mo + OP41TT	AR	-	10	8	1.5	
TP27	SD2/ICr1Ni1/2Mo + OP41TT	D	-	33	10	2.5	

NOTES: (1) 450°C - flux baked for 1 hour at 450°C before being used.

(2) AR - 'as received'.

(3) D - 'damp', i.e. flux exposed to the workshop atmosphere for 10 days, with increased moisture content.

TABLE 15 - Incidence of Cracking Identified by Magnetic Particle Inspection (Continuous Water Cooling Tests, TP28-39)

TEST PLATE	CONSUMABLES (Electrodes)	Condition of the Electrodes	Max. No. of Cracks > 1mm in a Longitudinal Section 100mm Long		Longest Crack (mm)	Average Crack Length (mm)	NOTES
			45°	vertical			
TP28	E8018 C1 (from manufacturer A)	B400°C(1)	3	-	3	1.5	Some fissures <1mm were found
TP29	As above	B300°C(1)	14	-	3.5	2.	Some fissures <1mm (the number was higher than for TP28)
TP30	As above	B300°C	12	-	2.5	1.5	As above
TP31	As above	AR (2)	12	-	3.5	2.0	Large number of fissures <1mm
TP32	As above	AR	8	-	3.	1.5	As above
TP33	As above	AR	5	-	2.5	2	As above. In this case only half of the joint was filled.
TP34	As above	D (3)	2	-	2.5	2.5	Low number of 45° cracks but very large number of fissures <1mm
TP35	E8018 C1 (from manufacturer B)	AR	20	-	6	3	Large number of fissures <1mm (especially on runs not containing chevron cracks)
TP36	Batch 2	B300°C	-	-	-	-	A few fissures <1mm
TP37	Batch 2	AR	4	-	2	1.5	Some fissures <1mm (the number was higher than for TP35).
TP38	Batch 2	D	-	-	-	<1	No 45° cracks but very large number of fissures <1mm and porosity.
TP39	E8013	AR	-	-	-	<1	Very large number of fissures and porosity.

NOTES : (1) B400°C and B300°C - electrodes baked for 1 hour at 400°C or 300°C, respectively, before testing.

(2) AR - 'as received'.

(3) D - 'damp' electrodes, i.e. electrodes exposed to the workshop atmosphere for 10 days, with high moisture content in the coating.

TABLE 16 - Incidence of Cracking Identified by Magnetic Particle Inspection (Continuous Water Cooling Tests, TP 40 - 56)

TEST PLATE	CONSUMABLES (Electrodes)	Condition of the Electrodes	Max. No. of Cracks > 1mm in a Longitudinal Section 100mm long		Longest Crack (mm)	Average Crack Length (mm)	NOTES
			45°	Vertical			
<u>Basic</u>							
TP40	B1	AR (1)	28	-	4	2	Large number of fissures < 1mm (especially on runs not containing chevron cracks).
TP41	B2	B400°C (2)	-	-	-	-	
TP42	B2	AR	35	-	4.5	2.5	As above
TP43	B3	AR	3	-	3	1.5	Large number of fissures < 1mm
TP44	B4	AR	3	2	3	2	As above
TP45	B5	B400°C	-	7	3	1	
TP46	B5	AR	-	12	7	1.5	Large number of fissures < 1mm
<u>Cellulosic</u>							
TP47	C1	AR	24	-	31	8	Large number of fissures < 1mm (especially on runs not containing longer cracks)
TP48	C2	AR	45	-	9	3.5	As above
TP49	C3	AR	7	-	5.5	3	As above
TP50	C4	AR	45	-	9	3.5	As above
TP51	C5	AR	-	50	34	2.5	As above
<u>Rutile</u>							
TP52	R1	AR	-	-	≅1	<1	Large number of fissures < 1mm, porosity and slag inclusions
TP53	R2	AR	-	-	≅1	<1	As above
TP54	R3	AR	-	-	≅1	<1	As above
TP55	R4	AR	-	7	7	2	As above
TP56	R5	AR	-	18	2.5	2	As above

NOTES: (1) AR - 'as received'.

(2) B400°C - electrodes baked for 1 hour at 400°C before testing.

TABLE 17 - Incidence of Cracking Identified by Magnetic Particle Inspection (Continuous Water Cooling Tests, TP57 - 60, 62 and 63)

TEST PLATE	CONSUMABLES (Electrodes)	Condition of the Electrodes	Max. No. of Cracks > 1mm in a Longitudinal Section 100mm Long		Longest Crack (mm)	Average Crack Length (mm)	NOTES
			45°	Vertical			
TP57	B0N1	AR(2)	-	-	<1	<1	Large number of fissures <1mm.
TP58	B2N1	AR	10	-	3.5	2	As above
TP59	B3N1	AR	10	1	2	1.5	As above
TP60	B4N1	AR	-	85	6	2.0	As above
TP61(1)	B4N1	B400°C(3)	-	11	3	1.5	A few fissures <1mm
TP62	B5N1	AR	-	145	10	2.5	
TP63	B5N1	B400°C	-	40	33	3	Some fissures <1mm
TP64(1)	B5N1	B400°C	-	16	3.5	2	A few fissures <1mm

NOTES (1) In this case the joint was not water cooled and the interpass temperature was 120°C; the dimensions of the parent plates, weld preparation and welding sequence were the same as for the Tulliani test.

(2) AR - 'as received'

(3) B400°C - electrodes baked for 1 hour at 400°C before testing.

TABLE 18 - Incidence of Cracking Identified by Magnetic Particle Inspection (Continuous Water Cooling Test, TP65)

TEST PLATE	CONSUMABLES (wire + shielding gas)	Condition of the Shielding Gas	Max. No. of Cracks > 1mm in a Longitudinal Section 100mm Long		Longest Crack (mm)	Average Crack Length (mm)	NOTES
			45°	Vertical			
65	SD3/No + Argon	Bubbled through a 200mm column of water at room temp- erature	-	45	5	1	The test was abandoned when the joint was about 1 filled due to very severe porosity problems, small fissures, <1mm, were also found.

TABLE 19 - Diffusible Hydrogen Levels for Weld Deposits with Manual Metal Arc Electrodes

ELECTRODE TYPE	ELECTRODE CONDITION	DIFFUSIBLE HYDROGEN ⁽¹⁾ (cc H ₂ /100g weld metal)
<u>Commercially available</u>		
E8018 C1 (from manufacturer A)	B400°C(2)	6.5
	B300°C(2)	8.5
	AR (3)	12.5
	D (4)	18.8
E8018 C1 (from manufacturer B)		
Batch 1	AR	17.4
Batch 2	AR	13.4
<u>Special Batches</u>		
<u>Basic</u>		
B1	AR	12.2
	B400°C	7.3
B3	AR	14.2
B4	AR	14.1
	B400°C	6.4
<u>Cellulosic</u>		
C1	AR	43.7
C2	AR	38.7
C3	AR	72.0
C4	AR	46.5
C5	AR	58.8
<u>Rutile</u>		
R4	AR	36.9
R5	AR	42.2

(1) According to the BS639 method.

(2) B400°C and B300°C, electrodes baked for 1 hour at 400°C and 300°C, respectively, before testing.

(3) AR - 'as received'.

(4) D - 'damp' electrodes, i.e. electrodes exposed to the workshop atmosphere, for 10 days, with high moisture content in the coating.

TABLE 20 - Moisture in the Submerged Arc Welding
Flux and Corresponding Weld Metal
Diffusible Hydrogen Levels

FLUX IDENTITY (Batch)	CONDITION OF THE FLUX	% H ₂ O (1) (at 1000°C)	DIFFUSIBLE HYDROGEN (2) (cc H ₂ /100g weld metal)
OP41TT	(037038) B450°C (3)	0.020	2.5
	AR (4)	0.033	3.7
	D (5)	0.057	6.2
OP41TT	(036014) D (5)	0.052	6.9

NOTES (1) Determined by the Gayley Wooding method.

(2) Determined according to a method similar to the one used
for the manual metal arc deposits.

(3) B450°C - flux baked for 1 hour at 450°C.

(4) AR - 'as received'.

(5) D - 'damp', i.e. flux exposed to the workshop atmosphere for
10 days, with increased moisture content.

TABLE 21 - Mechanical Properties of Hydrogen Charged Tensile Specimens Machined with the Axis at 45° with the Welding Direction

SPECIMEN NO.	CHARGING TIME (hrs)	Y.S. ₂ (N/mm ²)	U.T.S. ₂ (N/mm ²)	El% (l ₀ = 3.5d)	R.A.%	NOTES
1	24	-	560	-	-	(2)
2	0	550	620	28	67	(3)
3	48	560	620	24	63	(3)(4)
4	48	-	580	7	19	(3)
5	24	-	590	-	-	(5)

NOTES (1) The current density was 80 mA/cm²

(2) Specimen type Hounsfield No. 14. The specimen failed in the region of the shoulder thus no elongation (El%) or reduction of area (R.A.%) were considered.

(3) Specimen dimensions according to Figure 22a .

(4) There was an equipment fault during charging which probably resulted in a much lower charge than expected.

(5) Notched specimen, dimensions according to Figure 22b .

TABLE 22 - Mechanical Properties of Hydrogen Charged Tensile Specimens Machined with the Axis Parallel to the Welding Direction

SPECIMEN NO.	CHARGING TIME (hrs)	Y.S. ₂ (N/mm ²)	U.T.S. ₂ (N/mm ²)	El% (l ₀ = 3.5d)	R.A.%	NOTES
6	0	560	650	27	69	(2)
7	4	580	620	23	37	(2)
8	24	580	620	18	24	(2)
9	48	-	430	-	=0	(2)

NOTE (1) The current density was 80 mA/cm²

(2) Specimen type Hounsfield No. 14.

FIGURES

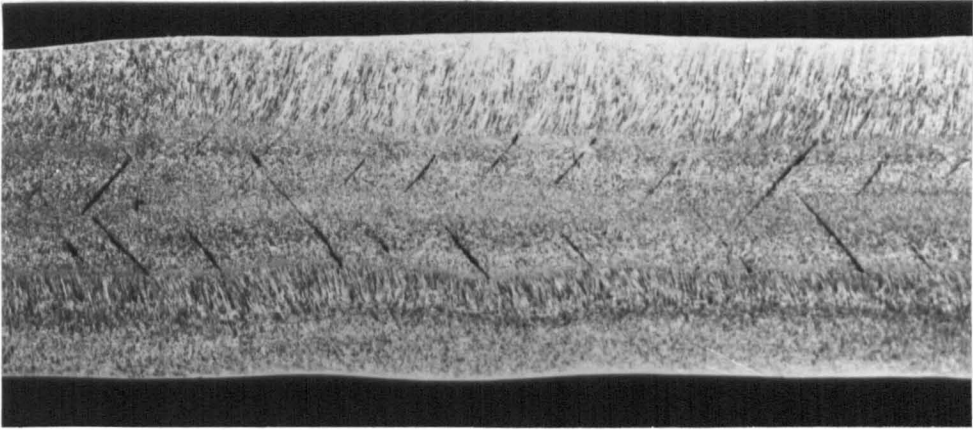
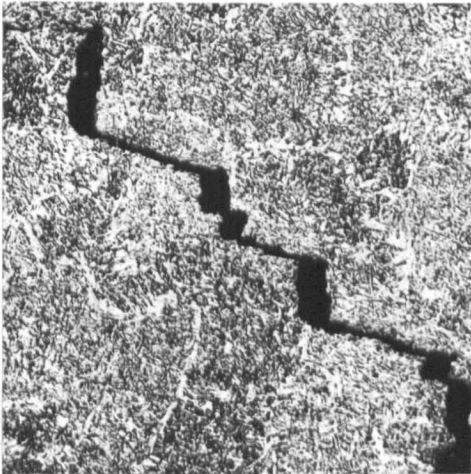


Figure 1 - Typical example of chevron cracking in a longitudinal section of an industrial sample. 1x.



(a)



(b)

Figure 2 - Details of a chevron crack.

- (a) Longitudinal section observed in the light microscope. 200x.
- (b) Fracture surface observed in the scanning electron microscope (from a direction perpendicular to the horizontal components). 80x.

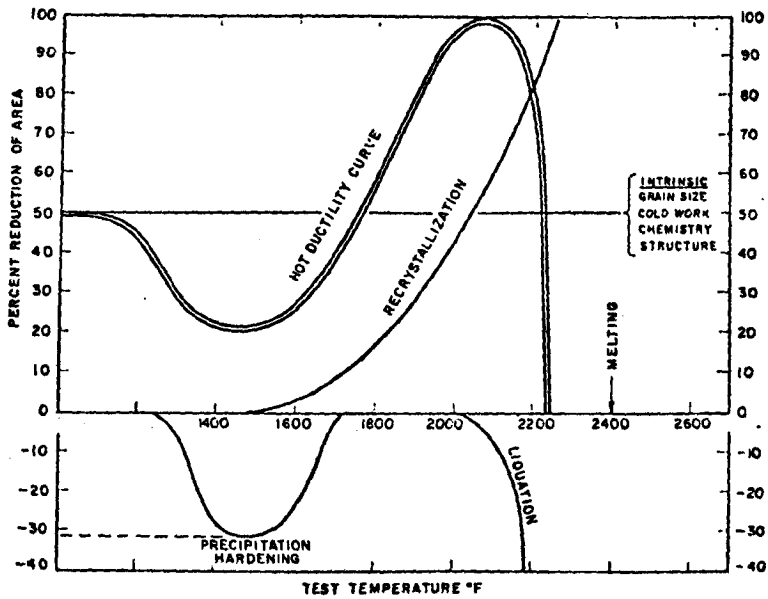
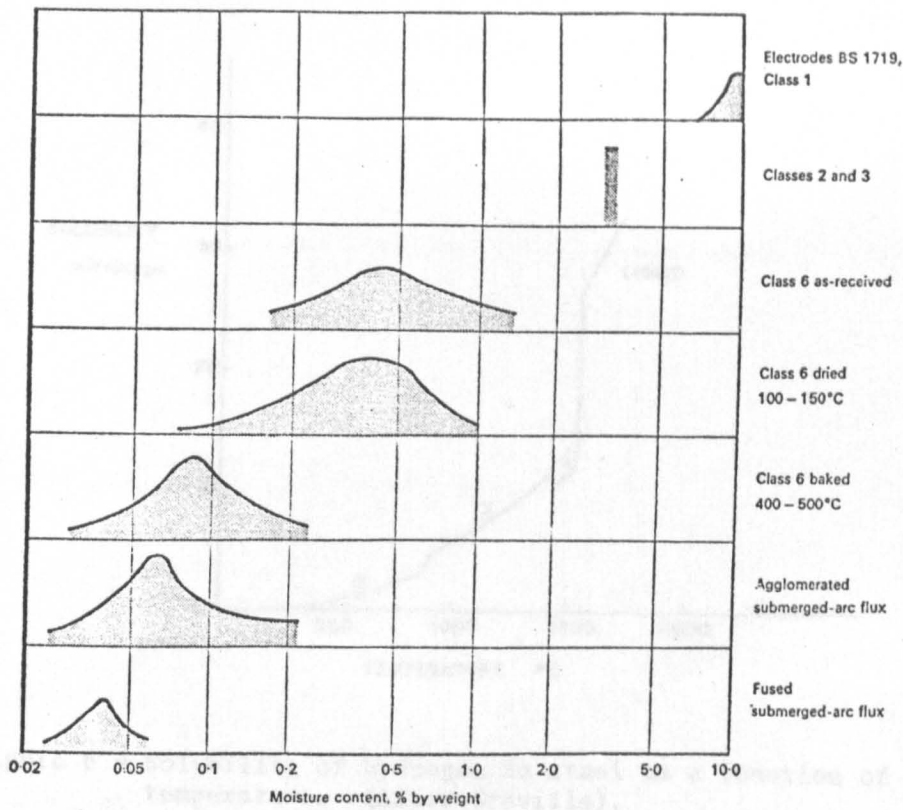
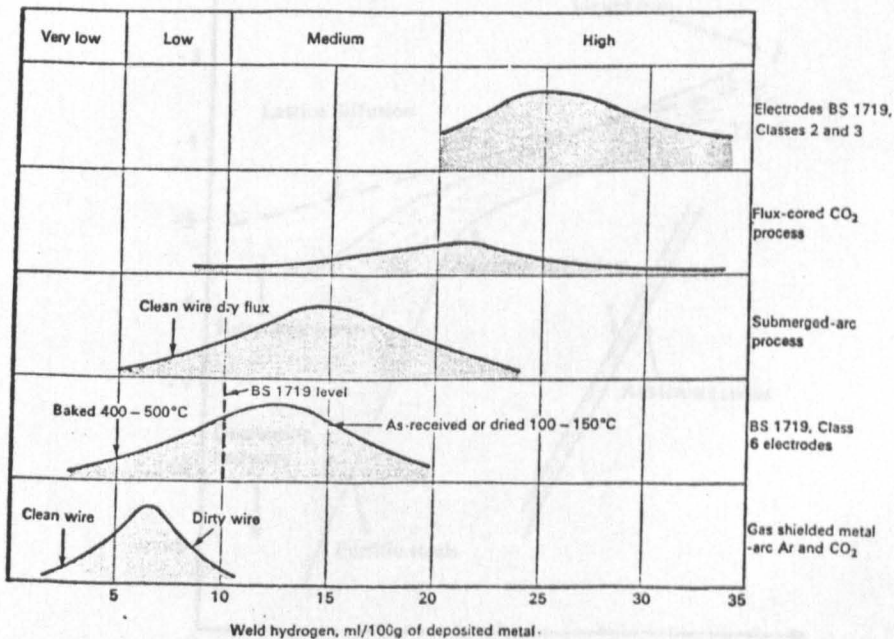


Figure 3 - Hypothetical hot ductility curve along with individual contributions which combine to make the curve.
(After Yeniscavich).



Note : Heights of curves indicate relative frequency of test results for each type of consumable.

Figure 4 - Typical potential hydrogen levels (moisture levels in coatings and fluxes). (After Coe).



Note: BS 1719, Class 1 electrodes cannot be shown on this diagram as they normally give weld hydrogen levels of between 70 and 100ml/100g. (Heights of curves indicate relative frequency of test results for each type of consumable)

Figure 5 - Typical hydrogen levels in weld metals deposited with different types of consumables. (After Coe).

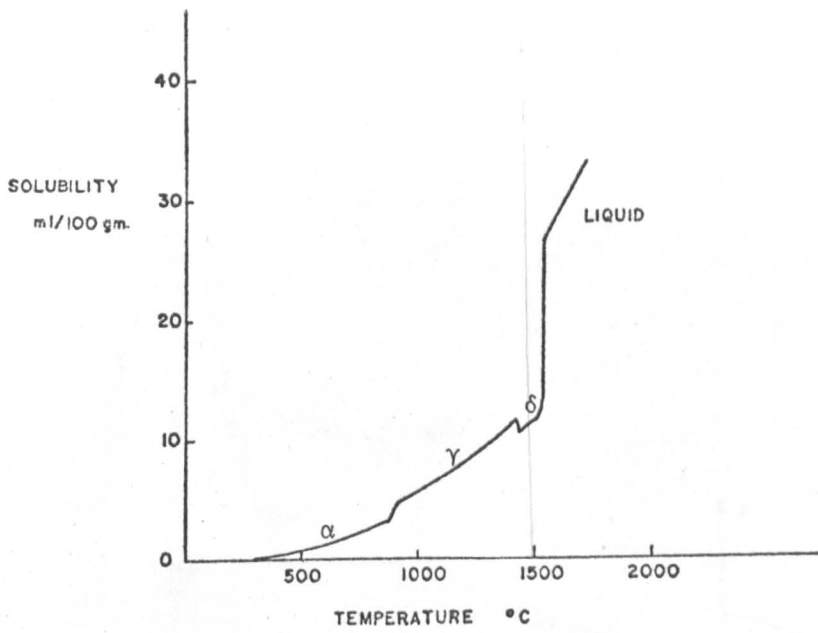


Figure 6 - Solubility of hydrogen in steel as a function of temperature. (After Graville).

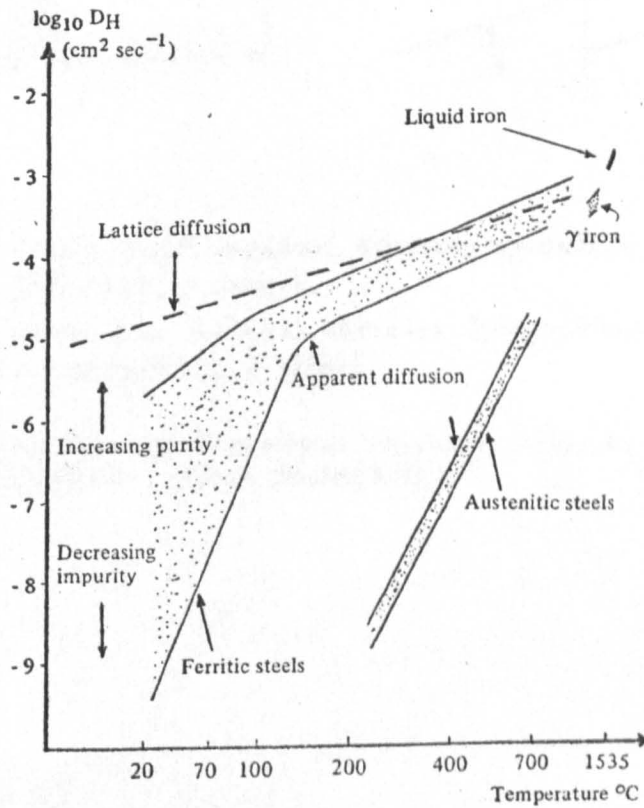
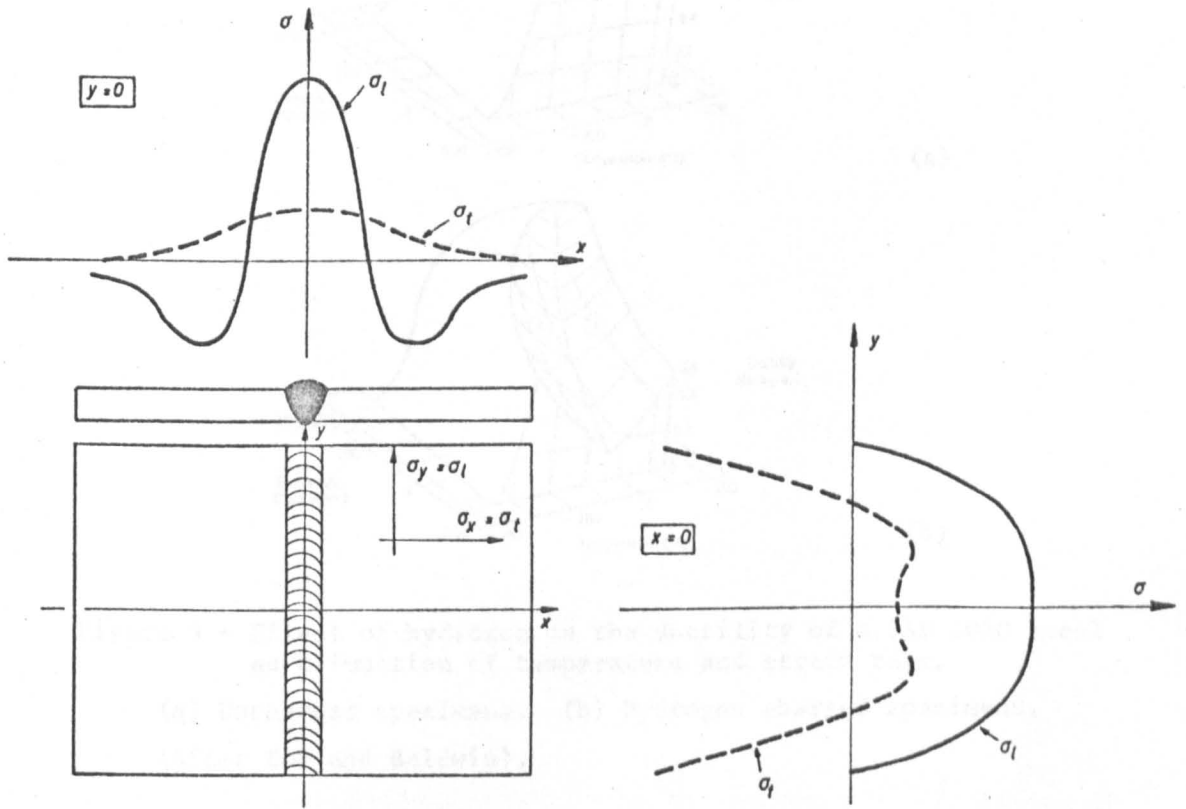


Figure 7 - Variation of overall hydrogen diffusivity coefficient, D_H , with temperature, for different steels. (After Coe).



Note : σ_l - longitudinal residual stresses (parallel to the welding direction, y axis).
 σ_t - transverse residual stresses (perpendicular to the welding direction, x axis).

Figure 8 - Distribution of residual stresses owing to shrinkage in a butt weld. (After Macherauch).

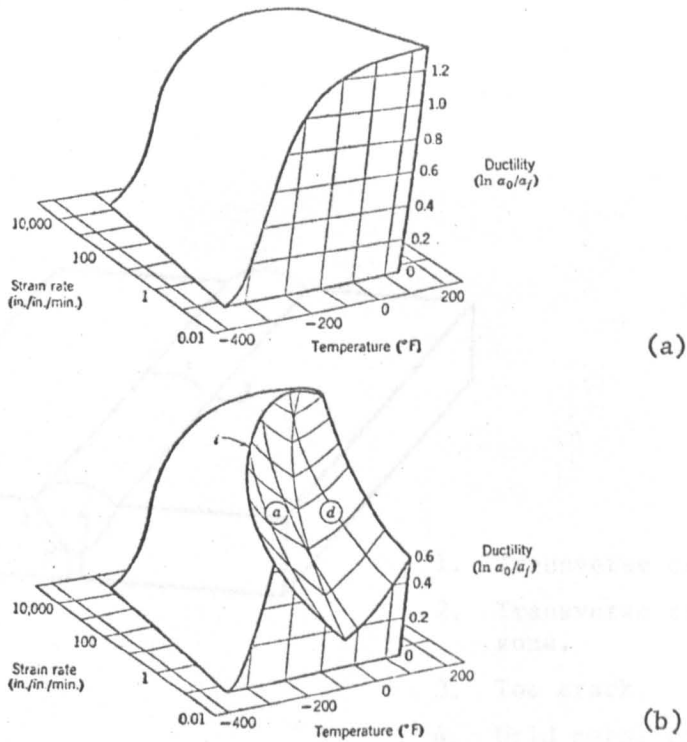


Figure 9 - Effect of hydrogen on the ductility of a SAE 1020 steel as a function of temperature and strain rate.

(a) Uncharged specimens. (b) Hydrogen charged specimens.
(After Toh and Baldwin).

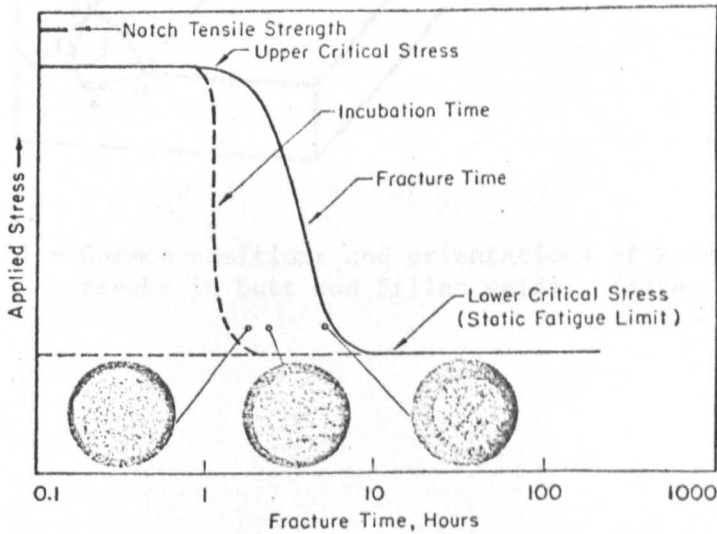
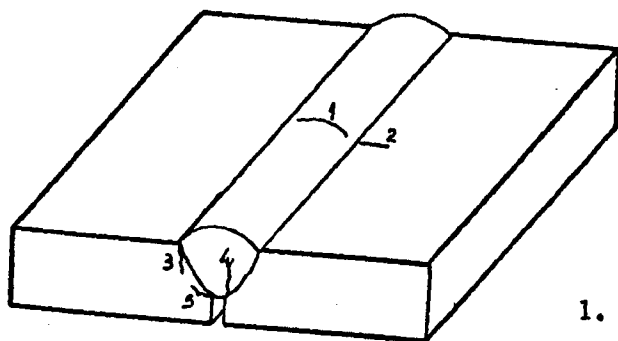


Figure 10 - Schematic representation of failure characteristics of a hydrogenated high strength steel. (After Troiano).



1. Transverse crack in weld metal.
2. Transverse crack in heat affected zone.
3. Toe crack.
4. Weld metal crack (longitudinal).
5. Root crack.
6. Underbead crack.

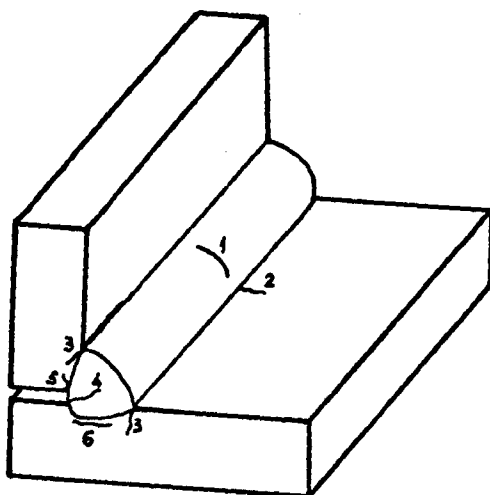
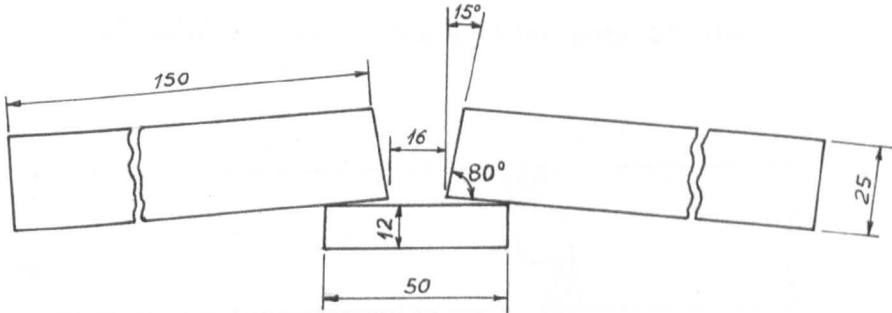
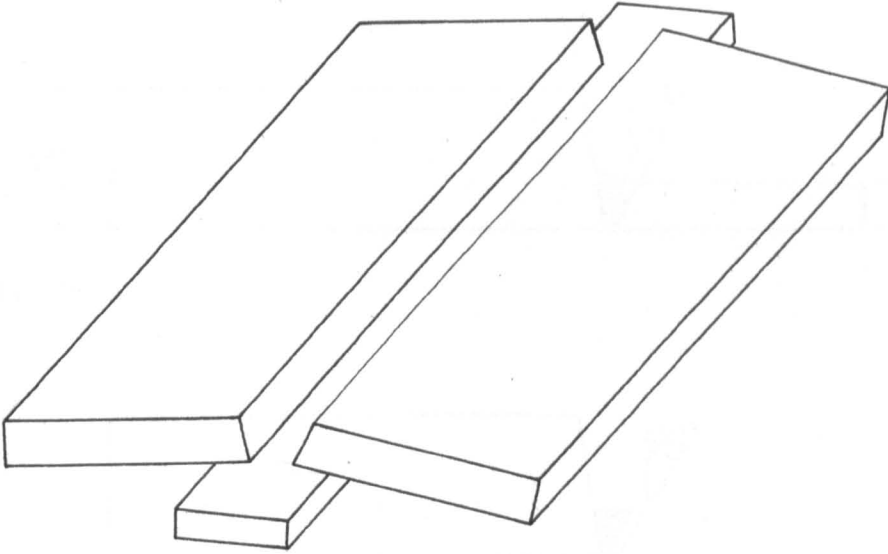


Figure 11 - Common positions and orientations of hydrogen induced cold cracks in butt and Fillet welds. (After Graville).



Note : All dimensions are in millimetres. The plates were 380mm long.
Figure 12 - Weld preparation for the Tuliani test.

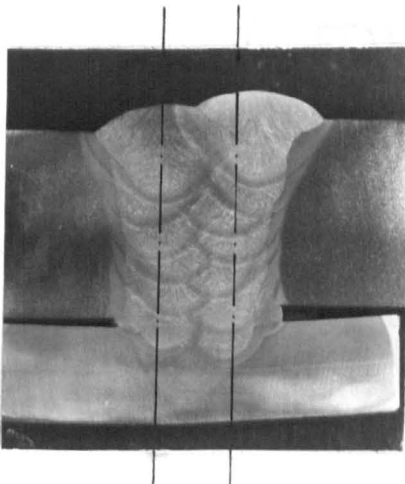
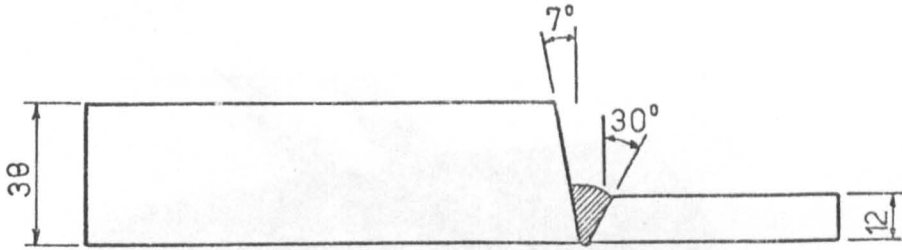
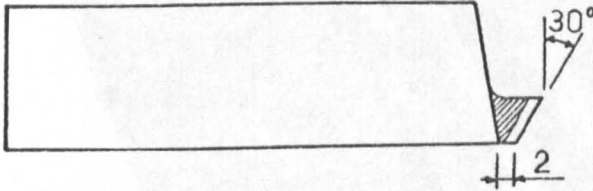


Figure 13 - Cross section of the joint after completing the weld.
Tuliani test, 1x.

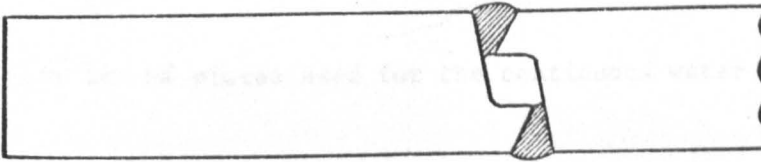


1. Weld.

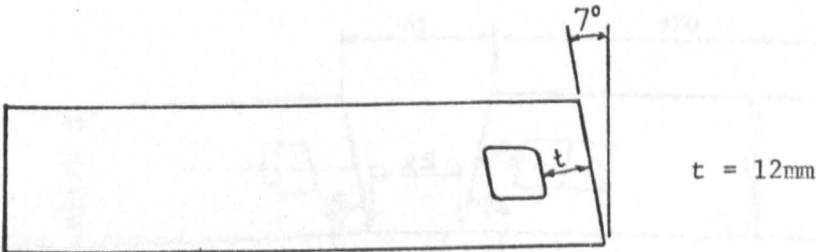


2. Oxi-cut and grind.

3. Repeat operations 1 and 2 for another pair of plates.



4. Weld.



5. Oxi-cut and grind the cut surface and excess weld.

6. Braze nozzles on each side of the plate as shown in Figure 15.

Figure 14 - Preparation of a channel in a plate for the continuous water cooling test.

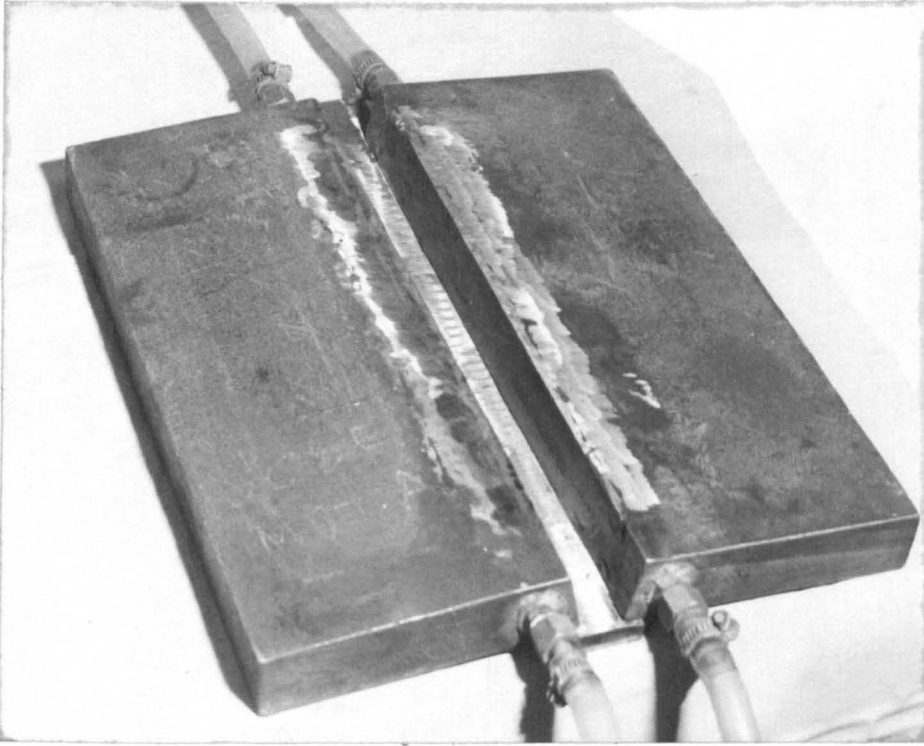
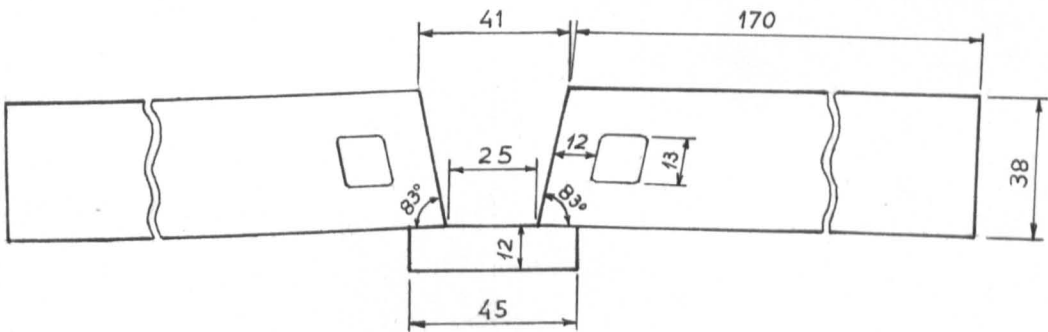
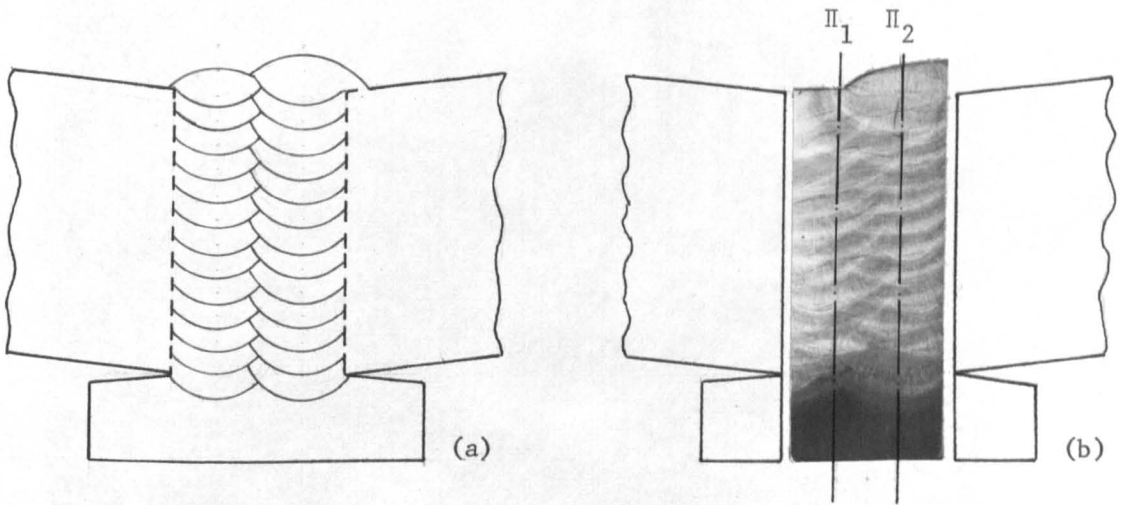


Figure 15 - Set of plates used for the continuous water cooling test.



Note : All the dimensions are in millimetres. The plates were 450mm long.

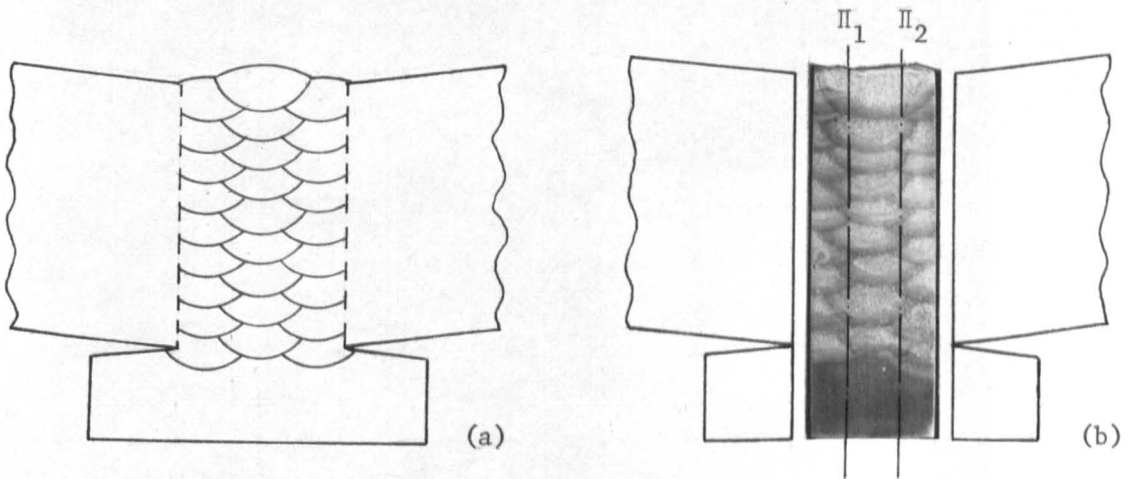
Figure 16 - Weld preparation used for the continuous water cooling test.



Note : The weld metal was subsequently sectioned through the planes Π_1 and Π_2 .

Figure 17 - (a) Welding sequence adopted for the series of submerged arc welds.

(b) Cross section of the weld metal and backing bar. 1x.



Note : The weld metal was subsequently sectioned through the planes Π_1 and Π_2 .

Figure 18 - (a) Welding sequence adopted for the series of manual metal arc welds.

(b) Cross section of the weld metal and backing bar. 1x.

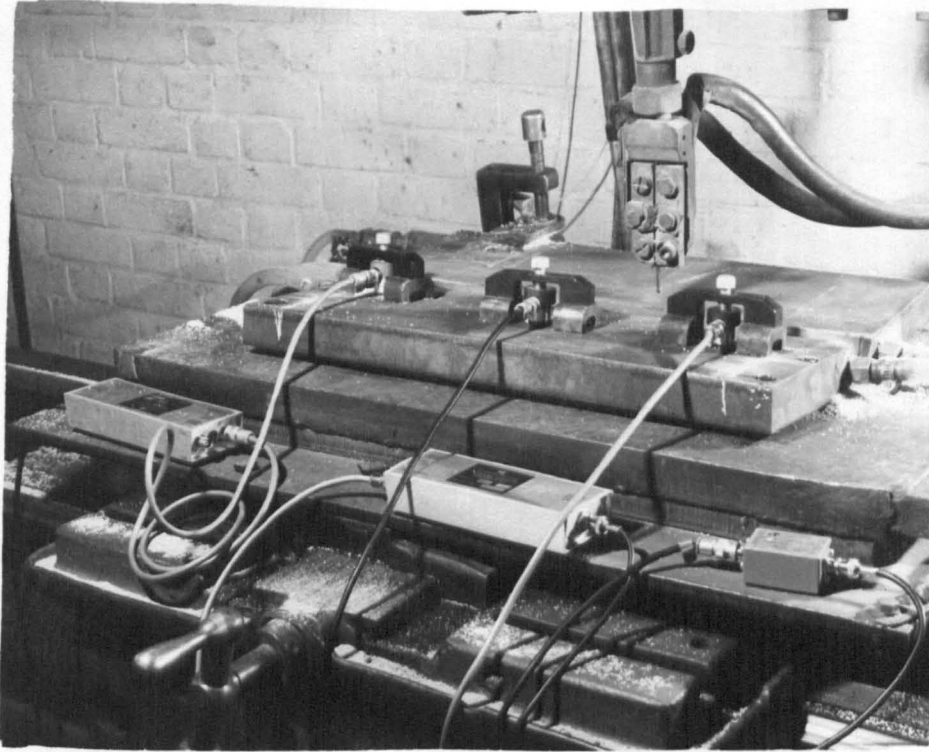


Figure 19 - Test plates with acoustic emission transducers to detect the occurrence of cracks in the deposited weld metal.

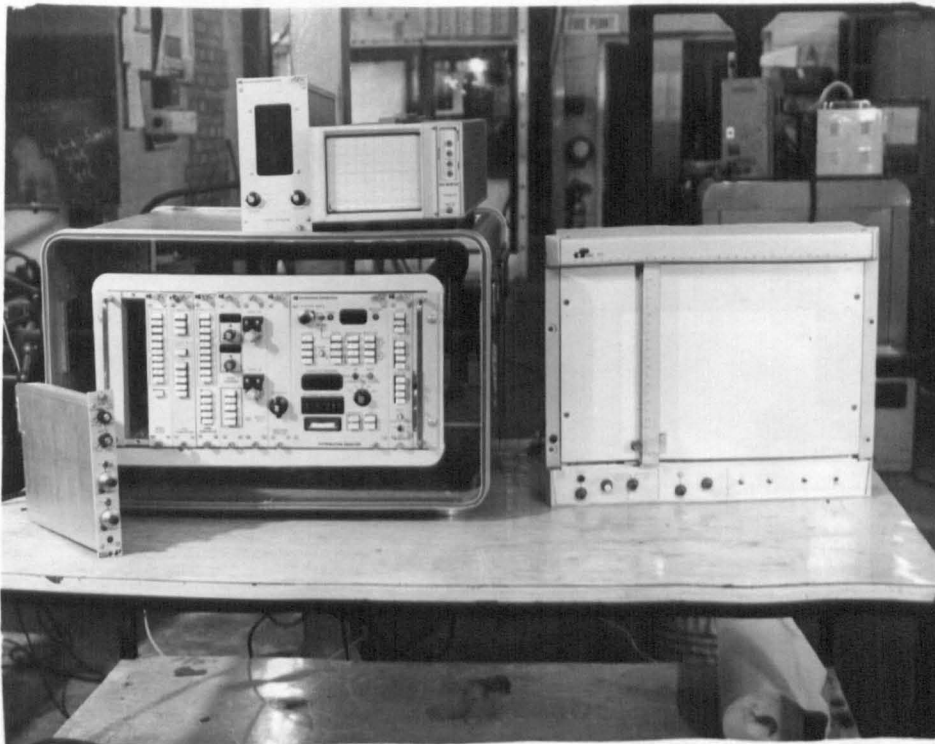


Figure 20 - Equipment used for the acoustic emission monitoring.

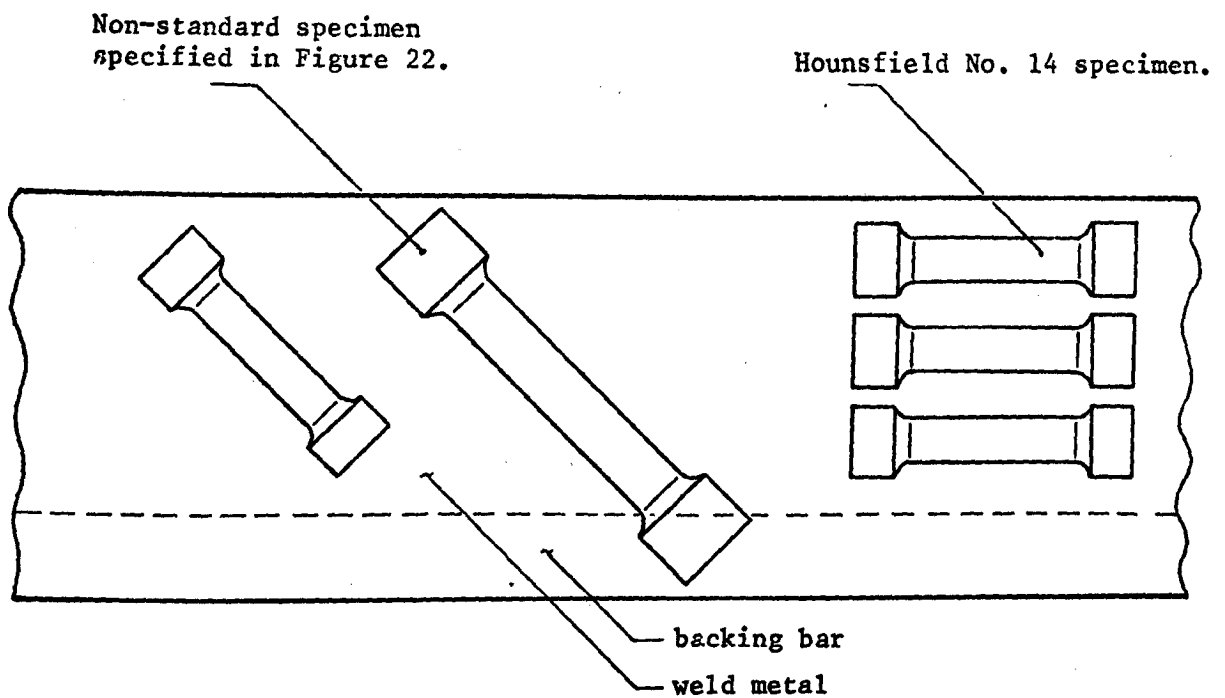
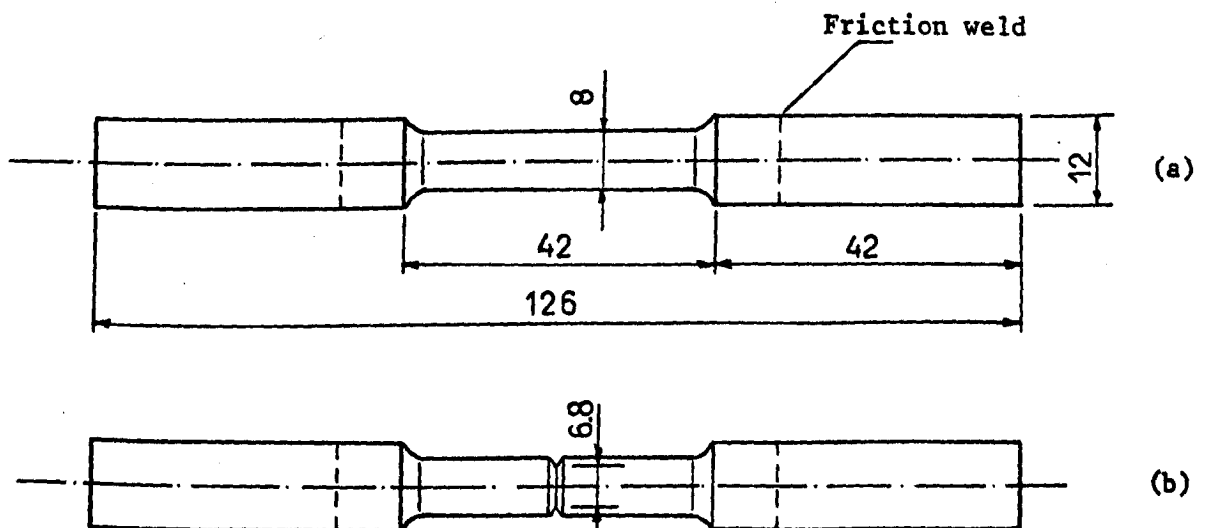


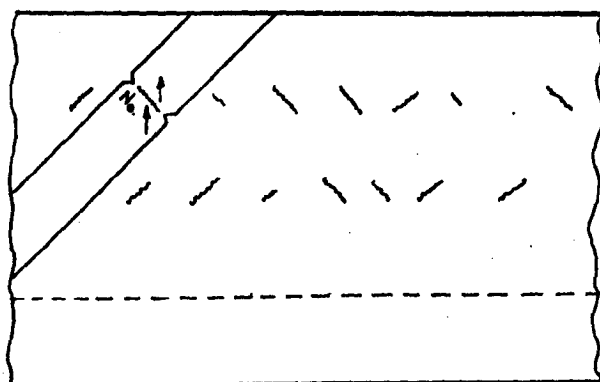
Figure 21 - Type and location of the tensile specimens in the section of weld metal.



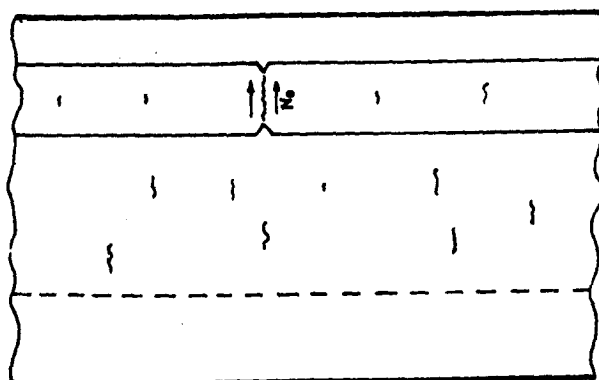
Note : All dimensions are in millimetres.

Figure 22 - (a) Dimensions of the non-standard weld metal tensile specimen.

(b) Detail of the notch used in one specimen.



(a)



(b)

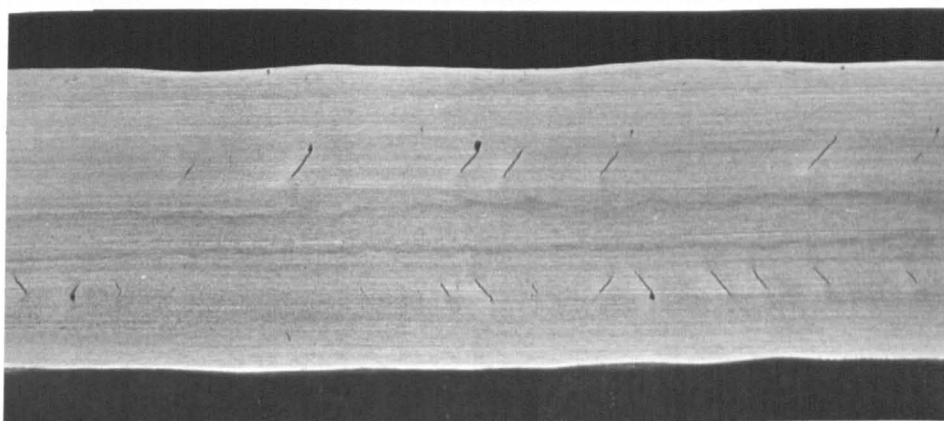
Figure 23 - Sectioning of weld metal specimens to prepare fracture surfaces to be examined in the scanning electron microscope.

(a) Chevron crack.

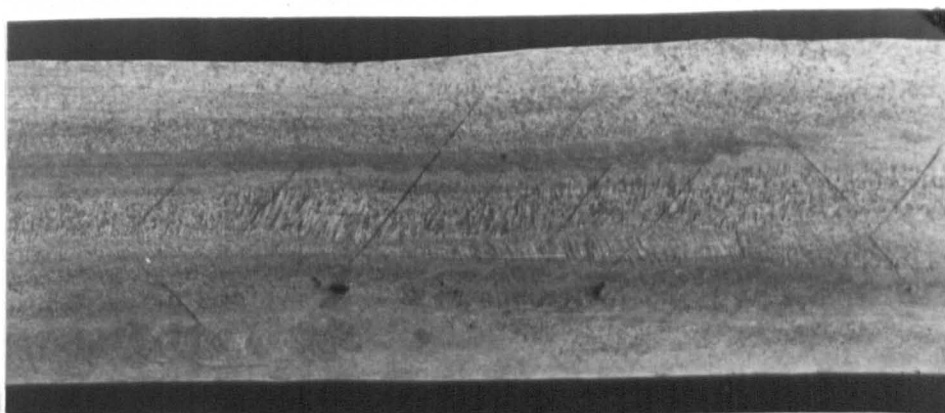
(b) Vertical crack.



(a)



(b)



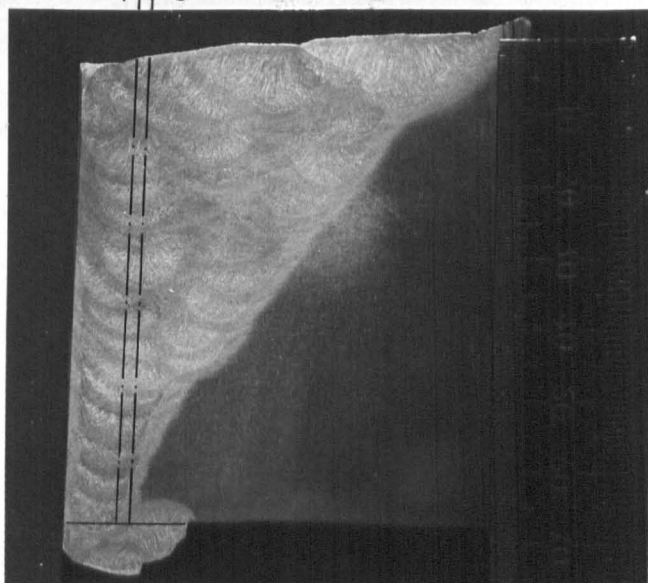
(c)

Figure 24 - Chevron cracks in the industrial sample A.

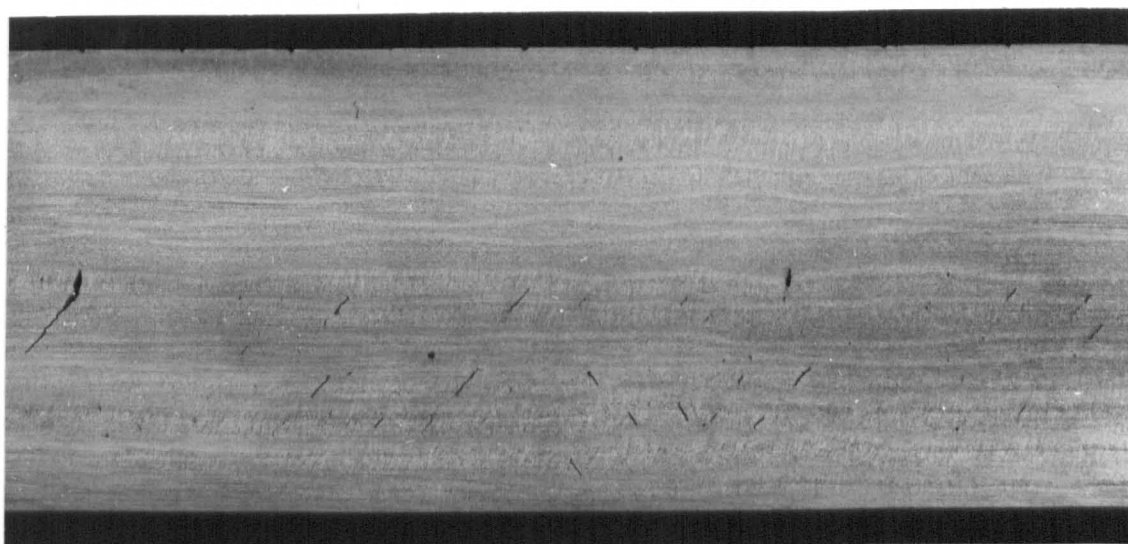
(a) Cross section of the joint where the cracks were found. 1x.

(b) Longitudinal section showing cracks of typical size. 1x.

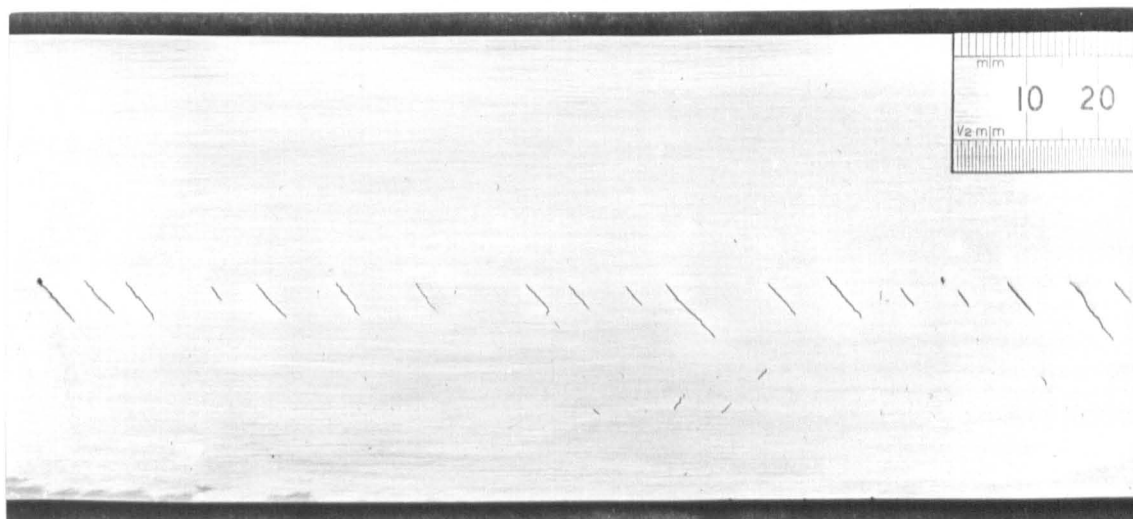
(c) Longitudinal section showing the longest cracks found. 1x.



(a)



(b)



(c)

Figure 25 - Chevron cracks in the industrial sample B.

(a) Cross section of the joint where the cracks were found. 1x.

(b) Longitudinal section corresponding to the plane π_1 . 1x.

(c) Longitudinal section corresponding to the plane π_2 . 1x.

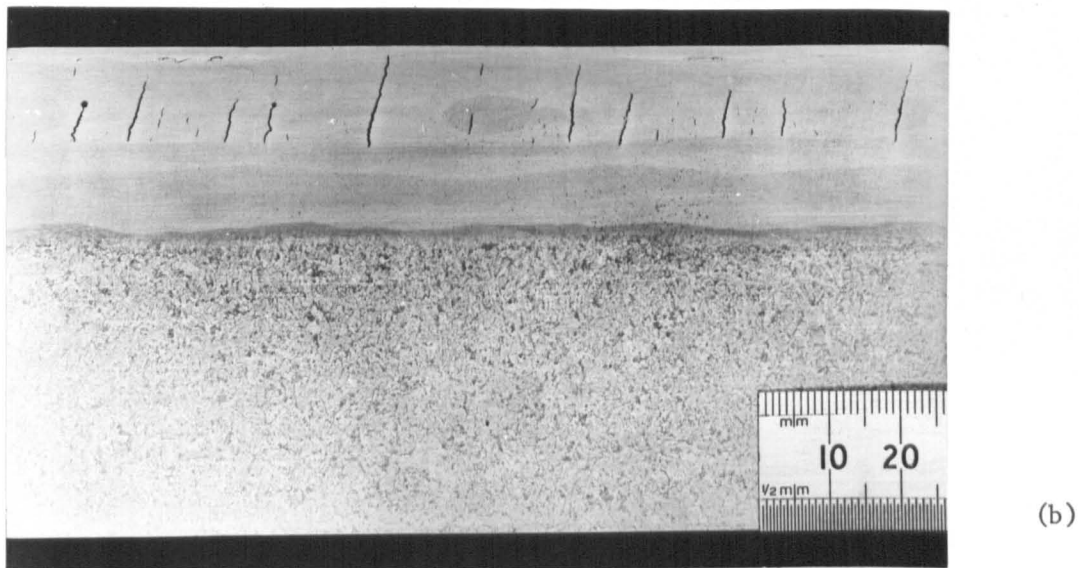
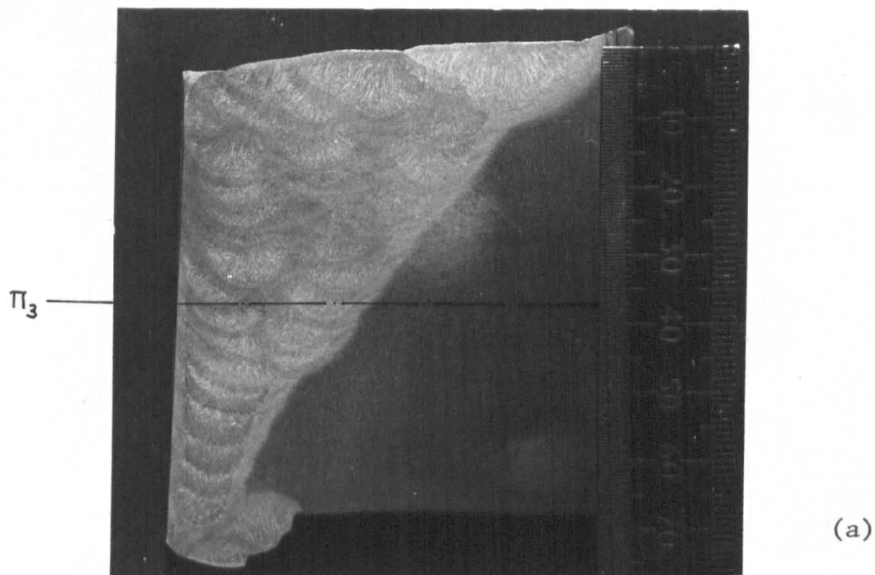


Figure 26 - Chevron cracks in the industrial sample B

- (a) Cross section of the joint where the cracks were found. 1x.
- (b) Longitudinal-horizontal section (corresponding to the plane Π_3). 1x.

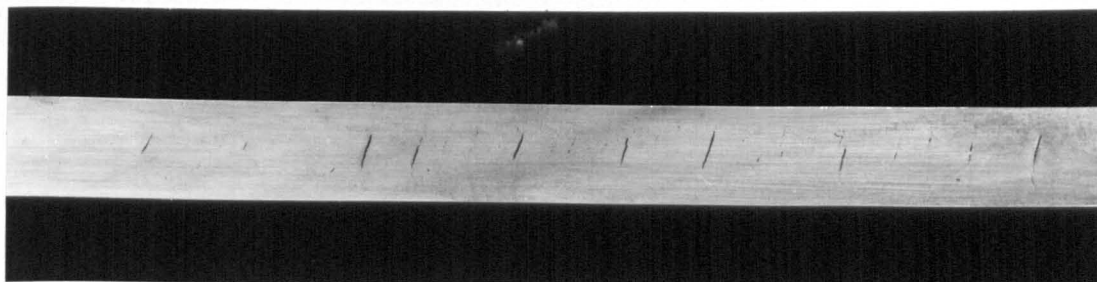
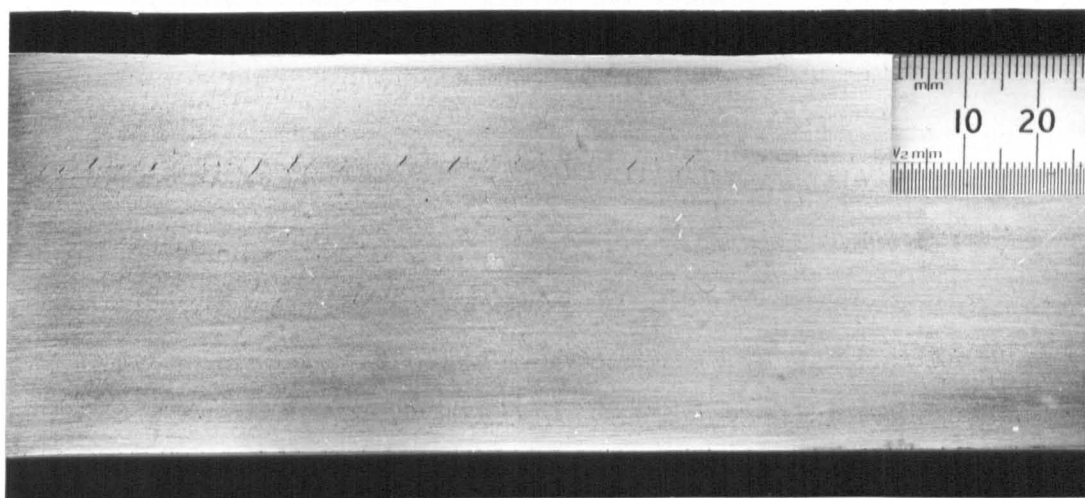
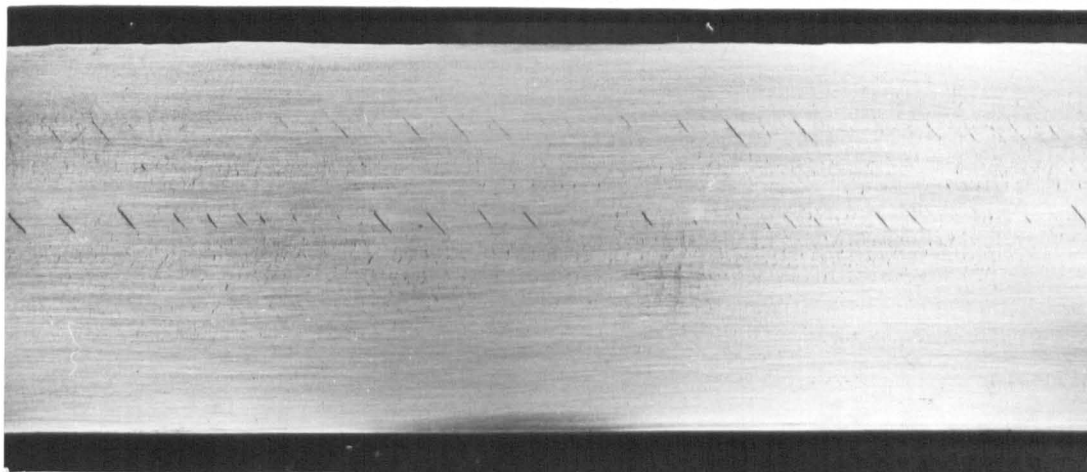


Figure 27 - Chevron cracks in a longitudinal horizontal section (parallel to the plane of the plates). Submerged arc weld with the wire-flux combination SD2/3Ni + OP41TT. TP17. 1x.



(a)



(b)

Figure 28 - Chevron cracks in submerged arc welds

(a) Deposited with the wire-flux combination S4 + OP41TT. TP9. 1x.

(b) Deposited with the wire-flux combination SD3/Mo + OP41TT. TP21. 1x.

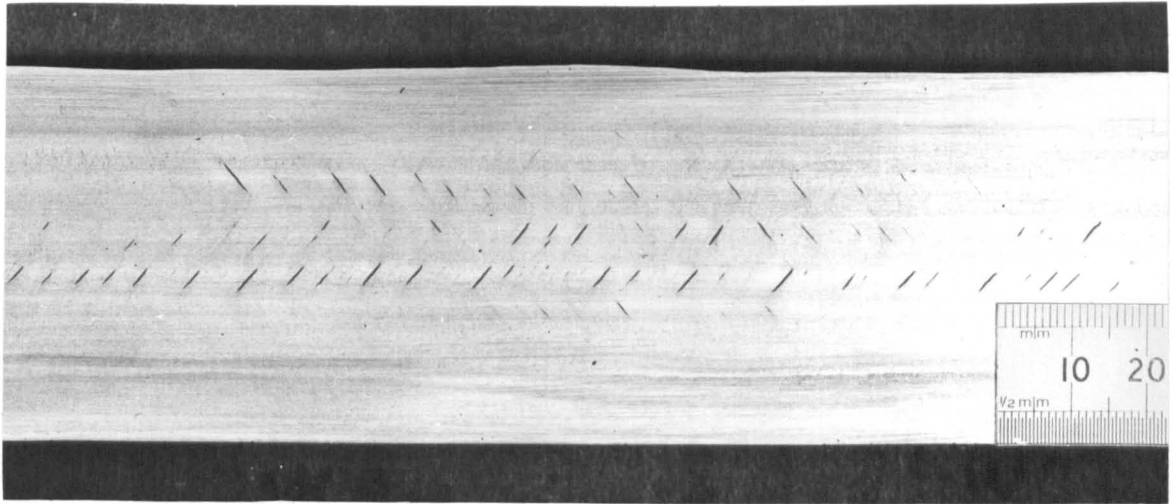


Figure 29 - Chevron cracks in a submerged arc weld deposited with the wire-flux combination SD2/3Ni + OP41TT. TP17. 1x.

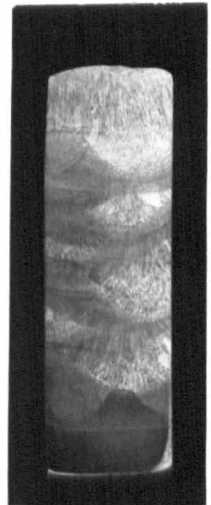
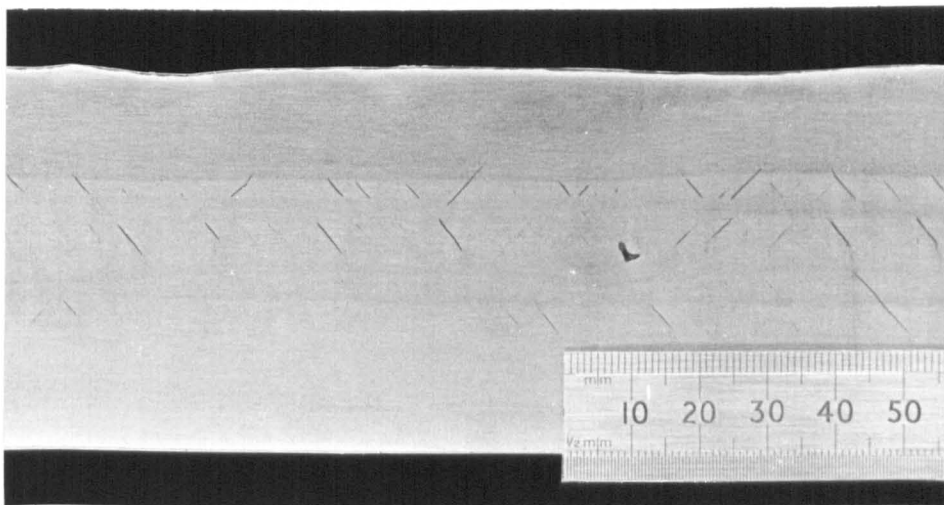
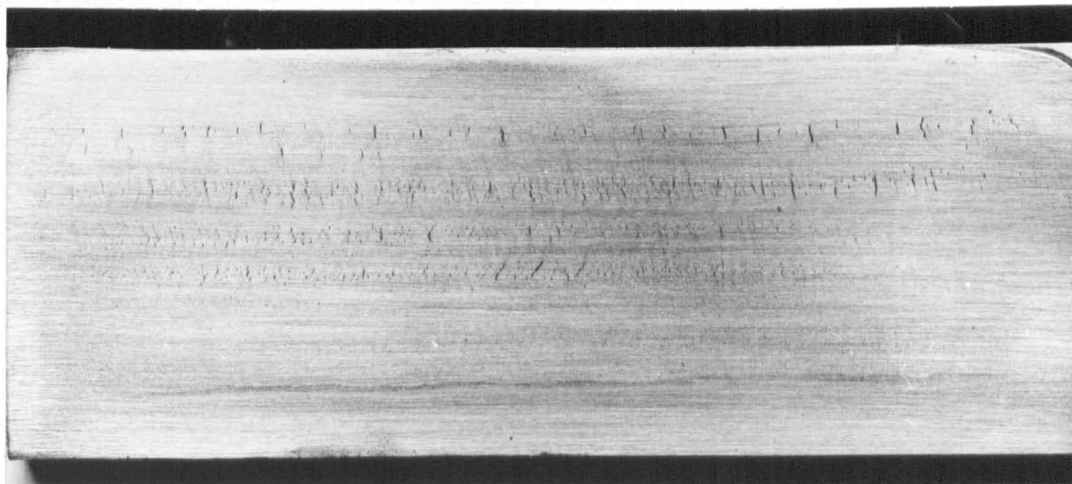
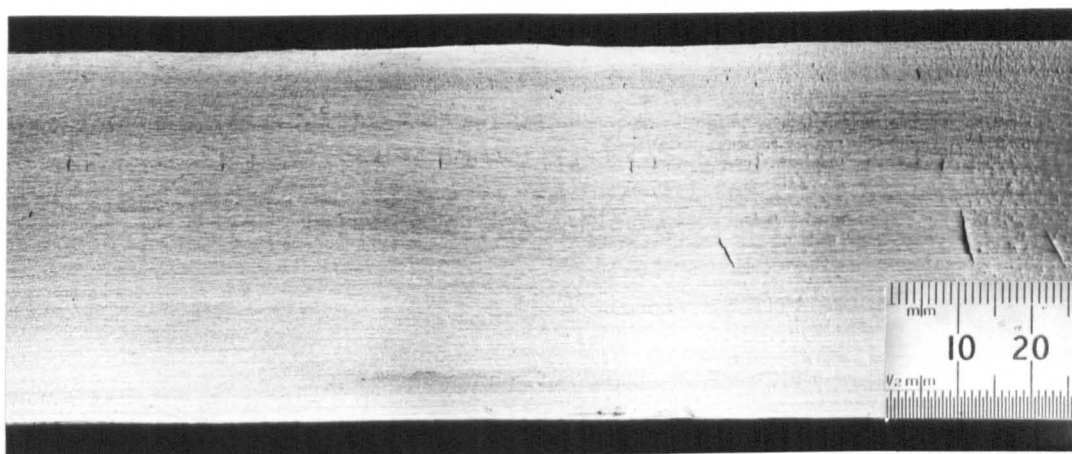


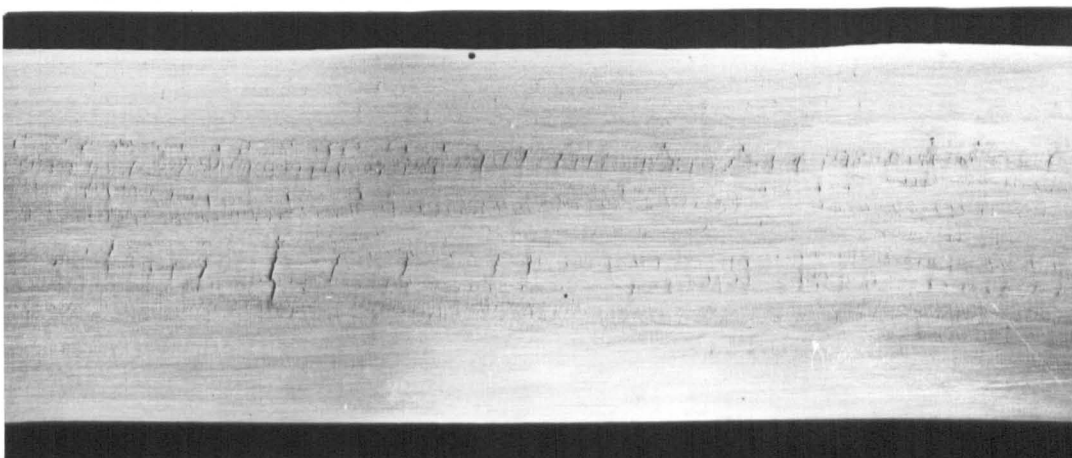
Figure 30 (a) Chevron cracks in a submerged arc weld deposited with the wire flux combination SD2/3Ni + OP41TT. High heat input weld made by Crouch (7). (b) Cross section of the weld metal and backing bar.



(a)



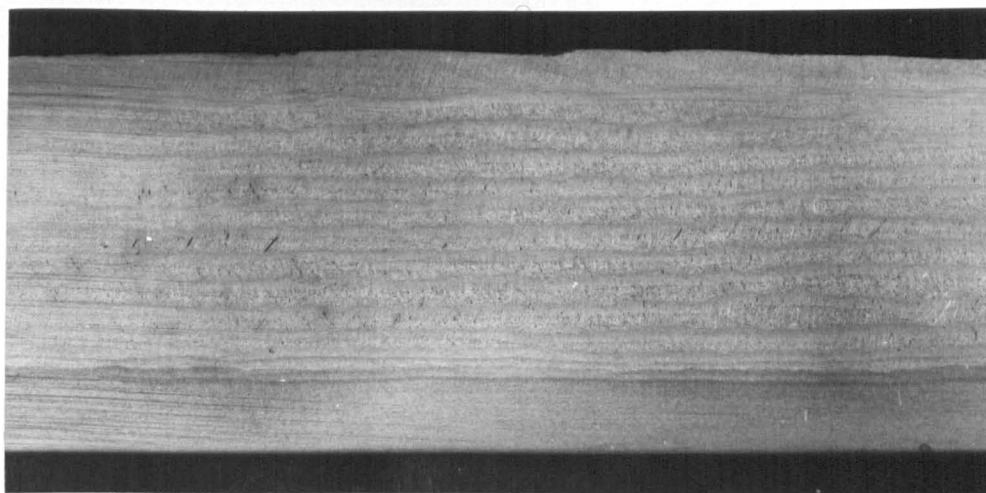
(b)



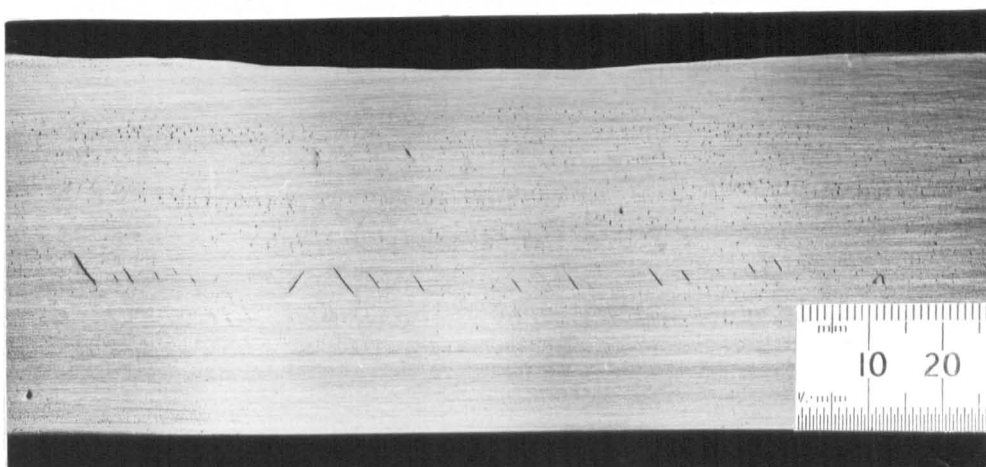
(c)

Figure 31 - Vertical cracks in high strength submerged arc welds

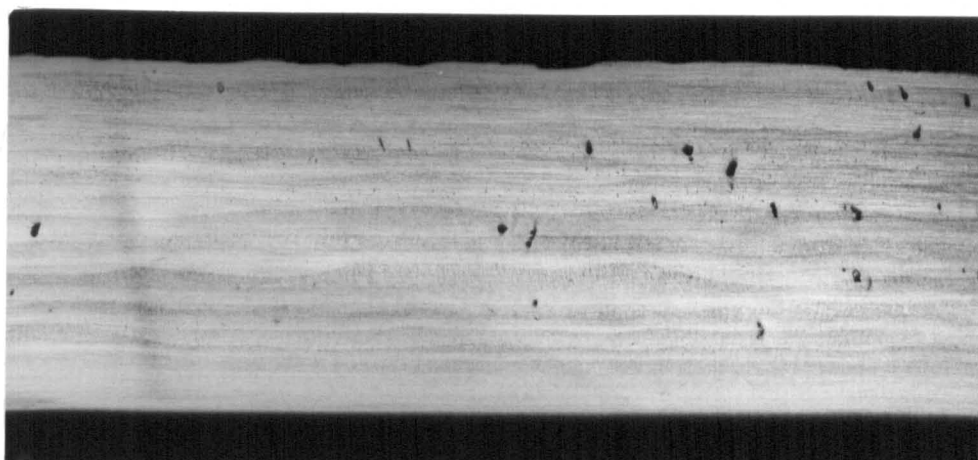
- (a) Deposited with the wire-flux combination $\text{SD3/1Ni}\frac{1}{2}\text{Mo} + \text{OP41TT}$ (damp). TP24. 1x.
- (b) Deposited with the wire-flux combination $\text{SD2/1Cr1Ni}\frac{1}{2}\text{Mo} + \text{OP41TT}$ (as received). TP26. 1x.
- (c) Deposited with the wire-flux combination $\text{SD2/1Cr1Ni}\frac{1}{2}\text{Mo} + \text{OP41TT}$ (damp). TP27. 1x.



(a)



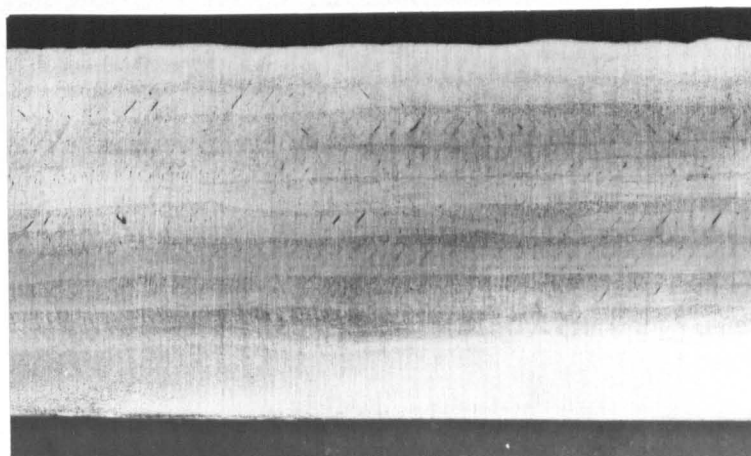
(b)



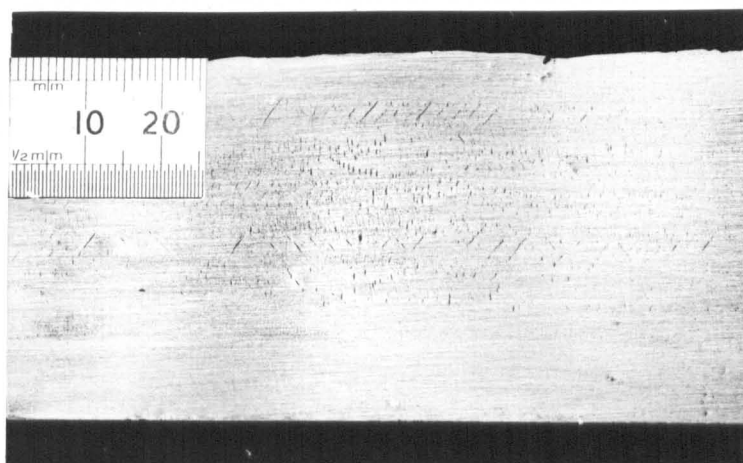
(c)

Figure 32 - Chevron cracks, fissures and porosity in manual metal arc welds deposited with E8018C1 electrodes.

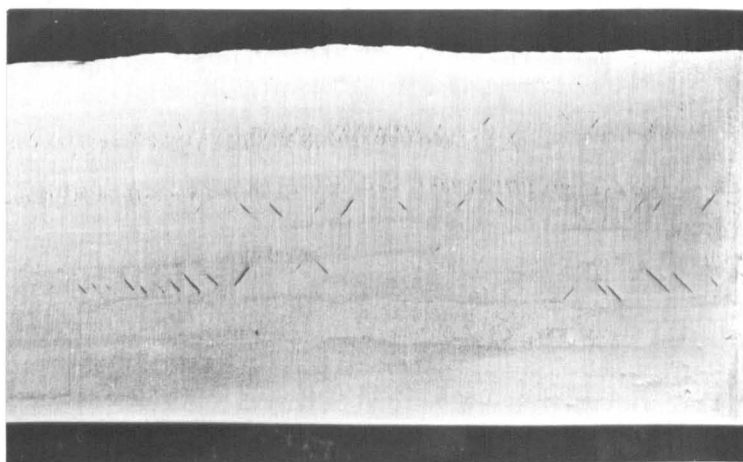
- (a) Weld with electrodes from manufacturer A. TP32. 1x.
- (b) Weld with electrodes from manufacturer B. (batch 1). TP35. 1x.
- (c) Weld with electrodes from manufacturer B. (batch 2). TP38. 1x.



(a)



(b)

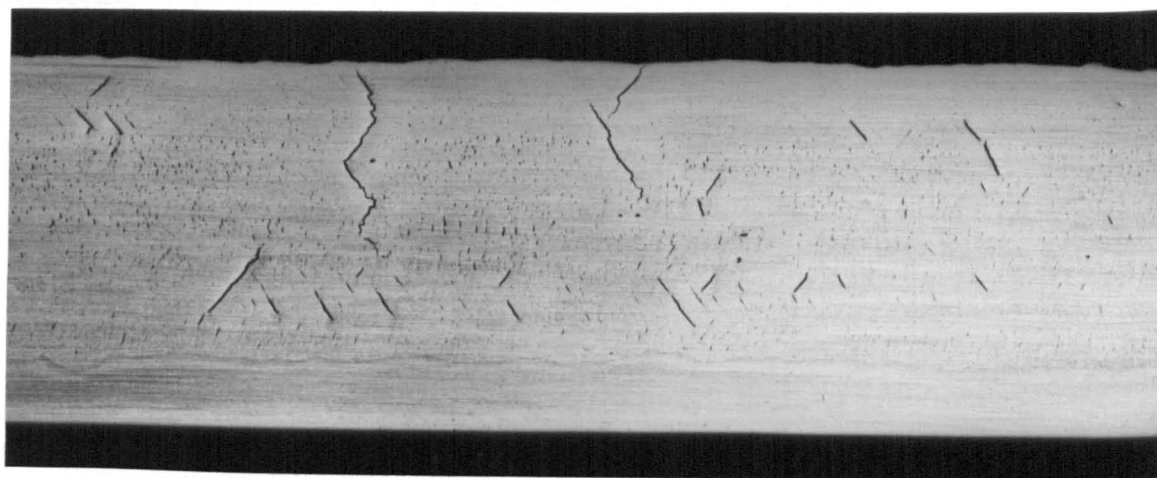


(c)

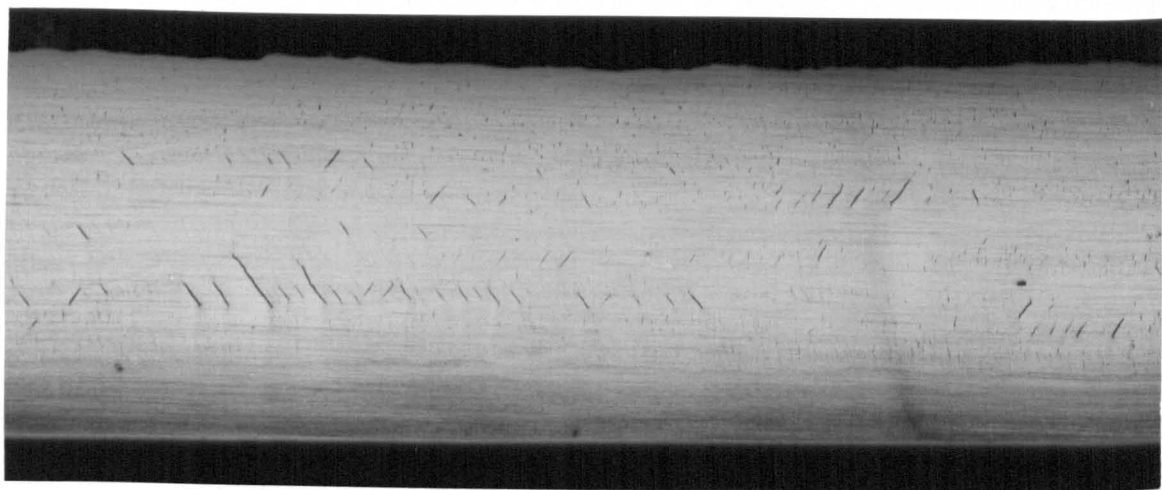
Figure 33 - Chevron cracks in manual metal arc welds

(a) Deposited with electrodes B1. TP40. 1x.

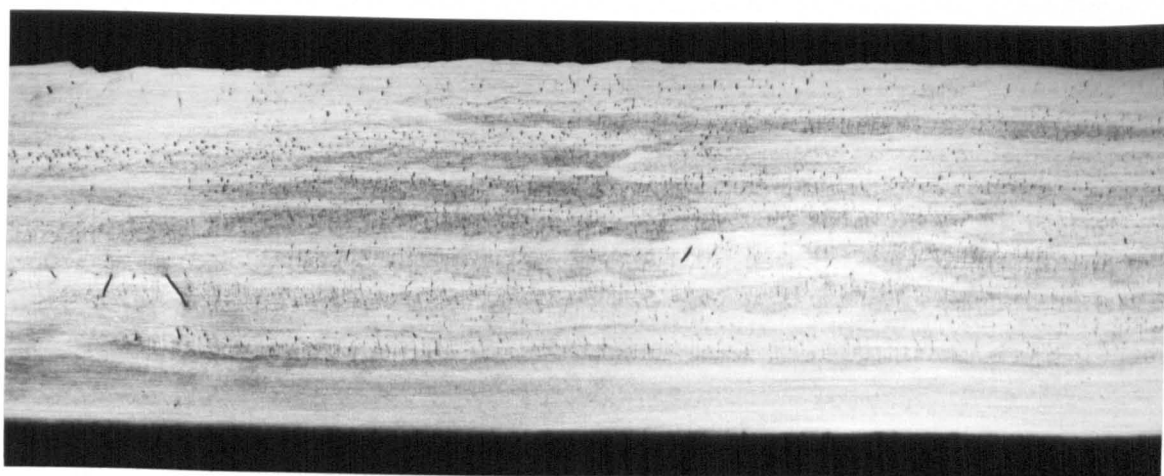
(b) and (c) Deposited with electrodes B2. TP42. 1x.



(a)



(b)



(c)

Figure 34 - Chevron cracks in manual metal arc welds.

(a) Deposited with electrodes C1. TP47. 1x.

(b) Deposited with electrodes C2. TP48. 1x.

(c) Deposited with electrodes C3. TP49. 1x.

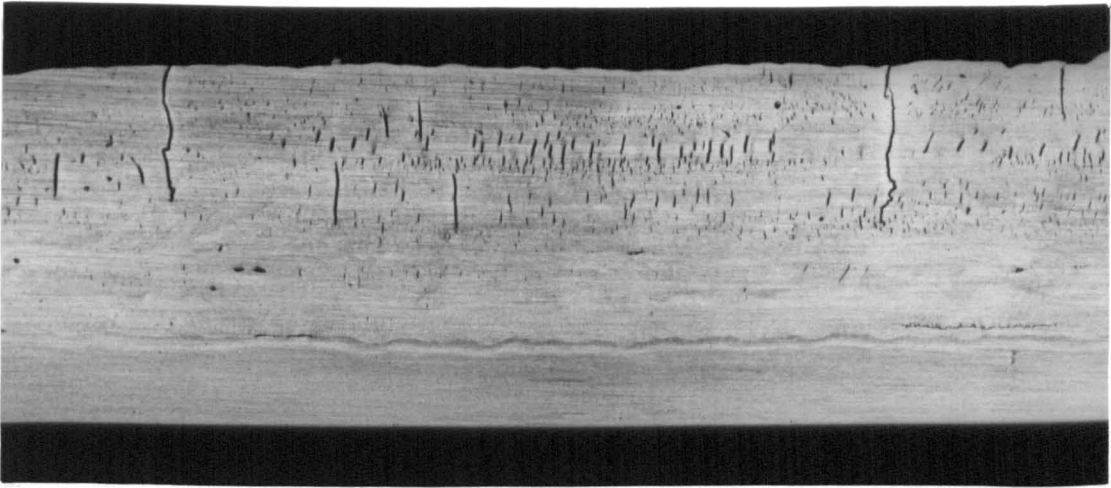


Figure 35 - Vertical cracks in a manual metal arc weld with electrodes C5. TP51. 1x.

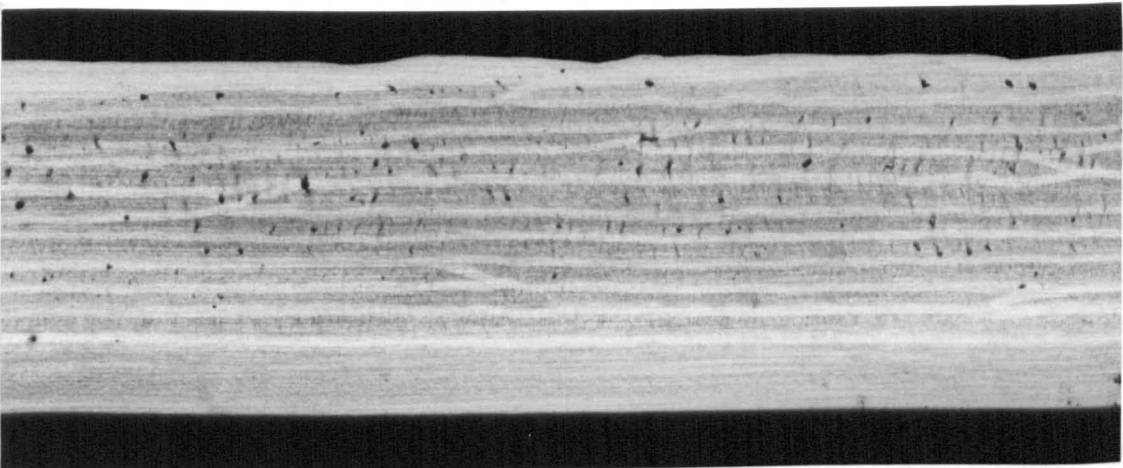


Figure 36 - Porosity in a manual metal arc weld with rutile electrodes R1. TP52. 1x.

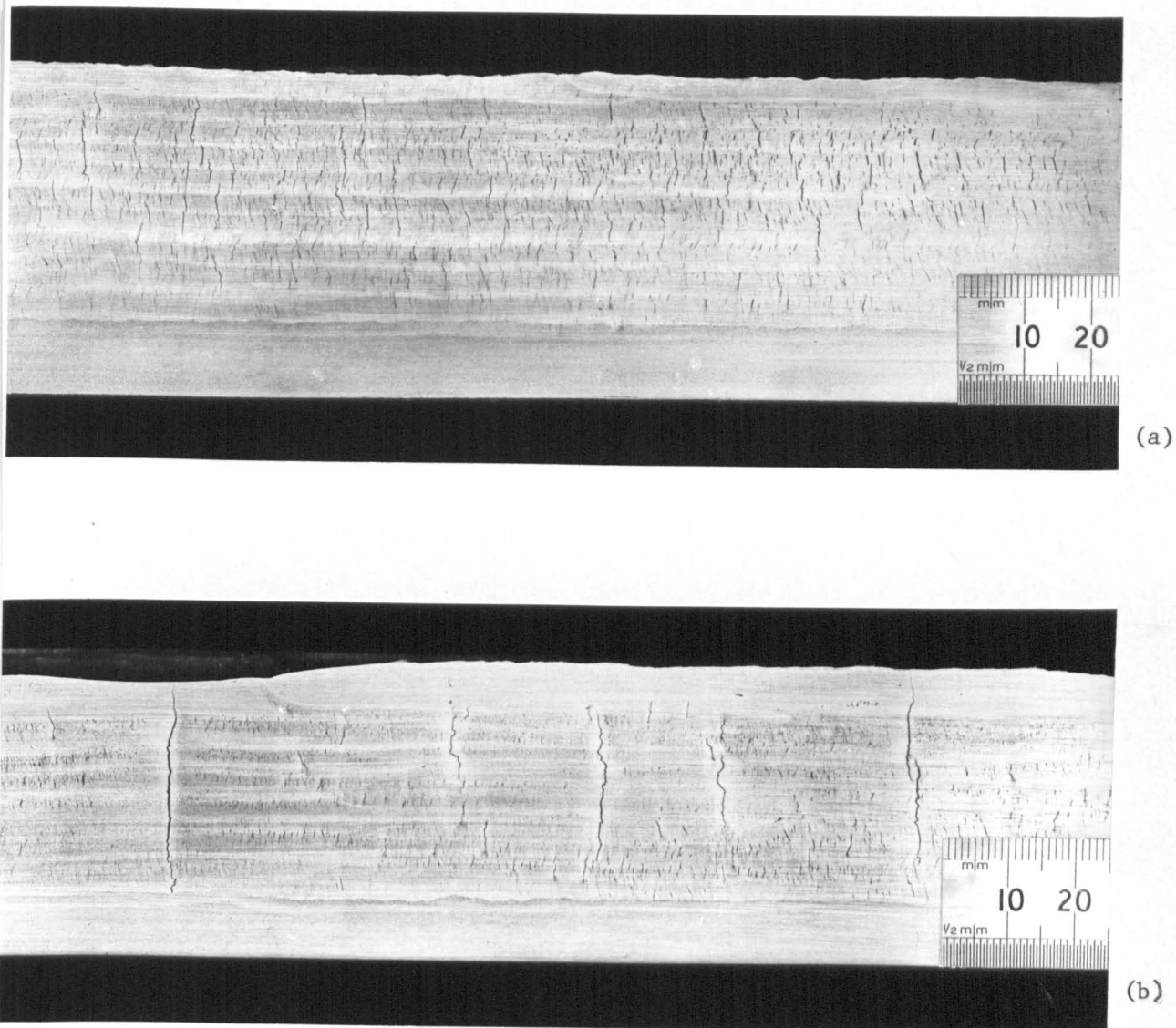
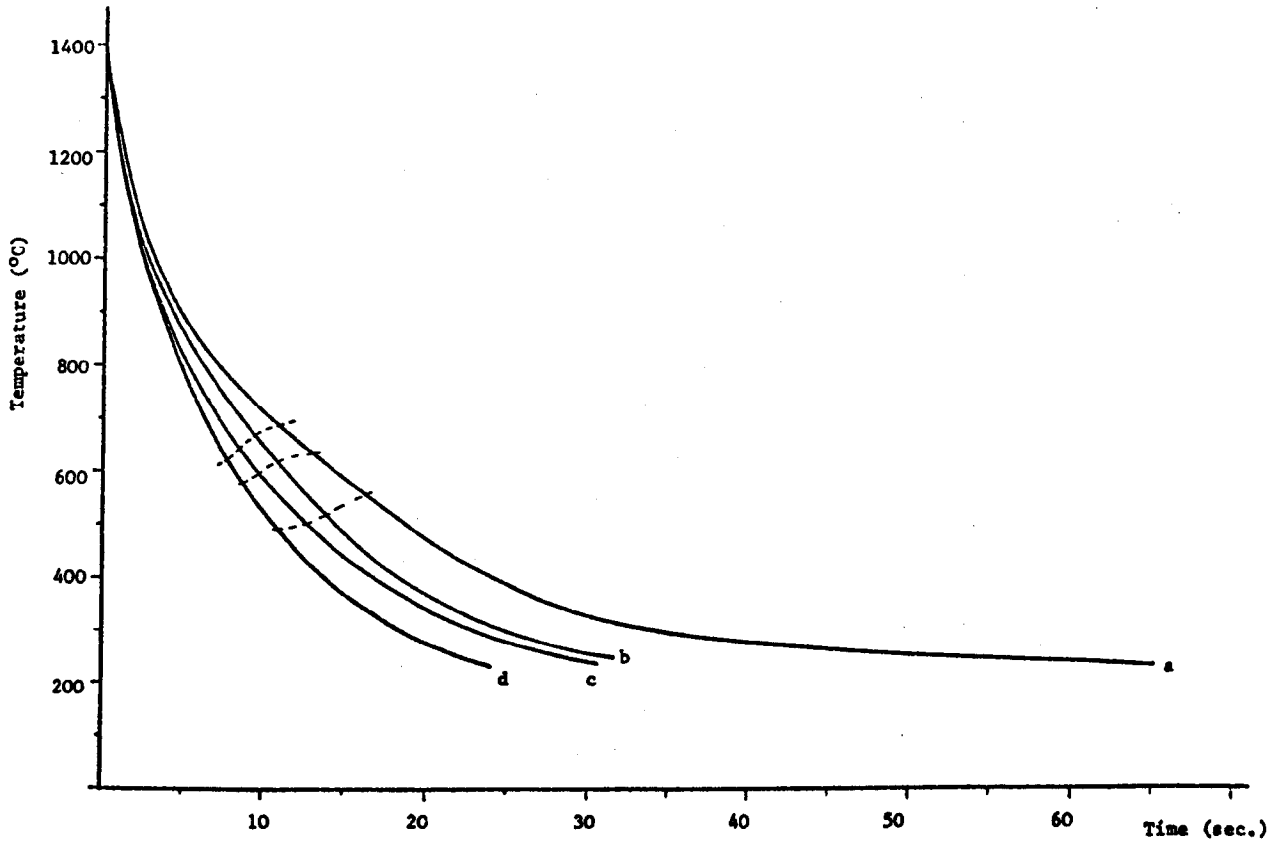


Figure 37 - Vertical cracks in manual metal arc welds with electrodes B5Ni.

(a) Weld with electrodes in the as received condition. TP62. 1x.

(b) Weld with electrodes baked at 400°C. TP63. 1x.

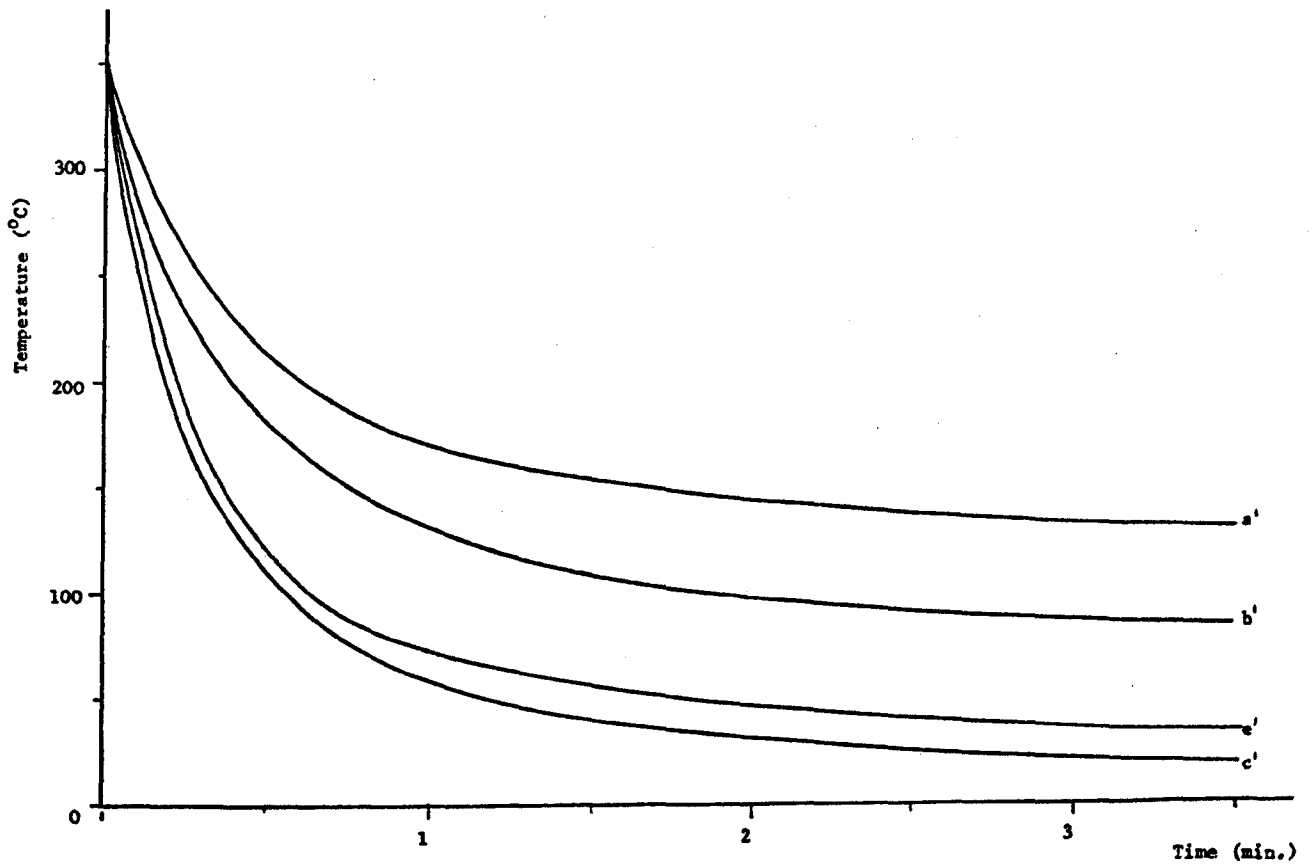


a. 90°C pre-heat, no water cooling.

b. No pre-heat, no water cooling.

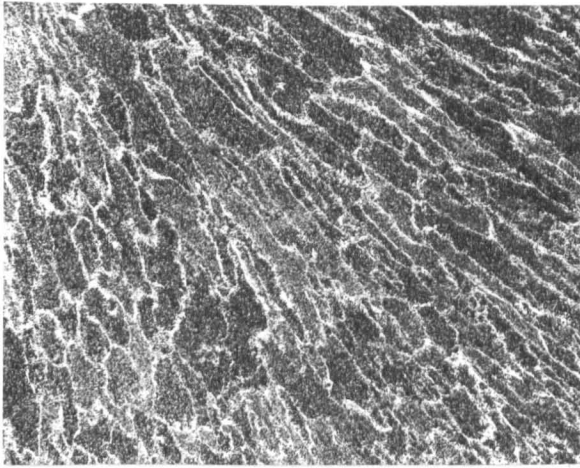
c and d. No pre-heat, cooling water flow rate 15ℓ/min.

Figure 38 - Weld metal cooling curves between 1400° and 300°C observed during the continuous water cooling test. (Heat input 2.4 kJ/mm, except for d which was 1.6 kJ/mm).

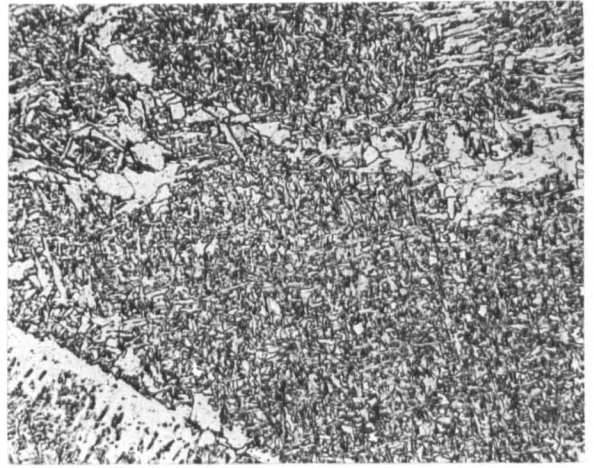


- a' 90°C pre-heat, no water cooling.
- b' No pre-heat, no water cooling.
- c' No pre-heat, cooling water flow rate 15ℓ/min.
- e' No pre-heat, cooling water flow rate 1ℓ/min.

Figure 39 - Weld metal cooling curves below 350°C observed during the continuous water cooling test. (Heat input 2.4 kJ/mm).



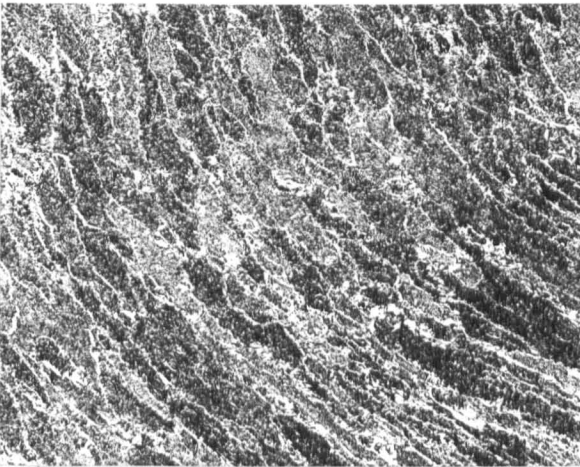
(a)



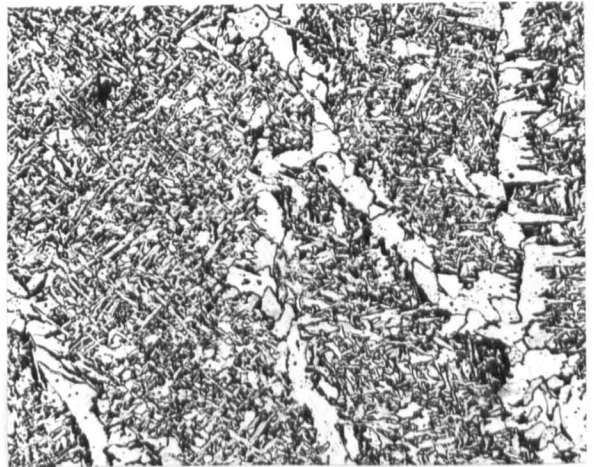
(b)

Figure 40 - Weld metal microstructure of the industrial sample A.

(a) 50x. (b) 500x (reduced 30% on reproduction).



(a)



(b)

Figure 41 - Weld metal microstructure of the industrial sample B.

(a) 50x. (b) 500x (reduced 30% on reproduction).

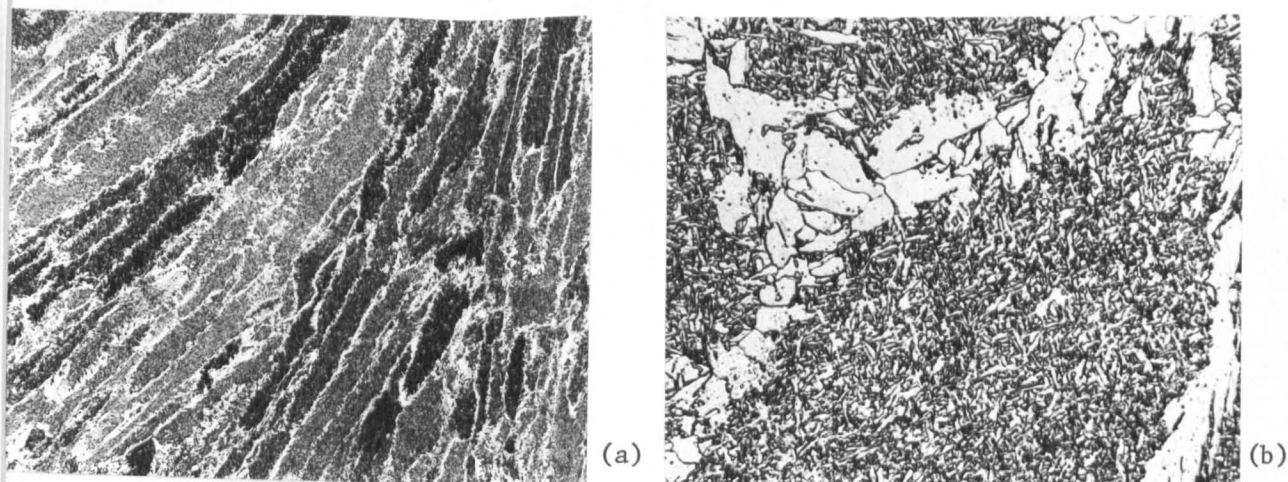


Figure 42 - Microstructure of a submerged arc weld deposited with the wire-flux combination. SD3 + OP41TT. TP6.

(a) 50x. (b) 500x (reduced 30% on reproduction).

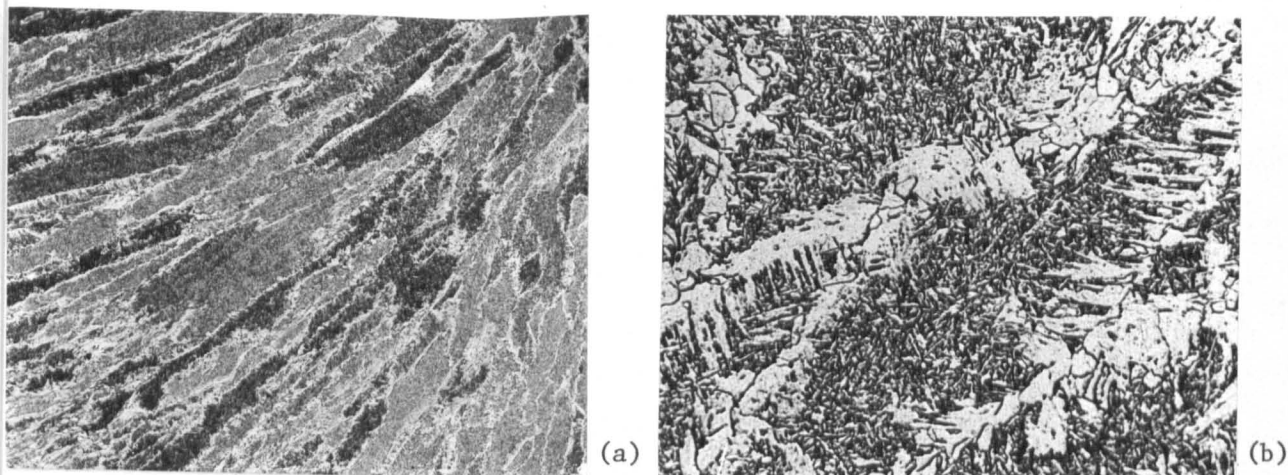


Figure 43 - Microstructure of a submerged arc weld deposited with the wire-flux combination S4 + OP41TT. TP9.

(a) 50x. (b) 500x (reduced 30% on reproduction).

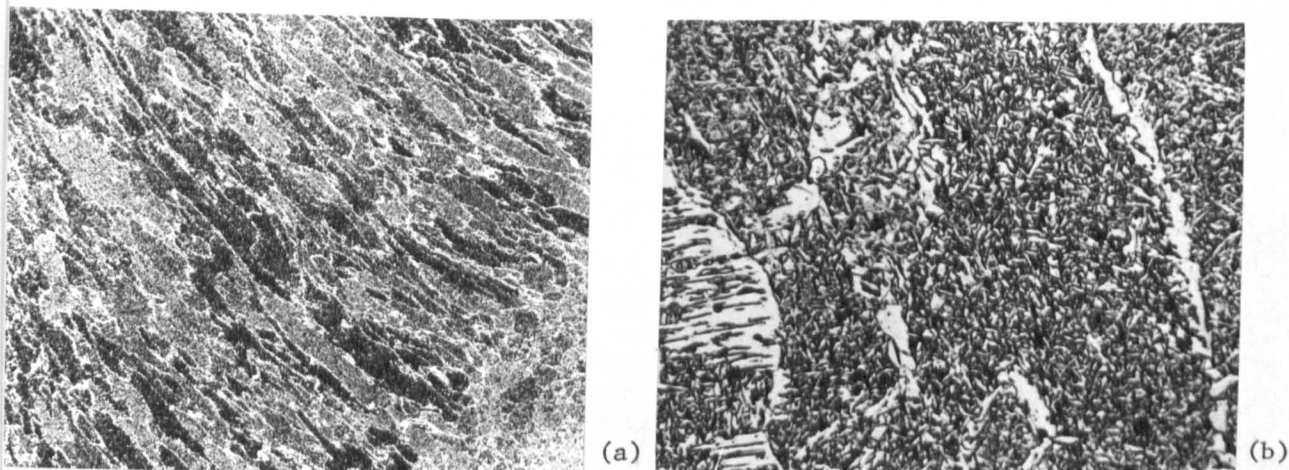
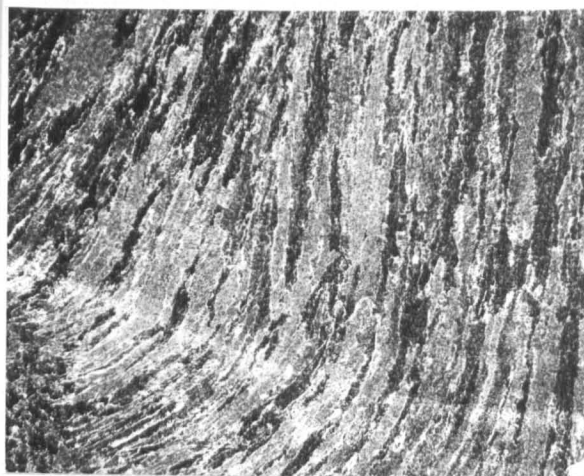
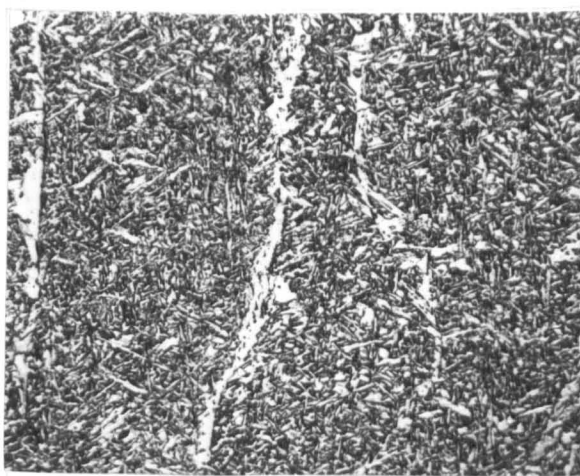


Figure 44 - Microstructure of a submerged arc weld deposited with the wire-flux combination SD3/1Ni + OP41TT. TP11.

(a) 50x. (b) 500x (reduced 30% on reproduction).



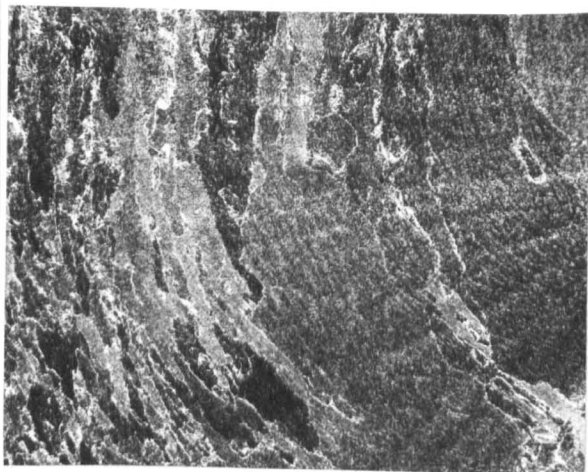
(a)



(b)

Figure 45 - Microstructure of a submerged arc weld deposited with the wire-flux combination SD2/3Ni + OP41TT. TP16.

(a) 50x. (b) 500x (reduced 30% on reproduction).



(a)

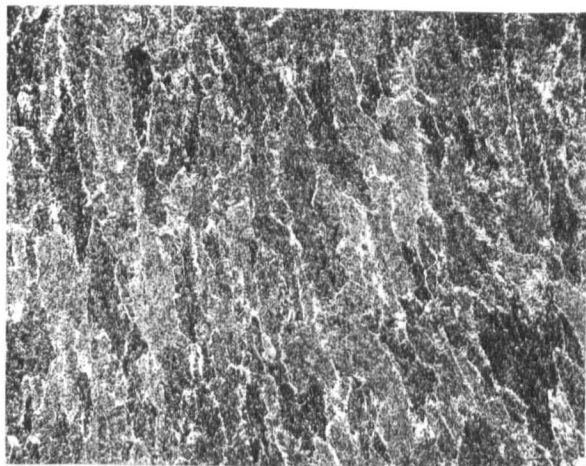


(c)

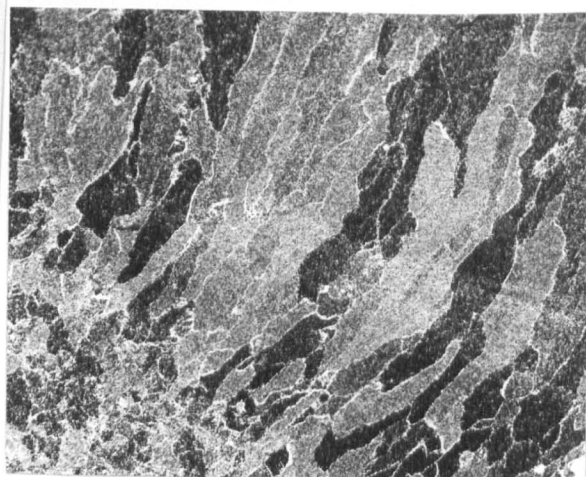
Figure 46 - Microstructure of a submerged arc weld deposited with the wire-flux combination SD2/3Ni + OP41TT. High heat input weld by Crouch (7).

(a) Detail showing very large grains, 25x.

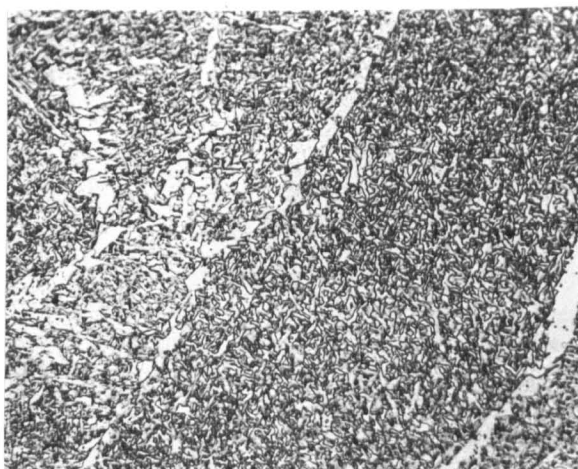
(b) 50x. (c) 500x (reduced 30% on reproduction).



(b)



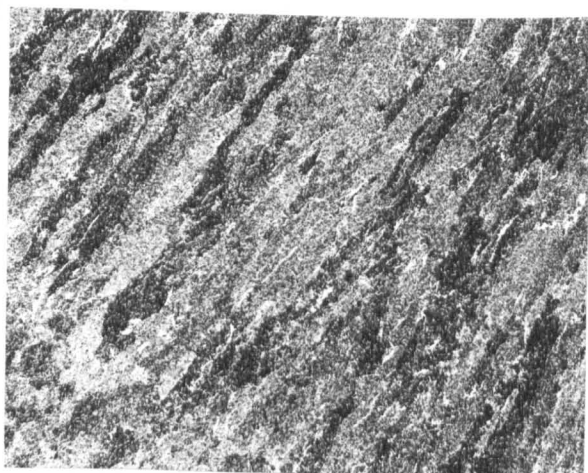
(a)



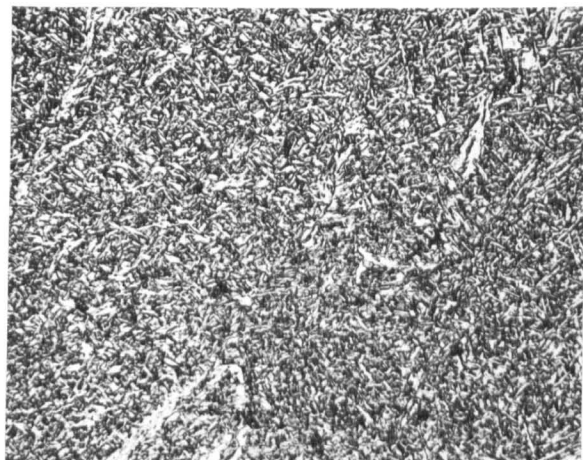
(b)

Figure 47 - Microstructure of a submerged arc weld deposited with the wire-flux combination SD3/ $\frac{1}{2}$ Mo + OP41TT. TP20.

(a) 50x. (b) 500x (reduced 30% on reproduction).



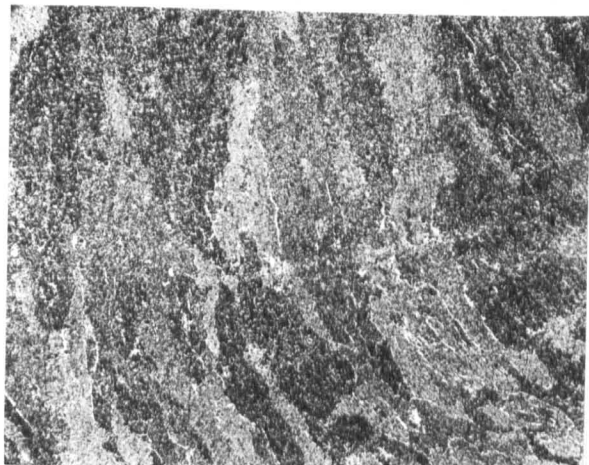
(a)



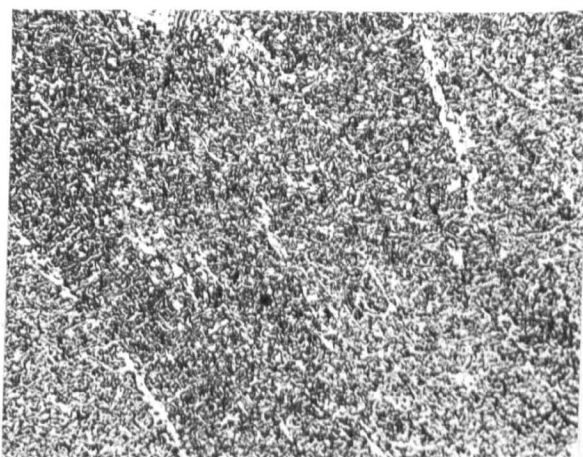
(b)

Figure 48 - Microstructure of a submerged arc weld deposited with the wire-flux combination SD3/1Ni $\frac{1}{2}$ Mo. TP24.

(a) 50x. (b) 500x (reduced 30% on reproduction).



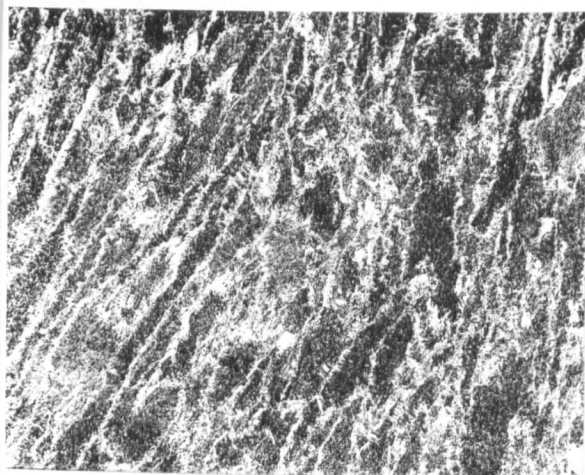
(a)



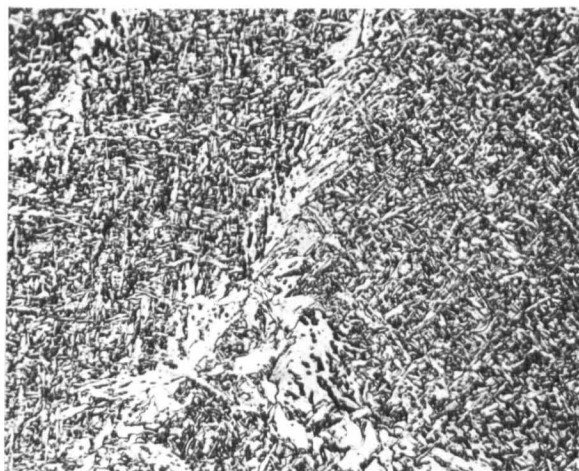
(b)

Figure 49 - Microstructure of a submerged arc weld deposited with the wire-flux combination SD2/1Cr1Ni $\frac{1}{2}$ Mo + OP41TT. TP26.

(a) 50x, (b) 500x (reduced 30% on reproduction).



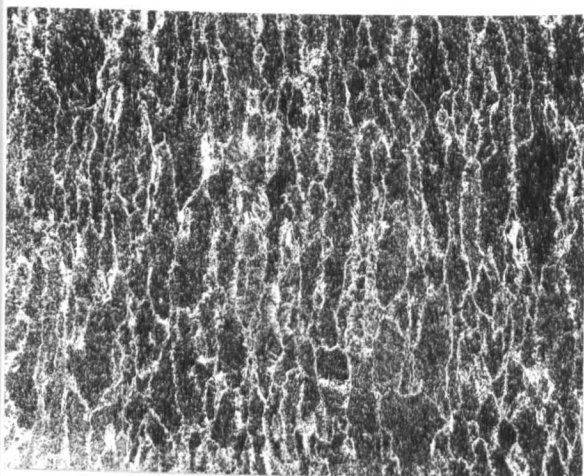
(a)



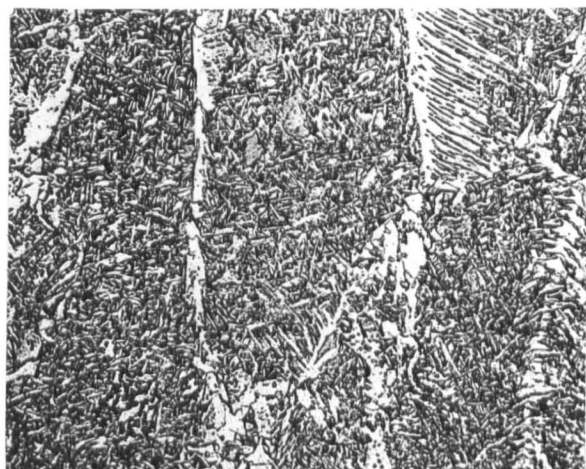
(b)

Figure 50 - Microstructure of a manual metal arc weld deposited with E8018C1 electrodes (from manufacturer A). TP30.

(a) 50x. (b) 500x (reduced 30% on reproduction)



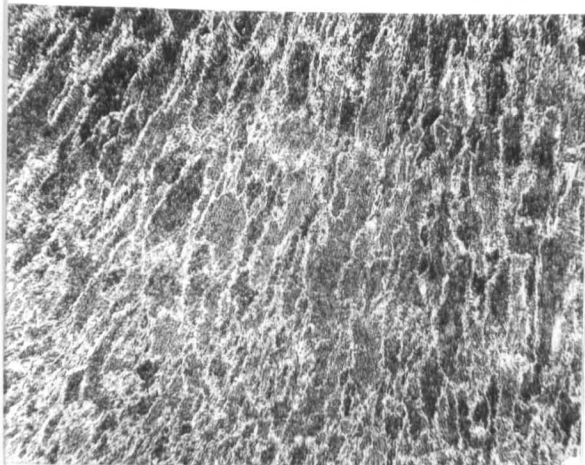
(a)



(b)

Figure 51 - Microstructure of a manual metal arc weld deposited with E8018C1 electrodes (from manufacturer B, batch 1). TP35.

(a) 50x. (b) 500x (reduced 30% on reproduction).



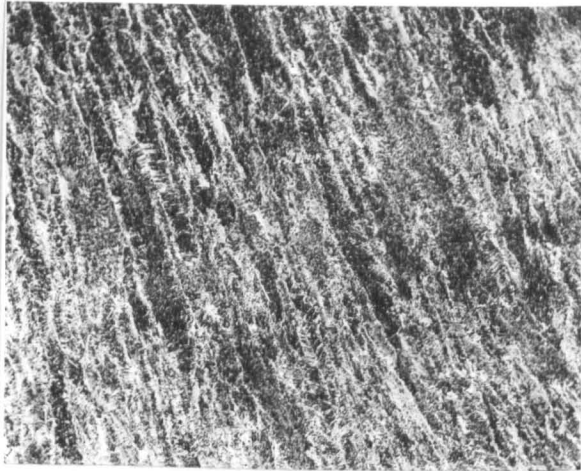
(a)



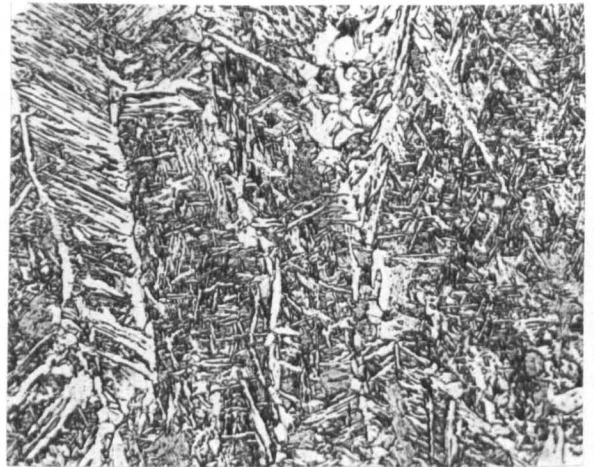
(b)

Figure 52 - Microstructure of a manual metal arc weld deposited with E8018C1 electrodes (from manufacturer B, batch 2). TP37.

(a) 50x. (b) 500x (reduced 30% on reproduction).



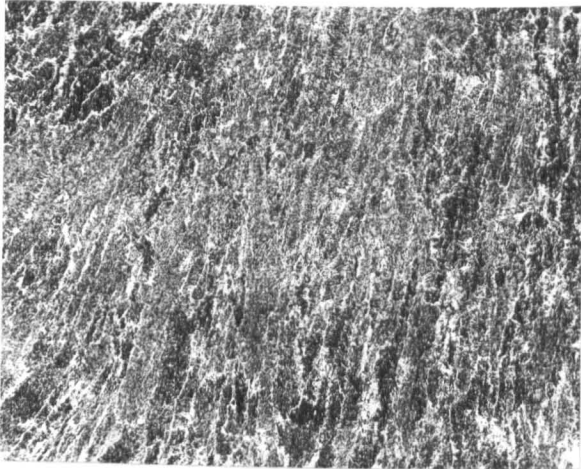
(a)



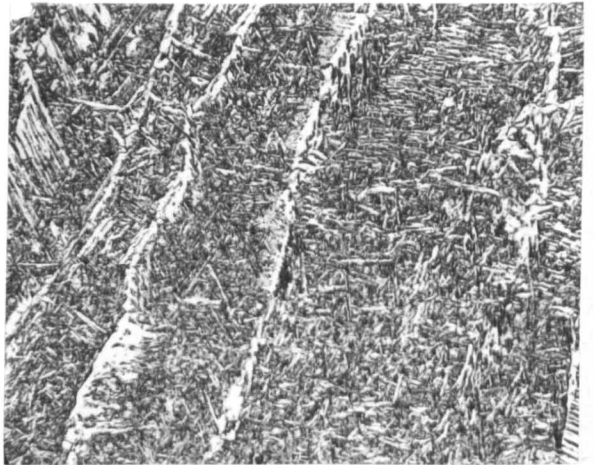
(b)

Figure 53 - Microstructure of a manual metal arc weld deposited with electrodes B1. TP40.

(a) 50x. (b) 500x (reduced 30% on reproduction).



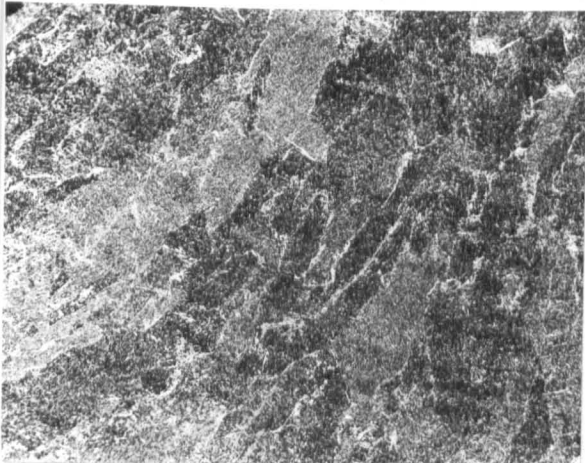
(a)



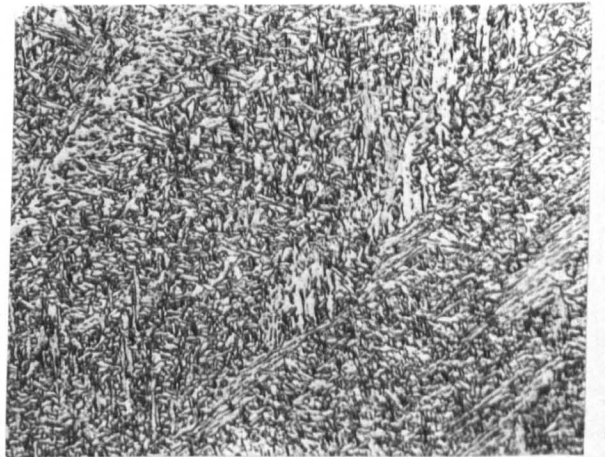
(b)

Figure 54 - Microstructure of a manual metal arc weld deposited with electrodes B2. TP42.

(a) 50x. (b) 500x (reduced 30% on reproduction).



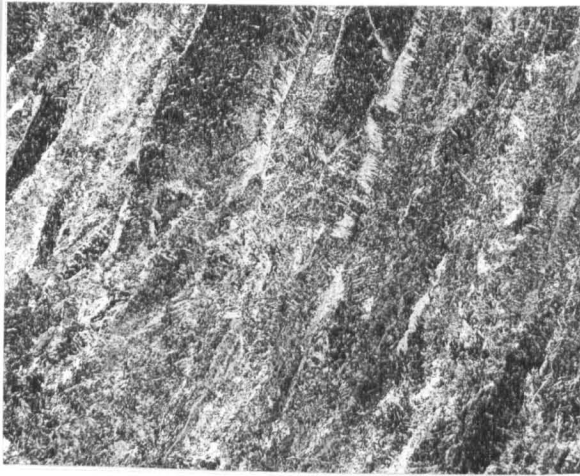
(a)



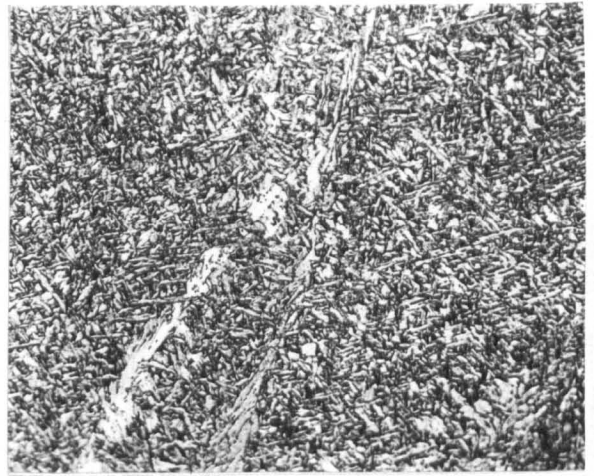
(b)

Figure 55 - Microstructure of a manual metal arc weld deposited with electrodes B3. TP43.

(a) 50x. (b) 500x (reduced 30% on reproduction).



(a)



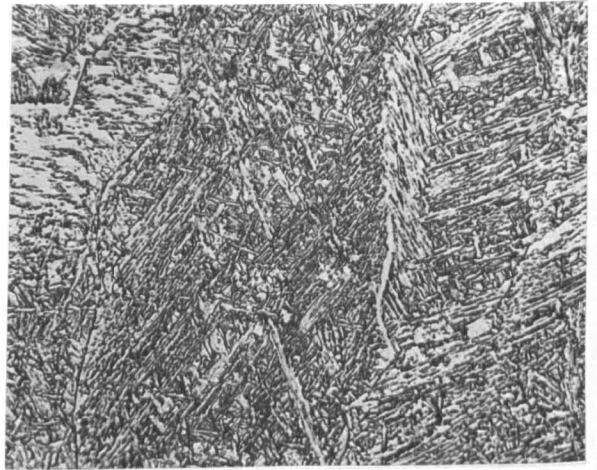
(b)

Figure 56 - Microstructure of a manual metal arc weld deposited with electrodes B4. TP44.

(a) 50x. (b) 500x (reduced 30% on reproduction).



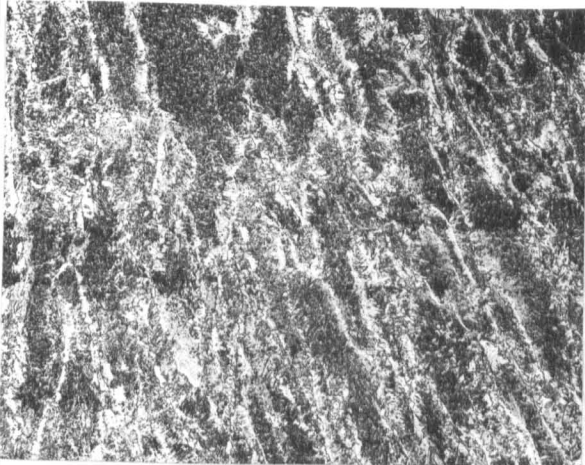
(a)



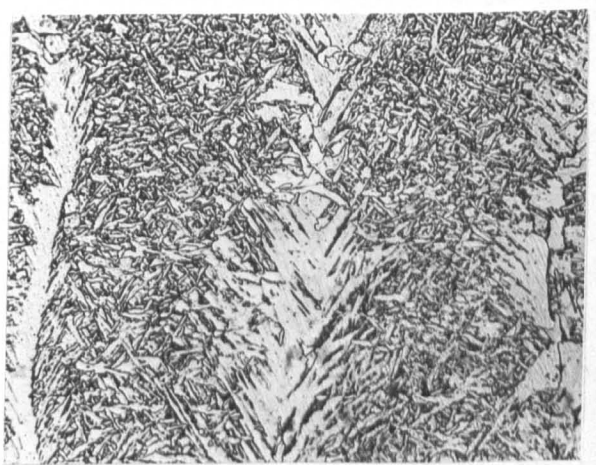
(b)

Figure 57 - Microstructure of a manual metal arc weld deposited with electrodes B5. TP46.

(a) 50x. (b) 500x (reduced 30% on reproduction).



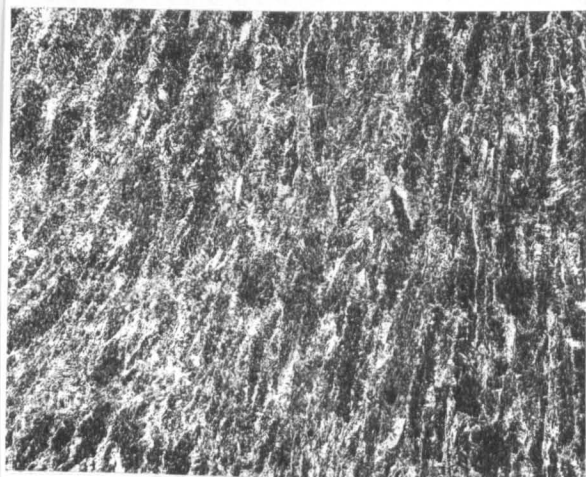
(a)



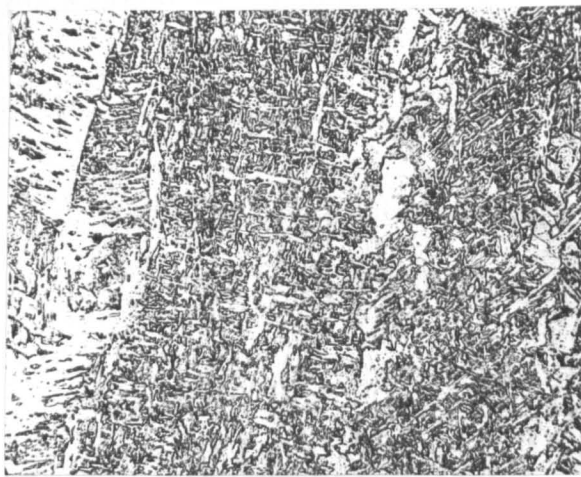
(b)

Figure 58 - Microstructure of a manual metal arc weld deposited with electrodes BONi. TP57.

(a) 50x. (b) 500x (reduced 30% on reproduction).



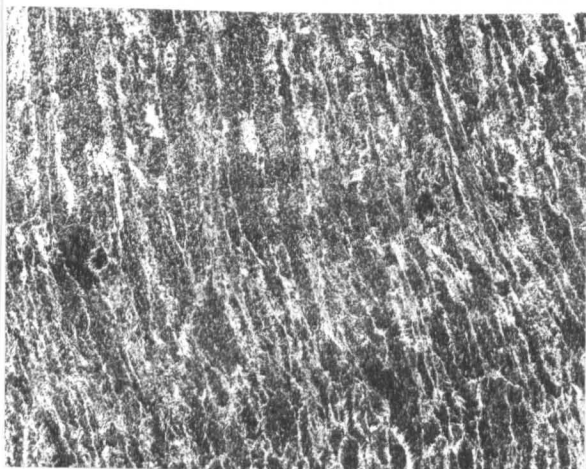
(a)



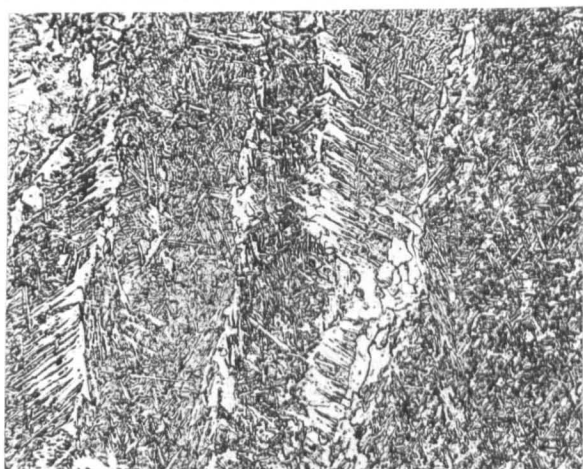
(b)

Figure 59 - Microstructure of a manual metal arc weld deposited with electrodes B2Ni. TP58.

(a) 50x. (b) 500x (reduced 30% on reproduction).



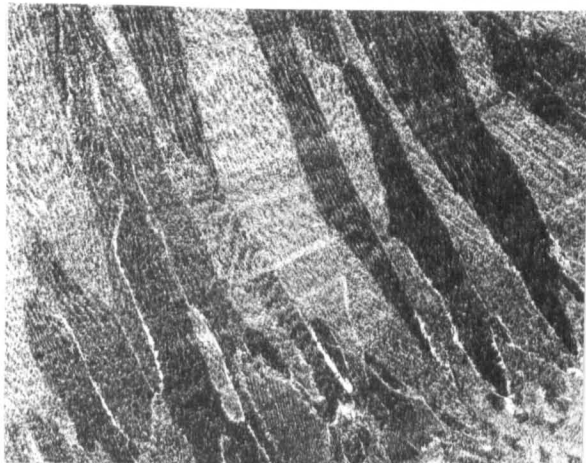
(a)



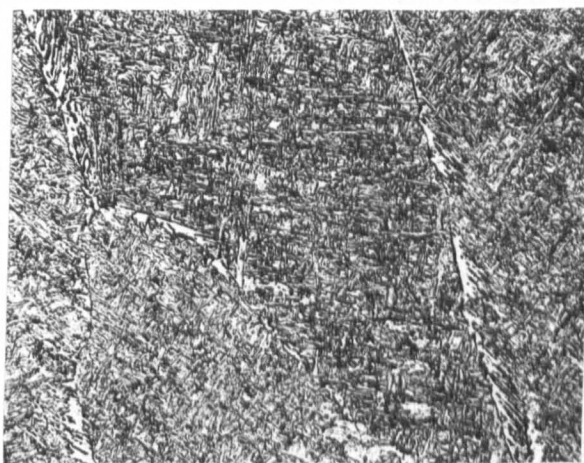
(b)

Figure 60 - Microstructure of a manual metal arc weld deposited with electrodes B3Ni. TP59.

(a) 50x. (b) 500x (reduced 30% on reproduction).



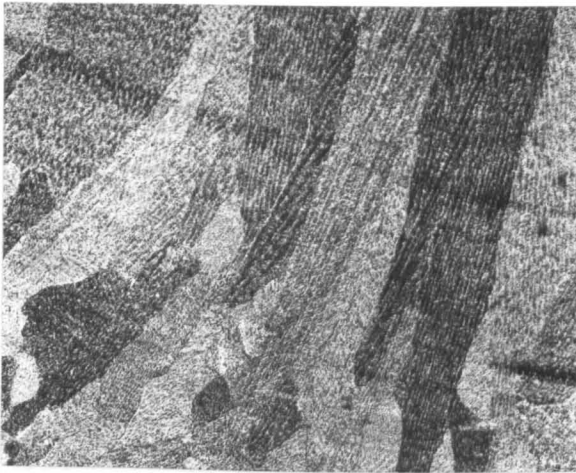
(a)



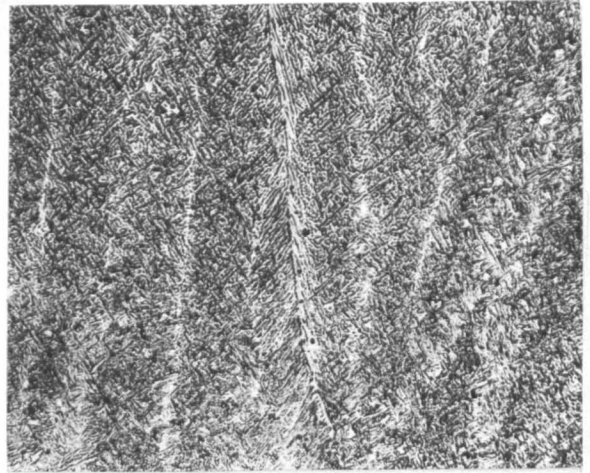
(b)

Figure 61 - Microstructure of a manual metal arc weld deposited with electrodes B4Ni. TP60.

(a) 50x. (b) 500x (reduced 30% on reproduction).



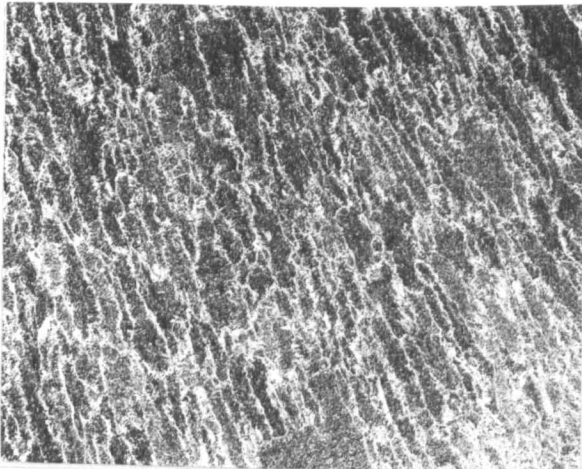
(a)



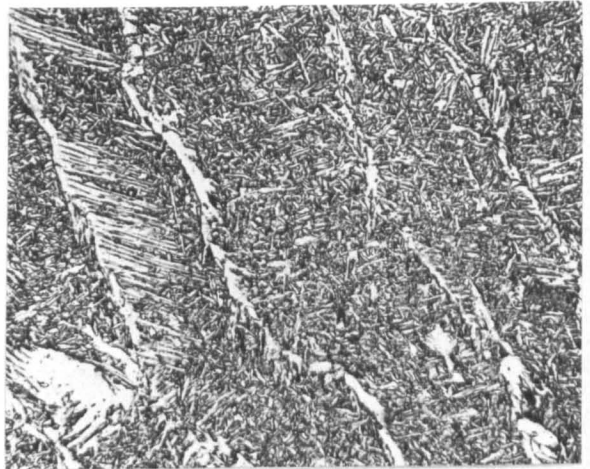
(b)

Figure 62 - Microstructure of a manual metal arc weld deposited with electrodes B5Ni. TP62.

(a) 50x. (b) 500x (reduced 30% on reproduction).



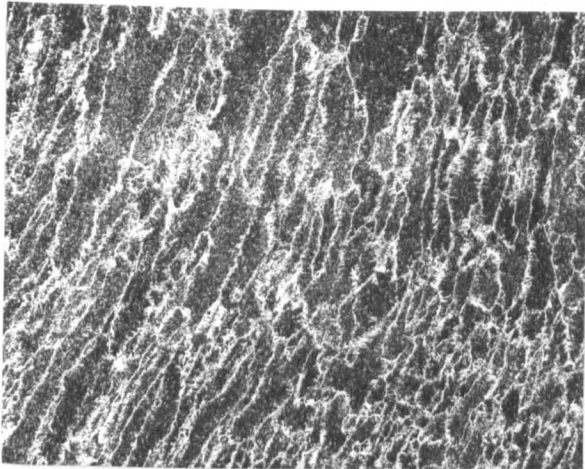
(a)



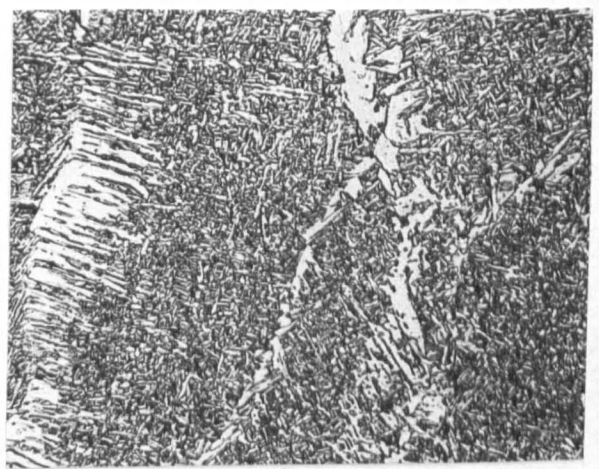
(b)

Figure 63 - Microstructure of a manual metal arc weld deposited with electrodes C1. TP47.

(a) 50x. (b) 500x (reduced 30% on reproduction.)



(a)



(b)

Figure 64 - Microstructure of a manual metal arc weld deposited with electrodes C2. TP48.

(a) 50x. (b) 500x (reduced 30% on reproduction.)

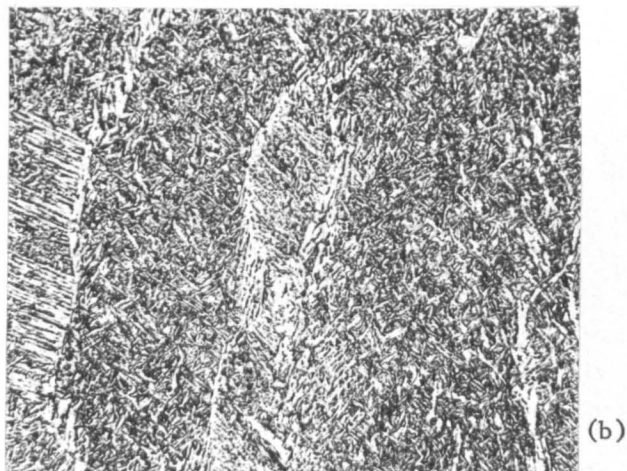
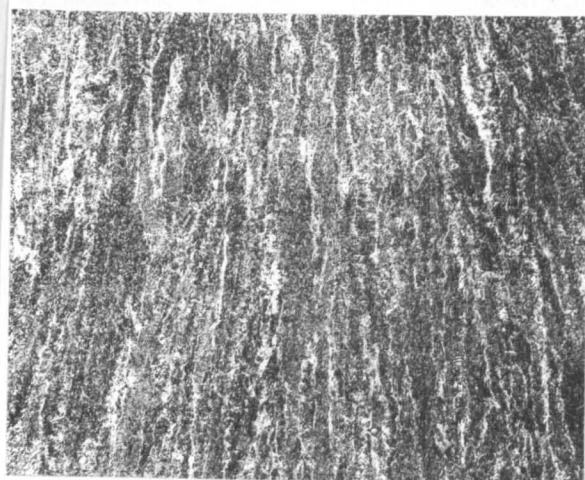


Figure 65 - Microstructure of a manual metal arc weld deposited with electrodes C3. TP49.

(a) 50x. (b) 500x (reduced 30% on reproduction).

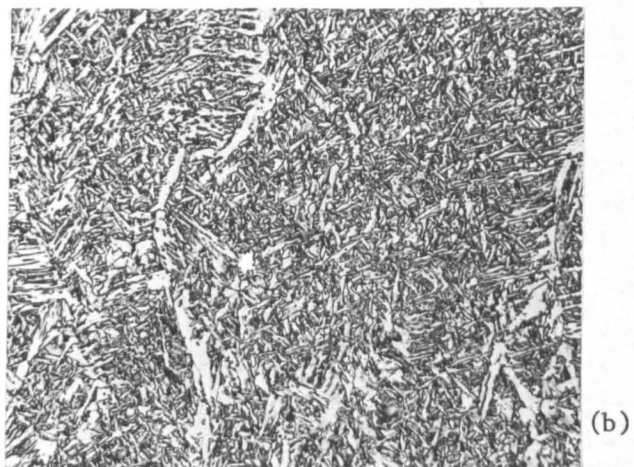
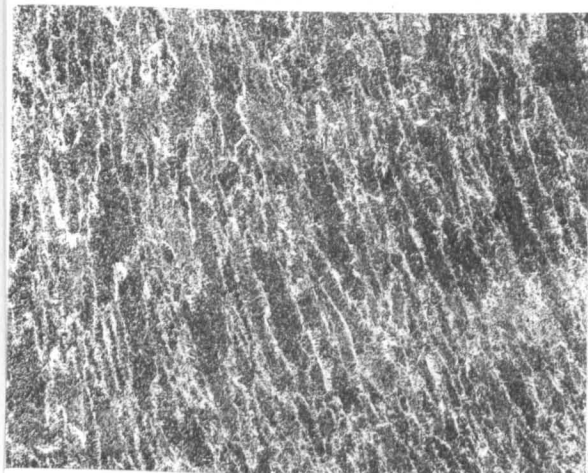


Figure 66 - Microstructure of a manual metal arc weld deposited with electrodes C4. TP50.

(a) 50x. (b) 500x (reduced 30% on reproduction).

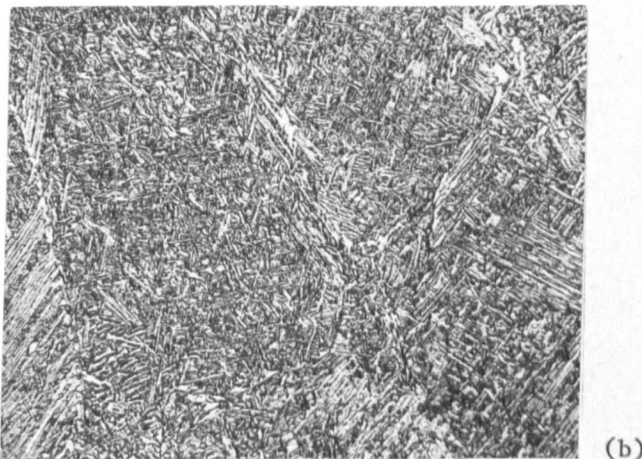
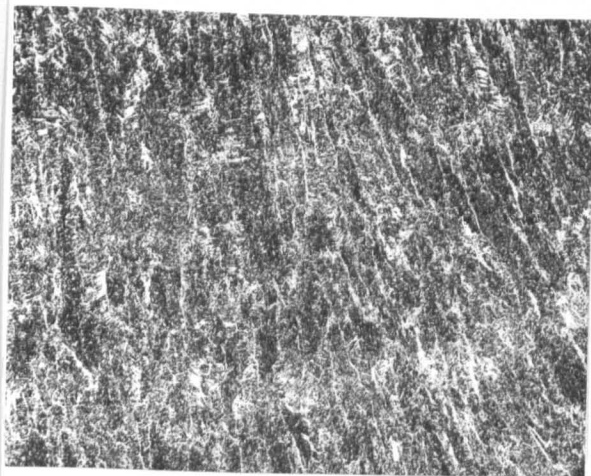
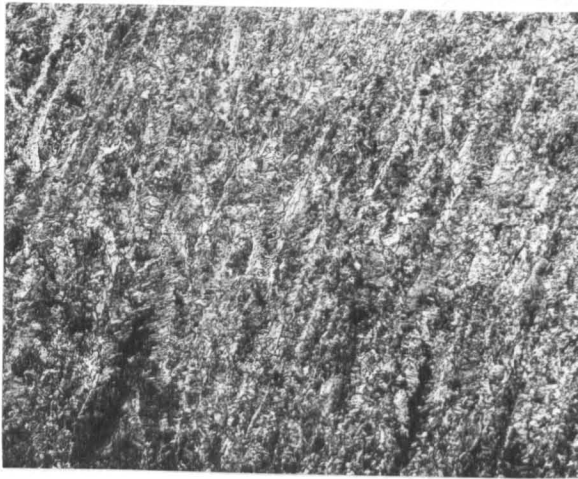


Figure 67 - Microstructure of a manual metal arc weld deposited with electrodes C5. TP51.

(a) 50x. (b) 500x (reduced 30% on reproduction).



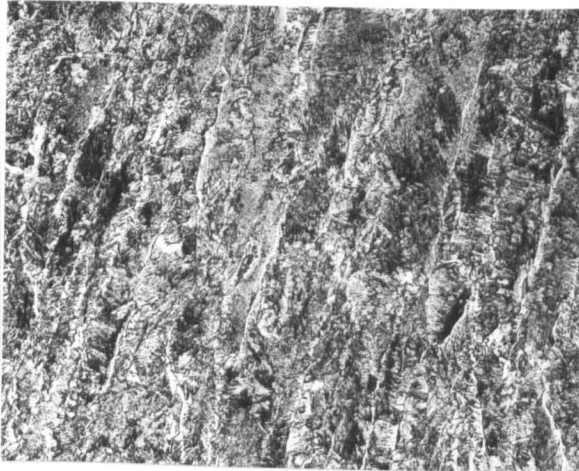
(a)



(b)

Figure 68 - Microstructure of a manual metal arc weld deposited with commercially available E6013 electrodes. TP39.

(a) 50x. (b) 500x (reduced 30% on reproduction).



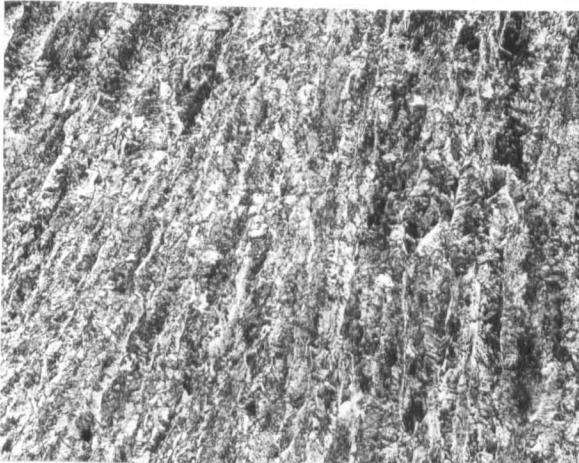
(a)



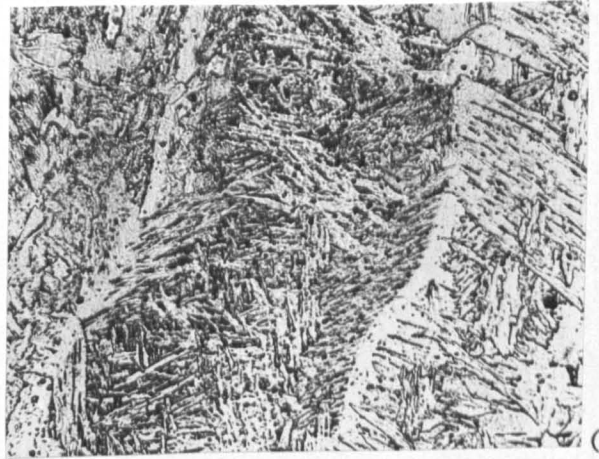
(b)

Figure 69 - Microstructure of a manual metal arc weld deposited with electrodes R1. TP52.

(a) 50x. (b) 500x (reduced 30% on reproduction).



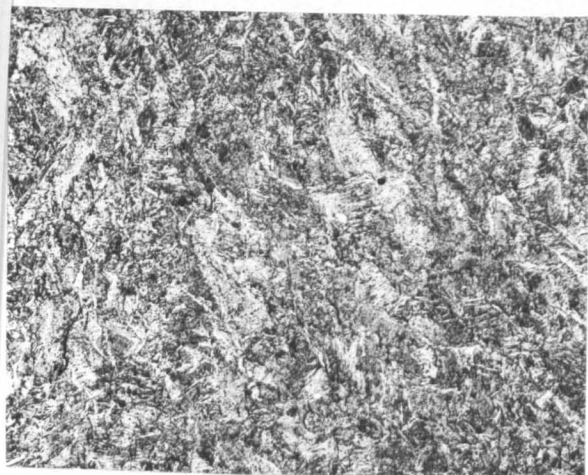
(a)



(b)

Figure 70 - Microstructure of a manual metal arc weld deposited with electrodes R2. TP53.

(a) 50x. (b) 500x (reduced 30% on reproduction).



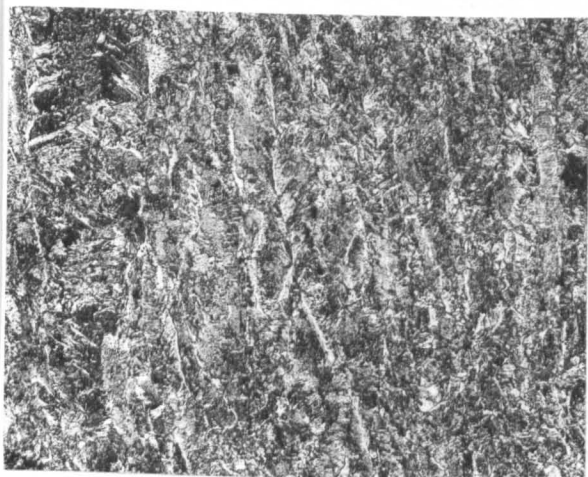
(a)



(b)

Figure 71 - Microstructure of a manual metal arc weld deposited with electrodes R3. TP54.

(a) 50x. (b) 500x (Reduced 30% on reproduction).



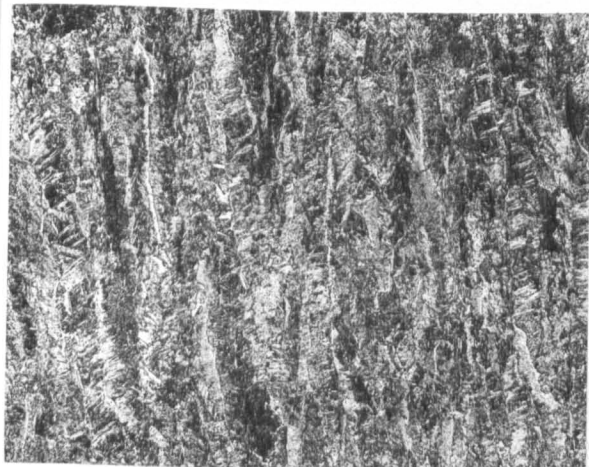
(a)



(b)

Figure 72 - Microstructure of a manual metal arc weld deposited with electrodes R4. TP55.

(a) 50x. (b) 500x (Reduced 30% on reproduction).



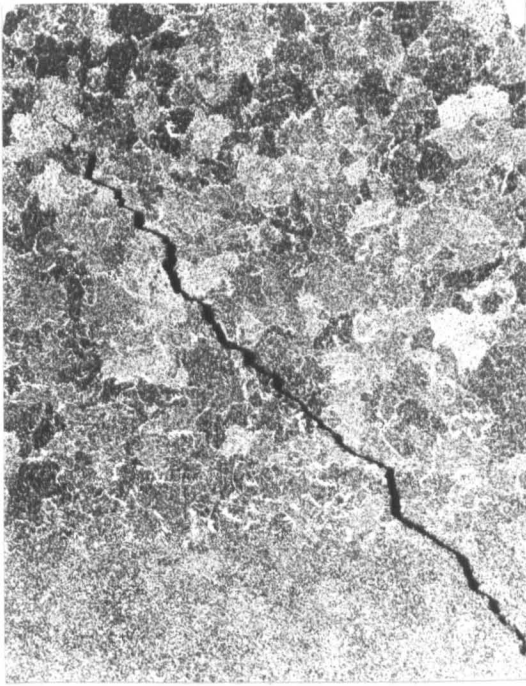
(a)



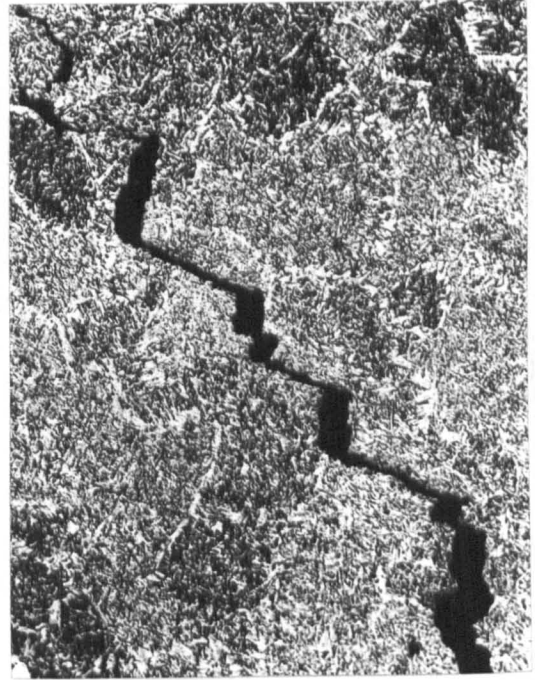
(b)

Figure 73 - Microstructure of a manual metal arc weld deposited with electrodes R5. TP56.

(a) 50x. (b) 500x (Reduced 30% on reproduction).



(a)

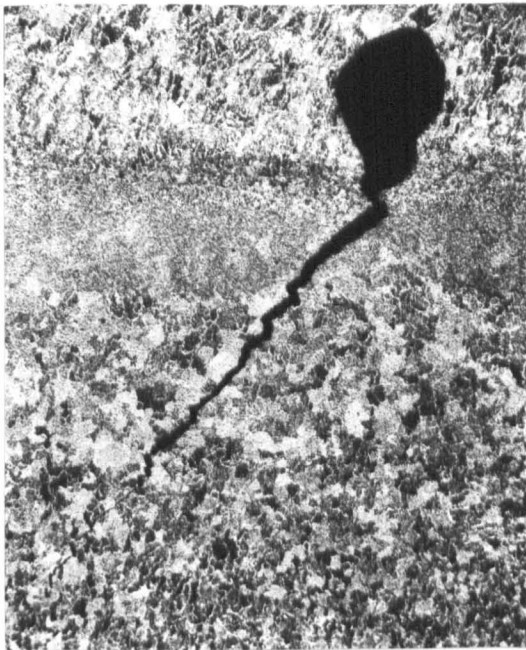


(b)

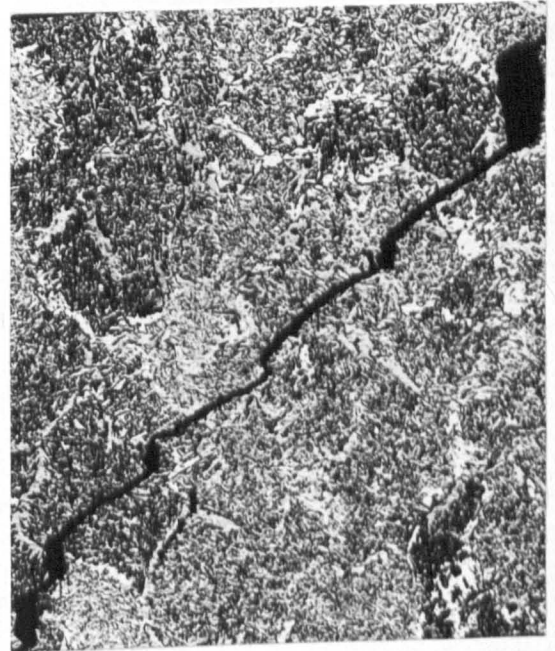
Figure 74 - Chevron crack in the industrial sample A.

(a) 40x.

(b) Detail, 200x.



(a)

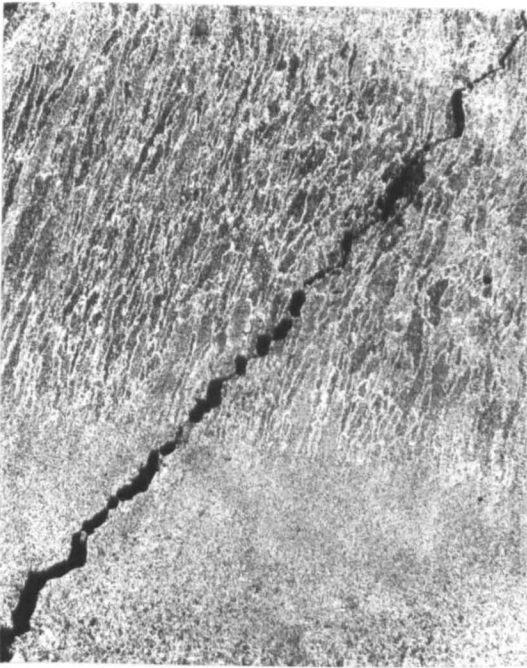


(b)

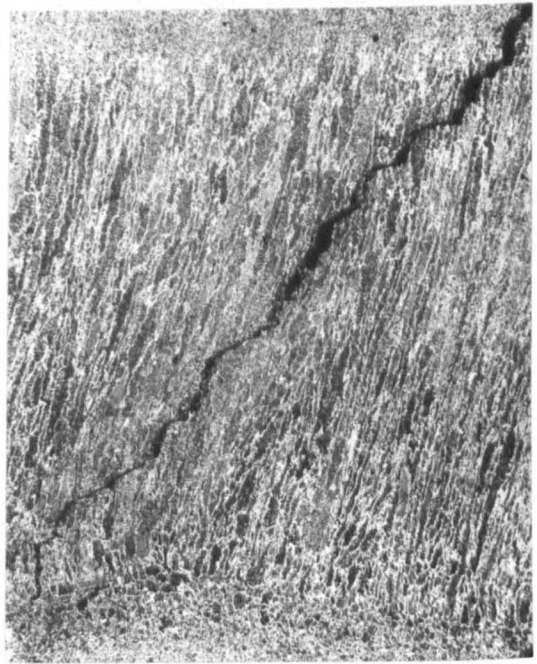
Figure 75 - Chevron crack associated with a pore. Industrial Sample A.

(a) 20x.

(b) Detail, 200x.



(a)

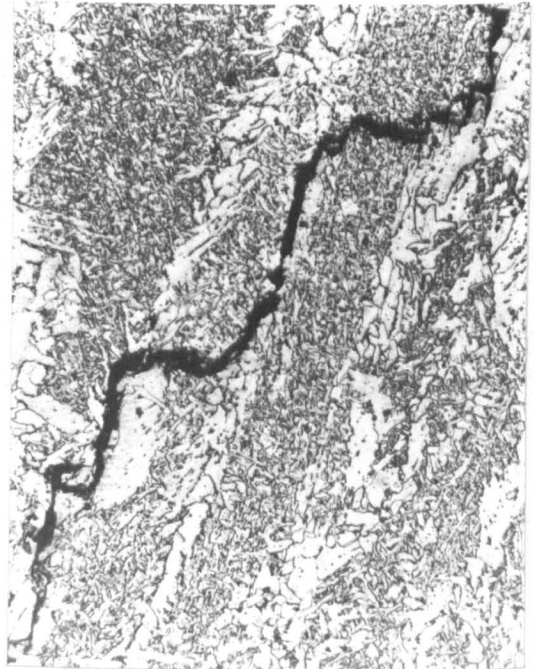


(b)

Figure 76 - Chevron cracks in the industrial sample B.
(a) and (b) 20x.



(a)



(b)



(c)



(d)

Figure 77 - Chevron crack in a submerged arc weld with the wire-flux combination SD3/1Ni + OP41TT. TP12.

(a) 40x.

(b), (c) and (d) details from (a). 400x.

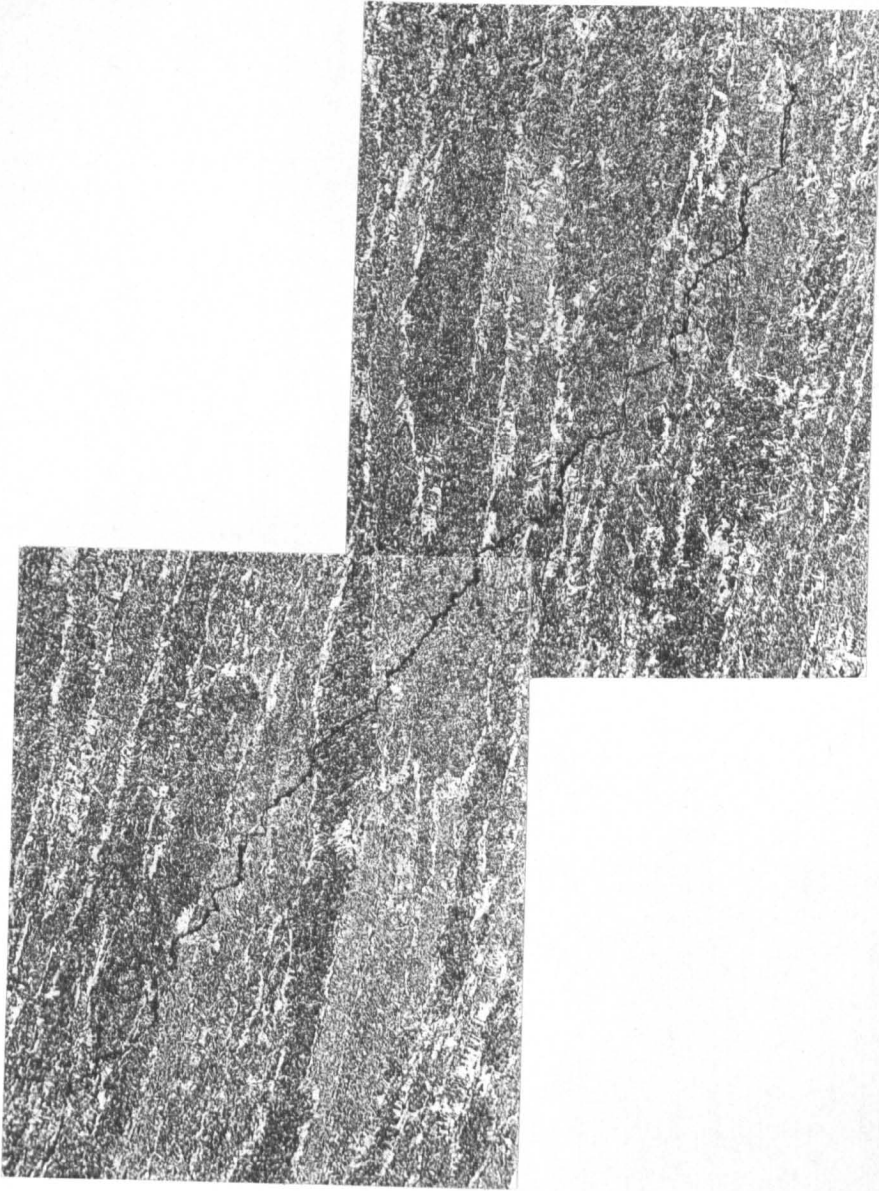
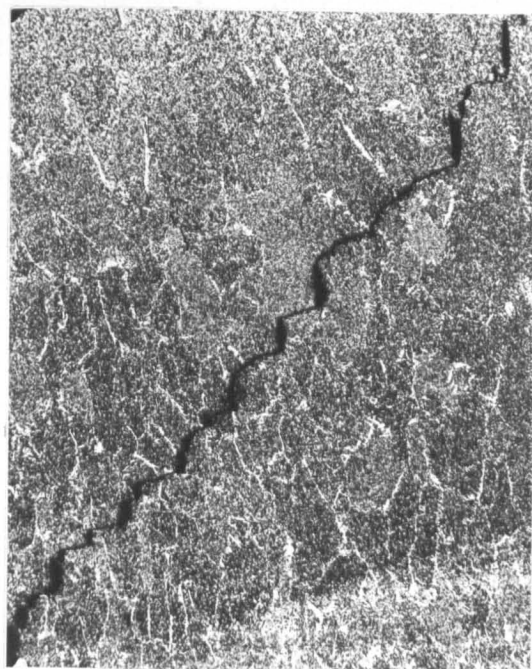
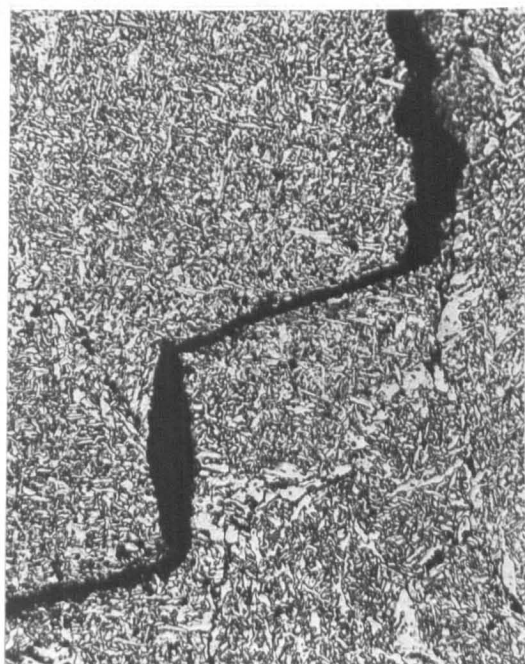


Figure 78 - Chevron crack in a submerged arc weld with the wire-flux combination SD2/3Ni + OP41TT. TP17. 120x.



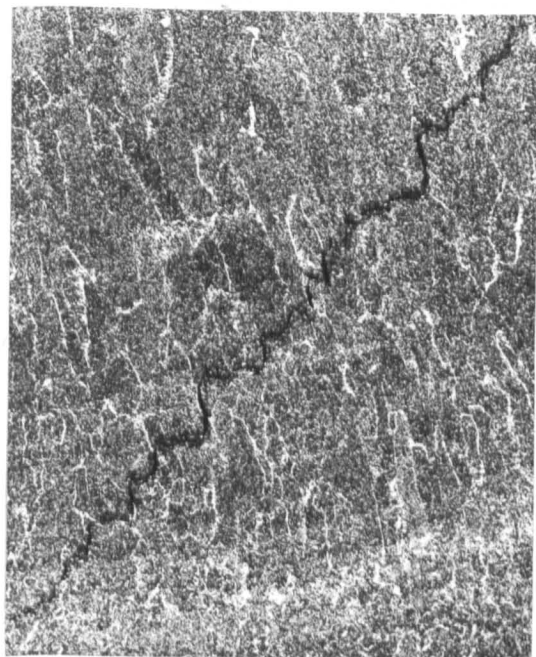
(a)



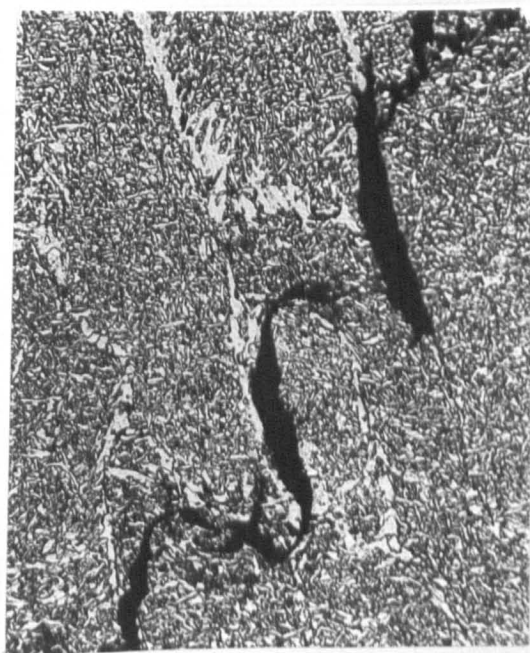
(b)

Figure 79 - Chevron crack in a submerged arc weld with the wire-flux combination SD3/Mo + OP41TT. TP21.

(a) 60x, (b) Detail, 400x.



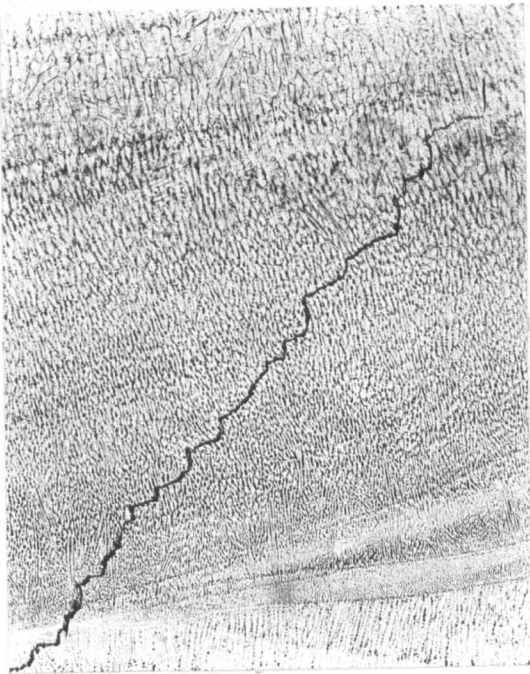
(a)



(b)

Figure 80 - Chevron crack in a submerged arc weld with the wire-flux combination SD3/Mo + OP41TT showing incomplete linking between vertical components. TP21.

(a) 60x. (b) Detail, 400x.



(a)



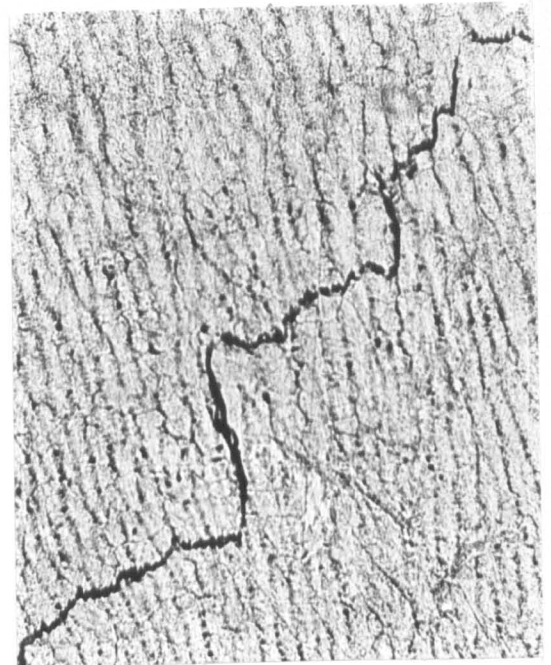
(b)

Figure 81 - Chevron crack in a submerged arc weld with the wire-flux combination SD3/Mo + OP41TT. TP21. (same crack as in Figure 79). Saspanansa etch.

(a) 40x. (b) Detail, 200x.



(a)



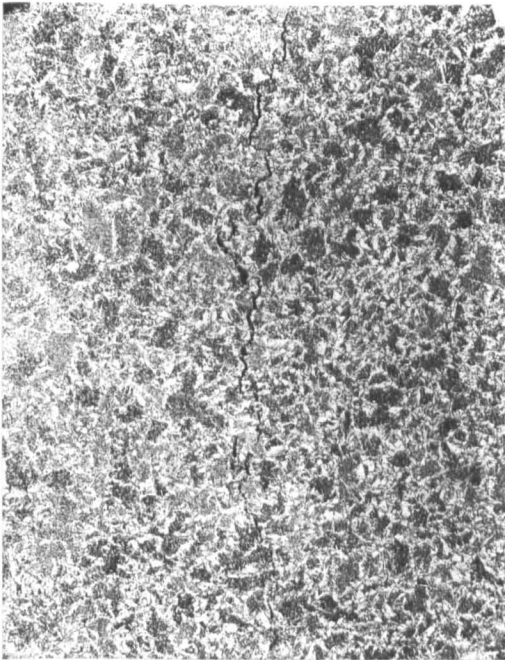
(b)

Figure 82 - Chevron crack in a submerged arc weld with the wire-flux combination SD3/Mo + OP41TT. TP21. (Same crack as in Figure 80). Saspanansa etch.

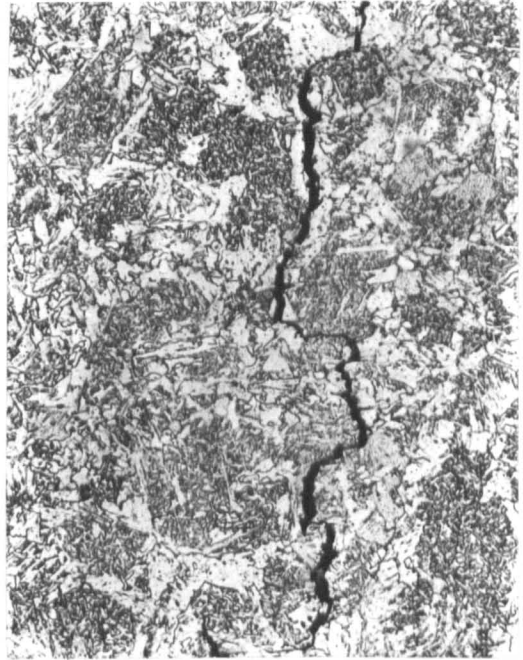
(a) 40x. (b) Detail, 200x.



Figure 83 - Detail of a chevron crack in a manual metal arc weld with electrodes E8018C1. TP29. 200x.



(a)



(b)

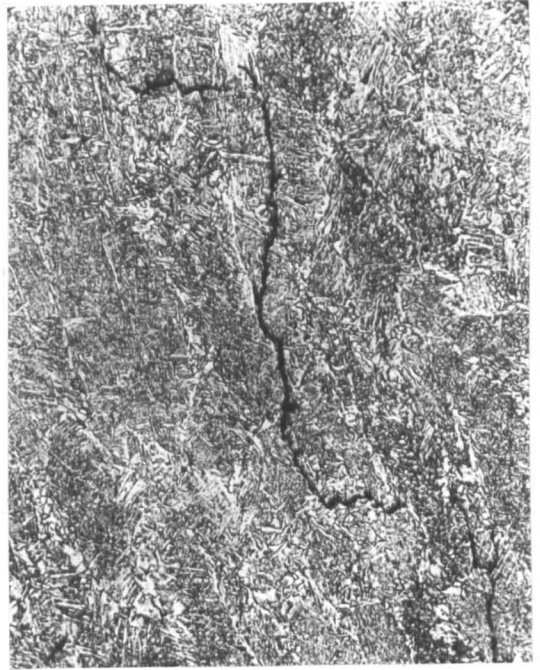
Figure 84 - Chevron crack in a manual metal arc weld with electrodes E8018C1 as observed in the longitudinal horizontal plane (parallel to the plane of the plates). TP29.

(a) 40x.

(b) Detail, 200x.



(a)

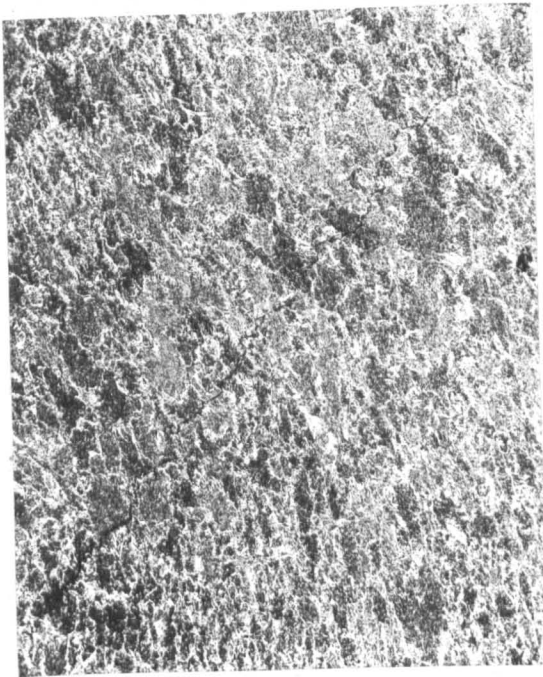


(b)

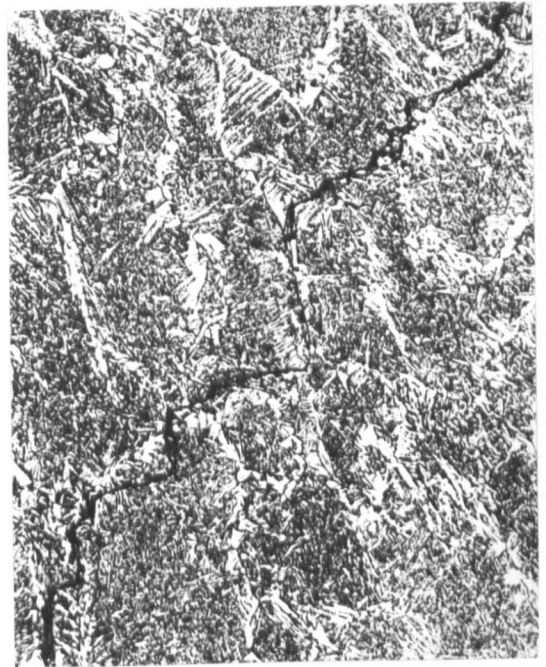
Figure 85 - Chevron crack in a manual metal arc weld with electrodes B1. TP40.

(a) 40x.

(b) Detail, 200x.



(a)

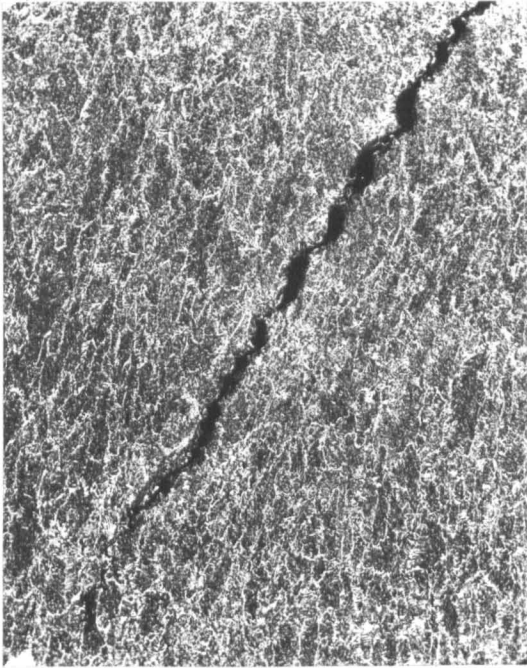


(b)

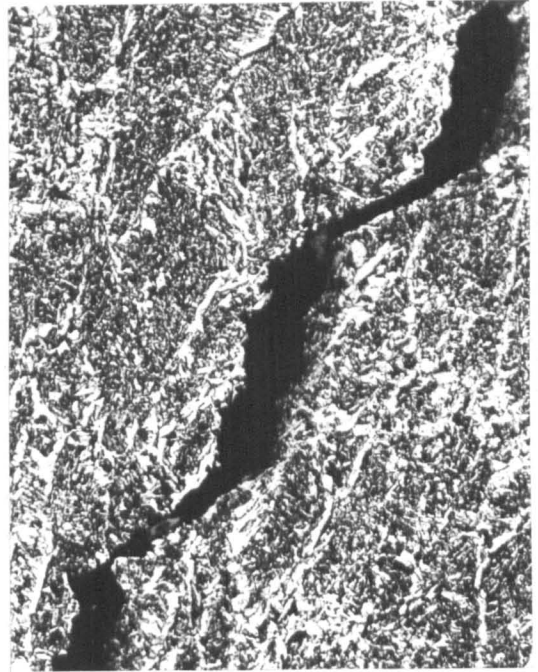
Figure 86 - Chevron crack in a manual metal arc weld with electrodes C1. TP47.

(a) 40x.

(b) Detail, 200x.



(a)

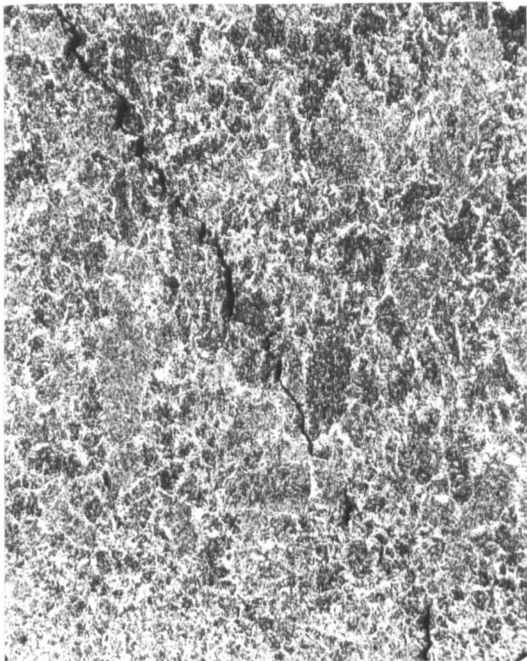


(b)

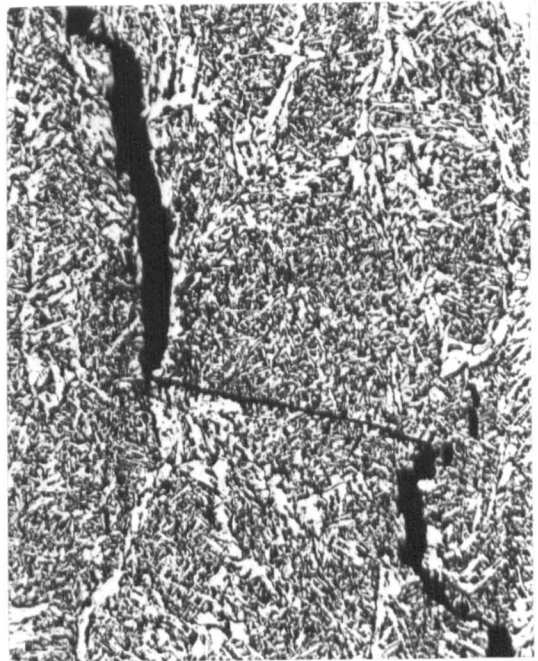
Figure 87 - Wide open chevron crack in a manual metal arc weld with electrodes C1. TP47.

(a) 40x.

(b) Detail, 200x.



(a)



(b)

Figure 88 - Chevron crack in a manual metal arc weld with electrodes C4. TP50.

(a) 60x.

(b) Detail 400x.

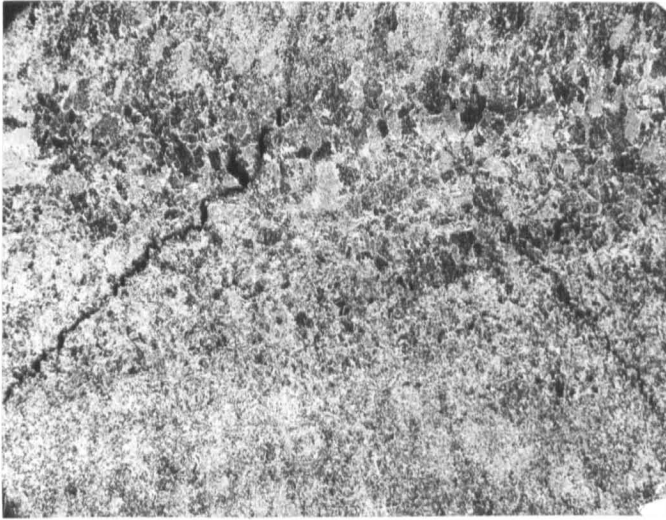
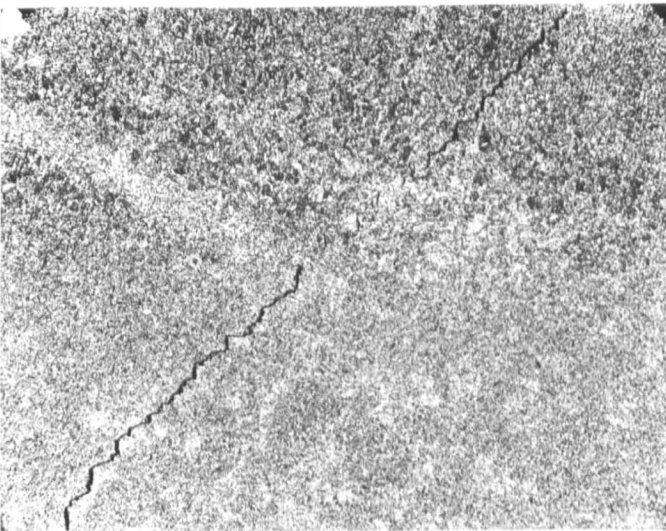


Figure 89 - Chevron cracks with different orientations in the same run. Manual metal arc weld with electrodes E8018C1. TP35. 20x.



(a)

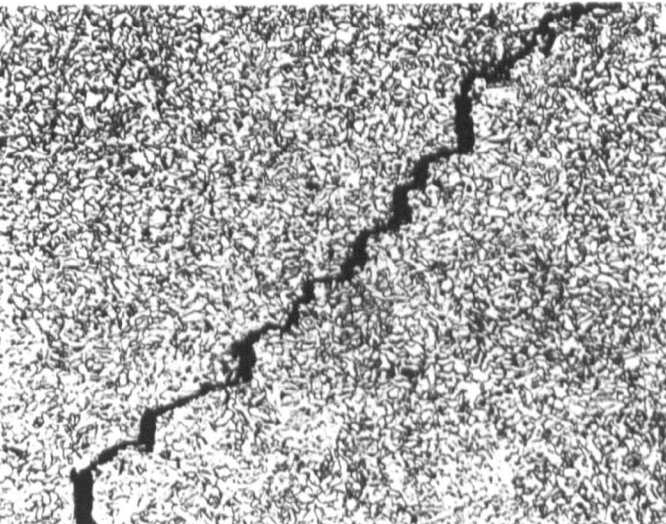
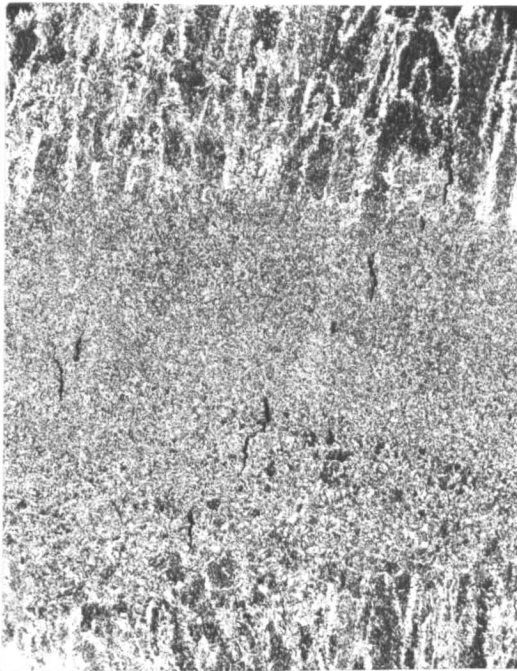
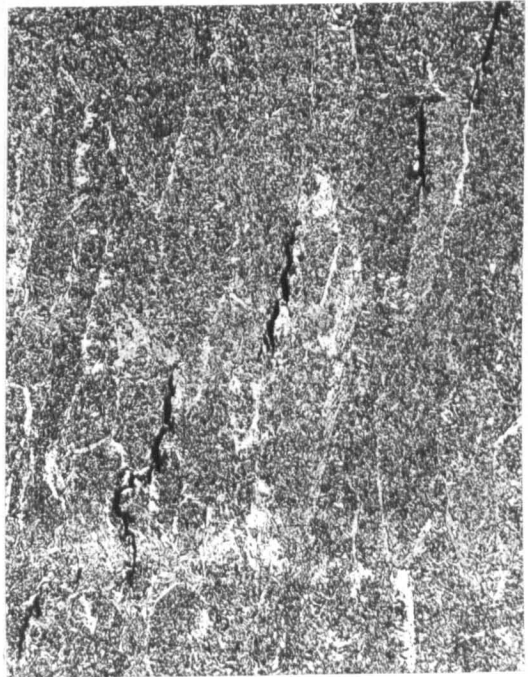


Figure 90 - Chevron crack in the refined region of a manual metal arc weld with electrodes B2. TP42.
(a) 40x. (b) Detail 200x

(b)



(a)

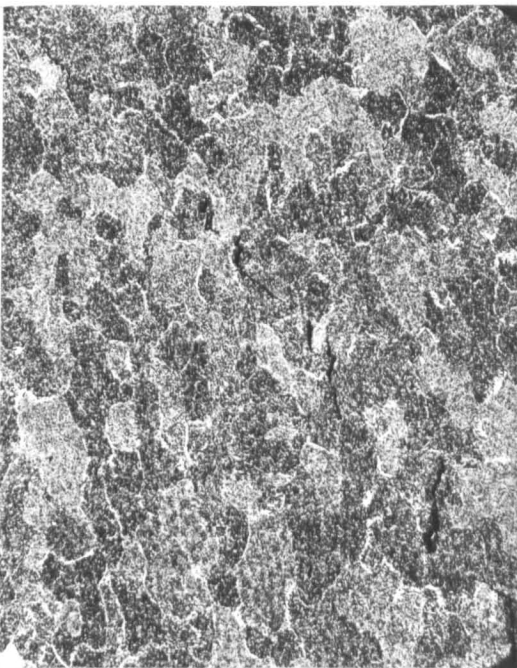


(b)

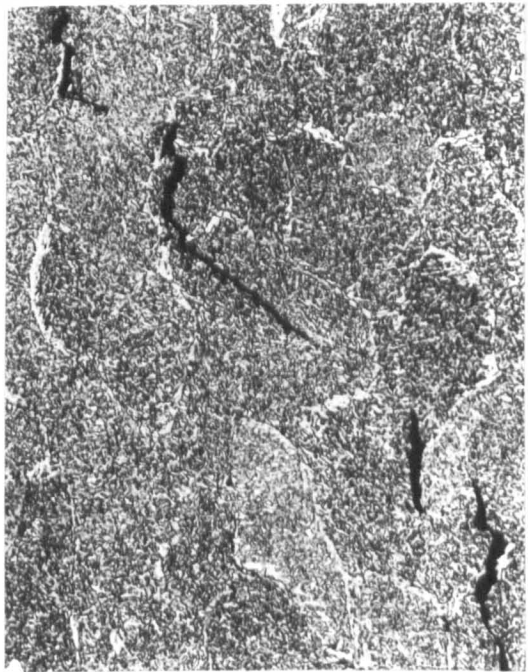
Figure 91 - Staggered, non-linked microcracks.

(a) Manual metal arc weld deposited with electrodes E8018C1. TP29. 60x.

(b) Submerged arc weld deposited with the wire-flux combination SD3/Mo + OP41TT. TP21. 200x.



(a)



(b)

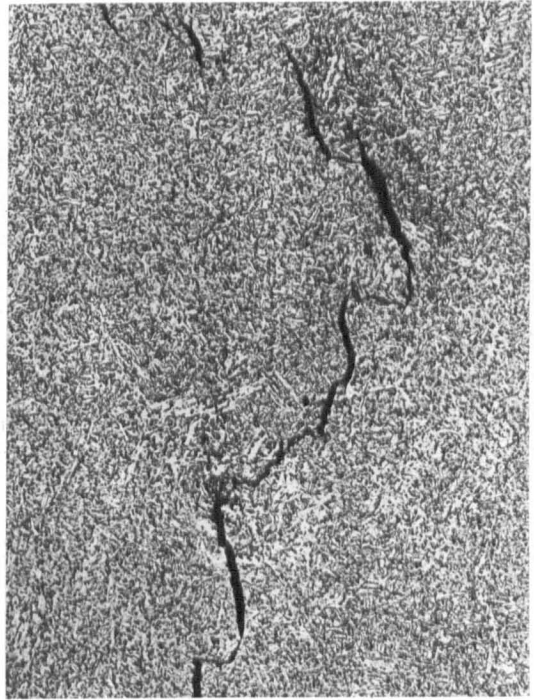
Figure 92 - Staggered microcracks at an intermediate stage of linking. Submerged arc weld deposited with the wire-flux combination SD3/Mo + OP41TT. TP21.

(a) 60x.

(b) Detail 200x.



(a)



(b)

Figure 93 - Vertical crack with a morphology reminiscent of a chevron crack. Submerged arc weld deposited with the wire-flux combination SD3/1Ni $\frac{1}{2}$ Mo + OP41TT. TP24.

(a) 40x.

(b) Detail 200x.



(a)



(c)

Figure 94 - Vertical cracks without typical cracking path. Submerged arc weld deposited with the wire-flux combination SD3/1Ni $\frac{1}{2}$ Mo + OP41TT. TP24.

(a) and (b) 80x.

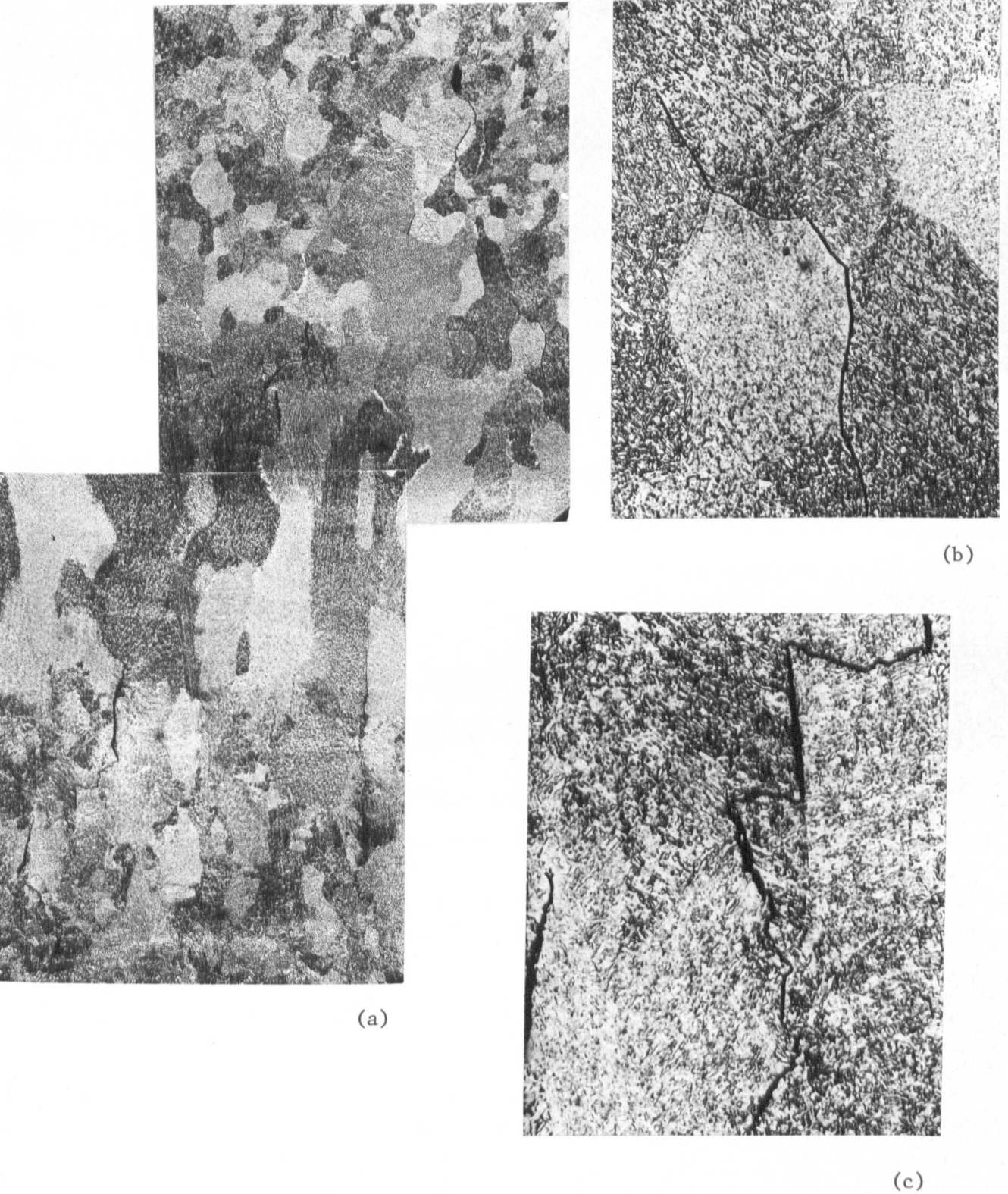
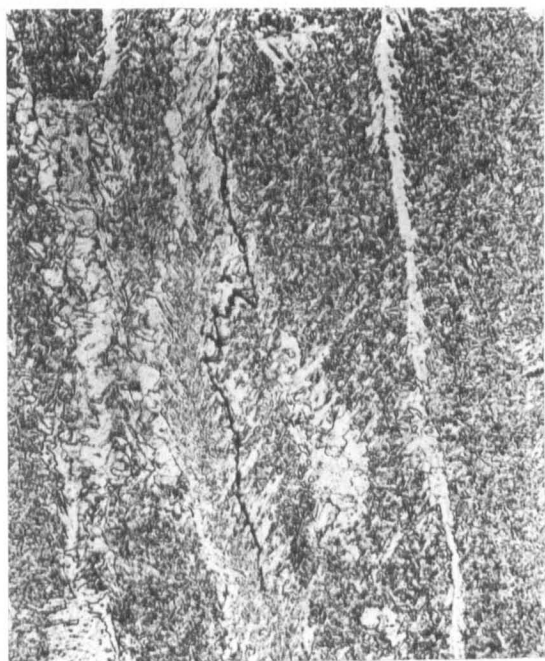


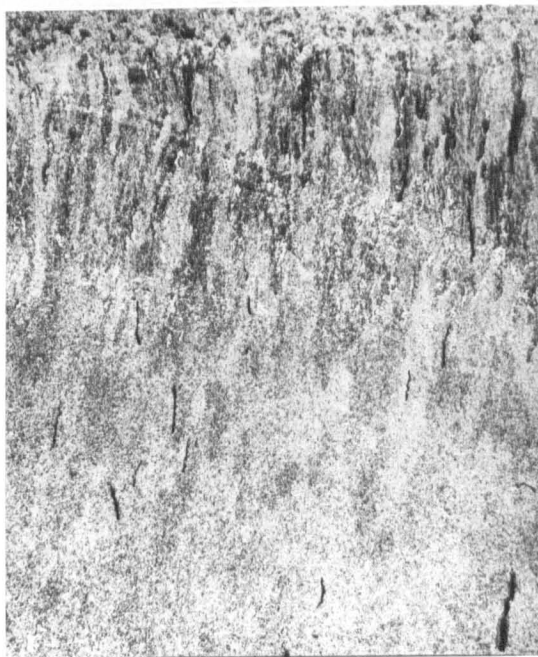
Figure 95 - Vertical cracks in a manual metal arc weld deposited with electrodes B5Ni. TP62.

(a) 40x.

(b) and (c) Details, 200x.



(a)

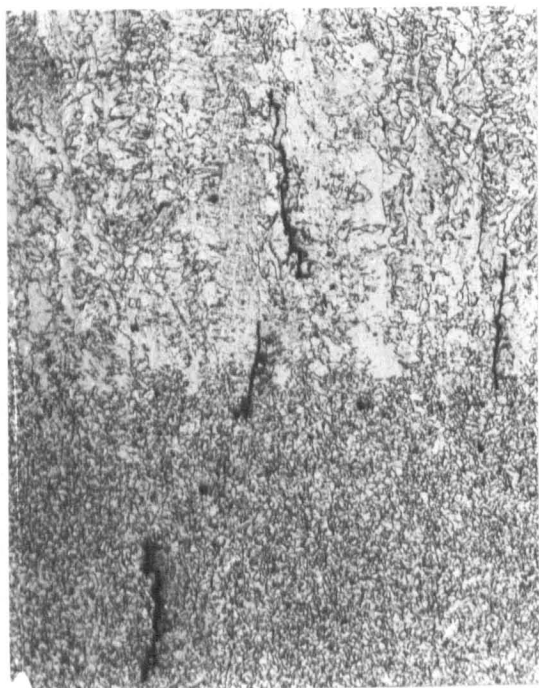


(b)

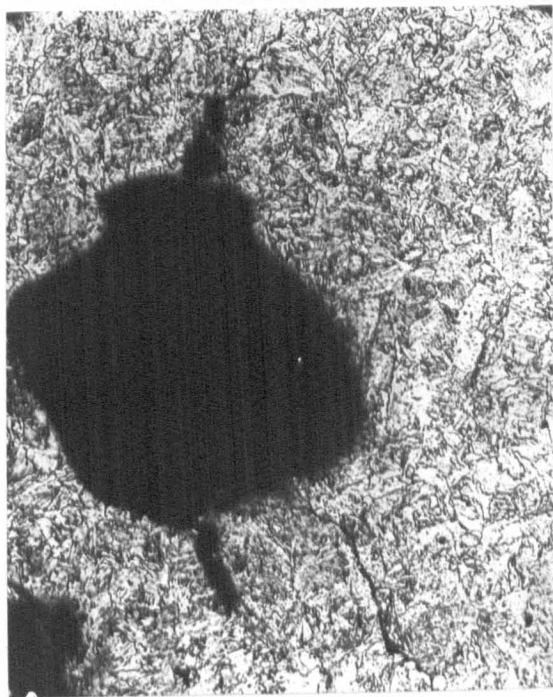
Figure 96 - Microfissures in manual metal arc welds.

(a) Deposited with electrodes E8018C1. TP29. 400x.

(b) Deposited with electrodes C3. TP49. 20x.



(a)



(b)

Figure 97 - Microfissures in manual metal arc welds.

(a) Deposited with electrodes E6013. TP39. 80x.

(b) Deposited with electrodes R4. TP55. 80x.

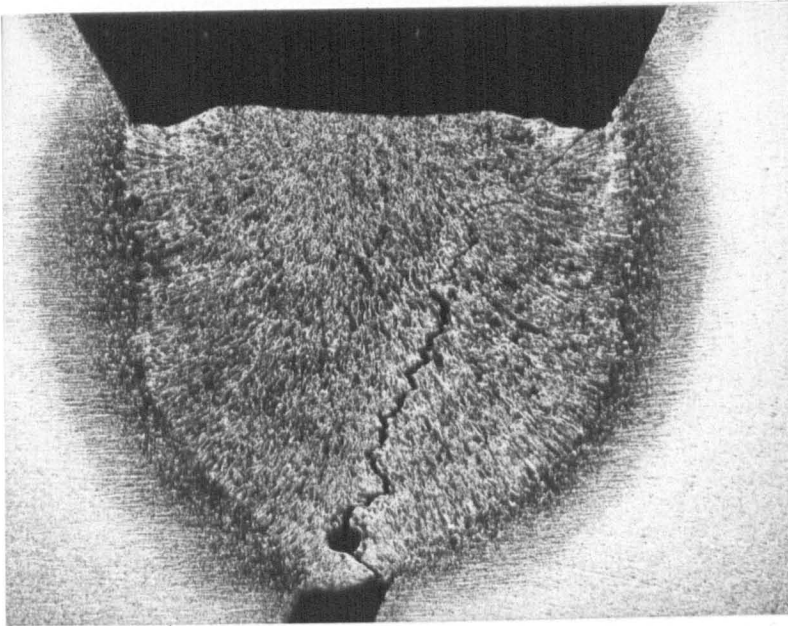
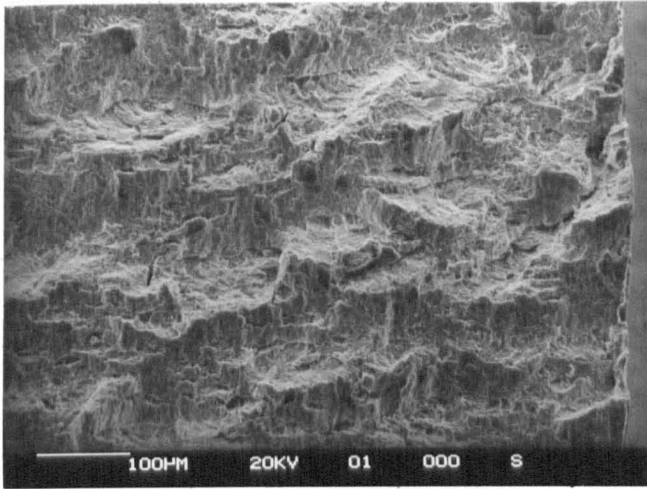
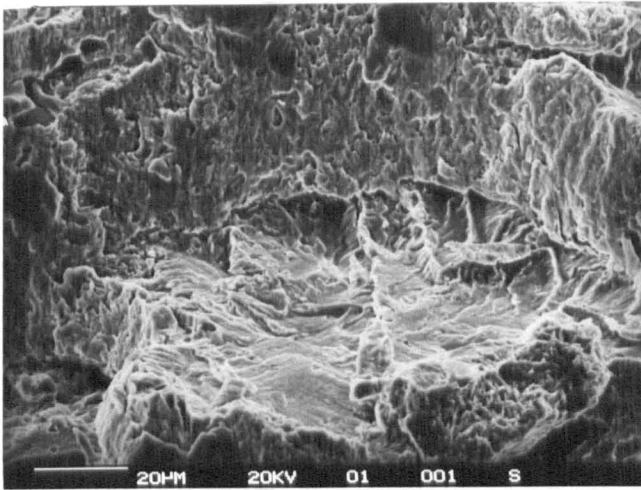


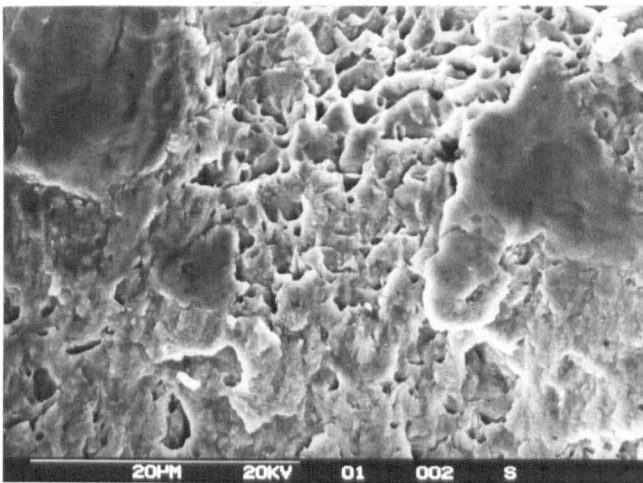
Figure 98 - Longitudinal crack with a staircase morphology produced in a Y groove Tekken test. Weld metal deposited with electrodes Cl. Cross section of the joint. 5x.



(a)



(b)



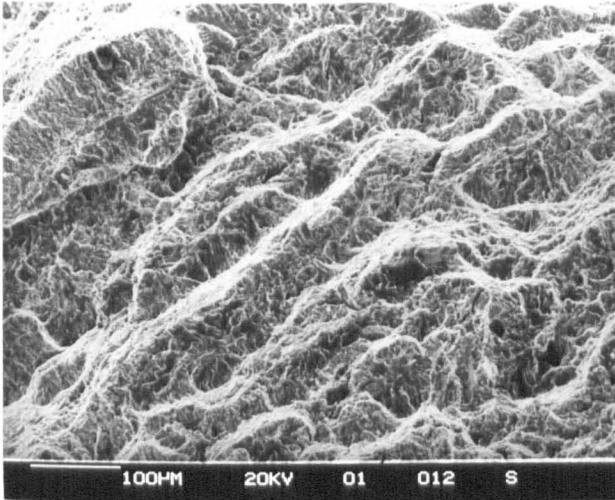
(c)

Figure 99 - Fracture surface of a chevron crack in the industrial sample B.

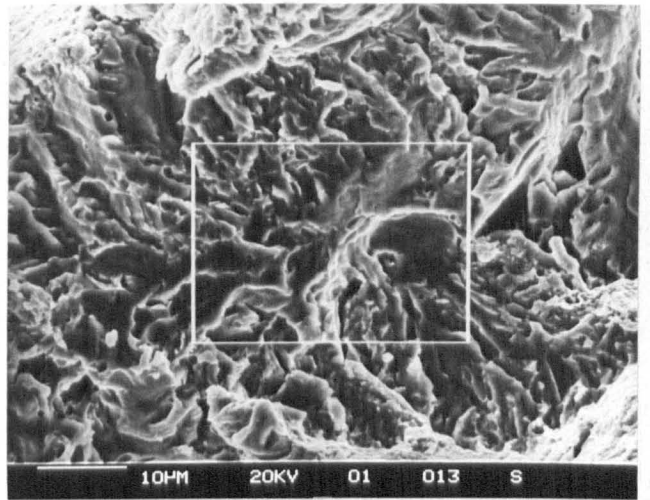
(a) General aspect.

(b) Detail of vertical and horizontal components.

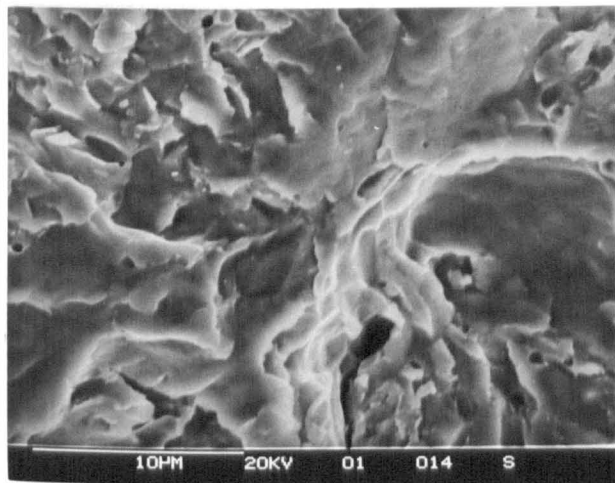
(c) Detail of a horizontal component.



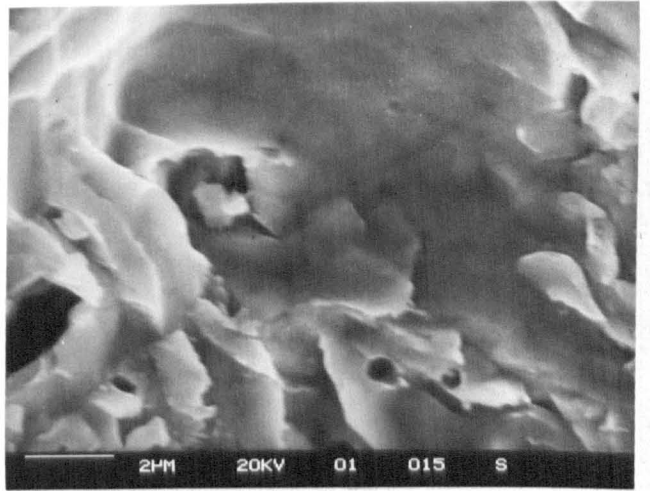
(a)



(b)



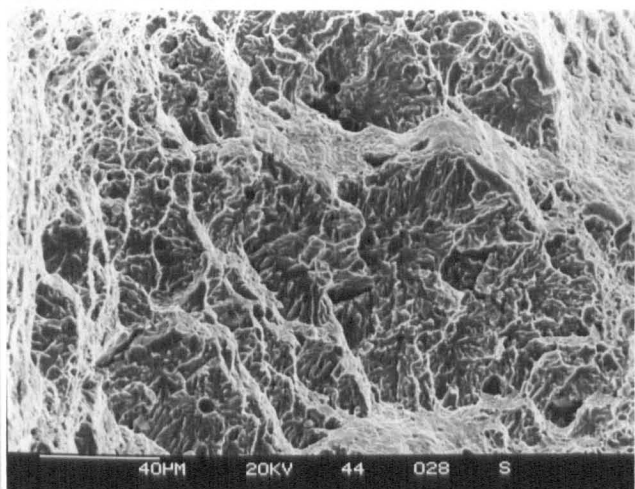
(c)



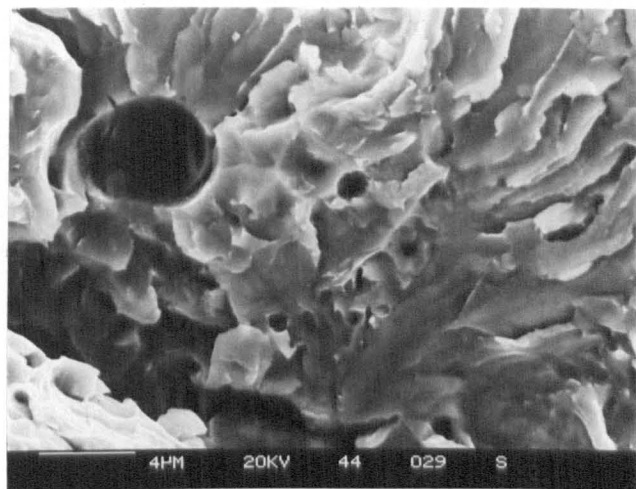
(d)

Figure 100 - Vertical components of a chevron crack in the industrial sample B.

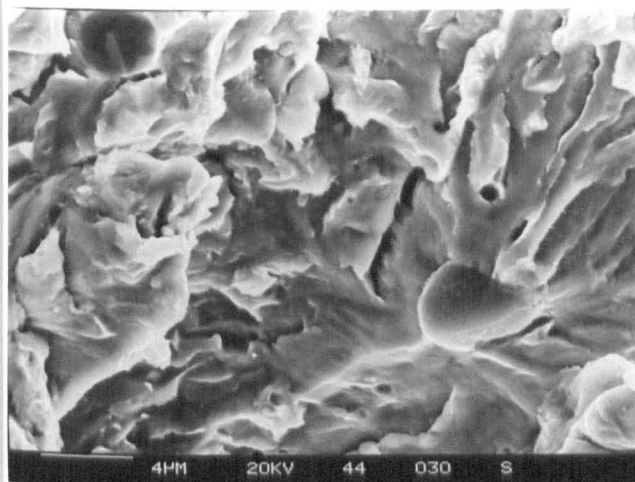
- (a) General aspect.
- (b) Detail from (a).
- (c) Detail from (b).
- (d) Detail from (c).



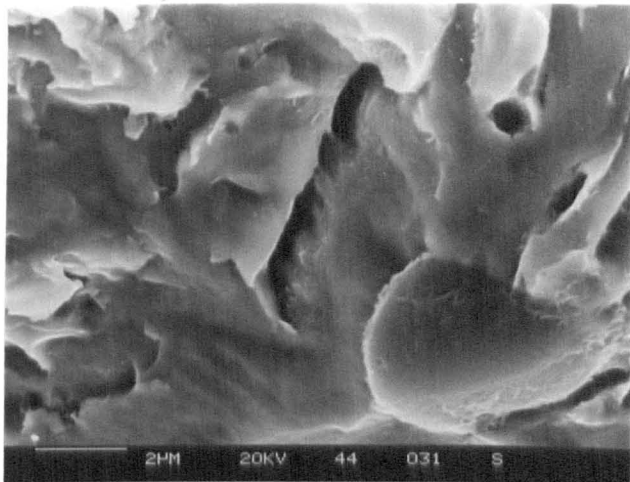
(a)



(b)



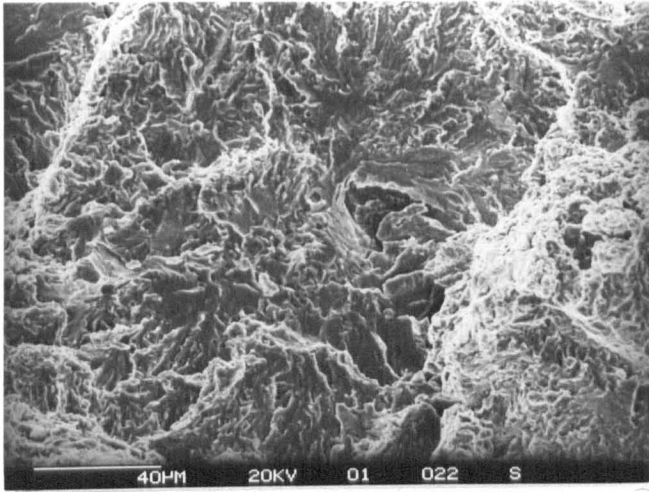
(c)



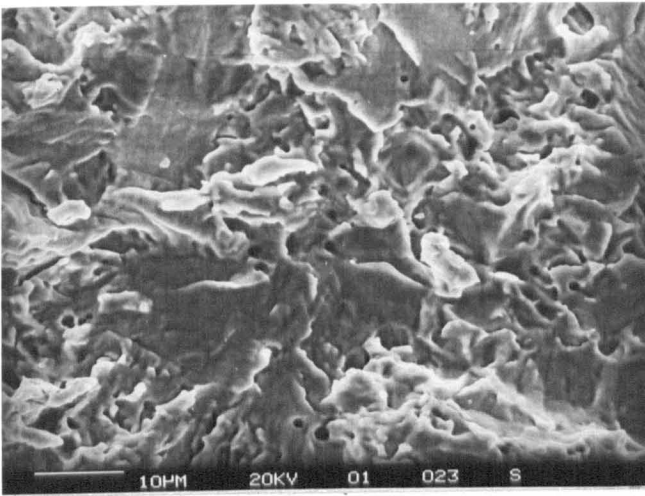
(d)

Figure 101 - Vertical components of a chevron crack observed in the industrial sample A.

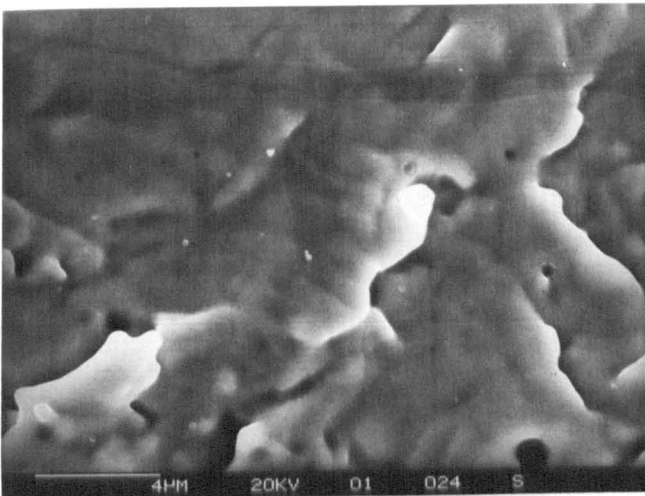
- (a) General aspect.
- (b) Detail from (a).
- (c) Another detail from (a).
- (d) Detail from (c).



(a)



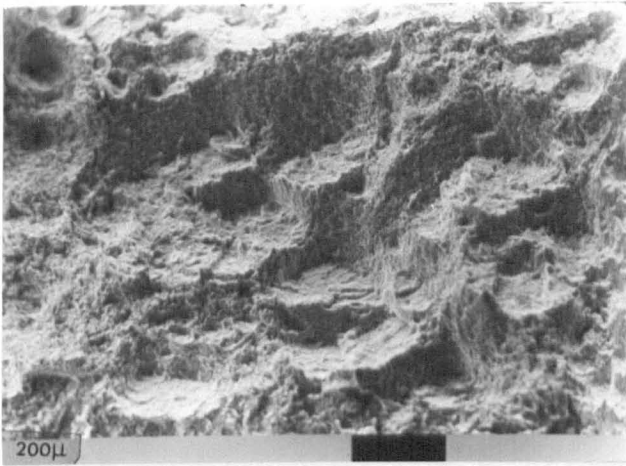
(b)



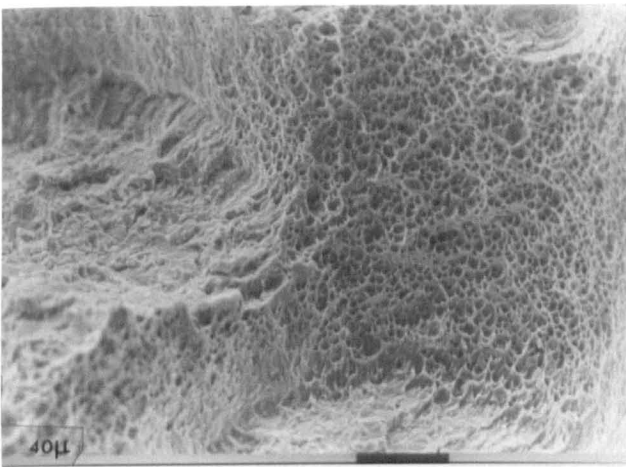
(c)

Figure 102 - Vertical component of a chevron crack which was exposed to high temperatures. Industrial sample B.

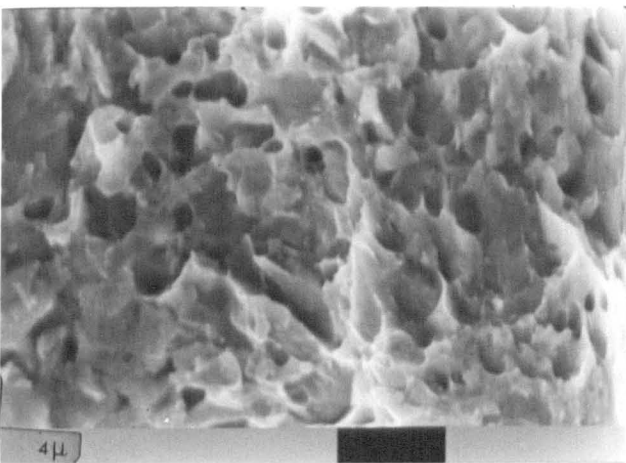
- (a) General aspect.
- (b) Detail from (a).
- (c) Detail from (b).



(a)



(b)



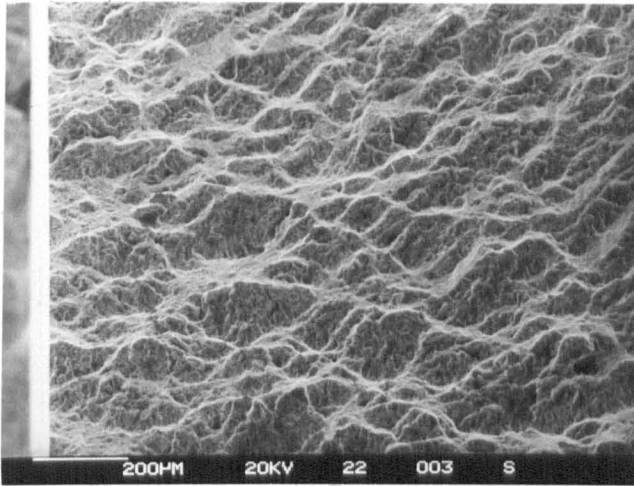
(c)

Figure 103 - Fracture surface of a chevron crack in a submerged arc weld. TP17.

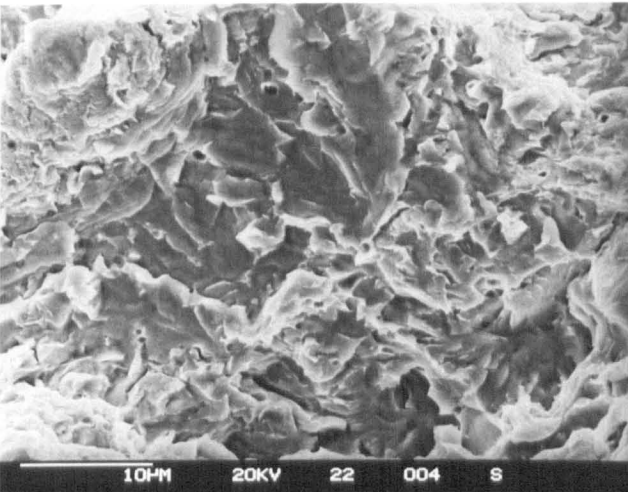
(a) General aspect.

(b) Detail from a horizontal component showing mainly dimples.

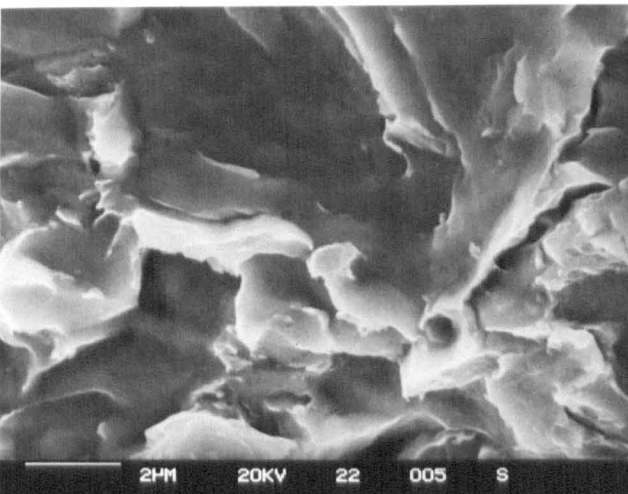
(c) Detail of a horizontal component showing dimples and quasi-cleavage.



(a)



(b)



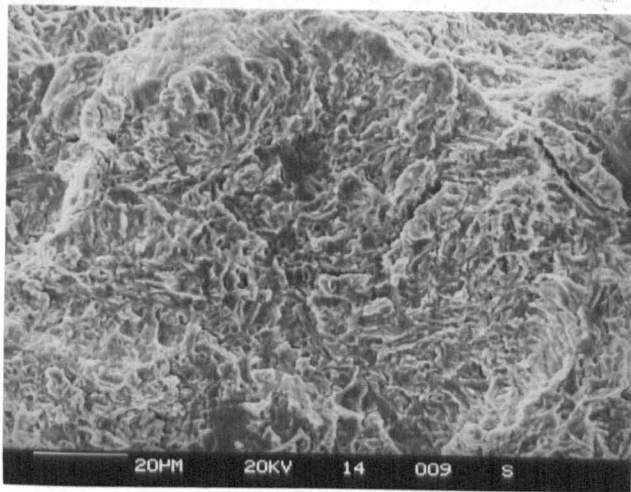
(c)

Figure 104 - Vertical components of a chevron crack in a submerged arc weld. TP17.

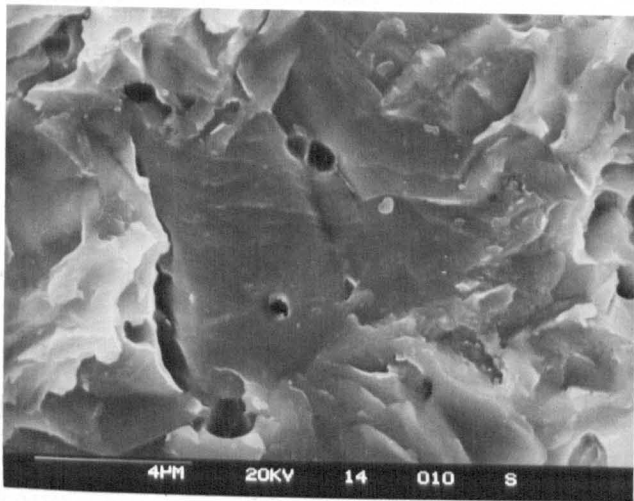
(a) General aspect.

(b) Detail from (a).

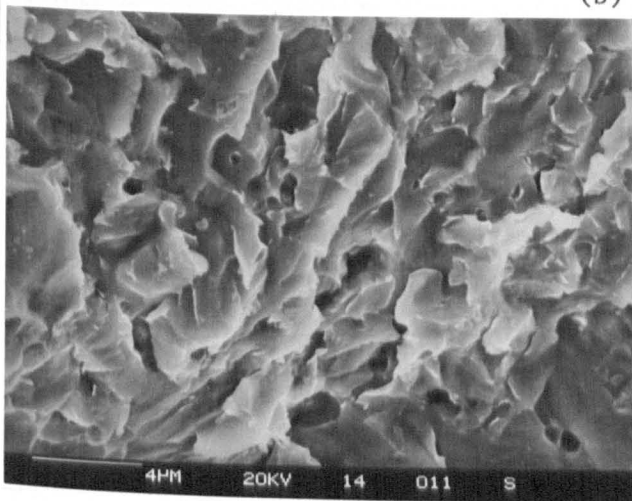
(c) Detail from (b).



(a)



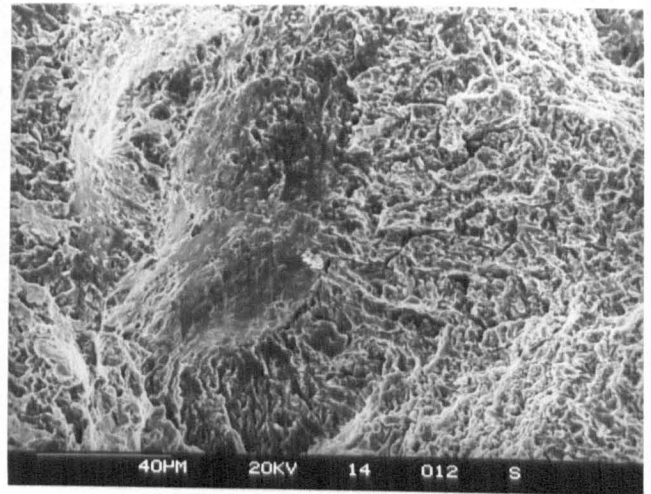
(b)



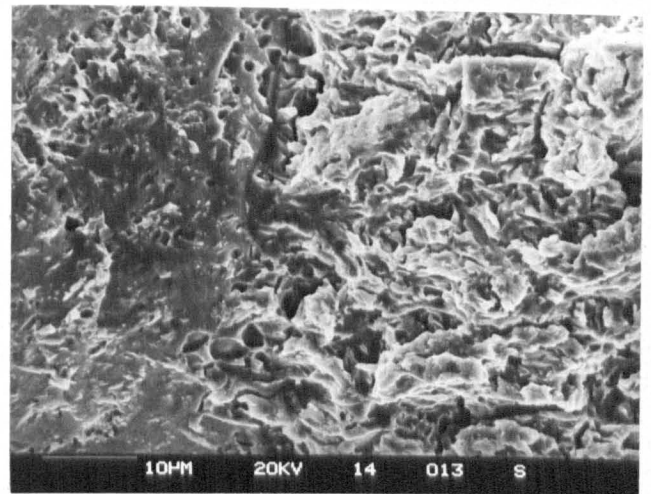
(c)

Figure 105 - Vertical component of a chevron crack in a submerged arc weld. TP21.

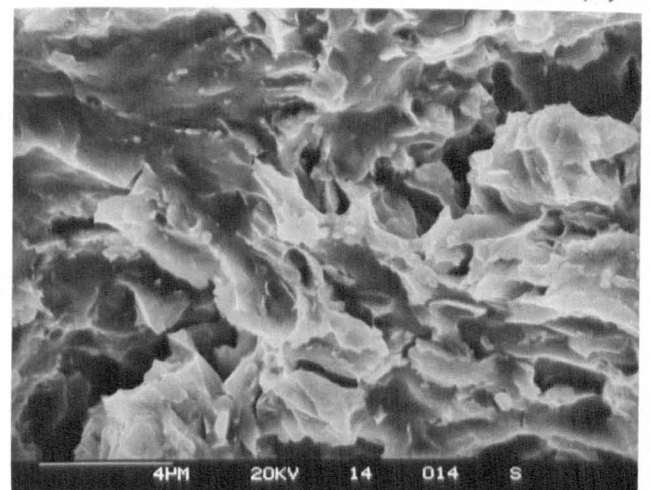
- (a) General aspect.
- (b) Detail from (a).
- (c) Another detail from (a).



(a)



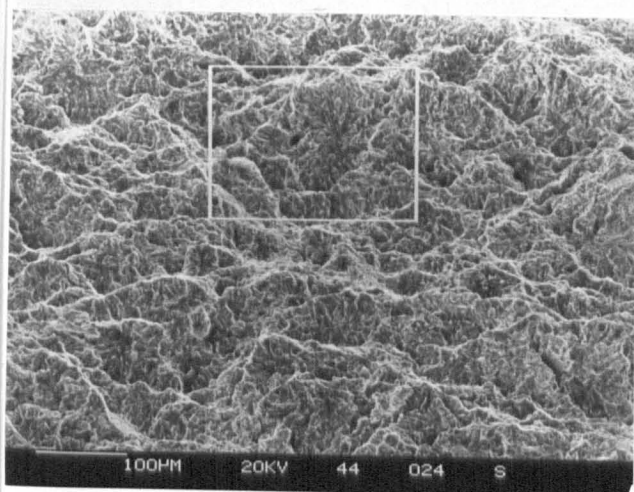
(b)



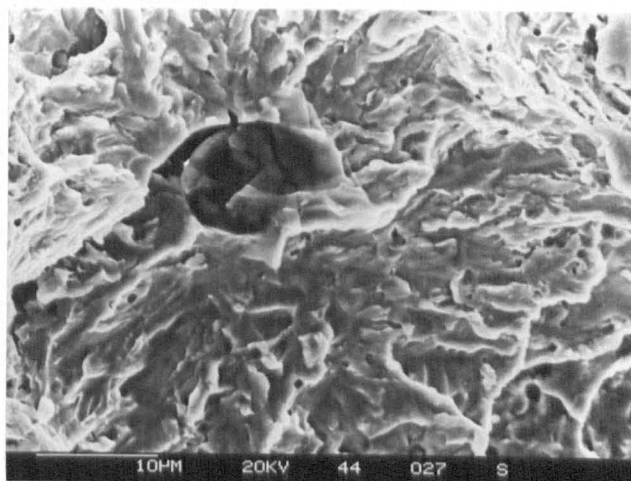
(c)

Figure 106 - Vertical component of a chevron crack showing inter and transgranular failure. Submerged arc weld. TP21.

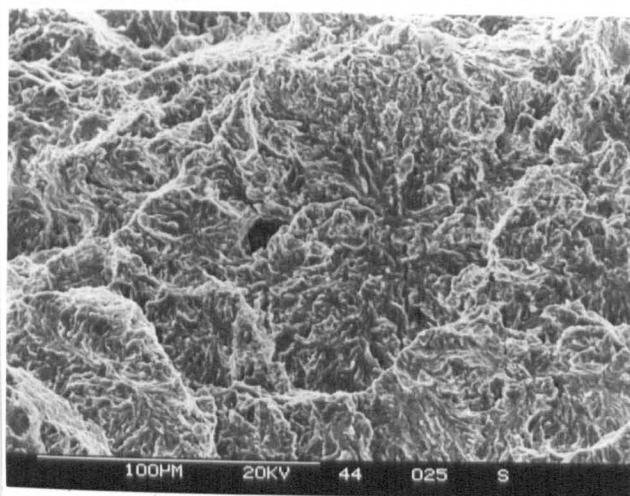
- (a) General aspect.
- (b) Detail from (a).
- (c) Detail from (b).



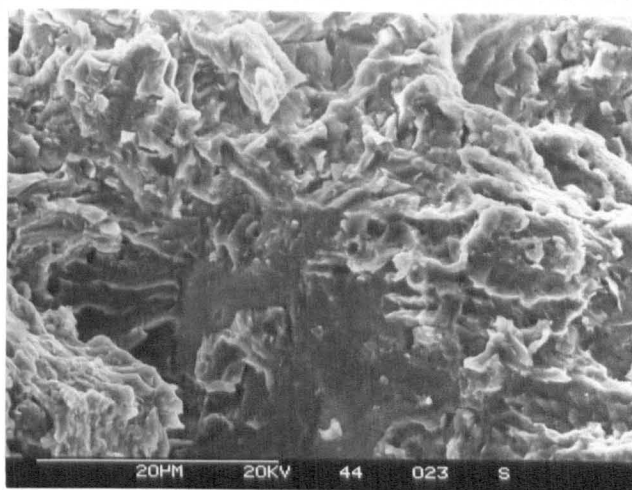
(a)



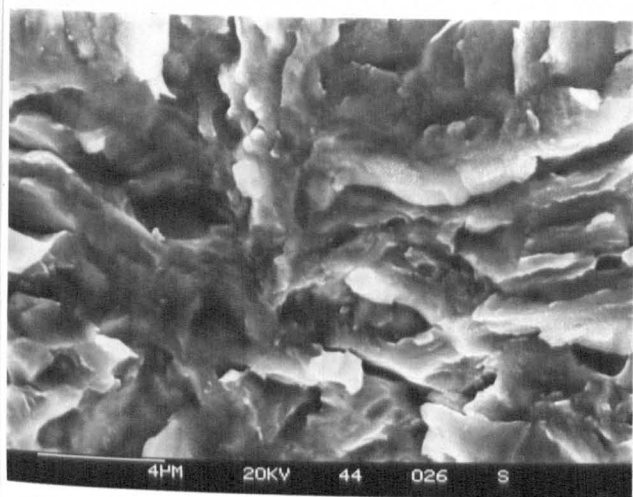
(d)



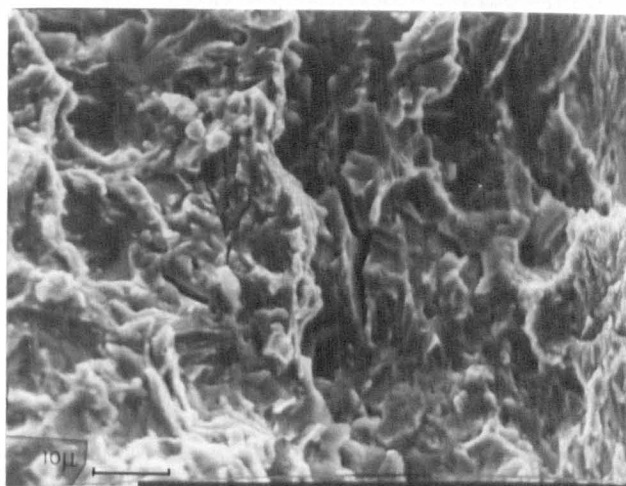
(b)



(e)



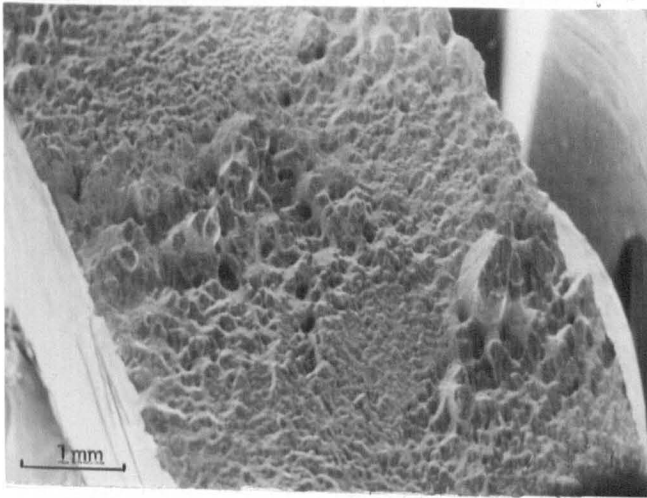
(c)



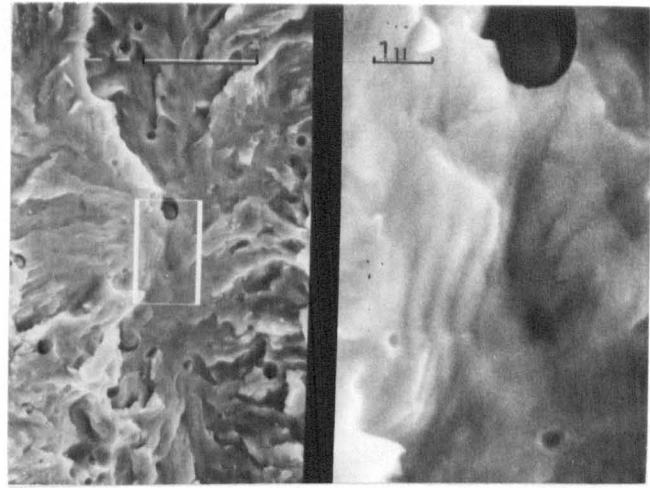
(f)

Figure 107 - Vertical components of a chevron crack in a manual metal arc weld. TP42.

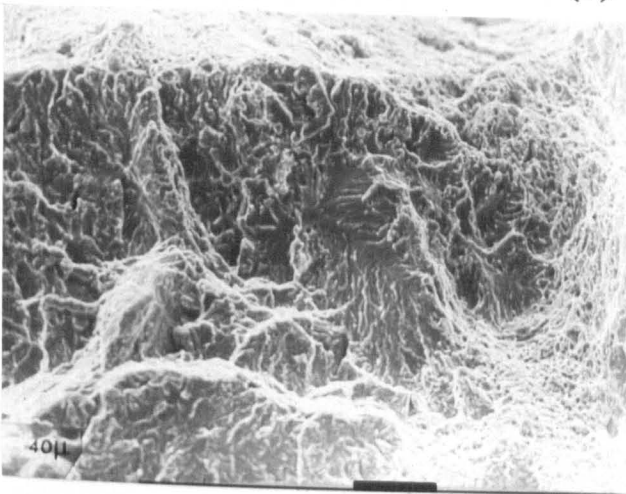
- (a) General aspect. (b) Detail from (a). (c) Detail from (b).
- (d) Detail of a component nucleated at an inclusion.
- (e) Detail of a component showing inter and transgranular failure.
- (f) Detail of the centre of a component without clear origin.



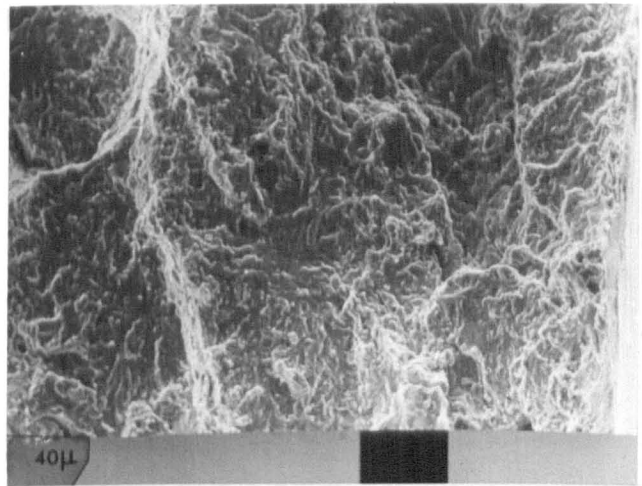
(a)



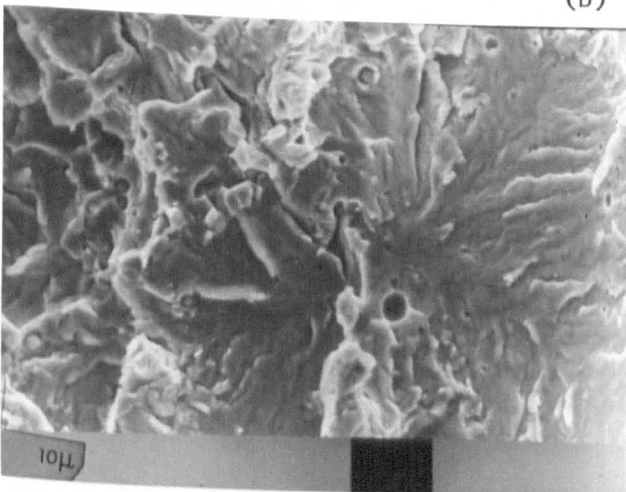
(d)



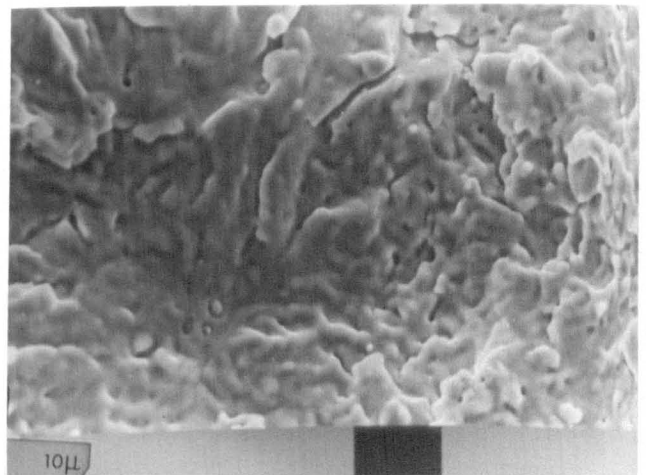
(b)



(e)



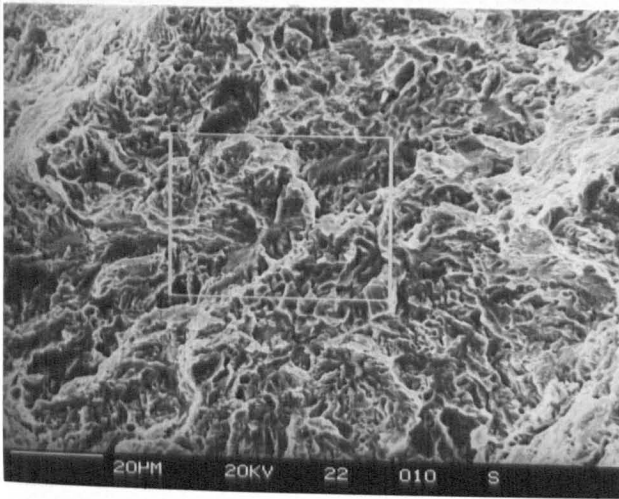
(c)



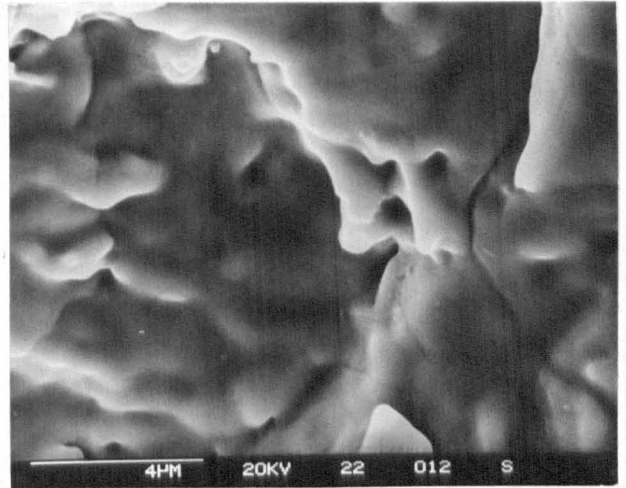
(f)

Figure 108 - Vertical components of a chevron crack in a manual metal arc weld.
TP47.

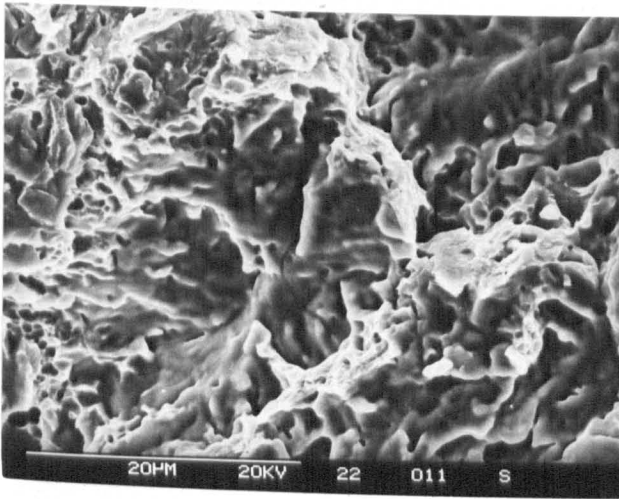
- (a) General aspect.
- (b) Detail from a component.
- (c) Detail from (b).
- (d) Detail of striations in the centre of a component.
- (e) Detail of a component exposed to high temperatures.
- (f) Detail from (e).



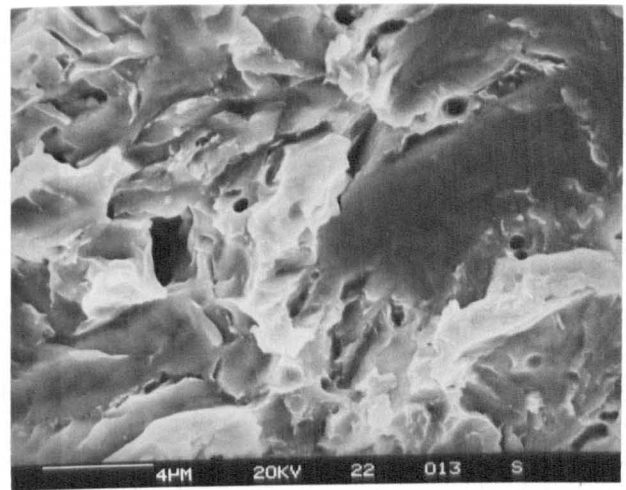
(a)



(c)



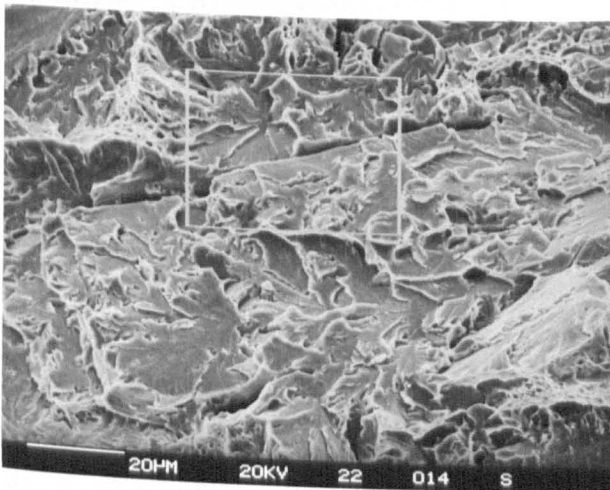
(b)



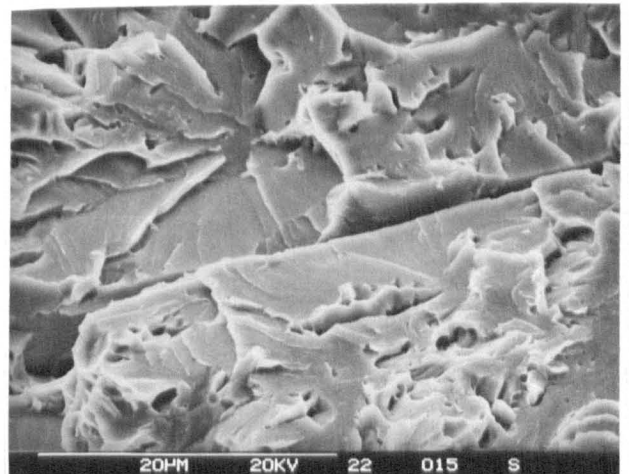
(d)

Figure 109 - Vertical component of a chevron crack in a submerged arc weld showing signs of high temperature exposure. TP17.

- (a) General aspect. (b) Detail from (a). (c) Detail from (b).
(d) Detail of quasi-cleavage in the outer regions of the component.



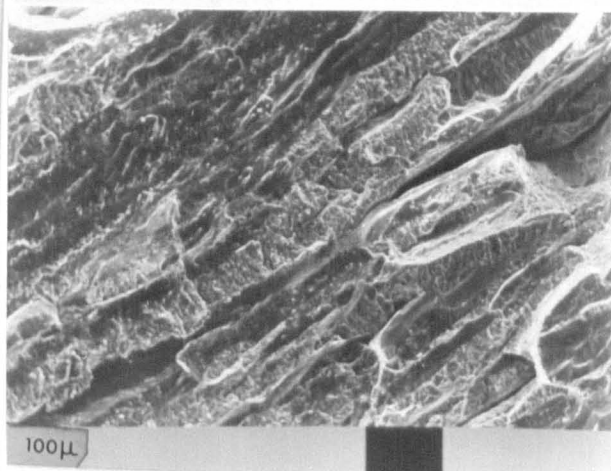
(a)



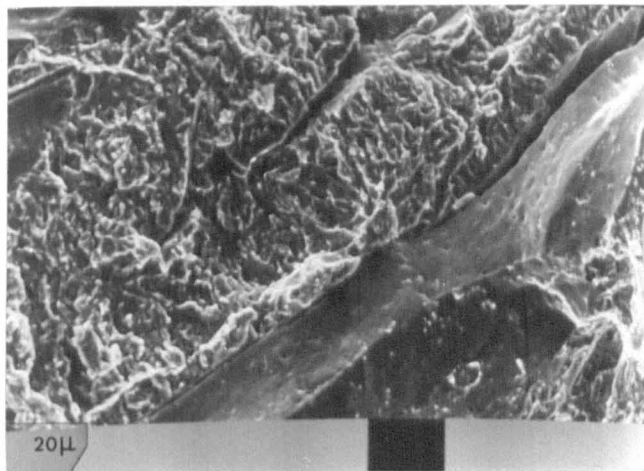
(b)

Figure 110 - Propagation of a chevron crack which was broken open after pre-cooling in liquid nitrogen.

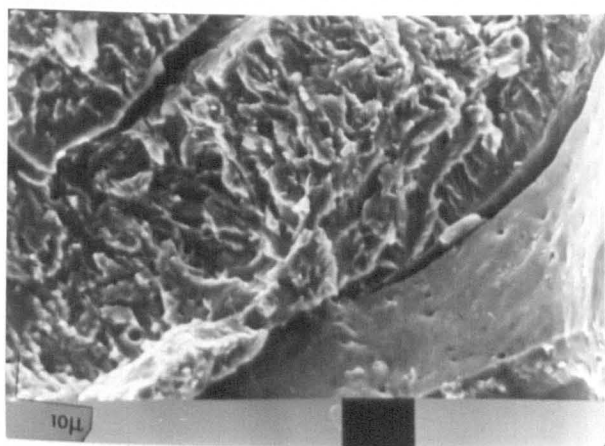
- (a) General view. (b) Detail from (a).



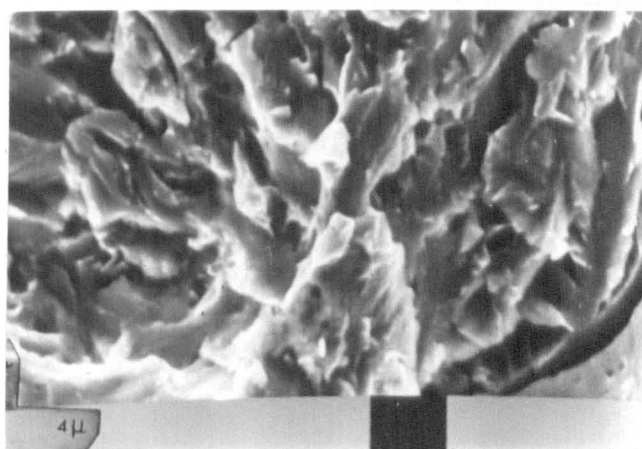
(a)



(b)



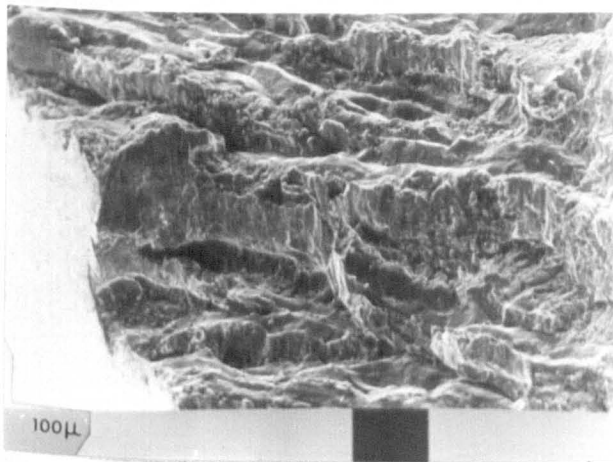
(c)



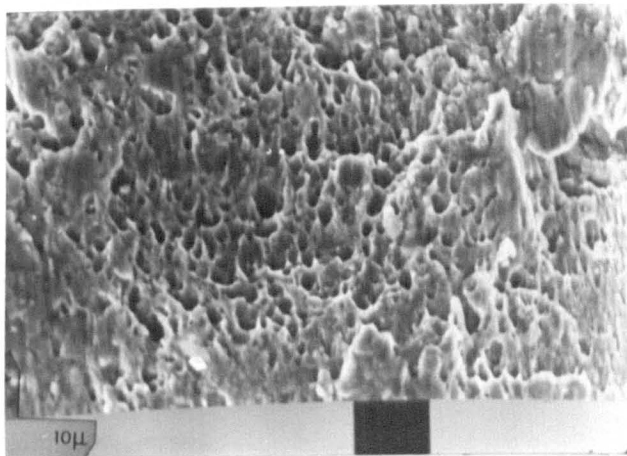
(d)

Figure 111 - Fracture surface of a vertical crack in a submerged arc weld. TP24.

- (a) General aspect. (b) Detail from (a). (c) Detail from (b).
(d) Detail of transgranular failure by quasi-cleavage.



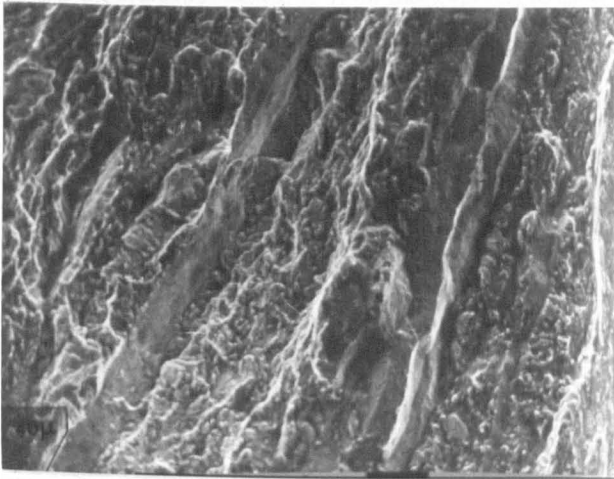
(a)



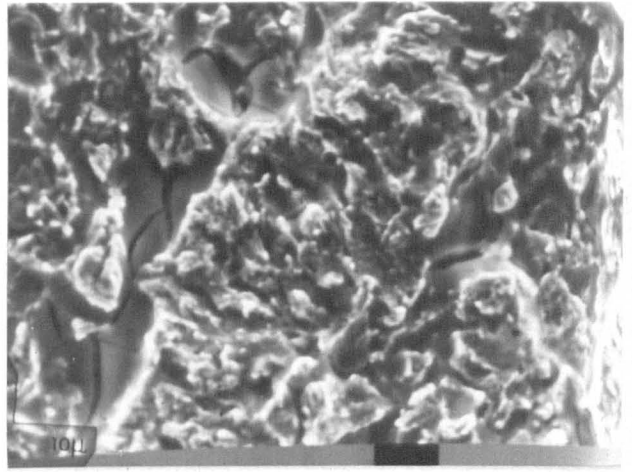
(b)

Figure 112 - Detail of areas of ductile failure linking brittle fracture regions. in a vertical crack. Submerged arc weld. TP24. (Crack also shown in Figure 93).

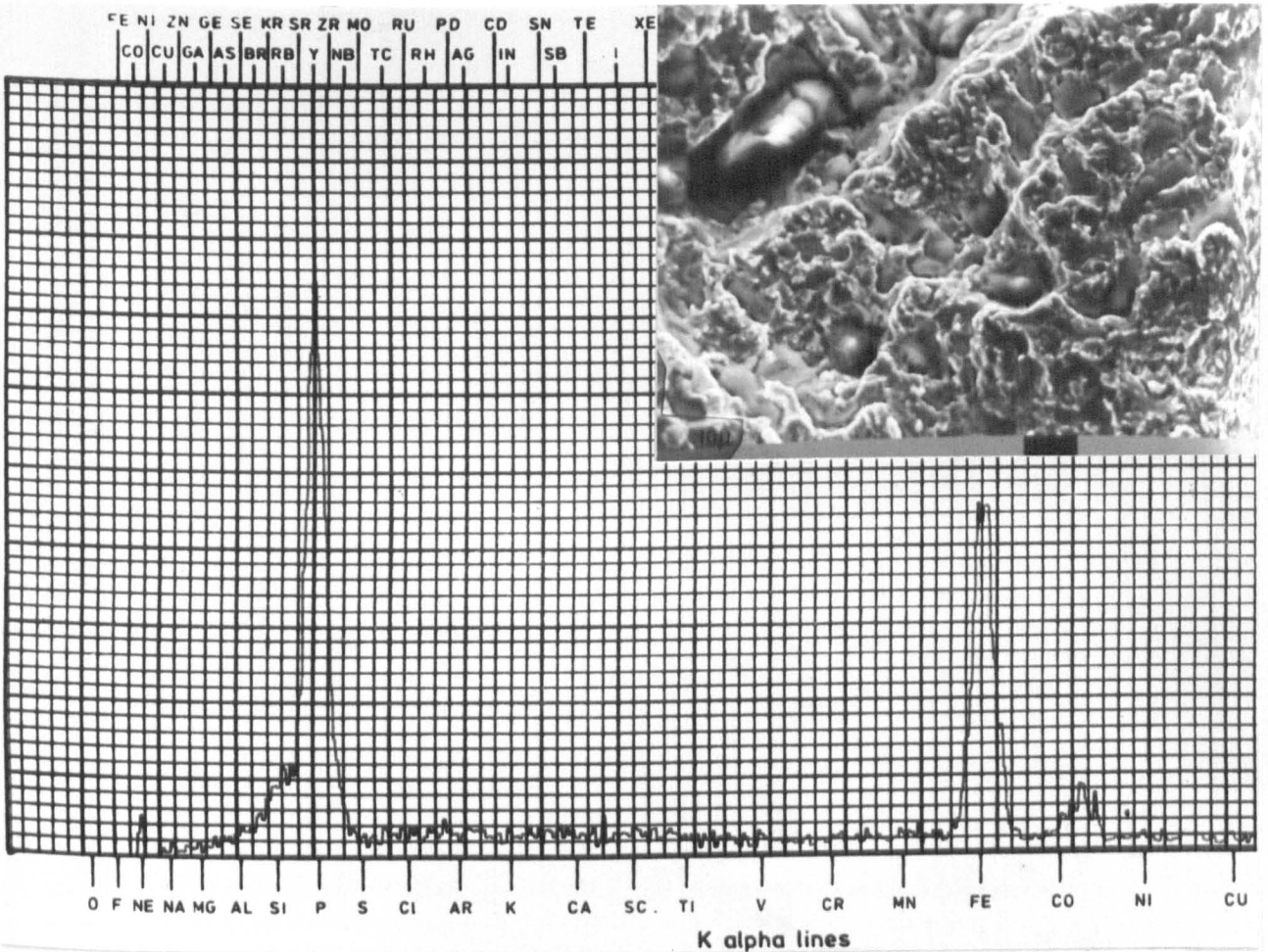
- (a) General aspect.
(b) Detail from (a) showing the aspect of the dimples.



(a)



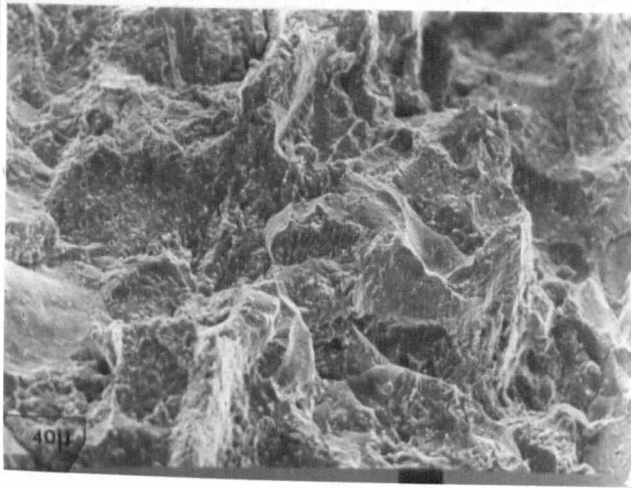
(b)



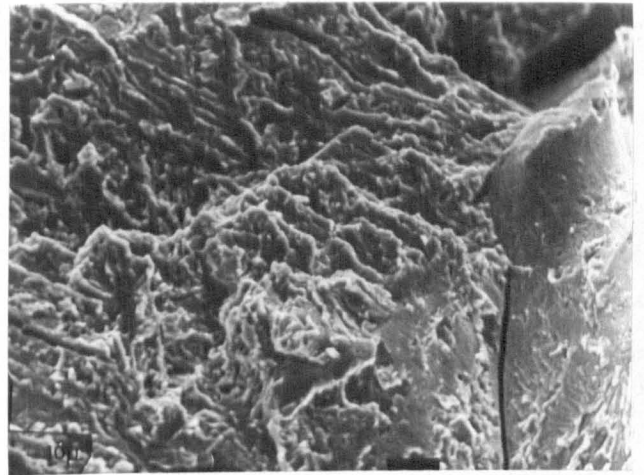
(c)

Figure 113 - Vertical crack in a submerged arc weld associated with phosphorous segregation. TP27.

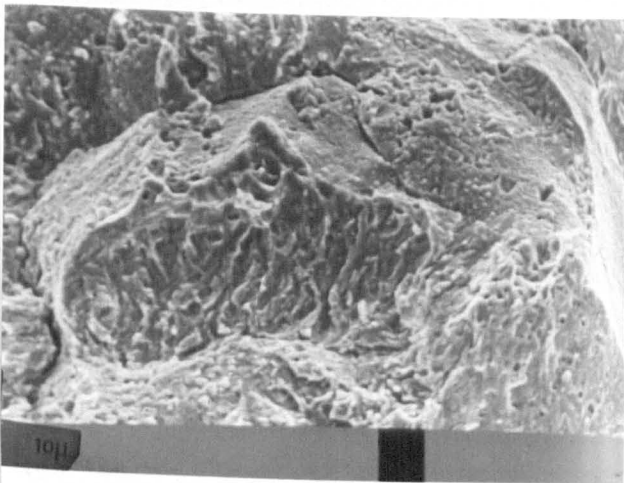
- (a) General aspect of the crack.
- (b) Detail of segregation.
- (c) Detail of segregation and chemical analysis.



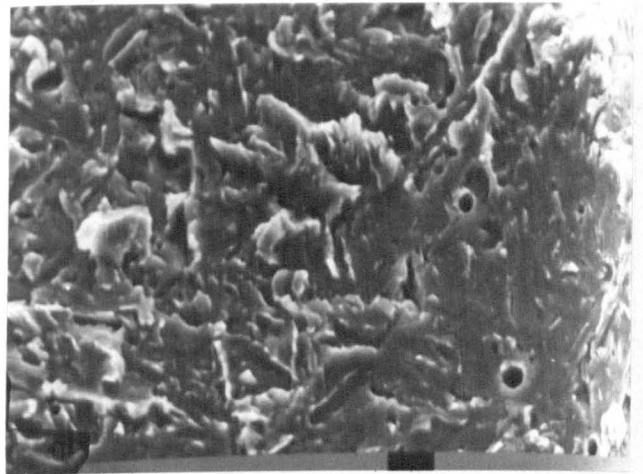
(a)



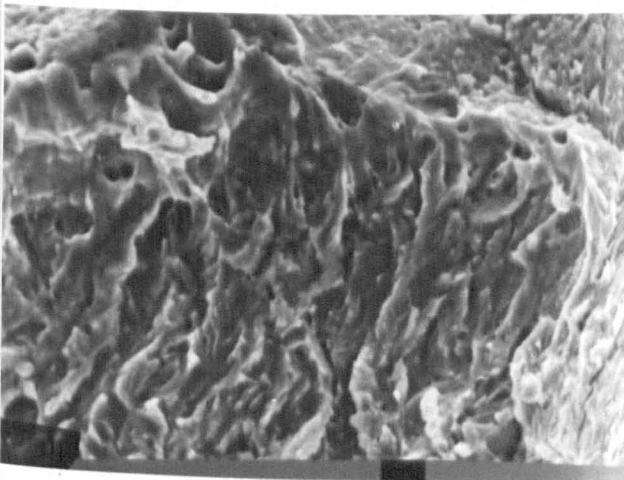
(d)



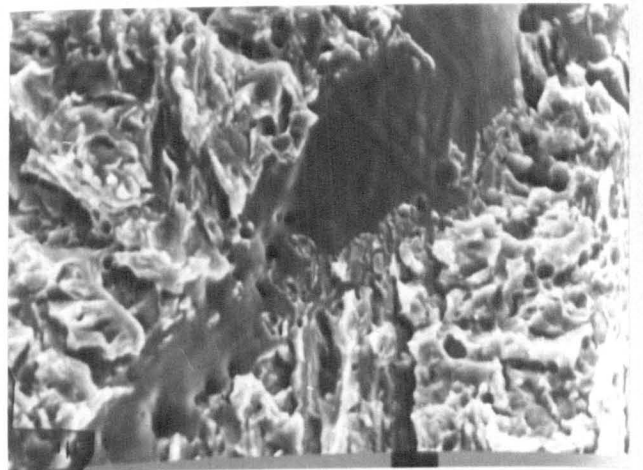
(b)



(e)



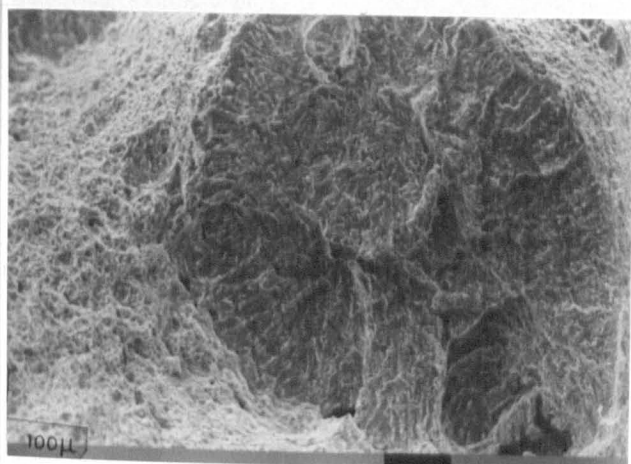
(c)



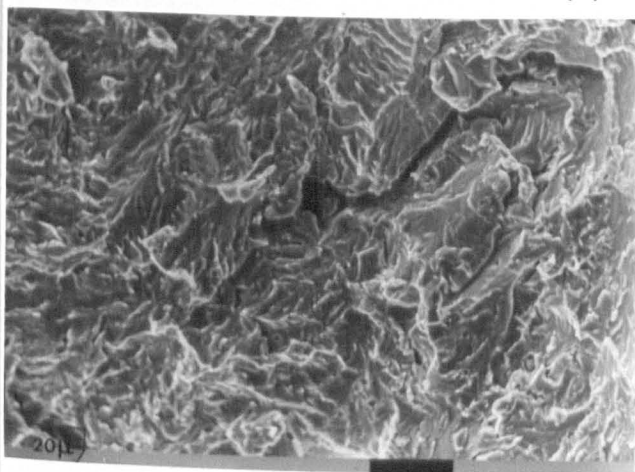
(f)

Figure 114 - Vertical crack in a manual metal arc weld deposited with electrodes B5Ni. TP62.

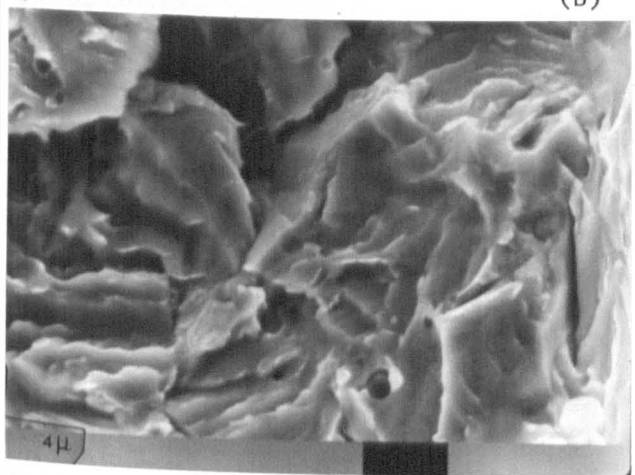
- (a) General aspect. (b) Detail from (a). (c) Detail from (b).
(d) Detail of inter and transgranular failure.
(e) and (f) Detail of less common features.



(a)



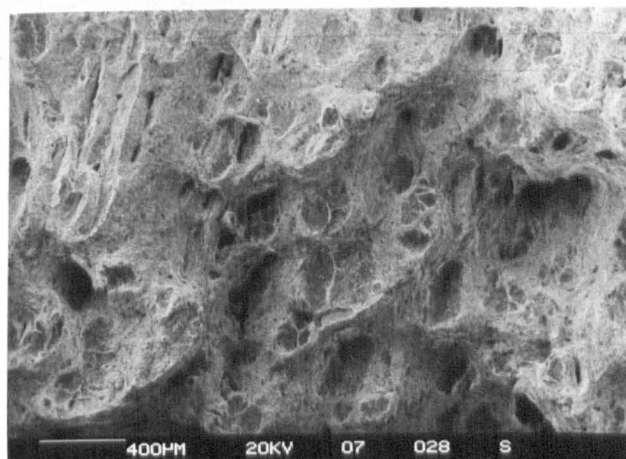
(b)



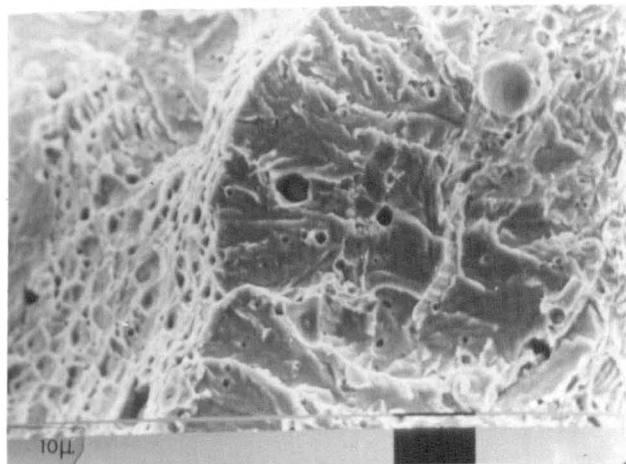
(c)

Figure 115 - Fissure in a submerged arc weld deposited with the wire-flux combination SD2/3Ni + OP41TT. High heat input weld by Crouch (7).

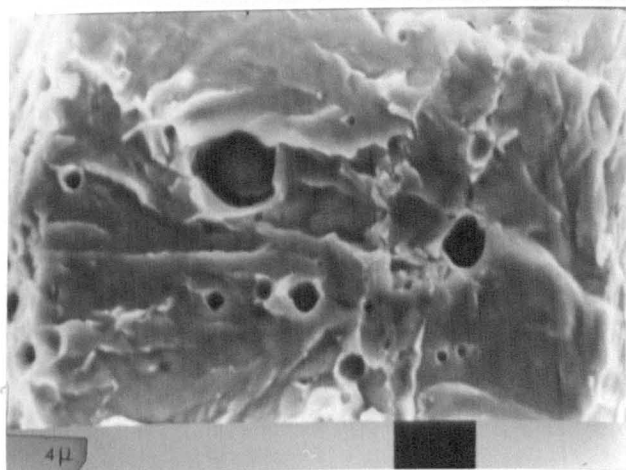
- (a) General aspect.
- (b) Detail from (a)
- (c) Detail from (b)



(a)



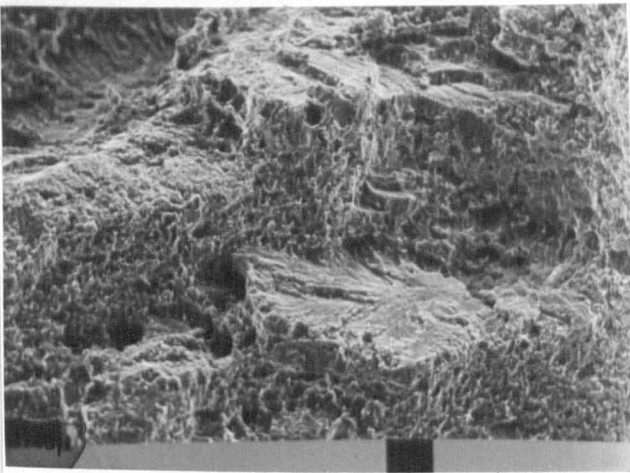
(b)



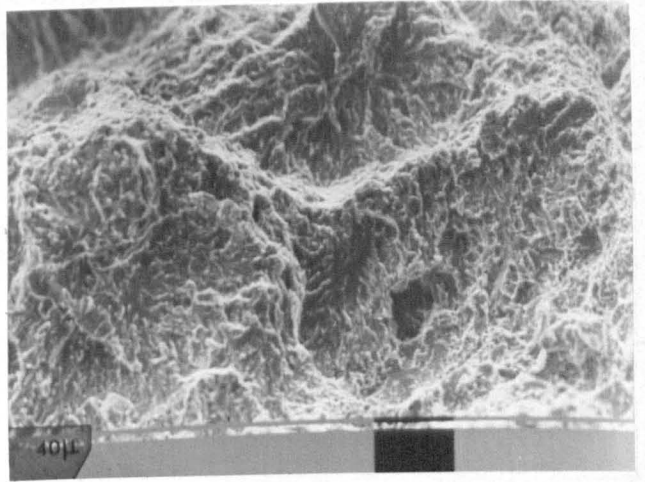
(c)

Figure 116 - Fissures in a manual metal arc weld deposited with electrodes E6013.TP39.

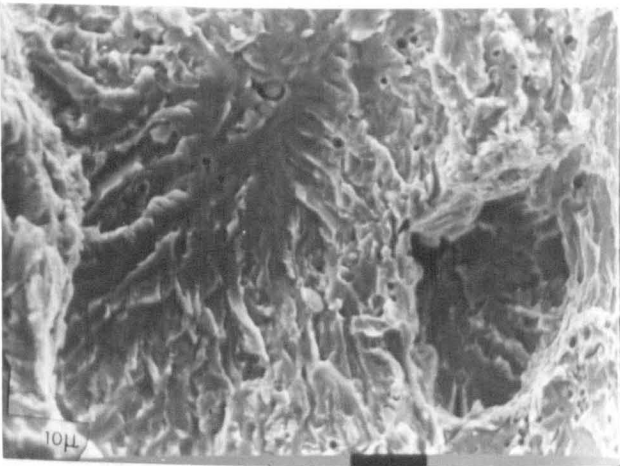
- (a) General aspect.
- (b) Detail of fissure.
- (c) Detail from (b).



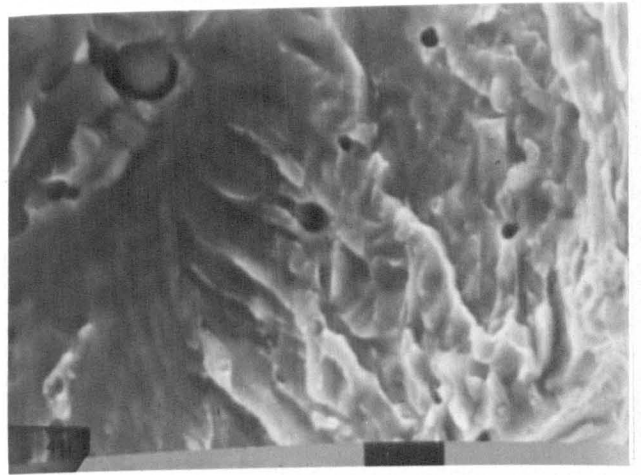
(a)



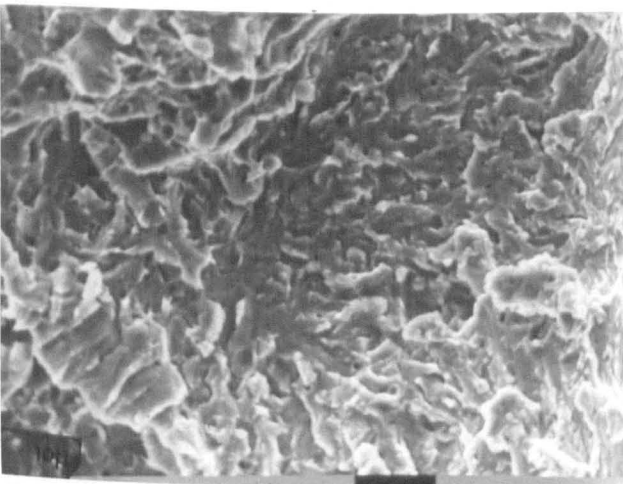
(b)



(c)



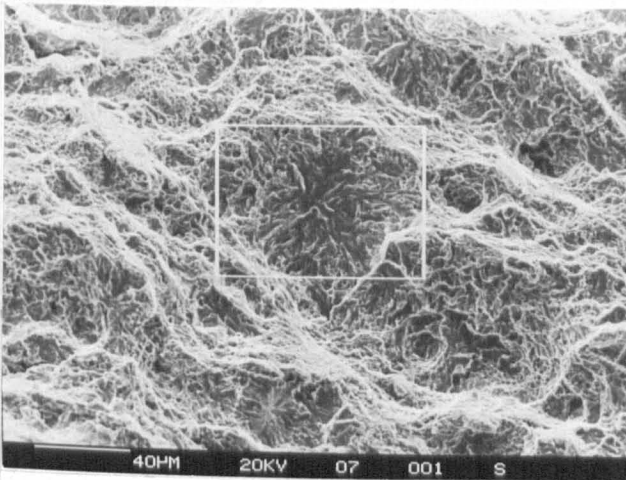
(d)



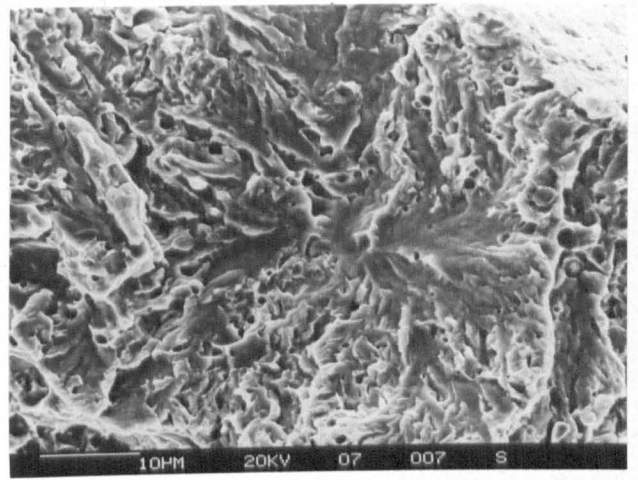
(e)

Figure 117 - Fracture surface of a longitudinal crack produced by the Y Groove test. Weld deposited with electrodes E8018C1.

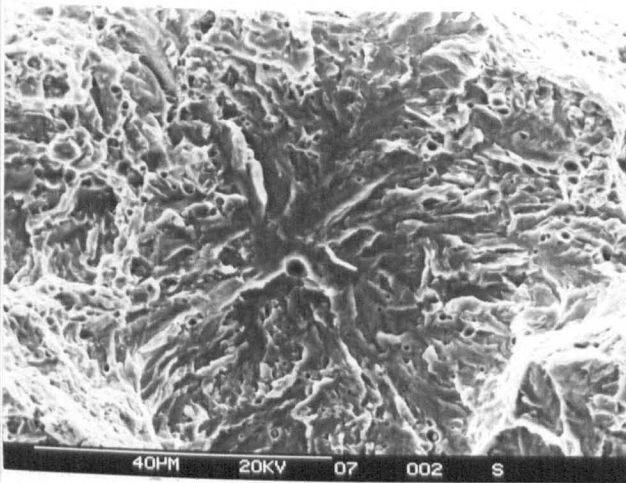
- (a) Detail of the staircase morphology (observed from an angle perpendicular to the ductile failure components).
- (b) Detail similar to the vertical components of chevron cracks (observed from a direction parallel to the ductile failure components).
- (c) Detail from (b).
- (d) Detail from (c).
- (e) Detail from (b).



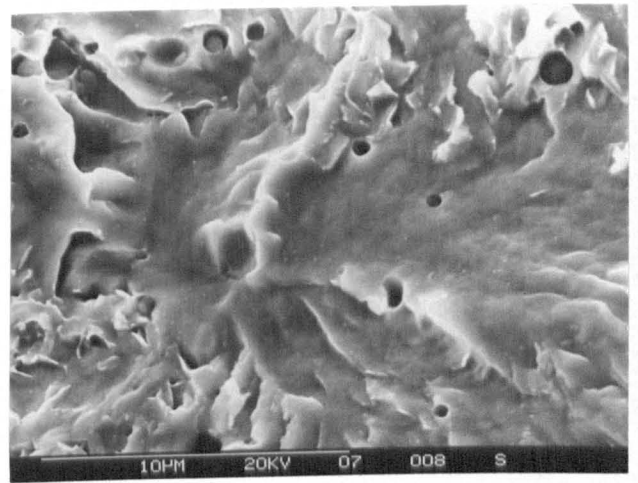
(a)



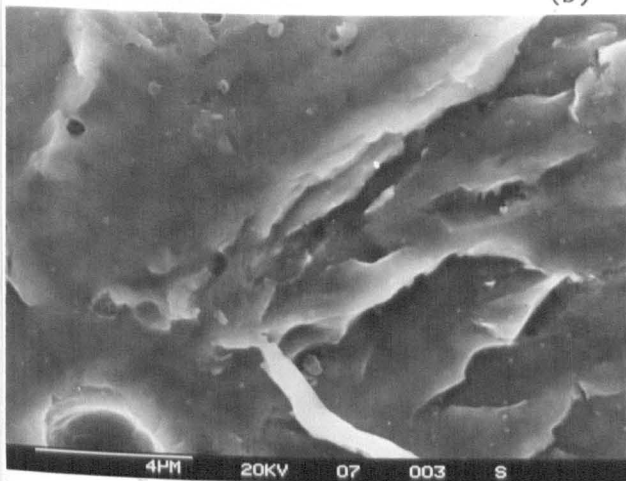
(d)



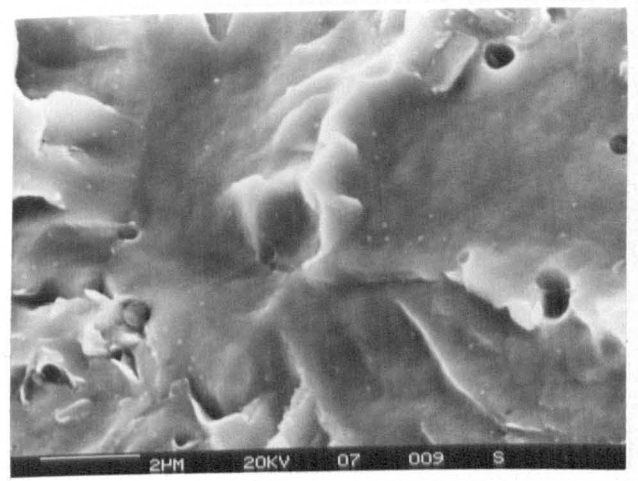
(b)



(e)



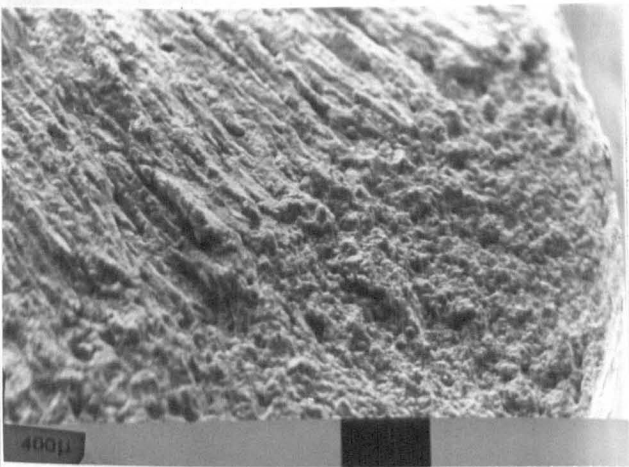
(c)



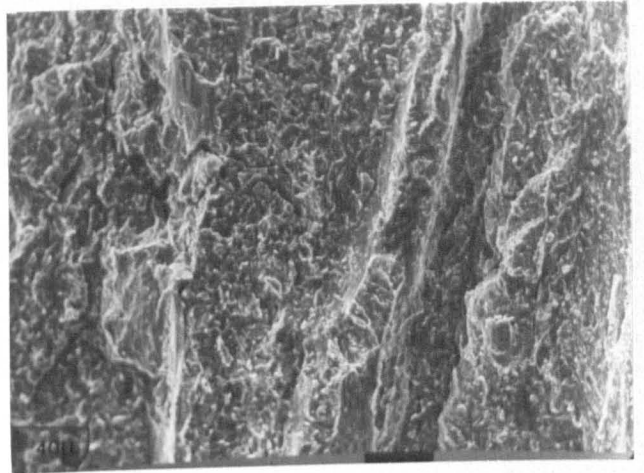
(f)

Figure 118 - Fracture surface of a longitudinal crack produced by the Y Groove test. Weld deposited with electrodes C2.

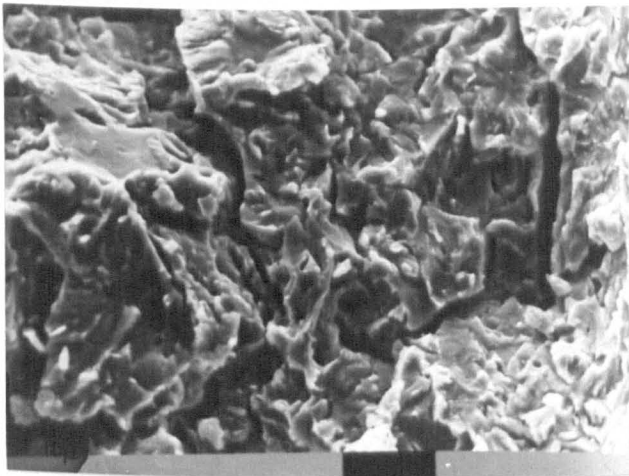
- (a) Detail similar to the vertical components of the chevron cracks.
(b) Detail from (a). (c) Detail from (b).
(d) Detail of another component. (e) Detail from (d).
(f) Detail from (e).



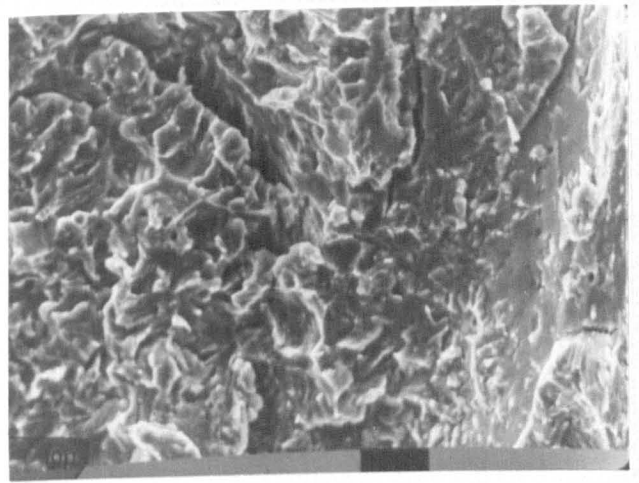
(a)



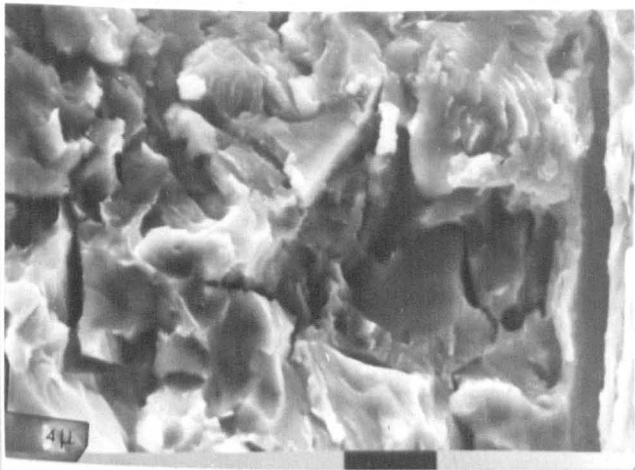
(d)



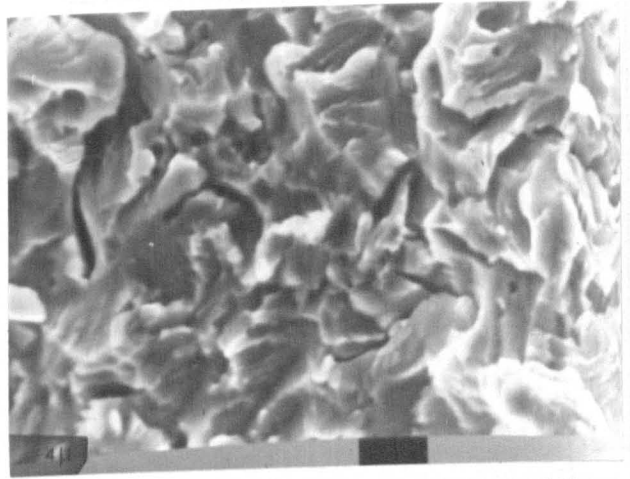
(b)



(e)



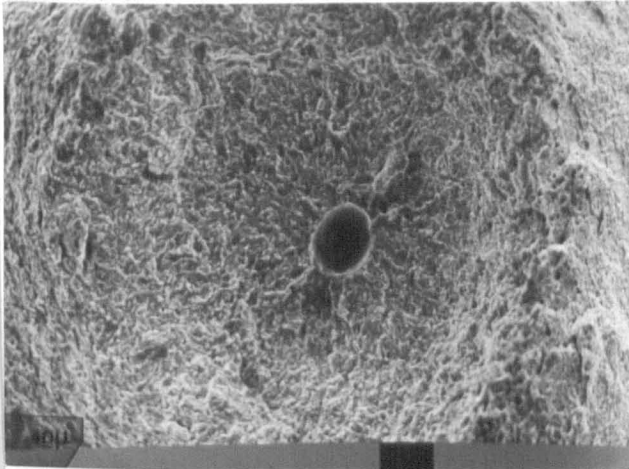
(c)



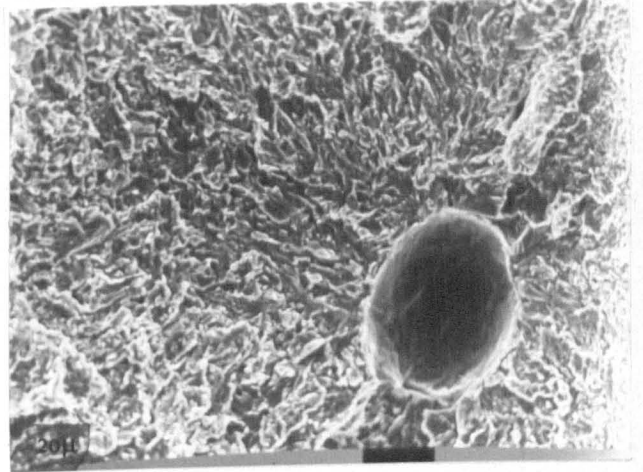
(f)

Figure 119 - Fracture surface of a hydrogen charged tensile specimen.
(Specimen 4 , Table 21).

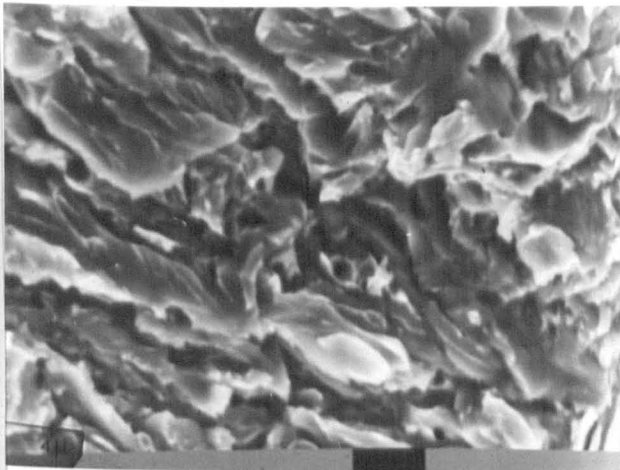
- (a) General aspect. (b) Detail from (a). (c) Detail from (b).
(d) Detail of the fracture surface in the columnar region.
(e) Detail from (d). (f) Detail from (d).



(a)



(b)



(c)

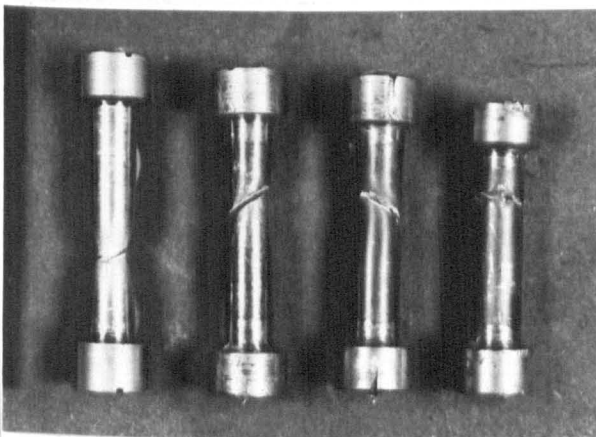
Figure 120 - Fish-eye in a hydrogen charged tensile specimen.

(Specimen 3, Table 21)

(a) General aspect

(b) Detail from (a)

(c) Detail from (b)



(6)

(7)

(8)

(9)

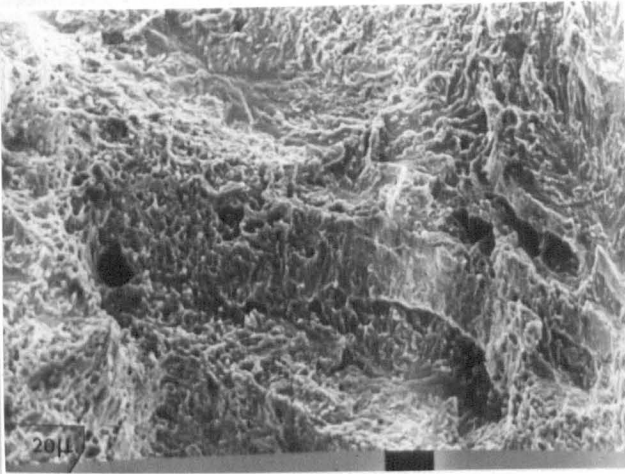
Figure 121 - Hydrogen charged tensile specimens after being tested. (Specimens referred to in Table 22). 1x.

(6) Non charged specimen.

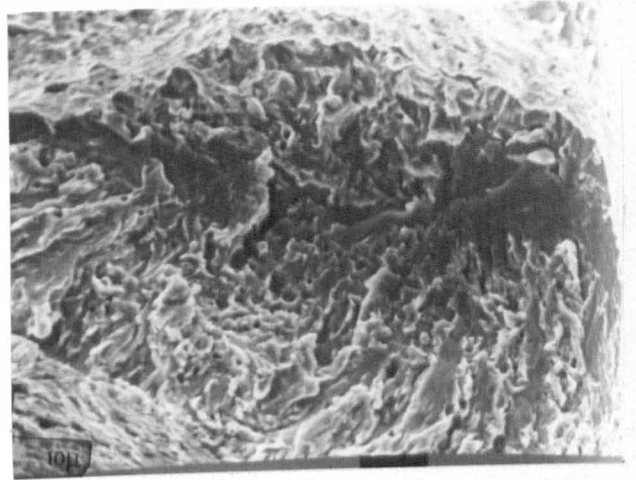
(7) Specimen charged for 4 hrs.

(8) Specimen charged for 24 hrs.

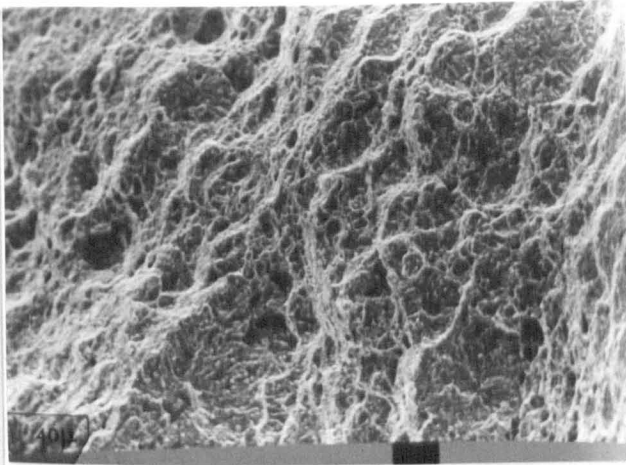
(9) Specimen charged for 48 hrs.



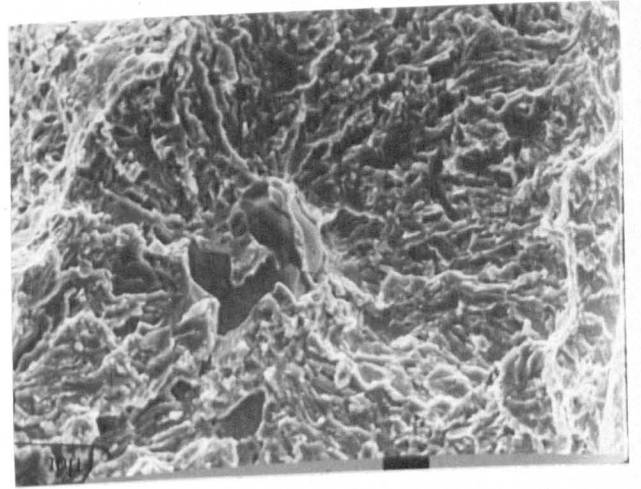
(a)



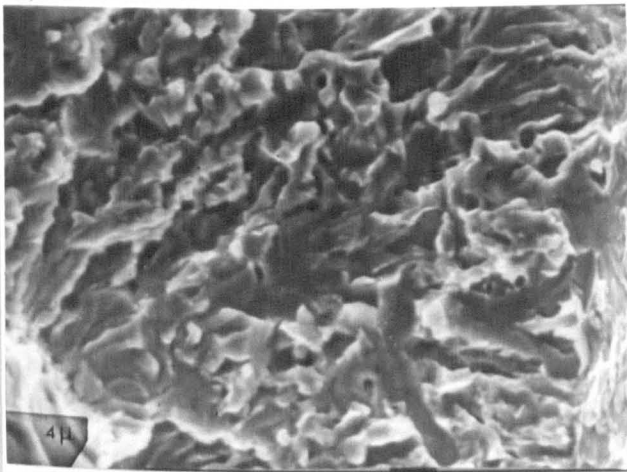
(b)



(c)



(d)

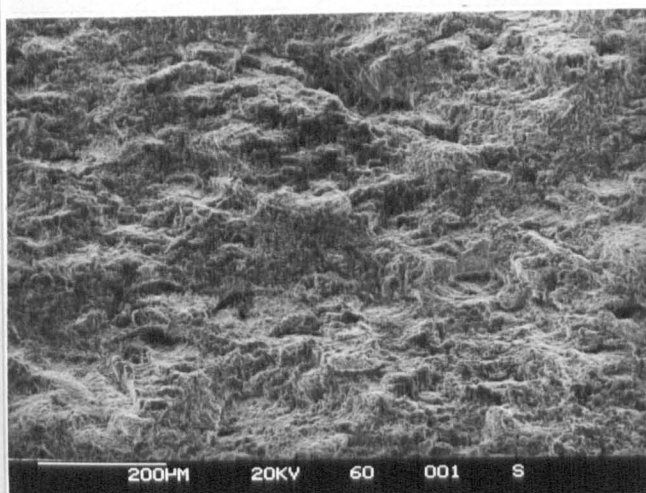


(e)

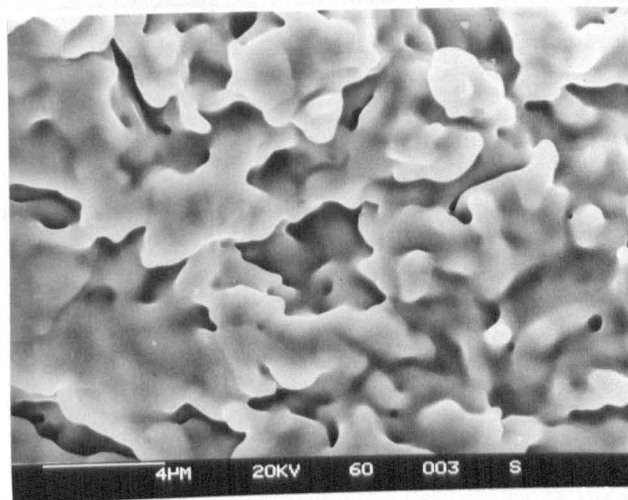
Figure 122 - Details from the fracture surface of hydrogen charged tensile specimens reminiscent of the staircase morphology of chevron cracks.

- (a) Specimen 7 (Table 22).
- (c) Specimen 9 (Table 22).
- (e) Detail from (d).

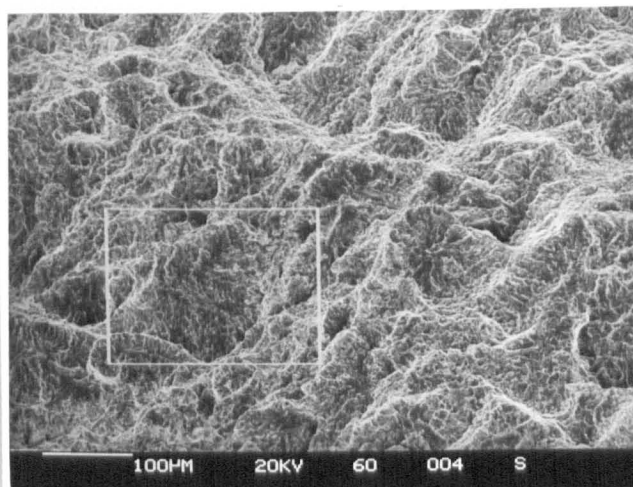
- (b) Detail from (a).
- (d) Detail from (c).



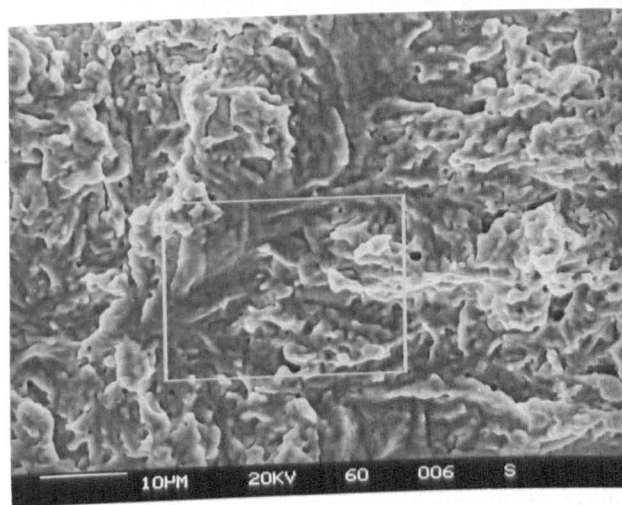
(a)



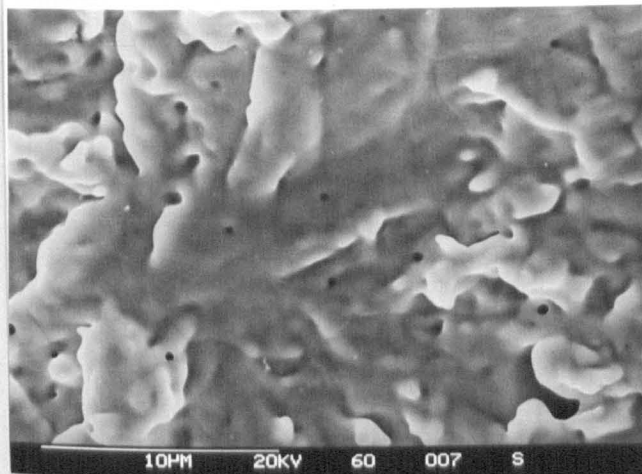
(b)



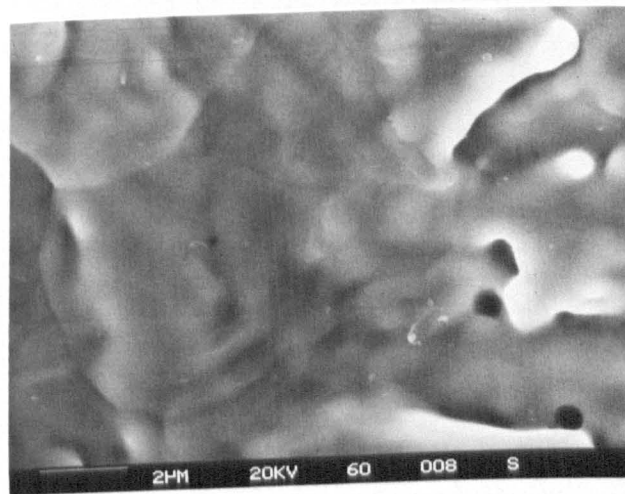
(c)



(d)



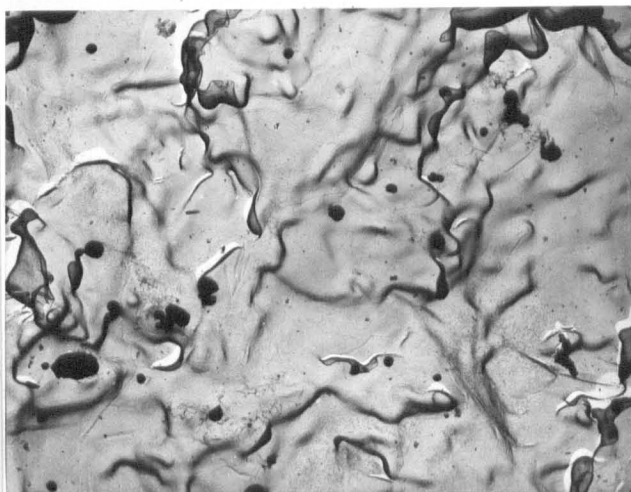
(e)



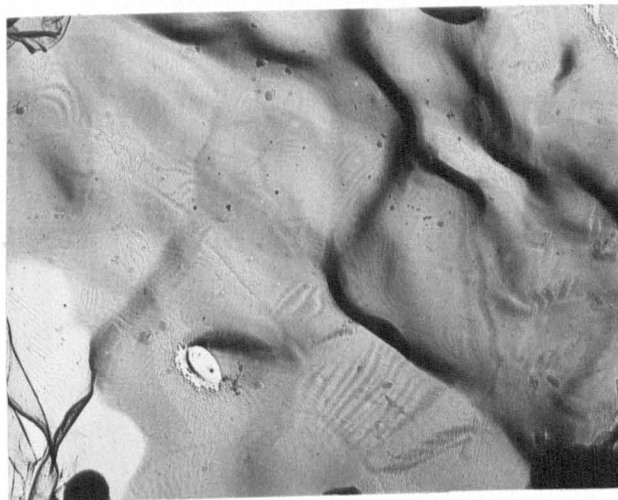
(f)

Figure 123 - Chevron crack in a submerged arc weld, which was reheated on purpose. TP21.

(a) Horizontal components. (b) Detail from (a) showing the effect of reheating. (c) Vertical components. (d) Detail from (c) showing the effect of reheating. (e) Detail from (d). (f) Detail from (d).



(a)

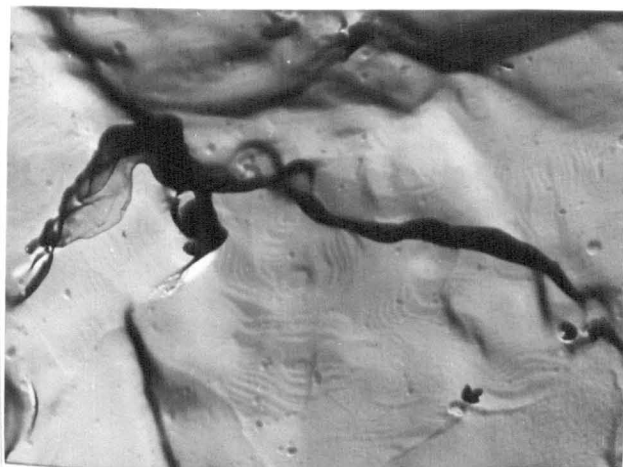


(b)

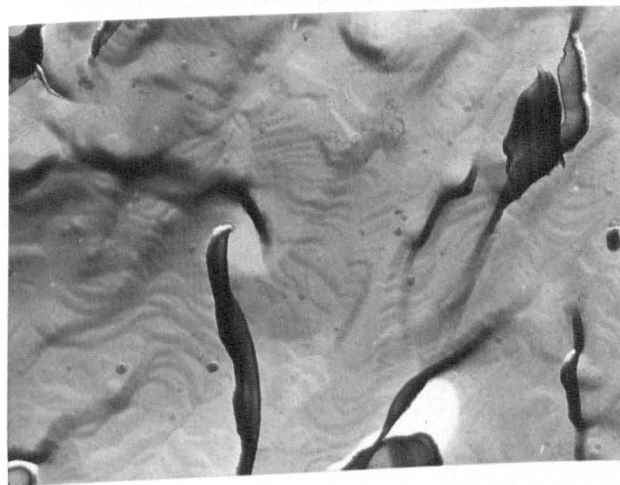
Figure 124 - Thermal facets on the fracture surface of a chevron crack reheated on purpose (same crack as in Figure 123). Single stage carbon extraction replica examined in the transmission electron microscope. TP21.

(a) General aspect, 5000x.

(b) Detail, 18000x.



(a)



(b)

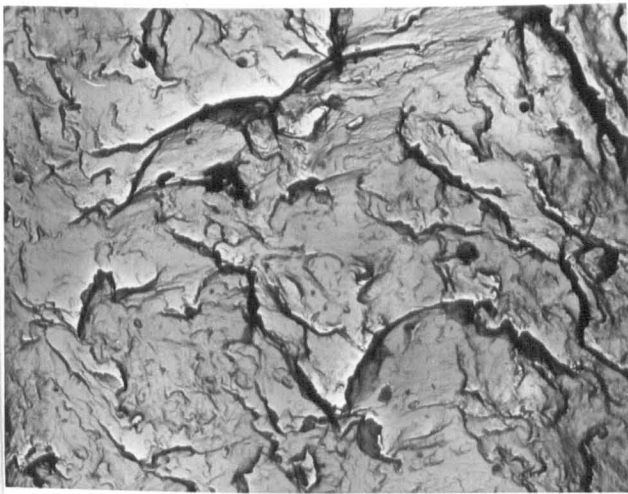
Figure 125 - (a) and (b) Thermal facets on the fracture surface of a chevron crack (same crack as in Figure 108). TP47. 15000x.



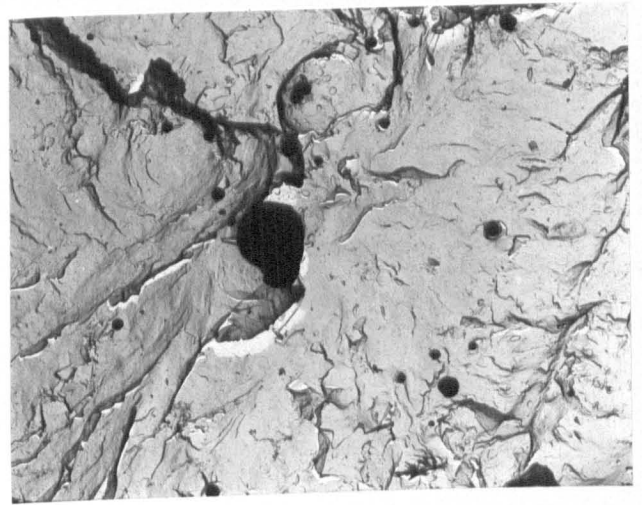
(a)



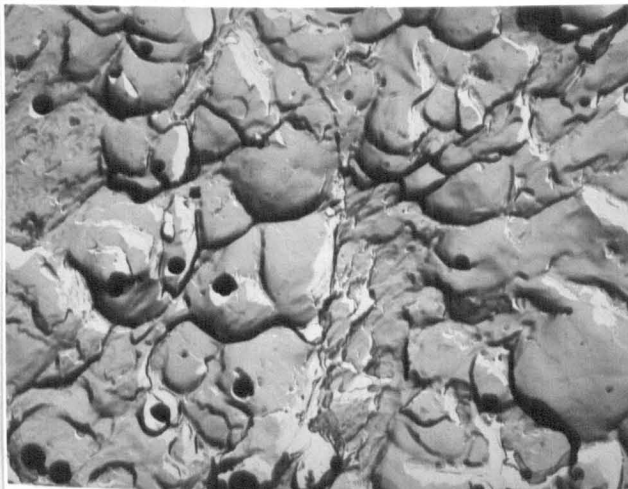
(b)



(c)



(d)



(e)

Figure 126 - Details from the fracture surfaces of chevron cracks. Single stage carbon extraction replicas examined in the transmission electron microscope.

(a) and (b) TP20, 7500x. (c) TP21, 5000x. (d) TP47, 5000x.

(e) Dimples corresponding to the horizontal components. TP47. 7500x.

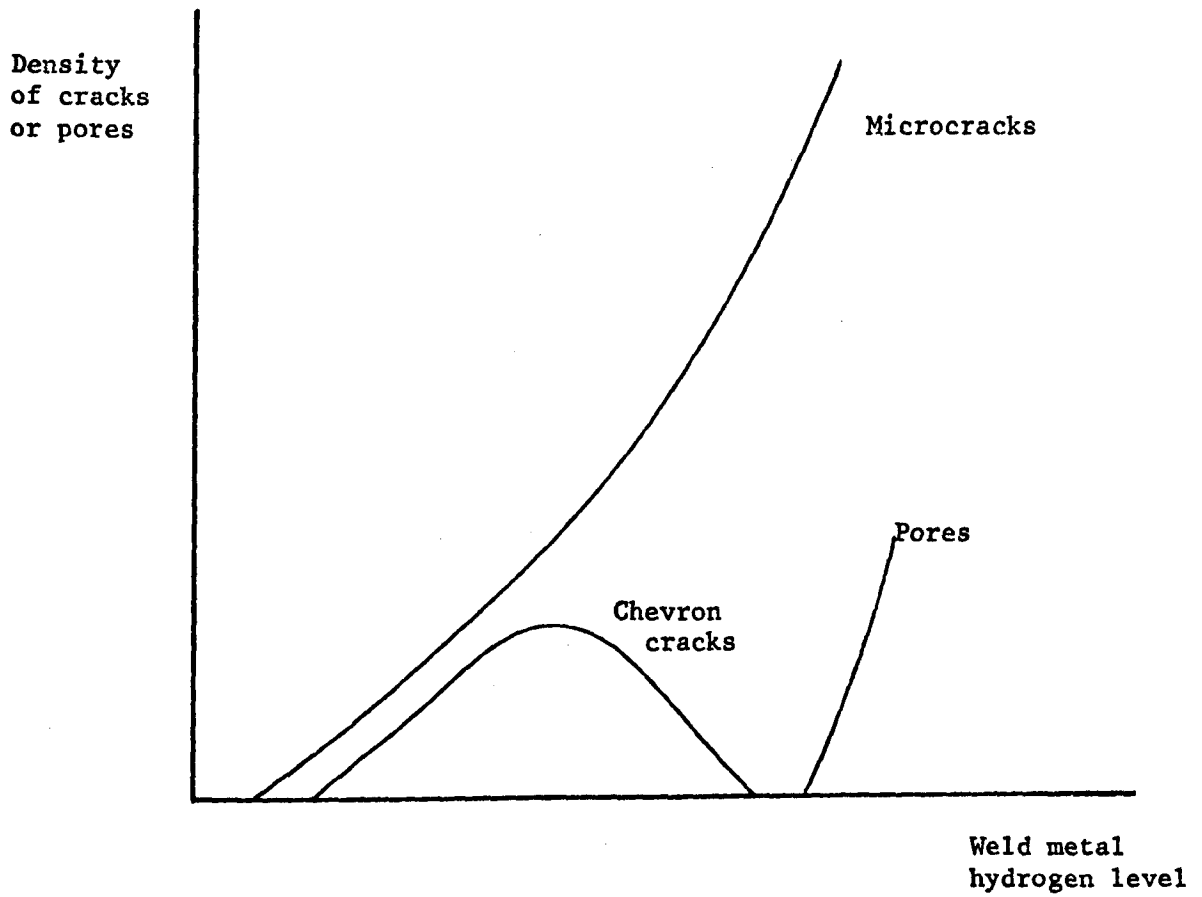


Figure 127 - Variation in the type and incidence of cracking with the hydrogen level in medium strength weld metals deposited with basic electrodes.

APPENDIX

APPENDIX

BIBLIOGRAPHY ON 'HYDROGEN IN METALS'

1. AEDELHADI, M.A. and HYSPECKA, L., GALLAND, J., AZOU, P. and BASTIEN, P. Delayed fracture and premature fracture in the presence of hydrogen in martensitic Fe-Ni-C alloys. Proc. of Int. Conf. on Stress Corrosion Cracking and Hydrogen Embrittlement of Iron Base Alloys. Unieux - Firminy, France, June 1973. p. 816.
2. ACHAR, B.S. and MIODOWNIK, A.P. The interaction of hydrogen and dislocations in iron-nickel alloys. International Congress 'L'Hydrogene dans les Metaux', Paris May-June 1972, Editions Science et Industrie, p.84.
3. ADLER, P.N., KAMYKOWSKI, E.A. and PADAWER, G.M. Localized hydrogen measurements in surfaces using the Lithium nuclear microprobe. Proc. of an Int. Conf. on Hydrogen in Metals. September 1973. Published by ASM. p. 623.
4. AIFANTIS, E.C. and GERBERICH, W.W. Diffusion of gases in linear elastic stress fields. Proc. of an Int. Conf. on Effect of Hydrogen on Behaviour of Materials. Jackson Lake Lodge, Moran, Wyoming, September, 1975. p. 350.
5. ALEX, F., HADNAGY, T.B., LYNN, K.G. and BYRNE, J.G. Positron annihilation studies of hydrogen embrittlement. Proc. of an Int. Conf. on Effect of Hydrogen on Behaviour of Materials. Jackson Lake Lodge, Moran, Wyoming; September 1975. p. 642.
6. ALLEN-BOOTH, D.M. and HEWITT, J. A mathematical model describing the effects of micro voids upon the diffusion of hydrogen in iron and steel. Acta Metallurgica, 1974, 22, 171 - 175.
7. AMBLER, J.F.R. and OLSON, P.G. Relative amounts and orientation of intergranular hydride in annealed zircaloy. Int. Congress 'L'Hydrogene dans les Metaux'. Paris, May - June, 1972. Editions Science et Industrie. p. 474.
8. ANDO, S., NAKAMURA, H. Effects of fish-eyes on fatigue strength of weld metal. IIW DOC II-267-63.
9. ANTONA, P.L., CASARINI, G. and DUMINI, W. Industrial cases of hydrogen cracking. Morphology and hypothesis of the phenomenon genesis. Int. Congress 'L'Hydrogene dans les Metaux'. Paris, May-June, 1972. Editions Science et Industrie. p. 520.
10. ARIKAWA, M. et al. Effect of weld metal strength and hydrogen content on cracking in the overhead welded fillet. IIW DOC II-539-70.
11. ASARO, R.J., WEST, A.J. and TILLER, W.A. Hydrogen induced phase transformations of austenite to martensite. Proc. of Int. Conf. on Stress Corrosion Cracking and Hydrogen Embrittlement of Iron Base Alloys. Unieux-Firminy, France, June, 1973. p. 1115.
12. ATEYA, B.G. and PICKERING, H.W. Conditions for which iron dissolution occurs in cracks during hydrogen charging of steels. Proc. of Int. Conf. on Stress Corrosion Cracking and Hydrogen Embrittlement of Iron Base Alloys. Unieux-Firminy, France, June 1973. p. 1183.
13. AZOU, P. Summary of the international congress on hydrogen in metals. Proc. of Int. Conf. on Stress Corrosion Cracking and Hydrogen Embrittlement of Iron Base Alloys. Unieux-Firminy, France. June 1973. p. 836.

14. BAILEY, N. Aspects of weldability of HY 130. Metal Construction and British Welding Journal, 1970, 2, p. 339.
15. BAILEY, N. Welding carbon-manganese steels. Metal Construction and British Welding Journal, 1970, 2, (10), 442 - 446.
16. BAILEY, N. Joint simulation testing against hydrogen cracking. Welding Institute Research Bulletin, 1971, 12, (10), 278 - 283.
17. BAILEY, N. The establishment of safe welding procedures. Welding Journal, 1972, 51, (4), 169s - 177s.
18. BAILEY, N., WATKINSON, F. Change : welding procedures to avoid hydrogen cracking. Welding Institute Research Bulletin, 1973, 14, (7), 193 - 196.
19. BAILEY, N. Hydrogen cracking and austenitic electrodes. Welding Institute Research Bulletin. 1974, 15, (4), 153 - 157.
20. BAILEY, N. Fish-eyes, hydrogen embrittlement and removal. Welding Institute Research Bulletin, 1974, 15, (12), 369 - 372.
21. BAILEY, N. Misalignment and cracking. Welding Institute Research Bulletin, 1976, 17, (4), 85 - 90.
22. BAILEY, N. and Miss M.L.E. DAVIS. Fluxes for S.A.W. ferritic steels - a literature survey. Part 2 : Weld properties and weld defects. Welding Institute Research Report 10/1976/M - May, 1976.
23. BAILEY, N. Cracking of C - $\frac{1}{2}$ Mo steel in hydrogen service - is there a problem? Welding Institute Research Bulletin, 1977, 18, (2), 33 - 39.
24. BAILEY, N. Hydrogen cracking and austenitic electrodes. Metal Construction, 1978, 10, (12), 580 - 583.
25. BAILLIE, J.G. Underbead and toe cracks. British Welding Journal, 1967, (14), (2), 51 - 61.
26. BAKER, R.G. and WATKINSON, F. The effect of hydrogen on the welding of low alloy steels. Iron and Steel Institute, London 1962. Special Report 73, pp 123 - 132.
27. BAKER, R.G., WATKINSON, W.F. and NEWMAN, R.P. The metallurgical implications of welding practice as related to low alloy steels. Proc. 2nd Commonwealth Welding Conference, 1965. pp 125 - 131.
28. BAKER, R.G. Weld cracking - a modern insight. British Welding Journal, 1968, 15, (6), 283 - 295.
29. BAKER, R.G. Some aspects of the practical control of weld cold cracking. Metals Technology Conference A-B, paper for the IIW 1976 Annual Assembly, first session.
30. BARBIN, L.M. The new moisture resistant electrodes. Welding Journal 1977, 56, (7), 15 - 18.
31. BARNETT, W.J. and TROIANO, A.R. Crack propagation in the hydrogen induced brittle fracture of steel. Transactions AIME, 1957, 209, 486 - 494.
32. BARTH, C.F., STEIGERWALD, E.A. and TROIANO, A.R. Hydrogen permeability and delayed failure of polarized martensitic steels. Corrosion, 1969, 25, p. 353.
33. BARTH, C.F. and STEIGERWALD, E.A. Evaluation of hydrogen embrittlement mechanisms. Metallurgical Transactions, 1970, 1, 3451 - 3455.

34. BASTIEN, P. and AZOU, P. Influence de l'amplitude et de la vitesse des deformations plastiques sur la segregation de l'hydrogene dans le fer et les aciers. Comptes Rendues, 1951, 232, 69 - 71.
35. BASTIEN, P. and AZOU, P. Influence de l'écrouissage sur le frottement interieur du fer et de l'acier, chargés ou non en hydrogene. Comptes Rendues Academie Science, 1951, 232, 1845.
36. BASTIEN, P. and AZOU, P. Effect of hydrogen on the deformation and fracture of iron and steel in simple tension. Proceedings of the 1st World Metallurgical Congress, ASM, 1951, p. 535 - 552.
37. BASTIEN, P.G. The phenomena of cracking and fracture of steel in the presence of moist hydrogen - corrosion under stress in the presence of moist hydrogen sulphide. Physical Metallurgy of Stress Corrosion Fracture. Metallurgical Society of the AIME, published Interscience, 1959.
38. BASTIEN, P. Action of hydrogen on iron and steels and industrial consequences. International Congress 'L'Hydrogene dans les Metaux', Paris, May - June 1972. Editions Science et Industrie, p. 11.
39. BAUER, G. and SCHMATZ, W. Study of the interaction of hydrogen and deuterium with the crystal lattice of Nb by quasielastic scattering of neutrons. Proc. of an Int. Conf. on Effect of Hydrogen on Behaviour of Materials. Jackson Lake Lodge, Moran, Wyoming. September 1973. p. 651.
40. BEACHEM, C.D. A new model for H₂-assisted cracking (H₂ embrittlement). Metallurgical Transactions 1972, 3, 437 - 451.
41. BEACHEM, C.D. and YODER, G.R. Elastic-plastic fracture by homogeneous microvoid coalescence tearing along alternating shear planes. Metallurgical Transactions, 1973, 4, 1145 - 1153.
42. BEACHEM, C.D. Microscopic versus macroscopic aspects of hydrogen-assisted cracking. Fifth Annual Spring Meeting, Institute of Metals Division, AIME, May 29 - June 1. 1973. Philadelphia, P.A.
43. BEACHEM, C.D. Electron fractographic support for a new model for hydrogen-assisted cracking. Proc. of Int. Conf. on Stress Corrosion Cracking and Hydrogen Embrittlement of Iron Base Alloys. Unieux-Firminy, France, June 1973, p. 376.
44. BEACHUM, E.P. An investigation into the causes of delayed cracking in steel weldments. PhD Dissertation, Lehigh University, 1960.
45. BEACHUM, E.P., JOHNSON, H.H., STOUT, R.D. Hydrogen and delayed cracking in steel weldments. Welding Journal, 1961, 40, 1961, 40, (4), 155s - 159s.
46. BECK, W., BOCKRIS, O'M, BREEN, J.Mc., NANIS, L. Hydrogen permeation in metals as a function of stress, temperature and dissolved hydrogen concentrations. Proceedings of the Royal Society, 1966, A290.;
47. BECK, W., JANKOWSKY, J. and FISCHER, P. Hydrogen permeation and dissolution of iron in dilute and very dilute solutions of sulphuric acid. International Congress 'L'Hydrogene dans les Metaux'. Paris, May - June, 1972. Editions Science et Industrie. p. 244.
48. BENSON, R.B., KIM, D.K., ATTERIDGE, D. and GERBERICH, W.W. The resistance to embrittlement by a hydrogen environment of selected high strength iron-manganese base alloys. Proc. of Int. Conf. on Stress Corrosion Cracking and Hydrogen Embrittlement of Iron Base Alloys. Unieux-Firminy, France, June 1973. p. 822.

49. BENSON, Jr. R.B. The resistance of selected high strength alloys to embrittlement by a hydrogen environment. Proc. of an Int. Conf. on Hydrogen in Metals, September 1973. Published by ASM. p. 183.
50. BERMAN, D.A., BECK, W. and DeLUCCIA, J.J. The determination of hydrogen in high strength steel structures by an electrochemical technique. Proc. of an Int. Conf. on Hydrogen in Metals. September 1973. Published by ASM. p. 595.
51. BERNSTEIN, I.M. The role of hydrogen in the embrittlement of iron and steel. Materials Science and Engineering, 1970, 6, (1), 1 - 19.
52. BERNSTEIN, I.M., GARBER, R. and PRESSOUYRE, G.M. Effect of dissolved hydrogen on mechanical behaviour of metals. Proc. of an Int. Conf. on Effect of Hydrogen on Behaviour of Materials, Jackson Lake Lodge, Moran, Wyoming, September 7 - 11, 1975, pp 37 - 58.
53. BERRY, J.T. and ALLAN, R.C. A study of cracking in low alloy steel welded joints. Welding Journal, 1960, 39, (3), 105s - 116s.
54. BHANSALI, K., LYNCH, C.T., VAHLDIEK, F. and SUMMITT, R. Effect of multi-functional inhibitors on crack propagation rates of high strength steel in corrosive environments. Proc. of an Int. Conf. on Effect of Hydrogen on Behaviour of Materials. Jackson Lake Lodge, Moran, Wyoming, September 1975. p. 185.
55. BIHARI, L.M. Relation of hydrogen cracking and high temperature ductility to chevron cracking in steel weld metal. MSc Thesis, Department of Materials, Cranfield Institute of Technology, 1978.
56. BILBY, B.A. and HEWITT, J. Hydrogen in steels - the stability of micro-cracks. Acta Metallurgica, 1962, 10, (6), 587 - 600.
57. BIRNBAUM, H.K., GROSSBECK, M. and GAHR, S. The effect of hydrogen in the mechanical properties and fracture of Zr and refractory metals. Proc. of an Int. Conf. on Hydrogen in Metals, September 1973. Published by ASM. p. 303.
58. BISSON, C L. and WILSON, W.D. Ab-initio calculations of self-diffusion of hydrogen in titanium hydride. Proc. of an Int. Conf. on Effect of Hydrogen on Behaviour of Materials. Jackson Lake Lodge, Moran, Wyoming, September 1971, p. 416.
59. BLAKE, P.D. Hydrogen contents of mild and alloy weld deposits, with some reference to the effects of hydrogen embrittlement in welded joints. British Welding Journal, 1957, 4, p. 146.
60. BLAKE, P.D. Measurements on the diffusible, residual and total hydrogen contents of weld metal. British Welding Journal, 1958, 5, 126 - 129.
61. BLAKE, P.D. Effect of diffusible hydrogen on the mechanical properties of weld metal. British Welding Journal, 1958, 5, p. 565.
62. BLAKE, P.D. and PUMPHREY, W.I. Effects of hydrogen in wrought steel and in ferrous weld metal. British Welding Journal 1959, 6, (5), 211 - 224
63. BLANCHARD, P. and TROIANO, A.R. La fragilization des metaux par l'hydrogene. Revue de Metallurgie 1960.
64. BLANCHET, J., CORIOU, H., GRAIL, L., MAHIEU, C., OTTER, C. and TURLUER, G. Historical review of the principal research concerning the phenomena of cracking of nickel base austenitic alloys. Proc. of Int. Conf. on Stress Corrosion Cracking and Hydrogen Embrittlement of Iron Base Alloys. Unieux-Firminy, France, June 1973, p. 1149.

65. BLAND, J. Effect of 'quench time' on weld metal. Welding Journal 1949, 28, 216s - 226s.
66. BLAND, J., GOLDSPIEL, S. New procedures for studying electrode coverings. Welding Journal 1950, 29, (10), 522s - 529s.
67. BLINK, W.P. van den. Note on the influence of the water content of an electrode coating on the hydrogen content of weld metal. Welding Journal, 1947, 26, (6), 369 - 370.
68. BLUNDY, R.F., ROYCE, R., POOLE, P. and SHREIR, L.L. Effect of pressure and stress on permeation of hydrogen through steel. Proc. of Int. Conf. on Stress Corrosion Cracking and Hydrogen Embrittlement of Iron Base Alloys. Unieux-Firminy, France, June, 1973, p. 636.
69. BOCKRIS, J. O'M., SUERAMANYAN, P.K. Hydrogen embrittlement and hydrogen traps. Journal of Electrochemical Society, 1971, 118, p. 1114.
70. BOCKRIS, J. O'M., BECK, W., GRENSHAW, M.A., SUBRAMANYAN, P.K. and WILLIAMS, F.S. The effect of stress on the chemical potential of hydrogen. Acta. Metallurgica, 1971, 19, (11), 1209 - 1218.
71. BOCKRIS, J. O'M., and ORIANI, R.A. Models of hydrogen embrittlement. Proc. of Int. Conf. on Stress Corrosion Cracking and Hydrogen Embrittlement of Iron Base Alloys. Unieux-Firminy, France, June, 1973. p. 225.
72. BOCKRIS, J. O'M. On hydrogen damage and electrical properties of interfaces. Proc. of Int. Conf. on Stress Corrosion Cracking and Hydrogen Embrittlement of Iron Base Alloys. Unieux-Firminy, France, June 1973 . p. 286.
73. BOILLOT, P., HANIN, M. and MAEDER, C. Quick determination of hydrogen in liquid steel. International Congress 'L'Hydrogene dans les Metaux'. Paris, May - June, 1972. Editions Science et Industrie. p. 382.
74. BOMBERRY, R.I. Fracture of high strength steels in gaseous hydrogen. Effects of Chemical Environment on Fracture Process. Third Tewksbury Symposium on Fracture, 4 - 6 June 1974. Edited by Osborn C.J. and Gifkins, R.C. Sponsored by Australian Institute of Metals.
75. BOND, A.P. and DUNDAS, H.J. Stress corrosion cracking of ferritic stainless steels. Proc. of Int. Conf. on Stress Corrosion Cracking and Hydrogen Embrittlement of Iron Base Alloys. Unieux-Firminy, France, June, 1973. p. 1136.
76. BONISZEWSKI, T. WATKINSON, F., BAKER, R.G. and TREMLETT, H.F. Hydrogen Embrittlement and Heat Affected Zone Cracking in Low Carbon Alloy Steels with Acicular Microstructures. British Welding Journal, 1965, 12, (1), 14 - 36.
77. BONISZEWSKI, T., WATKINSON, F., BAKER, R.G. Heat affected zone cold cracking in low alloy steels. Proceedings of the 2nd Commonwealth Welding Conference. Institute of Welding, London, April - May 1965, pp 117 - 124.
78. BONISZEWSKI, T. and BAKER, R.G. Hydrogen embrittlement in low carbon nickel and manganese steels. British Welding Journal, 1965, 12, (7), 349 - 362.
79. BONISZEWSKI, T. CTS weldability tests of $\frac{1}{2}$ Mo-B experimental steels. British Welding Journal 1965, 12, 593 - 612.
80. BONISZEWSKI, T. and Miss E.D. BROWN. Fissures in refined regions of multi-run weld metal. British Welding Journal, 1966, 13, 18 - 31.

81. BONISZEWSKI, T. and Mrs. J. MORETON. Effect of micro-voids and MnS (sulphide) inclusions in steel on hydrogen evolution and embrittlement. British Welding Journal 1967, 14, 321 - 336.
82. BONISZEWSKI, T. Hydrogen induced cold cracking - Discussion Section 2, Papers 3 and 4. Cracking in Welds - The Welding Institute Autumn Meeting, 1968, pp 115 - 116.
83. BONISZEWSKI, T. and MORETON, J. Hydrogen entrapment in mild steel weld metal micropores. IIW DOC II-A-238-69.
84. BONISZEWSKI, T. Hydrogen entrapment in mild steel with micropores. Metal Construction and British Welding Journal, 1969, 1, 269 - 276.
85. BONISZEWSKI, T. and WATKINSON, F. Effect of weld microstructure on hydrogen induced cracking in transformable steels. Metals and Materials, 1973, 7. Part I : February issue pp 90 - 96. Part II : March issue, pp 145 - 151.
86. BONISZEWSKI, T. and PAVELEY, D.A. Timing at temperature when drying welding electrodes before use. Metal Construction 1978, 10, (11), 530 - 531.
87. BOSWARD, I.G. The effect of excessive redrying on fortrex 35A and ferex 7018LT. BOC Murex Report No. D. 498. Welding R & D Laboratories, Waltham Cross.
88. BOUVEROT, R. Essais de soudabilité par implants effectués au laboratoire de la Société Babcock-Atlantique. IIW-DOC. IX-759-71.
89. BOWKER, P. and HARDIE, D. The effect of gaseous hydrogen on the tensile ductility of a high strength steel. International Congress 'L'Hydrogene dans les Metaux'. Paris, May - June, 1972. Editions Science et Industrie. p. 284.
90. BRADSTREET, B.J. Application of the cruciform test to a study of cracking in the T-1 steel weldments. Welding Journal, 1962, 41, (2), 62s-69s.
91. BRADSTREET, B.J. Moisture absorption in low hydrogen electrode coatings and porosity in welds. Welding Journal, 1964, 43, (1), 43s - 48s.
92. BRAIN, A.G. and SALTER, G.R. The hydrogen content of CO₂ weld metal. British Welding Journal, 1962, 9, 36 - 41.
93. BRESSANELLI, J.P. Effects of heat treatments on the resistance to hydrogen embrittlement of type 410 stainless steel. Transactions of the ASM, 1965, 58, p.3.
94. BRETIN, L., TOITOT, M. and BASTIEN, P. Hydrogen embrittlement of steels. Experimental methods and laboratory applications on industrial steels. International Congress 'L'Hydrogene dans les Metaux', Paris, May - June 1972. Editions Science et Industrie. p. 306.
95. BRIANT, C.L. Hydrogen assisted cracking of type 304 stainless steel. Metallurgical Transactions, 1979, 10A, (2), 181 - 189.
96. BROCKS, J.A. and THOMPSON, A.W. Hydrogen compatibility of joining processes for dispersion-strengthened materials. Proc. of an Int. Conf. on Hydrogen in Metals. September 1973. Published by ASM. p. 527.
97. BROUDEUR, R., FIDELLE, J.P. and AUCHERE, H. Experimental evidence of the role of dislocations in the transport of hydrogen. International Congress 'L'Hydrogene dans les Metaux', Paris, May - June 1972. Editions Science et Industrie. p. 106.

98. BROUDEUR, R., FIDELLE, J.P., DEVAUX, J. and RAPIN, M. Tritium diffusivity and solubility measurements in Z5 NCTD 26-15 (A286) austenitic stainless steel. International Congress 'L'Hydrogene dans les Metaux'. Paris, May - June 1972. Editions Science et Industrie. p.186.
99. BROWN, B.F., SMITH, J.A. and PETERSON, M.H. Electrochemical conditions at the tip of an advancing stress corrosion crack in AISI 4340 steel. Corrosion, 1970, 26, (12), p. 539.
100. BROWN, B.F. Stress corrosion cracking of high strength steels. The theory of stress corrosion cracking in alloys. NATO Science Committee, Research Evaluation Conference, Brussels, 1971
101. BROWN, I.T. and BALDWIN, W.M. Hydrogen embrittlement of steels. Transactions of the AIME, 1954, 200. 298 - 304.
102. BURKE, J., MEHTA, M.L. and NARAYAN, R. Hydrogen embrittlement of type 304L austenitic stainless steel. International Congress 'L'Hydrogene dans les Metaux'. Paris May - June 1972. Editions Science et Industrie. p. 149.
103. BURKE, J., JICKELS, A., MAULIK, P. and MEHTA, M. The effect of hydrogen on the structure and properties of Fe-Ni-Cr austenite. Proc. of an Int. Conf. on Effect of Hydrogen on Behaviour of Materials. Jackson Lake Lodge, Moran, Wyoming, September 1975, p. 102.
104. BURTE, H.M., ERBIN, E.F., HAHN, G.T., KOTFILA, R.J., SEEGER, J.W. and WRUCK, D.A. Hydrogen embrittlement of titanium alloys. Metal Progress, 1955, 67, 115 - 120.
105. BUSH, S.H. and DILLON, R.L. Stress corrosion in nuclear systems. Proc. of Int. Conf. on Stress Corrosion Cracking and Hydrogen Embrittlement of Iron Base Alloys. Unieux-Firminy, France. June 1973. p. 61.
106. BUZZARD, R.W. and CLEAVES, H.E. Hydrogen embrittlement of steel : Review of the literature. United States, National Bureau of Standards, Circular 511, 1951, p. 29.
107. CADIOU, L. and LEYMONIE, C. Development of a device to study delayed transverse cracking of submerged arc welds under the action of hydrogen. International Congress 'L'Hydrogene dans les Metaux'. Paris, May - June, 1972. Editions Science et Industrie. p. 511.
108. CAILLETET, M.
C.R. Acad. Sci. Paris, 1868, Vol. 66, p. 847.
109. CAIN, W.M. and TROIANO. Steel structure and hydrogen embrittlement. Petroleum Engineer, 1965, 37, p. 78.
110. CAMPBELL, J.E. Effects of hydrogen gas on metals at ambient temperature. DMIC Report S-31, April 1970.
111. CAMPBELL, W.P. Experiences with HAZ cold cracking tests on a C-Mn structural steel. Welding Journal, 1976, 55, (5), 135s - 143s.
112. CANE, M.W.F. and BAKER, R.G. Slow bend test for HAZ hydrogen cracking susceptibility and its correlation with welding experience. Welding Research International, 1973, 3, (2), 1 - 16.
113. CAPLAN, J.S. and LANDERMAN, E. Preventing hydrogen induced cracking after welding of pressure vessel steels by use of low temperature postweld heat treatments. Welding Research Council Bulletin No. 216, June, 1976.

114. CARTER, C.S. and HYATT, M.V. Review of stress corrosion cracking in low alloy steels with yield strength below 150 ksi. Proc. of Int. Conf. on Stress Corrosion Cracking and Hydrogen Embrittlement of Iron Base Alloys. Unieux-Firminy, France, June 1973. p. 524.;
115. CASKEY, Jr., G.R. The influence of a surface oxide film on hydriding of titanium. Proc. of an Int. Conf. on Hydrogen in Metals. September 1973. Published by ASM. p. 465.
116. CASKEY, Jr., G.R. and PILLINGER, W.L. Effect of trapping on hydrogen permeation in copper. Proc. of an Int. Conf. on Hydrogen in Metals. September 1973. Published by ASM. p. 683.
117. CAVET, R.H. and VAN NESS, H.C. Embrittlement of steels by high pressure hydrogen gas. Welding Journal, 1963, 42, p. 316s.
118. CHAKRAPANI, D.G. and E.N. PUGH. Hydrogen embrittlement in a Mg-Al alloy. Metallurgical Transactions, 1976, 7A, 173 - 178.
119. CHANDLER, W.T. and WALTER, R.T. Effects of high pressure hydrogen on steels. Paper presented to ASM and AWS. November 1967.
120. CHATTERJEE, S.S. and PICKERING, H.W. A means of inhibiting hydrogen entry into steel. Proc. of an Int. Conf. on Effect of Hydrogen on Behaviour of Materials. Jackson Lake Lodge, Moran, Wyoming, September 1975. p. 182.
121. CHEN, C.C. and ARSENAULR. Low temperature strengthening of group VA metal single crystals by hydrogen. Proc. of an Int. Conf. on Hydrogen in Metals, September 1973. Published by ASM. p. 393.
122. CHENE, J., PLUSQUELLEC, J., AZOU, P., BASTIEN, P. Influence of stress on the diffusion of hydrogen in iron armco. International Congress 'L'Hydrogene dans les Metaux'. Paris, May - June 1972. Editions Science et Industrie. p. 176.
123. CHEW, B. A void model for hydrogen diffusion in steel. Metal Science Journal, 1971, 5, 195 - 200.
124. CHEW, B. and FABLING, F.T. The effect of grain boundaries on the low temperature diffusion of hydrogen in decarburized mild steel. Metal Science Journal, 1972. 6, 140 - 142.
125. CHEW, B. Prediction of weld metal hydrogen levels obtained under test conditions. Welding Journal, 1973, 52, (9), 386s - 391s.
126. CHEW, B. and FABLING, E.T. Hydrogen control of basic-coated NMA welding electrodes. Part 1 - Baking procedures. CEEB Report R/M/N725. 1974.
127. CHEW, B. Moisture loss and regain by some basic flux covered electrodes. Welding Journal, 1976, 55, (5), 127s - 134s.;
128. CHRISTENSEN, N. Metallurgical aspects of welding mild steel. Welding Journal, 1949, 28 (8), 373s - 380s.
129. CHRISTENSEN, N. and ROSE. Hydrogen in mild steel weld metal. British Welding Journal, 1955, 2, (12), 550 - 558.
130. CHRISTENSEN, N., GJERMUNDSEN, K. and ROSE, R. Hydrogen in mild steel weld deposits. British Welding Journal, 1958, 5, (6), 272 - 281.
131. CHRISTENSEN, N. The role of hydrogen in arc welding with coated electrodes. Welding Journal, 1961, 40, (3), 145s - 154s.
132. CHRISTENSEN, N. and EVANS, G.M. The presence and growth of microfissures in multi run mild steel weld deposits. IIW. DOC II-A-94-62.

133. CHRISTENSEN, N. Effect of hydrogen in weld metal. IIW DOC II-238-62.
134. CHRISTENSEN, N. Hydrogen controlled weld metal and heat affected zone. IIW DOC II-A-118-63.
135. CHRISTENSEN, N. Investigations related to hard zone cracking. IIW DOC II-351-65 (ex DOC II-A-155-65).
136. CHRISTENSEN, N. Results of testing for the assessment of microfissures. IIW DOC II-380-66.
137. CHRISTENSEN, N. Implant testing based on delayed fracture. IIW DOC-448-73Z.;
138. CHRISTENSEN, N. Hydrogen microfissures in mild steel weld metal. IIW DOC II-350-75.
139. CISZEWSKI, A., RADOMSKI, T. and SMIALOWSKI, M. Effect of nonmetallic inclusions on the formation of microcracks in hydrogen charged 1% Cr steel. Proc. of Int. Conf. on Stress Corrosion Cracking and Hydrogen Embrittlement of Iron Base Alloys. Unieux-Firminy, France. June 1973. p. 674.
140. CLARK, Jr. W.G. The effect of hydrogen gas on the fatigue crack growth rate behaviour of HY-80 and HY-130 steels. Proc. of an Int. Conf. on Hydrogen in Metals, September 1973. Published by ASM, p. 149.
141. CLUM, J.A. The role of hydrogen in dislocation generation in iron alloys. Scripta Metallurgica, 1975, 9, 51 - 58.
142. COE, F.R. Hydrogen determinations in welding research. Iron and Steel Institute. Special Report No. 73. (1962). pp. 111 - 122.
143. COE, F.R. and MORETON, J. Diffusion of hydrogen in low alloy steel. Journal of the Iron and Steel Institute, 1966, 205, (4), 366 - 370.
144. COE, F.R. Hydrogen in weld metal. British Welding Research Association, Bulletin, 1967, 8, (3), 76 - 81.
145. COE, F.R. and WATKINSON, F. Weld metal hydrogen levels. Welding Institute Research Bulletin, 1969, 10, (2), 43 - 45.
146. COE, F.R. Welding steels without hydrogen cracking. The Welding Institute Publication. Abington Hall, Abington, Cambridge, 1973.
147. COE, F.R. Weld metal hydrogen levels and the definition of hydrogen controlled electrodes. IWN DOC-II-682-73 (ex doc. II-A-333-73).
148. COE, F.R. and CHANO, Z. Heat treatment and hydrogen removal. Welding Institute Research Bulletin, 1974, 15, (4), 97 - 101.
149. COE, F.R., CHANO, Z. Hydrogen distribution and removal for a single bead weld during cooling. Welding Research International, 1975, 5, (1), 33 - 90.
150. COE, F.R. Hydrogen diffusion in welding. An assessment of current knowledge. DOC IIS/IIW-491-75. Welding in the World. 1976, 14, (1/2), 1 - 10.
151. COLBUS, J. Effect of time after deposition on hydrogen content and mechanical properties of covered electrode weld metal. Welding Journal. 1957. 36, (11), 489s.
152. COMBETTE, P. and GRILHE, J. Hydrogen diffusion anomaly in nickel below 300K; Quantum diffusion of hydrogen? International Congress 'L'Hydrogene dans les Metaux', Paris May - June, 1972, Editions Science et Industrie, p. 45.

153. COMBETTE, P., RENARD, M. and GRILHE, J. Interaction between dislocations and hydrogen atoms in nickel : tensile tests, internal friction, electrical resistivity. International Congress 'L'Hydrogene dans les Metaux'. Paris, May - June, 1972. Editions Science et Industrie, p. 90.
154. COMBETTE, P., RENARD, M. and GOBIN, P.F. Influence of hydrogen on the internal friction of copper. International Congress 'L'Hydrogene dans les Metaux'. Paris, May - June 1972, Editions Science et Industrie. p. 103.
155. CONCLETON, J. Criteria for branching cracks. Proc. of Int. Conf. on Stress Corrosion Cracking and Hydrogen Embrittlement of Iron-Base Alloys. Unieux-Firminy, France. June, 1973. p. 473.
156. CONOPHAGCS, E., PLUSQUELLEC, AZOU, P. and BASTIEN, P. The influence of hydrogen on the internal friction of ferrous alloys. International Congress 'L'Hydrogene dans les Metaux'. Paris, May - June, 1972, Editions Science et Industrie. p. 97.
157. CONOPHAGOS, E., PLUSQUELLEC, J., HYSPECKA, L., AZOU, P. and BASTIEN, P. Interactions between hydrogen and structural defects in Fe-Ni and Fe-Ni-C alloys. Proc. of Int. Conf. on Stress Corrosion Cracking and Hydrogen Embrittlement of Iron Base Alloys. Unieux-Firminy, France, June, 1973. p. 831.
158. CORIOU, H., GRALL, L., BESNARD, A. and FENARD-LEGRY, G. Hydrogen charging in an austenitic nickel alloy. International Congress 'L'Hydrogene dans les Metaux'. Paris, May - June, 1972. Editions Science et Industrie. p. 241.
159. CORNET, M. and TALBOT-BESNARD, S. Embrittlement of high purity iron by hydrogen. Influence of low carbon addition. International Congress 'L'Hydrogene dans les Metaux'. Paris May-June 1972. Editions Science et Industrie. p. 277.
160. CORNET, M. and TALBOT-BESNARD, S. Present ideas about mechanisms of hydrogen embrittlement of iron and ferrous alloys. Metal Science, 1978, 12, (7), 335 - 339.
161. COTTERILL, P. The hydrogen embrittlement of metals. Progr. Material Science. 1961, 9, 201 -
162. COTTON, H.C. Weldability of structural and pressure vessel steels. Welding Institute Autumn Meeting, 1970, Paper 11.
163. COTTRELL, A.H. Theory of brittle fracture in steel and similar metals. Transactions of the Metallurgical Society of the AIME, 1958, 212, 192 - 202.
164. COTTRELL, C.L.M. Effect of hydrogen on the continuous cooling transformation diagram for a Mn-Mo steel. Journal Iron and Steel Institute, 1954, 176, (3), 273 - 282.
165. COTTRELL, C.L.M. Hydrogen - Barrier to welding progress. British Welding Journal. 1954. 1 (4), 167 - 176.
166. COTTRELL, C.L.M. Weldability of a C-Mn steel related to properties of the head affected zone. British Welding Journal, 1955, 2, (2), 75-80.
167. COTTRELL, C.L.M. and BRADSTREET, B.J. Calculated pre-heat temperatures to prevent hard zone cracking in low alloy steels. British Welding Journal, 1955, 2, (7), 310-312.

168. COX, T.B. and GUDAS, J.P. Investigation of the fracture of near-alpha titanium alloys in high pressure hydrogen environments. Proc. of an Int. Conf. on Effect of Hydrogen on Behaviour of Materials. Jackson Lake Lodge, Moran, Wyoming, September 1975. p. 287.
169. CRESSWELL, R.A. Use of argon hydrogen mixtures for tungsten inert-gas welding of stainless steel. Second Commonwealth Welding Conference (Proceedings), May 1965, pp 3 - 10.
170. CRIQUI, B., FIDELLE, J.P. and CLAUSS, A. Effects of internal and external hydrogen on mechanical properties of beta III titanium alloy sheet. Proc. of an Int. Conf. on Effect of Hydrogen on Behaviour of Materials, Jackson Lake Lodge, Moran, Wyoming, September 1975, p. 91.
171. CROUCH, S.J. The influence of heat input on weld metal transverse cracking. MSc Thesis, Department of Materials, Cranfield Institute of Technology, 1978.
172. DANA, A.V., SHORTSLEEVE, F.J. and TROIANO, A.R. Relation of flake formation in steel to hydrogen, microstructure and stress. Trans. American Institute of Mining and Metallurgical Engineers, 1955, 203, 895 - 905, Journal of Metals, Vol. 7.
173. DANIELS, R.D., QUIGG, R.J. and TROIANO, A.R. Hydrogen embrittlement and delayed failure in titanium alloys. Transactions of the A.S.M., 1959, 11, 843 - 860.
174. DAOU, J.N. and VIALARD, R. Some properties of α -phase in hydrogen-trivalent rare earths systems. International Congress 'L'Hydrogene dans les Metaux', Paris May - June 1972, Editions Science et Industrie, p. 76.
175. DAOU, J.N. and VIALARD, R. The mobility of hydrogen in trivalent-rare earths hydrides. International Congress 'L'Hydrogene dans les Metaux'. Paris, May - June, 1972. Editions Science et Industrie, p.123.
176. DARKEN, L.S. and SMITH, R.P. Behaviour of hydrogen in steel during and after immersion in acid. Corrosion, 1949, 5, p.1.
177. DAS, K.B. A hydrogen detector for measuring surface and volume hydrogen content in metals. Proc. of an Int. Conf. on Hydrogen in Metals. September 1973. Published by A.S.M. p. 609.
178. DAS, K.B., ROBERTS, E.C. and BASSETT, R.G. An investigation of blistering in 2024-T6 aluminium alloy. Proc. of an Int. Conf. on Hydrogen in Metals. September 1973. Published by ASM, p. 289.
179. DAUTOVICH, D.P. and FLOREEN, S. The stress intensities for slow crack growth in steels containing hydrogen. Metallurgical Transactions, 1973, 4, 2627 -
180. DAUTOVICH, D.P. and FLOREEN, S. The stress corrosion and hydrogen embrittlement behaviour of maraging steels. Proc. of Int. Conf. on Stress Corrosion Cracking and Hydrogen Embrittlement of Iron Base Alloys. Unieux-Firminy, France, June, 1973, p. 798.
181. DeGARMO, E.P. A theory for preheating of plain low carbon steels. Welding Journal, 1958, 37, (3), 93s - 96s.
182. De SANTE, D.F. and TETELMAN, A.S. The annealing of hydrogen induced microcracks in iron-3 pct silicon. Trans. Metallurgical Society AIME, 1968, 242, (7), 1473 - 1475.

183. DILLARS, J.L. and TALBOT-BESNARD, S. Determination of the diffusion coefficient of hydrogen by measuring permeability in high purity iron. International Congress 'L'Hydrogene dans les Metaux'. Paris, May - June, 1972. Editions Science et Industrie. p. 159.
184. DOLBY, R.E. and CANE, M.W. A new mechanical approach for assessing susceptibility to hydrogen induced HAZ cracking. Metal Construction and British Welding Journal, 1971, 3, (9), 351 - 354.
185. DOLBY, R.E. The weldability of low carbon structural steels. Welding Institute Research Bulletin, 1977, 18, (8), 209 - 216.
186. DONOVAN, J. Accelerated evolution of hydrogen from metals during plastic deformation. Metallurgical Transactions, 1976, 7A, 1677 -
187. DUNEGAN, H.L. and TETELMAN, A.S. Non destructive characterization of hydrogen embrittlement cracking by acoustic emission techniques. Engineering Fracture Mechanics, 1971, 2, 387.
188. DUTTON, R. and PULS, M.P. A theoretical model for hydrogen induced sub-critical crack growth. Proc. of an Int. Conf. on Effect of Hydrogen on Behaviour of Materials. Jackson Lake Lodge, Moran, Wyoming, September 1975. p. 516.
189. EBERHADT, E. and REICHE, H. Fisheyes on the fracture surface of bend tests, their avoidance and estimation (in German). Der Praktiker, 1972, 24, (11), 222 - 223.
190. EBERT, H.W. Hard Welds - their cause and prevention. Welding Journal, 1971, 50, p. 636.
191. EDWARDS, B.C., BISHOP, H.E., RIVIERE, J.C. and EYRE, B.L. An AES study of temper embrittlement in low alloy steels. Acta Metallurgica, 1976, 24, 957 - 967.
192. EFFINGER, H.T., RENQUIST, M.L., WACHTER, A.G. and WILSON, J.G. How hydrogen attacks and damages steel in refinery equipment. Oil and Gas Journal, 1951, 2, 99.
193. ELLERBROCH, H.G. et al. Diffusion of H in steel with cavities. Acta Metallurgica, 1972, 20, (1), 53 - 60.
194. ELLS, C.E. and SIMPSON, C.J. Stress induced movement of hydrogen in zirconium alloys. Proc. of an Int. Conf. on Hydrogen in Metals. September 1973. Published by ASM. p. 345.
195. ELSEA, A.R. and FLETCHER, E.E. Hydrogen induced delayed brittle failures of high strength steels. DMIC Report 196, January 1964.
196. ENGEL, N.N. and JOHNSON, J.E. The electron concentration concept applied on the effects of hydrogen in metals. International Congress 'L'Hydrogene dans les Metaux'. Paris, May - June, 1972, Editions Science et Industrie, p. 60.
197. EPELBOIN, I. and KEDDAM, M. Application of electrochemical methods to study the adsorption of hydrogen onto the metal-electrolyte interface. International Congress 'L'Hydrogene dans les Metaux'. Paris, May - June, 1972. Editions Science et Industrie. p. 230.
198. EPELBOIN, I., MOREL, Ph., TAKENOUTI, H. Action of some inhibitors on hydrogen adsorption onto iron in sulphuric solutions. International Congress 'L'Hydrogene dans les Metaux'. Paris, May - June 1972. Editions Science et Industrie. p. 234.

199. ERDMANN-JESNITZER, F. Interaction of hydrogen and dislocations in low carbon mild steels. International Congress 'L'Hydrogene dans les Metaux', Paris, May - June, 1972. Editions Science et Industrie. p. 16.
200. EVANS, G.M. and CHRISTENSEN, N. Microfissuring of multi run mild steel weld metal. British Welding Journal, 1963, 10, (10), 508 - 515.
201. EVANS, G.M. and ROLLASON, E.C. Influence of non-metallic inclusions on the apparent diffusion of hydrogen in ferrous materials. Journal of the Iron and Steel Institute, 1969, 207, (11), 1484 - 1490.
202. EVANS, G.M., SIMONSEN, T. and AUGLAND, B. Implant weldability testing of carbon-manganese steels. IIW-DOC. IX-698-70. Metal Construction 1970, 2, 108 - 109.
203. EVANS, G.M. and CHRISTENSEN, N. Apparent diffusivity of hydrogen in multirun metal arc weld deposits. Metal Construction and British Welding Journal, 1971, 3, (2), 47 - 49.
204. EVANS, G.M. and CHRISTENSEN, N. Correlation of weld metal hydrogen content with heat affected zone embrittlement. Metal Construction and British Welding Journal, 1971, 3, (5), 188 - 189.
205. EVANS, G.M. and CHRISTENSEN, N. Implant testing - effect of steel composition and hydrogen level. IIW-DOC. II-A-274-70. Metal Construction, 1971, 3, 263 - 265.
206. EVANS, G.M. and BAACH, H. Hydrogen content of welds. Metal Construction and British Welding Journal, 1975, 7, (10), 508 - 511.
207. EVANS, G.M. and BAACH, H. Hydrogen content of welds deposited by different welding processes. Metals Technology Conference A - B, paper for the IIW 1976 Annual Assembly, public session.
208. EVANS, G.M. and GARLAND, J.G. Water absorption and redrying characteristics of two high basic agglomerated fluxes. Oerlikon Electrodes Ltd. Technical Report.
209. FABLING, G.T. and CHEW, B. The performance of collecting fluids in diffusible hydrogen analysis. Welding Research International 1973, 3, (4), 81 - 87.
210. FARRAR, J.C.M. The effect of hydrogen on the formation of lamellar tearing. Welding Research Institute, 1977, 7, (2), 120 - 143.
211. FARRAR, R.A. The nature of chevron cracking in submerged arc weld metals. Welding Research Institute, 1977, 7 (2), 85 - 88.
212. FARRAR, R.A. and TAYLOR, L.G. A metallographic study of chevron cracking in submerged arc weld metals. Welding and Metal Fabrication, 1977, 47, 575 - 578.
213. FARREL, K. and QUARREL, A.G. Hydrogen embrittlement of an ultra-high-tensile steel. Journal of the Iron and Steel Institute, 1964, 202, 1002 - 1011.
214. FARREL, A.K. Hydrogen embrittlement of mild steel. Journal of the Iron and Steel Institute, 1965, 203, p. 457.
215. FARREL, K. Cathodic hydrogen absorption and severe embrittlement in a high strength steel. Corrosion, 1970, 26, p. 105.
216. FAST, V.D. Interaction of metals and gases. Academic Press, New York, 1965, p. 54.

217. FEDOROV, V.G. et al. Condition of crack formation when welding steel EP56. Welding Production, 1974, 21 (1), 52 - 54.
218. FEDOROV, V.G. Effects of flux on the resistance of welded joints in 10Kh 16N4B steel to the formation of cold cracks during welding. Avt. Svarka, 1976 (3), 31 - 33, also in Automatic Welding 1976, 29, (3), 26 - 28.
219. FEICHTINGER, H.K. and MARINCEK, B. A contribution to behaviour and determination of hydrogen during and after welding. Welding Research International, 1976, 6, (3), 1 - 10.
220. FESSLER, R.R., GROENEVELD, T.P. and ELSEA, A.R. Stress corrosion and hydrogen stress cracking in buried pipelines. Proc. of Int. Conf. on Stress Corrosion Cracking and Hydrogen Embrittlement of Iron Base Alloys. Unieux-Firminy, France. June, 1973. p. 135.
221. FIDELLE, J.P., ROUX, C. and RAPIN, M. Essais de fragilisation d'aciers a haute resistance par l'hydrogene et le deuterium sous pression. Contribution a l'etude du mecanisme de la fragilisation des aciers par l'hydrogene. Mem. Sc. Rev. Met., 1969, 66, 833. BISI Transl. 8242 (1970).
222. FIDELLE, J.P., BROUDEUR, R., PELLISSIER-TANON, A. and ROUX, C. Role de l'hydrogene dans la fissuration par corrosion sous contrainte des aciers austenitiques dans les solutions de chlorures. Etablissement d'un mecanisms possible applicable a ce type de fissuration. Symposium- on Stress Corrosion Cracking and Hydrogen Embrittlement, Paris, 23 - 24. 4. 1971.
223. FIDELLE, J.P., BROUDEUR, R. and ROUX, C. Influence of temperature on hydrogen gas embrittlement of 35 NCD 16 steel. International Congress 'L'Hydrogene dans les Metaux'. Paris, May - June, 1972. Editions Science et Industrie, p. 350.
224. FIDELLE, J.P. and BROUDEUR, R. Hydrogen gas embrittlement under the influence of strain rate, temperature and thickness : relationship with delayed failure. Proc. of an Int. Conf. on Effect of Hydrogen on Behaviour of Materials. Jackson Lake Lodge, Moran, Wyoming, September 1975. p. 507.
225. FIKKERS, A.T. Influence of external restraint on cold cracking (testing for hydrogen-induced cracking in normalized steels by the application of an external restraint). Metal Construction and British Welding Journal 1974, 6, (6), 188 - 193.
226. FIKKERS, A.T. and MULLER, T. Hydrogen induced cracking in weld metal. Welding in the World, 1976, 14, (11/12), 238 - 247.
227. FLANIGAN, A.E. An investigation of the influence of hydrogen on the ductility of arc welds in mild steel. Welding Journal, 1947, 26, (4), 193s - 214s.
228. FLANIGAN, A.E., BOCARSKY, S.I. and MCGUIRE, G.B. Effect of low temperature cooling rate on the ductility of arc welds in mild steel. Welding Journal 1950, 29 (9), 459s - 457s.
229. FLANIGAN, A.E. and KAUFMAN, M. Microcracks and the low-temperature cooling rate embrittlement of welds. Welding Journal, 1951, 30, (12), 613s - 622s.
230. FLANIGAN, A.E. and MICLEU, T. Relation of pre-heating to embrittlement and microcracking in mild steel welds. Welding Journal, 1953, 32, (2), 99s - 106s.

231. FLANIGAN, A.E. and SAPERSTEIN, Z.P. Isothermal studies on the weld-metal microcracking of arc welds in mild steel. Welding Journal 1956, 35, (11), 541s - 556s.
232. FLANIGAN, A.E. and TUCKER, M.S. Temperature dependence of the rate of immunization against underbead cracking in arc welded low alloy steel. Welding Journal 1966, 45 (8), 368s - 373s.
233. FLANIGAN, A.E. and LEE, E.U. On the escape of dissolved hydrogen from weld metal. Welding Journal, 1966, 45, (10), 477s - 480s.
234. FLETCHER, E.E. and ELSEA, A.R. Hydrogen movement in steel-entry, diffusion and elimination. DMIC Report 219, June 30, 1965, Batelle Memorial Institute, Columbus, Ohio.
235. FOLKARD, E., SCHABEREITER, H., RABENSTEINER, G and RETTENBACHER, H. The content of diffusible hydrogen in weld joints and its influence. International Congress 'L'Hydrogene dans les Metaux'. Paris, May - June, 1972. Editions Science et Industrie. p. 501.
236. FORD, F.P. Quantitative examination of slip-dissolution and hydrogen-embrittlement theories of cracking in aluminium alloys. Metal Science, 1978, 12 (7), 326 - 334.
237. FRANDSEN, J.D., MORRIS, W.L. and MARCUS, H.L. Fatigue crack propagation of a nickel-copper alloy in low pressure hydrogen. Proc. of an Int. Conf. on Hydrogen in Metals. September 1973. Published by ASM. p. 633.
238. FRANDSEN, J.D. and MARCUS, H.L. Crack growth and fracture in gaseous hydrogen. Proc. of an Int. Conf. on Effect of Hydrogen on Behaviour of Materials. Jackson Lake Lodge, Moran, Wyoming, September 1975, p. 233.
239. FROHMBERG, R.P., BARNETT, W.J. and TROIANO, A.R. Delayed failure and hydrogen embrittlement in steel. Transactions of the A.S.M., 1955, 47, 892 - 925.
240. FUJII, T. On the prevention of hydrogen induced weld cracking in steel weldments. IIW DOC. IX-876-74.
241. FUJITA, T. and YAMADA, Y. Physical metallurgy and SCC in high strength steels. Proc. of Int. Conf. on Stress Corrosion Cracking and Hydrogen Embrittlement of Iron Base Alloys. Unieux-Firminy, France. June, 1973. p. 736.
242. FUKUI, S. and ASADA, C. Delayed fracture characteristics of low alloy steel in aqueous environments. Transactions Iron and Steel Institute of Japan, 1969. 9, p. 448.
243. GALEY, J., FOULARD, J. and KARINTHI, P. Elimination of hydrogen by flushing a neutral gas in liquid metals. International Congress 'L'Hydrogene dans les Metaux'. Paris, May - June, 1972. Editions Science et Industrie. p. 388.
244. GALLAND, J. These Doctorat d'Etat, Paris, No. 02487 (1968).
245. GALLAND, J., CHENE, J., AZOU, P., BASTIEN, P. Kinetics of desorption of hydrogen in iron and steels. International Congress 'L'Hydrogene dans les Metaux'. Paris, May - June, 1972. Editions Science et Industrie. p. 214.
246. GANGLOFF, R.P. and WEI, R.P. Embrittlement of 18 Ni maraging steel by low pressure gaseous hydrogen. Proc. of an Int. Conf. on Effect of Hydrogen on Behaviour of Materials. Jackson Lake Lodge, Moran, Wyoming, September 1975. p. 249.

247. GARBER, R., BERNSTEIN, I.M. and THOMPSON, A.W. Effect of hydrogen on ductile fracture of spheroidized steel. *Scripta Metallurgica*, 1976, 10, (4), 341 - 345.
248. GARLAND, J.G. and BAILEY, N. Fluxes for submerged arc welding ferritic steels - a Literature Survey. Part 1 : Manufacture, quality control and weldability. Welding Institute Research Report. M/84/75.
249. GAROFARD, F., CHOU, Y.T. and AMBEGAOKAR, V. Effect of hydrogen on stability of microcracks in iron and steel. *Acta Metallurgica*, 1960, 8, (8), 504 - 512.
250. CAYLEY, C.T. and WOODING, W.H. Determining total water content in electrode coverings. *Welding Journal*, 1950, 29, (8), 629 - 635.;
251. GELAS, B. de, SERAPHIN, L. and TRICOT, R. Hydrogen in titanium and its alloys. International Congress 'L'Hydrogene dans les Metaux'. Paris, May - June, 1972. Editions Science et Industrie. p. 433.;
252. GELD, P.V., RYABOV, R.A. and SALY, V.I. Permeability and diffusivity of hydrogen in iron and alloys on iron base. International Congress 'L'Hydrogene dans les Metaux'. Paris, May - June, 1972. Editions Science et Industrie. p. 167.
253. GERBERICH, W.W. and HARTBOWER, C.E. Monitoring crack growth of hydrogen embrittlement and stress corrosion cracking by acoustic emission. Proc. of Fundamental Aspects of Stress Corrosion Cracking Conference, Ohio State University, 11 - 15 September, 1967, p. 420 - 438.
254. GERBERICH, W.W. and CHEN, Y.T. A threshold stress intensity concept for environmental cracking. *International Journal of Fracture*, 1973, 9, 369 - 371.
255. GERBERICH, W.W. Effect of hydrogen on high strength and martensitic steels. Hydrogen in Metals - Proc. of an Int. Conf. 23 - 27 September, 1973. Published by ASM. pp 115 - 148.
256. GERBERICH, W.W. and CHEN, Y.T. The effect of thickness on hydrogen-induced slow crack growth. *Scripta Metallurgica*, 1974, 8, 243 - 248.
257. GERBERICH, W.W. and CHEN, Y.T. Hydrogen controlled cracking - an approach to threshold stress intensity. *Metallurgical Transactions A*, 1975, 6A, 271 - 278.
258. GERBERICH, W.W., CHEN, Y.T. and JOHN, C. St. A short time diffusion correlation for hydrogen induced crack growth kinetics. *Metallurgical Transactions A*, 1975, 6A, 1485 - 1498.
259. GERBERICH, W.W., GARRY, J. and LESSAR, J.F. Grain size and concentration effects in internal and external hydrogen embrittlement. Proc. of an Int. Conf. on Effect of Hydrogen on Behaviour of Materials. Jackson Lake Lodge, Moran, Wyoming, September 1975, p. 70.
260. GEST, R.N. and TROIANO, A.R. Hydrogen embrittlement and stress corrosion cracking in aluminium alloys. International Congress 'L'Hydrogene dans les Metaux'. Paris, May - June 1972. Editions Science et Industrie. p. 427.
261. GIBALA, R. Internal friction in hydrogen charged iron. *Trans. AIME*, 1967, 239, 1574 - 1585.
262. GIBALA, R. Hydrogen - defect interactions in iron-base alloys. Proc. of Int. Conf. on Stress Corrosion Cracking and Hydrogen Embrittlement of Iron Base Alloys. Unieux-Firminy, France. June 1973. p. 244.

263. GILMAN, J.J. Stress corrosion in plastic solids including the role of hydrogen. *Philosophical Magazine*, 1972, p. 801.
264. GILMAN, J.J. The role of surface hydrides in stress corrosion cracking. *Proc. of Int. Conf. on Stress Corrosion Cracking and Hydrogen Embrittlement of Iron-Base Alloys*. Unieux-Firminy, France, June 1973. p. 326.
265. GIRARDT, U. Comparative microfissure tests on single and multi-run welds and diffusible hydrogen determinations. IIW DOC II-A-132-64.
266. GOLD, E. and KOPPENAAL, T.J. Anomalous ductility of TRIP steel. *Transactions of the ASM*, 1969, 62, 607 - 610.
267. GOLDBREICH, M. The development of a new constant load cold cracking test. Study to obtain the master degree at the Delft Technological University (Department of Welding Technology).
268. GOLTSOV, V.A. and KAGAN, G.E. Diffusion, penetration and solubility of hydrogen in palladium alloys. *International Congress 'L'Hydrogene dans les Metaux'*. Paris, May - June 1972. Editions Science et Industrie. p. 249.
269. GOVE, K.B. and CHARLES, J.A. Hydrogen and dynamic strain-ageing in ferrite. *Metal Science*, 1974, 8, 367 -
270. GRANJON, H. Information on cracking tests. IIW. DOC. 93-62 (ex DOC. IX-290-61) also in *Welding in the World*, 1963, 1, (2), 58 - 91.
271. GRANJON, H. Studies on cracking of and transformation in steels during welding. *Welding Journal*, 1962, 42, (1), 1s - 11s.;
272. GRANJON, H. and DEBIEZ, S. Contribution a l'etude de la fissuration a froid dans les soudures sur acier par la methode des implants. IIW-DOC IX-559-67.
273. GRANJON, H. The 'implants' method for studying the weldability of high strength steels. *Metal Construction and British Welding Journal* 1969, 1, (11), 509 - 515.
274. GRANJON, H., DEBIEZ, S and GAILLARD, R. Etude de la soudabilite des aciers par la methode des implants : resultats actuels et perspectives nouvelles. IIW-DOC IX-708-70.
275. GRANJON, H. et al. Continuous cooling transformation and cold cracking of weld metal in steel welded joints. *Revue de Metallurgie*, 1971, 68, 5, 355 - 364.
276. GRANJON, H. Cold cracking in welding of steels. *Proceedings of the 1st International Symposium on Cracking and Fracture in Welds*. Tokyo, Japan, November 1971, Japan Welding Society, pp 1B1.1 - 1B1.11.
277. GRANJON, H. Cold cracking in the welding of steels. IIW DOC. IX-748-71 Also in *Welding in the World*, 1971, 9, (11-12), 382 - 397.
278. GRANJON, H. and DEBIEZ, S. Note on acoustic emission associated with cold cracking in the welding of steel. (Note sur l'emission acoustique associee a la fissuration a froid en soudage d'acier). (in French). *Proc. 8th World Conf. on Non Destructive Testing*, Cannes, 1976. Published : 75880 Paris, Cedex 18, France. Comité Français d'Etude des Essais Non Destructifs, 1976. Paper No. 3k14.
279. GRANJON, H. 1977 Portevin Lecture. *Welding in the World*, 1977, 15, (7/8), 121 - 134.
280. GRANT, N.J. and LUNDSFORD, J.L. How important is hydrogen embrittlement? *Iron Age*, 1955, 175, (6), 92 - 94.

281. GRAVILLE, B.A. Effect of temperature and strain rate on hydrogen embrittlement of steel. *British Welding Journal*, 1967, 14, 337 - 342.
282. GRAVILLE, B.A. Effect of fit-up on heat affected zone cold cracking. *British Welding Journal*, 1968, 15, 183 - 190.
283. GRAVILLE, B.A. Effect of hydrogen concentration on hydrogen embrittlement. *British Welding Journal*, 1968, 15, 191 - 195.
284. GRAVILLE, B.A. Weld cooling rates and heat affected zone hardness in a carbon steel. *Welding Journal* September 1973, 52, (9), 377s - 385s.
285. GRAVILLE, B.A. and READ, J.A. Optimization of fillet weld sizes. *Welding journal*, April 1974, 53(4), 161s - 169s.
286. GRAVILLE, B.A., McPARLAN, M. Weld metal cold cracking. *Metal Construction*, 1974, 6, (2), 62 - 63.
287. GRAVILLE, B.A. The principles of cold cracking control. Published by Dominion Bridge Co. Ltd., Montreal, Canada. 1975. 137pp.
288. GRAVILLE, B.A. Welding of H.S.L.A. (microalloyed) steels. A.S.M./A.T.M. Conference, Italy, 1976.
289. GRAY, H.R. Hydrogen environment embrittlement. NASA, Technical Memo. NASA TMX-68088, 1972.
290. GRAY, H.R. and JOYCE, J.P. Hydrogen environment embrittlement of turbine disc alloys. *Proc. of an Int. Conf. on Effect of Hydrogen on Behaviour of Materials*. Jackson Lake Lodge, Moran, Wyoming. September, 1975. p. 578.
291. GREEN, J.A.S., HAYDEN, H.W. and MONTAGUE, W.J. The influence of loading mode on the stress corrosion. Susceptibility of various alloy-environment systems. *Proc. of an Int. Conf. on Effect of Hydrogen on Behaviour of Materials*. Jackson Lake Lodge, Moran, Wyoming. September, 1975. p. 200.
292. GROENEVELD, T.P. and ELSEA, A.R. Hydrogen-stress cracking in natural-gas-transmission pipelines. *Proc. of an Int. Conf. on Hydrogen in Metals*. September 1973. Published by ASM. p. 727.
293. GUILLES, N.L. and ONO, K. The effect of hydrogen on internal friction of several titanium alloys. *Proc. of an Int. Conf. on Effect of Hydrogen on Behaviour of Materials*. Jackson Lake Lodge, Moran, Wyoming, September 1975. p. 666.
294. GUIONNET, M., JECKO, G., RAGUIN, J., WITTMANN, A. Contribution to sampling and determination of hydrogen in liquid steel. *International Congress 'L'Hydrogene dans les Metaux'*. Paris, May-June 1972. Editions Science et Industrie. p. 372.
295. GULBRANSEN, E.A. A model for the stress corrosion cracking of metals based on the morphology and structure of localized corrosion processes. *Proc. of Int. Conf. on Stress Corrosion Cracking and Hydrogen Embrittlement of Iron-Base Alloys*. Unieux-Firminy, France. June, 1973. p. 218.
296. HAMILTON, I.G. Trends in user requirements for welding consumables. *Proc. of Int. Conf. on Welding Research Related to Power Plant*. Eds. N.F. Eaton and L.M. Wyatt, C.E.G.B. 1972. Paper 21, 285-292.

297. HANADA, R. A resistometric study of the hydrogen and deuterium in group Va metals at low temperatures. Proc. of an Int. Conf. on Effect of Hydrogen on Behaviour of Materials. Jackson Lake Lodge, Moran, Wyoming, September 1975. p. 676.
298. HANCOCK, G.G. and JOHNSON, H.H. Hydrogen, oxygen and subcritical crack growth in a high strength steel. Trans. of the Metallurgical Society of AIME, April 1966. 236, 513 - 516.
299. HANNA, G.L., TROIANO, A.R. and STEIGERWALD, A. A mechanism for the embrittlement of high strength steel by aqueous environments. Trans. ASM, 1964, 57, p. 668.
300. HARASAWA, H. and HART, P.H.M. A preliminary evaluation of the effect of restraint on HAZ cold cracking of butt welds in C-Mn steels. Welding Research International, 1978, 8, (2), 129 - 165. Also in Welding Institute Members Report 40/1977/M.
301. HARDIE, D. The importance of the matrix in hydride embrittlement of zirconium. International Congress 'L'Hydrogene dans les Metaux. Paris, May - June 1972. Editions Science et Industrie. p. 497.
302. HARDIE, D. and BOWKER, P. The effect of gaseous hydrogen environment of the fracture behaviour of a HY-150 type steel. Proc. of an Int. Conf. on Effect of Hydrogen on Behaviour of Materials. Jackson Lake Lodge, Moran, Wyoming, September 1975. p. 251.
303. HARDIE, D. and MURRAY, T.I. Effect of hydrogen on ductility of a high strength steel in hardened and tempered conditions. Metals Technology, 1978, 5, (5), 145 - 149.
304. HARRIS, D. and PICKERING, H.W. On anodic cracking during cathodic hydrogen charging. Proc. of an Int. Conf. on Effect of Hydrogen on Behaviour of Materials. Jackson Lake Lodge, Moran, Wyoming, September, 1975. p. 229.
305. HARRISON, R.P., JONES, D de G. and NEWMAN, J.F. Caustic cracking of temper embrittled steels. Proc. of Int. Conf. on Stress Corrosion Cracking and Hydrogen Embrittlement of Iron-Base Alloys. Unicux. Firminy, France, June 1973. p. 659.
306. HART, M. Diffusible weld metal hydrogen from FEREX 7018 LT. BOC Murex Report No. D462. R & D Laboratories, Waltham Cross.
307. HART, P. and WATKINSON, F. Development and use of the implant cracking test. Welding Journal, 1972, 52, (7), 349s - 357s.
308. HART, P.H.M. Higher preheat- not always a panacea for hydrogen cracking. Welding Institute Research Bulletin, 1974, 15, (12), 375 - 377.
309. HART, P.H.M., WATKINSON, E. Weld metal implant test ranks Cr-Mo hydrogen cracking resistance. Welding Journal, 1975, 54, (9), 288s - 295s.
310. HART, P.H.M. and BROOKS, T.L. The effects of sulphur on HAZ hydrogen cracking in C-Mn steels. Welding Institute Report 43/1977/M.
311. HART, P.H.M. Low sulphur levels in C Mn steels and their effect on HAZ hardenability and hydrogen cracking. Int. Conf. on Trends in Steels and Consumables for Welding. The Welding Institute, London, 13 - 16 November 1978. Paper No. 20.
312. HARTBOWER, C.E., GERBERICH, W.W. and CRIMMINS, P.P. Monitoring subcritical crack growth by detection of elastic waves. Welding Journal, 1968, 47, (1), 1s - 18s.

313. HAYWARD, D.O. and TRAPNELL. Chemisorption. Butterworths, Washington, (1964).
314. HEROLD, A. and RAT, J.C. Electromigration of isotopes of hydrogen in some transition metals. International Congress 'L'Hydrogene dans les Metaux.' Paris, May - June 1972. Editions Science et Industrie, p. 49.
315. HEROLD, A. and MARECHE, J.F. Solubility of hydrogen and deuterium in some metals and alloys. International Congress 'L'Hydrogen dans les Metaux.' Paris, May - June 1972. Editions Science et Industrie, p. 210.
316. HERRES, S.A. Practical importance of hydrogen in metal arc welding of steel. Transactions of the American Society for Metals. 1947, 39, 162 - 189.
317. HERZOG, E. Developing steels to resist hydrogen sulphide. Industrial and Engineering Chemicals, 1961, 53, p. 64A.
318. HESS, P.D. and TURNBULL, G.K. Effects of hydrogen on properties of aluminium alloys. Proc. of an Int. Conf. on Hydrogen in Metals, September 1973. Published by ASM, p. 277.
319. HETTCHE, C.R. and COX, A.R. Fracture resistance of low carbon alloy irons. Metallurgical Transactions, 1972, 3, 2327 - 2335.
320. HEWITT, J. The study of hydrogen in low alloy steels by internal friction techniques. Iron and Steel Institute Special Report No. 73 on the Harrogate Conference on Hydrogen in Steel, Published 1962, p. 83.
321. HEWITT, J. and MURRAY, J.D. Effect of sulphur on the production and fabrication of carbon-manganese steel forgings. Conference on Cracking in Welds. Welding Institute Autumn Meeting, November, 1968. Published in Metal Construction and British Welding Journal. Supplement 2s, 24 - 31.
322. HILL, M.L. and JOHNSON, E.W. The solubility of hydrogen in alpha iron. Transactions Metals Society, AIME, 1961, 221, 622 - 629.
323. HIRTH, J.P. Stress corrosion cracking from the viewpoint of the defect solid state. Proc. of Int. Conf. on Stress Corrosion Cracking and Hydrogen Embrittlement of Iron-Base Alloys. Unieux-Firminy, France, June 1973. p. 1.
324. HOAGLAND, R.A., ROSENFELD, A.R. and HAHN, G.T. Mechanisms of fast fracture and arrest in steels. Metallurgical Transactions, 1972, 3, 123 - 136.
325. HOBSON, J.D. and SYKES, C. Effect of hydrogen on the properties of low alloy steels. Journal of the Iron and Steel Institute, 1951, 171, p. 209.
326. HOBSON, J.D. and HEWITT, J. The effect of hydrogen on the tensile properties of steel. Journal of the Iron and Steel Institute, 1953, 174, 131 - 140.
327. HOBSON, J.D. The diffusion of hydrogen in steel at temperatures -78° to 200°C. Journal Iron and Steel Institute, 1958, 189, (4), 315-321.
328. HOFMANN, W. and VIBRANS, G. Effect of hydrogen on fatigue strength of welded steel. Schweissen und Schneiden, 1960, 12, (3), 95-101.

329. HOFMANN, W. and RAULS, W. Ductility of steel under the influence of external high pressure hydrogen. *Welding Journal*, 1965, 44, p. 225s.
329. HOLZWORTH, M.L. and LOUTHAN, Jr. M.R.
Corrosion, 1968, 24, p. 110 -
330. HOPKIN, G.L. A suggested cause and a general theory for the cracking of alloy steels on welding. *Transactions Institute of Welding*, 1944, 7, 76 - 78.
331. HORIUTI, J. and TOYA, T. Chemisorbed hydrogen. Report from the Institute for Metal Catalysis, Hokkaido University, Sapporo, Japan, 1968.
332. HOULDCROFT, P.T. and GRIFFITHS, D.M. A bend test for welds in thick plate. *British Welding Journal*, 1963, 10, 266 - 269.
333. HOWARD, D.B. Evaluating iron powder electrodes for production use. *Welding Journal*, 1955, 34, (8), 752 - 758.
334. HOWDEN, D.G. and MILNER, D.R. Hydrogen absorption in arc melting. *British Welding Journal*, 1963, 10, (6), 304 - 316.
335. HOYT, S.L., SIMS, C.E., and BANTA, H.M. Metallurgical factors of under-bead cracking. *Metals Technology*, 1945, Technical Publication 1847, 1 - 24, also in *Welding Journal* 1945, 24, 433s - 445s.
336. HRIVNAK, I. The mutual relationship and interdependence of developments in steel metallurgy and welding technology. 1978 Houdremont Lecture (Annual Assembly of the IIW, public session).
337. HUDAK, S.J. and WEI, R.P. The kinetics of hydrogen enhanced crack growth in 18Ni maraging steel. *Proc. of an Int. Conf. on Hydrogen in Metals*, September, 1973. Published by ASM. p. 165.
338. HUDGINS, C.M., McGLASSON, R.L., and MEHDIZADEH, P. Hydrogen sulphide cracking of carbon and alloy steels. *Corrosion*, 1966, 22, p.238.
339. HUGHES, P.C., CAMBORN, I.R. and LIEBERT, B.B. Fracture of a low alloy steel in corrosive environments. *Journal of the Iron and Steel Institute* 1965, 203, p. 156.
340. HUMMITSCH, W. Effect of storage time on the hydrogen content and mechanical properties of arc welds made with covered electrodes. *British Welding Journal*, 1959, 6 (4), 155 - 160.
341. HURD, D.T. An introduction to the chemistry of the hydrides. Wiley, New York, 1952.
342. HYSPECKA, L., ABDELHADI, GALLAND, J. The increase of brittleness of austeno-martensitic structure of iron-nickel alloys in the presence of hydrogen. *International Congress L'Hydrogene dans les Metaux*. Paris, May - June 1972. Editions Science et Industrie. p. 267.
343. HYSPECKA, L. and MAZANEC, K. Contribution to study of premature and delayed fractures in structural steels. *International Congress L'Hydrogene dans les Metaux*. Paris, May - June 1972. Editions Science et Industrie. p. 330.
344. IINO, M. The extension of hydrogen blister-crack array in linepipe steels. *Metallurgical Transactions* 1978, 9A, (11), 1581 - 1590.
345. IINO, M. The elastic interaction between solute atoms and stress field at the tip of cracks and notches. *Engineering Fracture Mechanics*, 1978, 10, 1 - 13.

346. IIW-DOC-153-64. Determination of total hydrogen contents in weld metal. Welding in the World, 1965, 3, 1, 12 - 21.
347. IIW-DOC-288-68. Note on the carbon equivalent. Welding in the World, 1968, 6, (2), 78 - 81.
348. IIW-DOC-314-68. Recommended procedure for the determination of total water contents of electrode coatings by combustion (potential hydrogen contents). Welding in the World, 1969, 7, (1), 6 - 15.
349. IIW-DOC-314-68. IIW Method for the determination of water in electrode coatings. Welding in the World. 1969, 7, (1), 7 - 15.
350. IIW-DOC-315-68. Tentative procedure for the determination of hydrogen in mild and low alloy steel weld metal. Welding in the World, 1969, 7, (1), 16 - 27.
351. IIW-DOC-323 - 69. Note on the underbead hardness and the susceptibility to cold cracking. Welding in the World, 1969, 7, (2), 100-103.
352. IIW-DOC-361-71. Measurement of hydrogen in weld metal - recommendations concerning the presentation of experimental results. Welding in the World. 1971, 9, (1/2), 40 - 45.
353. IIW-DOC-447-73. Recommendation for the use of the implant test as a complementary information test on susceptibility to cold cracking in welding of steels. Welding in the World, 1974, 12, (1/2), 9 - 16.
354. IIW-452-74. Weld metal hydrogen levels and the definition of hydrogen controlled electrodes. Welding in the World, 1974, 12, (3/4), 69 - 76.
355. IIW-DOC-II-477-75. Recommended method of testing for the assessment of the microfissuring tendency of mild and low alloy steel weld metal deposited by manual arc welding covered electrodes. Welding in the World, 1975, 13, (5/6), 155 - 160.
356. IIW-DOC-II-778-75. Recommended methods of reporting weld metal hydrogen contents. Welding in the World, 1977, 15, (3/4), 69 - 72.
357. IIW-DOC-536-77. Japanese studies on structural restraint severity in relation to weld cracking (preliminary report). Welding in the World, 1977, 15, (7/8), 155 - 189.
358. IIW-DOC-IX-1093-78. Rapport de synthese sur les essais de fissuration.
359. INAGAKI, M, SUZUKI, H., and NAKAMURA, H. Effect of restraint and hydrogen on root cracking of high strength steel welds. (NRIM TRC test). IIW-DOC-IX-408-64.
360. INAGAKI, M., NAKAMURA, H., SUZUKI, H. Effect of microstructure on root cracking in high strength steel welds and behaviour of hydrogen. IIW-DOC-IX-439-65.
361. INAGAKI, M., NAKAMURA, H. and MITANI, Y. Cold cracking in multi layer welds of low-alloy high strength steel. IIW-DOC-IX-625-69.
362. INTERRANTE, C.G. and STOUT, R.D. Delayed cracking in steel weldments. Welding Journal, 1964, 43, (4), 145s - 160s.
363. INTERRANTE, C.G., DALDER, N.C. and YEO, R.B.G. Effect of moisture on cold cracking of carbon-manganese steel. Welding Journal, 1969, 48, (9), 384s - 388s.
364. INTERRANTE, C.G. Interpretative Report on effect of hydrogen in pressure vessels. Welding Research Council Bulletin No. 145, October, 1969.

365. ISONO, E., et al. An application of acoustic emission to the weld cracking test. Proc. of the 1st International Symposium on Cracking and Fracture in Welds. Japan Welding Society, Tokyo, Japan, November 1971, pp IB7.1 - IB7-10.
366. ITO, Y. and BESSIO, K. Cracking parameter of high strength steels related to HAZ cracking. Journal Japan Welding Society. 1968, 37, (9), 983 - 991.
367. ITO, Y. and BESSIO, K. A production of welding procedure to avoid heat affected zone cracking. IIW-DOC-IX-631-69.
368. IVENS, P.F. Weldability of HY-80 steel. IIW-DOC-IX-702-70.
369. JACOBS, A.J. and CHANDLER, W.T. Inhibition of hydrogen environment embrittlement by SO_2 . Scripta Metallurgica, 1975, 9, 767 - 769.
370. JAFFEE, R.I., LENNING, G.A. and CRAIGHEAD, C.M.
Transactions of the AIME, 1956, 206, 907 -
371. JAFFEE, R.I. and WILLIAMS, D.N. The effect of composition on the hydrogen embrittlement of alpha-beta titanium alloys. Transactions of the ASM, 1959, 51, 820 - 841.
372. JENKINS, N. and PARKER, D.H. The determination of moisture in electrode coatings. Welding Research International, 1974, 4, (1), 82 - 87.
373. JOHN, C. St. and GERBERICH, W.W. The effect of loading mode on hydrogen embrittlement. Metallurgical Transactions 1973, 4, 589 - 594.
374. JOHNSON, H.H. and TROIANO, A.R. Crack initiation in hydrogenated steel. Nature, 1957, 179, p. 777.
375. JOHNSON, H.H., SCHNEIDER, E.J. and TROIANO, A.R. The recovery of embrittled cadmium plated steel. Iron Age, 1958, 182, 47 - 50.
376. JOHNSON, H.H., MORLET, J.G. and TROIANO, A.R. Hydrogen crack initiation and delayed failure in steel. Transactions of the AIME, 1958, 212, 528 - 536.
377. JOHNSON, H.H. and WILLNER, A.M. Moisture and stable crack growth in a high strength steel. Applied Metals Research, 1965, 4, p.33.
378. JOHNSON, H.H. On hydrogen brittleness in high strength steels. Proc. of Conf. on Fundamental Aspects of Stress Corrosion Cracking. R.W. Staehle, ed. Ohio State University, National Association of Corrosion Engineers, 1967, p. 439.
379. JOHNSON, H.H. and PARIS. Subcritical flaw growth. Journal of Engineering Fracture Mechanics. 1968, 1, p.1.
380. JOHNSON, H.H. Hydrogen gas embrittlement. Proc. of an Int. Conf. on Hydrogen in Metals, 23 - 27 September 1973, Published by ASM, pp 35 - 48.
381. JOHNSON, H.H. Hydrogen brittleness in hydrogen and hydrogen-oxygen gas mixtures. Proc. of Int. Conf. on Stress Corrosion Cracking and Hydrogen Embrittlement of Iron-Base Alloys. Unieux-Firminy, France, June 1973. p. 382.
382. JOHNSON, H.H., KUMNICK and QUICK, N. Hydrogen trapping. Proc. of an Int. Conf. on Effect of Hydrogen on Behaviour of Materials. Jackson Lake Lodge, Moran, Wyoming, September 1975, p. 348.

383. JOHNSON, H.R., DINI, J.W. and ZEHR, S.W. On the embrittlement of uranium and U-0.8 Ti alloy by hydrogen and water. Proc. of an Int. Conf. on Hydrogen in Metals. September 1973. Published by ASM. p. 325.
384. JOHNSON, W.H.
Proc. Roy. Soc., 1875, No. 158, 168 - 179.
385. JOLLEY, G. and THOMASON, P.F. The importance of the tempering of martensite to the problem of hydrogen cracking in weld heat affected zones. International Congress L'Hydrogene dans les Metaux. Paris, May - June 1972. Editions Science et Industrie. p. 518.
386. JONES, T.E.M. Cracking of low alloy steel weld metal. British Welding Journal, 1959, 6, (7), 315 - 323.
387. KAMDAR, M.H. Crack nucleation in Fe-3% Si in a hydrogen environment. Proc. of an Int. Conf. on Hydrogen in Metals, September 1973. Published by ASM, p. 107.
388. KANE, J.L. Mechanical properties, microstructure and susceptibility to cracking in the HAZ of controlled-rolled, niobium treated, low carbon, manganese steels. British Welding Journal, 1968, 15, (8), 395 - 407.
389. KARPENKO, G.V., KRYPYAKEVYCH, R.I. and SLABOVSKY, I.S. A study of electron structure of hydrogen solid solutions in some transitional metals. International Congress L'Hydrogene dans les Metaux. Paris, May - June 1972. Editions Science et Industrie, p. 57.
390. KARPENKO, G.V., CHVED, M.M., and YAREMTCHENKO, N.Y. Influence of electrolytical charging in hydrogen on the character of the deformation and destruction of the iron. International Congress L'Hydrogene dans les Metaux. Paris, May - June 1972. Editions Science et Industrie. p. 272.
391. KARPENKO, G.V., VASSILENKO, I.I., FEDTCHENKO, V.S. and KHITARICHVICI, M.G. Lowering of mechanical strength of steel by absorption of hydrogen gas and hydrogen sulfid. International Congress L'Hydrogene dans les Metaux. Paris, May - June 1972. Editions Science et Industrie. p. 355.
392. KASS, W.J. Hydrogen transport in 4130 steel. Proc. of an Int. Conf. on Effect of Hydrogen on Behaviour of Materials. Jackson Lake Lodge, Moran, Wyoming, September 1975, p. 327.
393. KAZINCZY, F. de. A theory of hydrogen embrittlement. Journal of the Iron and Steel Institute, 1954, 177, 85 - 92.
394. KAZINCZY, F. de. Effect of hydrogen on the yielding of mild steel. Acta Metallurgica 1959, 7, (11), 706 - 708.
395. KERNS, G.E. and STAEHLE, R.W. Slow crack growth in hydrogen and hydrogen sulphide gas. Scripta Metallurgica, 1972, 6, p. 631.
396. KERNS, G.E., WANG, M.T. and STAEHLE, R.N. Stress corrosion cracking and hydrogen embrittlement in high strength steels. Proc. of Int. Conf. on Stress Corrosion Cracking and Hydrogen Embrittlement of Iron Base Alloys. Unieux-Firminy, France. June 1973. p. 700.
397. KEVILLE, B.R. An investigation to determine the mechanism involved in the formation and propagation of chevron cracks in submerged arc weldments. Welding Research International, 1976, 6(6), 47 - 66.

398. KHODOSOV, E.F., SHEPILOV, N.A. and KURISHCO, V.I. Electron-nuclear interactions in metal-hydrogen systems on the basis of the transition metals. International Congress L'Hydrogene dans les Metaux. Paris, May - June 1972, Editions Science et Industrie, p. 54.
399. KIHARA, H. Welding cracks and notch toughness of the heat affected zone in high strength steels. Conference Houdremont 1968, IIW DOC-313-68/Welding in the World, 1968, 6, (4), 196 - 235.
400. KIHARA, H., TERAII, K., YAMADA, S. and NAGANO, T. Study on preheating temperature in welds of high strength steel structure. IIW-DOC-IX-667-70.
401. KIKUTA, Y., SUGIMOTO, K., OCHIAI, S.I. and IWATA, K. The interaction of hydrogen and dislocations and its parallelism with hydrogen embrittlement in iron and steels. International Congress L'Hydrogene dans les Metaux. Paris, May - June 1972. Editions Science et Industrie. p. 144. Also IIW-DOC-II-616-72.
402. KIKUTA, Y., ARAKI, T. and OCHIAI, S.I. The diffusivity of hydrogen and its effect on the embrittlement of steel. International congress L'Hydrogene dans les Metaux. Paris, May - June 1972. Editions Science et Industrie. p. 295.
403. KIM, C.D. and LOGINDON, A.W. Techniques for investigating hydrogen-induced cracking of steels with high yield strength. Corrosion, 1968, 24, p. 313.
404. KIM, Y.G. and ALESZKA, J. Fatigue failure of hydrogen embrittled high strength steels. Metallurgical Transactions 1975, 6A, 1461 - 1465.
405. KITADA, T. The Japanese approach to cold cracking. The Welding Institute Research Bulletin, 1974, 15, (8), 223 - 227.
406. KLIER, E.F., MUVDI, B.B. and SACHS, G. Hydrogen embrittlement in a ultra-high-strength 4340 steel. Trans. American Institute of Mining and Metallurgical Engineers, 1957, 209, 106 - 112, Journal of Metals Vol. 9.
407. KLINGER, L.J., BARNET, W.J., FROMBERG and TROIANO, A.R. The embrittlement of alloy steel at high strength levels. Transactions of the ASM, 1954, 46, p. 1557.
408. KOLACHEV, B.A. Hydrogen Embrittlement of Nonferrous Metals. Israel Program for Scientific Translations, 1968, Jerusalem.
409. KONING, H.J., LANGE, K.L. and DAHL, W. Influence of alloying elements in the diffusion of hydrogen in alpha-iron between room temperature and 300°C. International Congress L'Hydrogene dans les Metaux. Paris, May - June 1972. Editions Science et Industrie. p. 172.
410. KORTOVICH, C.S. and STEIGERWALD, E.A. A comparison of hydrogen embrittlement and stress corrosion cracking in high strength steels. Engineering Fracture Mechanics, 1972, 4, p. 637.
411. KOWAKA, M. and NAGATA, S. Stress corrosion cracking of mild and low alloy steels in CO-CO₂-H₂O. Proc. of Int. Conf. on Stress Corrosion Cracking and Hydrogen Embrittlement of Iron-Base Alloys. Unieux-Firminy, France, June 1973. p. 680.
412. KOWAKA, M., TERASAKI, F., NAGATA, S., IKEDA, A. The test method to hydrogen induced cracking of rolled steels under wet hydrogen sulfide environment. Sumitomo Metals, 1975. 27 (1), 12 - 25.

413. KOYANAGY, K. and BRADSTREET, B.J. Effect of pre-heat, arc energy and moisture on the time delay for hard zone cracking. Proc. of the 2nd Commonwealth Welding Conference, The Institute of Welding, London, 26 April - 16 May, 1965. pp 132 - 135.
414. KRAFFT, J.M. and SMITH, H.L. Ligament instability model for stress corrosion and fatigue crack propagation in a 4340 steel. Proc. of Int. Conf. on Stress Corrosion Cracking and Hydrogen Embrittlement of Iron Base Alloys. Unieux-Firminy, France. June 1973. p. 482.
415. KRYPYAKEVYCH, R.I., SIDORENKO, V.M., KACHMAR, B.P. The effect of the electric field and stresses on hydrogen permeability of certain metals. International Congress L'Hydrogene dans les Metaux. Paris, May - June 1972. Editions Science et Industrie. p. 114.
416. KUDVA, V.V. Effect of cathodic charging on the crack sensitivity of steel weldments. MSc Thesis, Lehigh University, 1963.
417. KUMAR, R. and QUARREL, A.G. The effect of hydrogen upon martensite formation in low alloy steels. Journal of the Iron and Steel Institute, 1957, 187, 195 - 204.
418. KYTE, W.S. and CHEW, B. Postweld heat treatment for hydrogen removal. Welding Journal, 1979, 58, (2), 54s - 58s.
419. LACOMBE, P., AUCOUTURIER, M., LAURENT, J.P. and LAPASSET, G. Autoradiography of tritium and hydrogen embrittlement. Proc. of Int. Conf. on Stress Corrosion Cracking and Hydrogen Embrittlement of Iron Base Alloys. Unieux-Firminy, France, June 1973. p. 423.
420. LAPASSET, G., LAURENT, J.P., AUCOUTURIER, M., LACOMBE, P. Correlation between hydrogen localization observed through high resolution autoradiography and the trapping mechanism in iron and in a maraging steel. International Congress L'Hydrogene dans les Metaux, Paris, May - June 1972. Editions Science et Industrie. p. 108.
421. LAPUJOULADE, J. Chemisorption of hydrogen on transition metals. International Congress L'Hydrogene dans les Metaux, Paris, May - June, 1972, Editions Science et Industrie, p. 37.
422. LATANISION, R.M. and OPPERHAUSER Jr. H. The intergranular embrittlement of nickel by cathodically produced hydrogen. Proc. of an Int. Conf. on Hydrogen in Metals, September 1973. Published by ASM, p. 539.
423. LATANISION, R.M. The intergranular embrittlement of nickel by hydrogen: The effect of grain boundary segregation. Metallurgical Transactions, 1974, 5, 483 - 492.
424. LAURENT, J.P., LAPASSET, G., AUCOUTURIER, M. and LACOMBE, P. The use of electron high resolution autoradiography in studying hydrogen embrittlement. Proc. of an Int. Conf. on Hydrogen in Metals. September 1973. Published by ASM. p. 559.
425. LEACH, J.S.L. The possible role of surface films in stress corrosion cracking. Proc. Int. Conf. on Stress Corrosion Cracking and Hydrogen Embrittlement of Iron Base Alloys. Unieux-Firminy, France, June 1973. p. 16.
426. LEE, K.S. and STOLOFF, N.S. Fatigue of vanadium-hydrogen alloys. Proc. of an Int. Conf. on Effect of Hydrogen on Behaviour of Materials. Jackson Lake Lodge, Moran, Wyoming, September 1975. p. 404.

427. LEE, T.D., GOLDENBERG, T. and HIRTH, J.P. Effect of hydrogen on fracture of U-notched bend specimens of spheroidized AISI 1095 steel. Metallurgical Transactions, 1979, 10A, (2), 199 - 208.
428. LEEUWEN, H.P. Van. The kinetics of hydrogen embrittlement : a quantitative diffusion model. Engineering Fracture Mechanics, 1974, 6, 141 - 161.
429. LEEUWEN, H.P. Van. An analysis of hydrogen-induced cracking. Proc. of an Int. Conf. on Effect of Hydrogen on Behaviour of Materials. Jackson Lake Lodge, Moran, Wyomig, September 1975. p. 480.
430. LEEUWEN, H.P. Van. A failure criterion for internal hydrogen embrittlement. Engineering Fracture Mechanics, 1977, 9, 291 - 296.
431. LEFEVRE, Flakes in welds. Welding Journal, 1947, 26, (1), 57s - 64s.;
432. LEGRAND, J., COUDERC, C. and FIDELLE, J.P. Microfractography of 20 CND 10 steel embrittled by thermal processing and hydrogen. Int. Congress L'Hydrogene dans les Metaux. Paris, May - June 1972. Editions Science et Industrie. p. 316.
433. LESSAR, J.F. and GERBERICH, W.W. Grain size effects in hydrogen assisted cracking. Metallurgical Transactions A, 1976, 7A, 953 - 960.
434. LILLYS, P. and NEHRENBURG, A.E. Effect of tempering on stress corrosion cracking and hydrogen embrittlement of martensitic stainless steels. Transaction of the ASM, 1956, 58, p. 327.
435. LINDEN, H. Von der, SCHONHERR, W. Compilation of cold cracking tests. IIW-DOC-IX-779-72.
436. LINNERT, G.E. Welding metallurgy, Vol. 2. A.W.S., New York, 1967.
437. LIU, H.W. and FICALORA, P.J. Catalytic dissociation, hydrogen embrittlement and stress corrosion cracking. International Journal of Fracture Mechanics, 1972, 8, p. 223.
438. LORENTZ, R.E. and LEACH, P.D. Arc welding of thick cross sections. Welding Research Council Bulletin. No. 82, October 1962.
439. LOUNAMAA, K. and BAGGSTRÖM, G. Cracking in hydrogen charged tensile test specimens. Journal of the Iron and Steel Institute, 1965, 203, 702 - 706.
440. LOUTHAN, M.R., DEXTER, A.H. and DONOVAN, J.A. Effect of microvoids on H diffusion, Journal of the Iron and Steel Institute, 1972, 210, (1), 57 - 58.
441. LOUTHAN, Jr. M.R., CASKEY, G.R., DONOVAN, J.A. and RAWL, D.E. Hydrogen embrittlement of metals. Materials Science and Engineering, 1972, 10, 357 - 368.
442. LOUTHAN, Jr. M.R. Effects of hydrogen on the mechanical properties of low carbon and austenitic steels. Proc. of an Int. Conf. on Hydrogen in Metals. 23 - 27 September 1973, Published by ASM, pp 53 - 75
443. LOUTHAN, M.R., DERRICK, R.G., DONOVAN, J.A. and CASKEY, G.R. Hydrogen transport in iron and steel. Proc. of an Int. Conf. on Effect of Hydrogen on Behaviour of Materials. Jackson Lake Lodge, Moran, Wyoming, September 1975. p. 337.
444. LOUTHAN, Jr., M.R. and McNITT, R.P. The role of test techniques in evaluating hydrogen embrittlement mechanisms. Proc. of an Int. Conf. on Effect of Hydrogen on Behaviour of Materials. Jackson Lake Lodge, Moran, Wyoming, Sept 7 - 11, 1975, pp 496 - 506.

445. MAGNANI, N.J. Cracking of U-0.75wt % Ti in hydrogen and water vapour. Proc. of an Int. Conf. on Effect of Hydrogen on Behaviour of Materials. Jackson Lake Lodge, Moran, Wyoming, September 1975. p.188.
446. MAKARA, A.M. et al. Cold transverse cracks in low-alloy high strength welds. Automatic Welding, 1971, 24, (11), 1 - 4.
447. MAKARA, A.M. et al. Interconnection between cold cracks and the structures of high strength welds. Automatic Welding, 1972, 25, (7), 1 - 5.
448. MAKAROV, E.L., FJODOROW, W.G. Testing of thin plates of high strength steels to evaluate their resistance to cold cracking in a biaxial state of stress in welding. Baumann Hochschule No. 133, Moscow 1969.
449. MALLET, M.W. The water-gas reaction applied to welding arc atmospheres. Welding Journal 1946, 25, 396 - 399.
450. MALLET, M.W. and RIEPPEL, P. Arc atmospheres and underbead cracking. Welding Journal, 1946, 25, p. 748.
451. MALLET, M.W. and RIEPPEL, P.J. Underbead cracking of welds cathodically charged with hydrogen. Welding Journal, 1950, 29, (7), 343s - 347s.
452. MALUTCHKOV, O.T., LILEEVA, J.J. and TCHERTKOV, A.A. Diffusion of hydrogen in transition metals hydrides and their alloys. International Congress L'Hydrogene dans les Metaux. Paris, May - June 1972. Editions Science et Industrie. p. 261.
453. MARANDET, B. Effect of cold work on the dissolution and the diffusion of hydrogen in unalloyed carbon steels. Proc. of Int. Conf. on Stress Corrosion Cracking and Hydrogen Embrittlement of Iron Base Alloys. Unieux-Firminy, France, June 1973. p. 774.
454. MARKWORTH, A.J., KANNINEN, M.F. and GEHLEN, P.C. An atomic model of an environmentally-affected crack in BCC iron. Proc. of Int. Conf. on Stress Corrosion Cracking and Hydrogen Embrittlement of Iron Base Alloys. Unieux-Firminy, France, June 1973. p. 447.
455. MARQUEZ, J.A., MATSUSHIMA, I. and UHLIG, H.H. Effect of cold rolling on resistance of Ni-Fe alloys to hydrogen cracking. Corrosion, 1970, 26, p. 215.
456. MARSHALL, R.P. and LOUTHAN, Jr. M.R.
Transactions of the ASM, 1963, 56, 693 -
457. MARSHALL, S., VARVEY, T.M. and ILEWELYN, D.S. Relationship between hydrogen content and ductility of steels. Electric Furnace Proceedings, American Institute of Mining and Metallurgical Engineers, 1948, 6, 59 -
458. MASUEUCHI, K. and MARTIN, D.C. Investigation of residual stresses by use of Hydrogen cracking. Part 1 - Welding Journal, 1961, 40, (12), 553s - 563s. Part 2 - Welding Journal, 1966, 45, (9), 401s - 563s.
459. MASUBUCHI, K. and MARTIN, D.C. The mechanism of cracking in HY-80 steel weldments. Welding Journal, 1962, 41, (8), 375s - 384s.
460. MATHIAS, H., KATZ, Y. and NADIV, S. Hydrogenation effects in austenitic steels with different stability characteristics. Metal Science, 1978, 12, (3), 129 - 137.

461. McCLINTOCK, F.A. Continuum description of cracks at macro and micro levels and interaction of crack morphology with environment. Proc. of Int. Conf. on Stress Corrosion Cracking and Hydrogen Embrittlement of Iron Base Alloys. Unieux-Firminy, France, June 1973. p.455.
462. McCOY, R.A. Development of a high manganese steel resistant to hydrogen embrittlement. Proc. of an Int. Conf. on Hydrogen in Metals. 23 - 27 September 1973. Published by ASM pp 169 - 176.
463. McCRIGHT, R.D. Effects of environmental species and metallurgical structure on the hydrogen entry into steel. Proc. of Int. Conf. on Stress Corrosion Cracking and Hydrogen Embrittlement of Iron Base Alloys. Unieux-Firminy, France. June 1973. p. 306.
464. McDONALD, R.D. Susceptibility to cracking at welds in heavy sections of galvanized structural steels due to hydrogen embrittlement induced by pickling and corrosion. Welding Research Abroad, 1972, June, p. 23.
465. McGUIRE, M.F., HEHEMANN, R.F. and TROJANO, A.R. Stress corrosion cracking and hydrogen embrittlement in 410 stainless steel. International Congress L'Hydrogene dans les Metaux. Paris, May - June, 1972. Editions Science et Industrie. p. 325.
466. McINTYRE, P., PRIEST, A.H. and NICHOLSON, C.E. Hydrogen induced sub-critical flaw growth in steels under static and cyclic loading conditions. British Steel Corporation Laboratories. Report MG/38/72 (1972).
467. McINTYRE, P. Influence of environment on crack growth in high strength steels. Proc. of a Conf. on Mechanics and Mechanisms of Fracture. Churchill College, Cambridge, 4 - 6 April 1973. Paper 8.
468. McINTYRE, P. The relation between stress corrosion cracking and sub-critical flow growth in hydrogen and hydrogen sulphide gases. Proc. of Int. Conf. on Stress Corrosion Cracking and Hydrogen Embrittlement of Iron Base Alloys, Unieux-Firminy, France. June 1973, p. 788.
469. McLELLAN, R.B. and HARKINS, C.G. Hydrogen interactions with metals. Materials Science and Engineering, 1975, 18, 5 - 35.
470. McMAHON, C.J., Jr., YOSHINO, K. and FENG, H.C. Hydrogen embrittlement in impure steels. Proc. of Int. Conf. on Stress Corrosion Cracking and Hydrogen Embrittlement of Iron Base Alloys, Unieux-Firminy, France. June 1973, p. 649.
471. McNITT, R.P. and PLETTA, D.H. Hydrogen embrittlement and high cycle fatigue of 4340 steel. Proc. of an Int. Conf. on Hydrogen in Metals September 1973. Published by ASM. p. 109.
472. McPARLAN, M. and GRAVILLE, B.A. Hydrogen cracking in weld metals. Welding Journal, 1976, 55, 95s - 102s.;
473. MEITZNER, C.F. and STOUT, R.D. Microcracking and delayed cracking in welded quenched and tempered steels. Welding Journal, 1966, 45, (9), 393s - 400s.
474. MILLET, E.J. Origin and distribution of hydrogen in steel weld metals. British Welding Journal, 1956, 3, p. 497.
475. MILLION, A. and MILLION, C. Remarks on delayed failure mechanisms. Int. Congress L'Hydrogene dans les Metaux. Paris, May - June 1972. Editions Science et Industrie. p. 319.

476. MILLS, R.L. and EDESKUTY, F.L. Tests for hydrogen embrittlement of steels used in tank farm cylinders. CA-3602-MS, VC25, TID-4500, Los Alamos Scientific Laboratory of the University of California. 1966.
477. MIODOWNIK, A.P. The interaction of hydrogen with dislocations, stacking faults and other interfaces. Proc. of Int. Conf. on Stress Corrosion Cracking and Hydrogen Embrittlement of Iron Base Alloys. Unieux-Firminy, France, June 1973. p. 272.
478. MISHIMA, Y., ISHINO, S. and KAWANISHT, H. Grain boundary hydride precipitates in zircaloy-2. International Congress L'Hydrogene dans les Metaux. Paris, May - June 1972. Editions Science et Industrie. p. 469.
479. MISHIMA, Y., ISHINO, S. and KAWANISHT, H. Some observations on the dissolution and precipitation of zirconium hydrides in α -zirconium by electron microscopy. International Congress L'Hydrogene dans les Metaux. Paris, May - June, 1972. Editions Science et Industrie. p. 489.
480. MOISIO, T. Brittle fracture in failed ammonia plant. Metal Construction and British Welding Journal. 1972, 4, p.3.
481. MONTGRAIN, L. and SWANN, P.R. Electron microscopy of hydrogen embrittlement in a high purity Al-Zn-Mg alloy. Proc. of an Int. Conf. on Hydrogen in Metals. September 1973. Published by ASM. p. 575.
482. MOON, D.M. Correlation of the pressure, temperature and yield strength dependence of hydrogen embrittlement to a generalized threshold stress intensity model. Scripta Metallurgica, 1974, 8, 1435 -
483. MORETON, J., COE, F.R. A survey of knowledge of the sources, distribution and movement of hydrogen in weld metal. IIW-DOC II-512-69.
484. MORETON, Mrs. J., COE, F.R. and BONISZEWSKI, T. Hydrogen movement in weld metals. Welding Institute Research Bulletin, 1970, 11 (8), 233 - 235. Also published in Metal Construction and British Welding Journal, Part 1 - 1971, 3, (5), 185 - 189; Part 2, 1971, 3, (6), 223 - 228.
485. MORETON, Mrs. J., PARKER, D.H. and JENKINS, N.
Welding Institute Report M/61/71 (1971).
486. MORLET, J.G., JOHNSON, H.H. and TROIANO, A.R. A new concept of hydrogen embrittlement in steel. Journal of the Iron and Steel Institute, 1958, 189, 37 - 44.
487. MOTA, J.M.F. and APPS, R.L. Transverse 45° cracking - chevron cracking - in C-Mn and low alloy weld metals. IIW-DOC-LX-1080-78 for Annual Assembly, 1978.
488. MOTA, J.M.F., JUBB, J.E.M. and APPS, R.L. Chevron cracking : initiation and propagation. Welding and Metal Fabrication, 1978, 46, (9), 625 - 627.
489. MOTA, J.M.F., APPS, R.L. and JUBB, J.E.M. Chevron cracking in manual metal arc welding - International Conference on Trends in Steels and Consumables for Welding, Welding Institute Autumn Meeting, London, 14 - 16 November 1978, Paper No. 18, preprint pages 509 - 517.
490. MOTT, N.F. Fracture in metals. Journal of the Iron and Steel Institute 1956, 183, 233 - 243.

491. NADKARNI, S.V. and JATKAR, A.D. Cracking of weldment in quenched and tempered high strength steel with reference to its use in penstock pipes. Proc. of the 1st International Symposium on Cracking and Fracture in Welds. November 1971, Tokyo - Japan Welding Society. pp 1A5.1 - 1A5.6.
492. NAKAMURA, H. et al. Effects of pre and post heating on weld cracking of low alloy steels. Proc. of 1st International Symposium on Cracking and Fracture in Welds. The Japan Welding Society, Tokyo, Japan. November 1971. pp 1B6 1 - 13.
493. NAKASATO, F. and BERNSTEIN, I.M. Crystallographic and fractographic studies of hydrogen-induced cracking in purified iron and iron-silicon alloys. Metallurgical Transactions A, 1978, 9A, 1978, 1317 - 1326.
494. NANTIS, L. and NAMBOODHIRI, T.K.G. Analysis of the permeation technique for the study of hydrogen entry into iron-base alloys. Proc. of Int. Conf. on Stress Corrosion Cracking and Hydrogen Embrittlement of Iron Base Alloys. Unieux-Firminy, France. June 1973, p. 432.
495. NELSON, G.A. and EFFINGER, R.T. Blistering and embrittlement of pressure vessel steels by hydrogen. Welding Journal, 1955, 34, (1), 12s - 21s.
496. NELSON, H.G., WILLIAMS, D.F. and TETELMAN, A.S. Embrittlement of a ferrous alloy in a partially dissociated hydrogen environment. Metallurgical Transactions, 1971, 2, (4), 953 - 959.
497. NELSON, H.G., WILLIAMS, D.P. and STEIN, J.E. Environment hydrogen embrittlement of an α - β titanium alloy effect of microstructure. Metallurgical Transactions, 1972, 3, 469 - 475.
498. NELSON, H.G. The kinetic and mechanical aspects of hydrogen-induced failure in metals. NASATN D-6691. Washington, DC, April 1972.;
499. NELSON, H.G. Environmental hydrogen embrittlement of an α - β titanium alloy : effect of hydrogen pressure. Metallurgical Transactions, 1973, 4, (1), 364 - 367.
500. NELSON, H.G. and WILLIAMS, D.P. Quantitative observation of hydrogen-induced slow crack growth in a low alloy steel. Proc. of Int. Conf. on Stress Corrosion Cracking and Hydrogen Embrittlement of Iron Base Alloys. Unieux-Firminy, France. June 1973. p. 390.
501. NELSON, H.G. Hydrogen-induced slow crack growth of a plain carbon pipeline steel under conditions of cyclic loading. Proc. of an Int. Conf. on Effect of Hydrogen on Behaviour of Materials. Jackson Lake Lodge, Moran, Wyoming, September 1975. p. 602.
502. NEWMAN, J.F. and SHREIR, L.L. Effect of carbon content and structure of steels on solubility and diffusion coefficient of hydrogen. Journal of the Iron and Steel Institute, 1969, 207, (10), 1369-1372.
503. NEWMAN, J.F. and SHREIR, L.L. The effect of temperature upon the solubility and diffusion coefficient of cathodic hydrogen (H_2) in steel. Corrosion Science, 1971, 11, p. 25.
504. NIELSEN, N.A. Hydrogen induced cracking of low strength stainless steels. Proc. of Int. Conf. on Stress Corrosion Cracking and Hydrogen Embrittlement of Iron Base Alloys. Unieux-Firminy, France. June 1973, p. 1108.
505. NORBERG, R.E. Nuclear magnetic resonance of hydrogen into palladium wires. Physical Review, 1952, 86, 745 -

506. NUTTALL, K. Some aspects of slow crack growth in hydrided Zr-2.5 wt % Nb. Proc. of an Int. Conf. on Effect of Hydrogen on Behaviour of Materials. Jackson Lake Lodge, Moran, Wyoming, September 1975, p. 441.
507. NUTTALL, K., McCODEYE, D.P., ROGOWSKI, A.J. and HAVELOCK, F. Metallographic observations of the interaction of hydride, stress and crack growth at 600°K in a Zr - 2.5% Nb alloy. Scripta Metallurgica, 1976, 10, 979 - 982.
508. ODEGARD, B.C., BROOKS, J.A. and WEST, A.J. The effect of hydrogen on mechanical behaviour of nitrogen strengthened stainless steel. Proc. of an Int. Conf. on Effect of Hydrogen on Behaviour of Materials. Jackson Lake Lodge, Moran, Wyoming, September 1975, p. 116.
509. ODEGARD, D., EVANS, G.M., CHRISTENSEN, N. Apparent diffusivity of hydrogen in multi-run metal arc weld deposits. Metal Construction and British Welding Journal, 1971, 1, (2), 47 - 49.
510. OISHI, M. and OHWA, T. On the microcracks in the weld metal and hydrogen contents in the heat affected zone. IIW-DOC-II-265-63.
511. OKADA, H. Stress corrosion cracking and hydrogen cracking of structural steels. Proc. of Int. Conf. on Stress Corrosion Cracking and Hydrogen Embrittlement of Iron Base Alloys. Unieux-Firminy, France. June 1973, p. 124.
512. OKUMURA, T. and HORIKAWA, K. Transverse crack in S.A.W. of 80kg/mm² tensile strength steel. Proc. of the 1st International Symposium on Cracking and Fracture in Welds. The Japan Welding Society, Tokyo, Japan. November 1971. pp 1A7.1 - 1A7.17.
513. ORIANI, R.A. Hydrogen in metals. Proceedings from a Symposium on Stress Corrosion Cracking. 1967, p. 32.
514. ORIANI, R.A. Diffusion and trapping of hydrogen in steel. Acta Metallurgica, 1970, 18, (1), 147 - 157.
515. ORIANI, R.A. Consequence of strain induced electric field at roots of cracks. Scripta Metallurgica, 1971, 5, (8), 697 - 700.
516. ORIANI, R.A. A mechanistic theory of hydrogen embrittlement of steels. Ber. Bunsenges, 1972, 76, (8), 848 - 857.
517. ORIANI, R.A. and JOSEPHIC, P.H. Testing the decohesion theory of hydrogen induced crack propagation. Scripta Metallurgica, 1972, 6, (8), 681 - 687.
518. ORIANI, R.A. A review of proposed mechanism for hydrogen assisted cracking in metals. Fifth Annual Spring Meeting, Institute of Metals Division, AIME, May 29 - June 1, 1973, Philadelphia, P.A.
519. ORIANI, R.A. A decohesion theory for hydrogen induced crack propagation. Proc. of Int. Conf. on Stress Corrosion Cracking and Hydrogen Embrittlement of Iron Base Alloys. Unieux-Firminy, France. June 1973. p. 351.
520. ORIANI, R.A. and JOSEPHIC, P.H. Equilibrium aspects of hydrogen induced cracking of steels. Acta Metallurgica, 1974, 22, 1065 - 1074.
521. PALCZEWSKA, W. The effect of catalytic poisons on the kinetics of heterogeneous recombination of hydrogen atoms. Bulletin de l'Academie Polonaise des Sciences, Series des Sciences Chimiques, 1959, 12, p. 743.

522. PALCZEWSKA, W. and RATAJCZYKOWA, I. Investigations on the mechanism of the penetration of hydrogen from the gas phase into iron. Third International Congress on Metallic Corrosion, Moscow, May, 1966. Vol. 2, p. 64.
523. PAPP, J., HEHEMANN, R.F and TROIANO, A.R. Hydrogen embrittlement of high strength FCC alloys. Proc. of an Int. Conf. on Hydrogen in Metals. September 1973. Published by ASM. p. 657.
524. PARKINS, R.N. Environmental aspects of stress corrosion cracking in low strength ferritic steels. Proc. of Int. Conf. on Stress Corrosion Cracking and Hydrogen Embrittlement of Iron Base Alloys. Unieux-Firminy, France. June 1973. p. 601.
525. PARRISH, P.A., DAS, K.B., CHEN, C.M. and VERINK, E.D. Inhibition of hydrogen embrittlement of D6aC steel in aqueous oxidising media. Proc. of an Int. Conf. on Effect of Hydrogen on Behaviour of Materials. Jackson Lake Lodge, Moran, Wycmig, September 1975. p. 169.
526. PATERSON, K.A., SCHWANEBECK, J.C. and GERBERICH, W.W. In situ scanning Auger analysis of hydrogen induced fracture in Ti-6Al-6V-2Sn. Metallurgical Transactions A, 1978, 9A, 1169 - 1172.
527. PATON, N.E. and WILLIAMS, J.C. Effect of hydrogen on titanium and its alloys. Proc. of an Int. Conf. on Hydrogen in Metals. September, 1973. Published by ASM. p. 409.
528. PATON, N.E. and BUCK, O. The effect of hydrogen and temperature on the strength and modulus of beta phase titanium alloys. Proc. of an Int. Conf. on Effect of Hydrogen on Behaviour of Materials. Jackson Lake Lodge, Moran, Wycmig, September 1975. p. 83.
529. PEDDER, C. and HART, P.H.M. Implant cracking test equipment. Welding Institute Research Bulletin, 1971, 12, (12), 339 - 340.
530. PEDDER, C. and HART, P.H.M. CTS testing procedures : the present position. Welding Institute Research Bulletin. 1975, 16, (9), 264 - 266.
531. PELLINI, W. and ESCHBACHER, E.W. Effect of hydrogen on the ductility of weldments. Welding Journal, 1954, 33, (1), 16.
532. PELLOUX, R.M. and VAN DEN AVYLE, J.A. Testing and diagnosis of hydrogen susceptibility. Proc. of an Int. Conf. Hydrogen in Metals - 23 -27 September 1973. Published by ASM, pp 547 - 558.
533. PERKINS, W.G. Computational investigation of the effects of barrier layers on the permeation of hydrogen through metals. Proc. of an Int. Conf. on Effect of Hydrogen on Behaviour of Materials. Jackson Lake Lodge, Moran, Wyomig, September 1975, p. 355.
534. PETCH, N.J. and STABLES, P. Delayed fracture of metals under static load. Nature, 1952, 169, 842 - 843.
535. PETCH, N.J. The lowering of fracture-stress due to surface adsorption. Philosophical Magazine, 8th series, 1956, Vol. 1, 331 - 337.
536. PETERSON, D.T. and JENSEN, C.L. Electromigration of hydrogen and deuterium in vanadium and niobium by a resistance method. Metallurgical Transactions AIME, 1978, 9A (11), 1673 - 1677.

537. PHELPS, E.H. A review of stress corrosion behaviour of steels with high yield strength. Proc. of Conf. on Fundamental Aspects of Stress Corrosion Cracking. R.W. Staehle, ed. Ohio State University. National Association of Corrosion Engineers, 1967, p. 398.
538. PLUSQUELLEC, P., AZOU, P. and BASTIEN, P.
Mem. Sci. Rev. Met., 1968, 65, (1), 11.
539. PODGURSKI, H.H. and ORIANI, R.A. Nitrogenation of Fe-Al alloys. III - Absorption of hydrogen in nitrogenated Fe-Al alloys. Metallurgical Transactions 1972, 3, (8), 2055 - 2063.
540. POTTHOF. Micro-patches in weld metal of unalloyed welding electrodes. IIW-DOC-II-A-321 - 72.
541. POWELL, G.L. A method for measuring the hydrogen content of metals. Proc. of an Int. Conf. on Hydrogen in Metals. September 1973. Published by ASM. p. 585.
542. PREECE, C.M. Liquid metal embrittlement in iron alloys. Proc. of Int. Conf. on Stress Corrosion Cracking and Hydrogen Embrittlement of Iron Base Alloys. Unieux-Firminy, France, June 1973. p. 625.
543. PRESSOUYRE, G.M. and BERNSTEIN, I.M. A quantitative analysis of hydrogen trapping. Metallurgical Transactions AIME, 1978, 9A, (11), 1571 - 1580.
544. PRIEST, A.H., McINTYRE, P. and NICHOLSON, C.E. Hydrogen induced sub-critical flaw growth in steels under static and cyclic loading conditions. Proc. of the Third Int. Conf. on Fracture, Munich, April 1973.
545. PROCHOROV, N.N. and MAKAROV, E.L. Method for evaluating the resistance of steels to cold cracking in welding. Svar. Proiz. 1958, No. 9.
546. PROCHOROV, N.N. and others. The strength of steel during the conversion of austenite in welding. Svar. Proiz. 1959, No. 8.
547. PROCHOROV, N.N. and MAKAROV, E.L. Procedure for the determination and regulation of the resistance of steels to cold cracking in welding. Avt. Svarka, 1961, No. 11.
548. PROCTOR, R.P.M. and PAXTON, H.W. The effect of prior austenite grain size on the stress corrosion cracking susceptibility of AISI 4340 steel. Transactions of the ASM, 1969, 62, p. 989.
549. PROTOPAPAS, P., DEPUYT, P.J. and PARLEE, N.A.D. The diffusion of hydrogen in liquid metals and alloys. International Congress L'Hydrogene dans les Metaux. Paris, May - June 1972. Editions Science et Industrie. p. 419.
550. PUGH, E.N. A post conference evaluation of our understanding of the failure mechanisms. Proc. of Int. Conf. on Stress Corrosion Cracking and Hydrogen Embrittlement of Iron Base Alloys. Unieux-Firminy, France, June 1973. p. 37.
551. QUIGG, R.J. and TROIANO, A.R. Hydrogen embrittlement in steels, titanium alloys and several face centered cubic alloys. WADC Report 59 - 172 (April 1959). R.J. Quigg, PhD Thesis, Case Institute of Technology, Cleveland.
552. QUINN, T. Heat affected zone properties of low carbon line pipe steels. MSc Thesis, Materials Department, Cranfield Institute of Technology, September 1977.

553. RACK, H.J. The relationship between thermal embrittlement and hydrogen cracking in 18Ni (250) maraging steel. Proc. of an Int. Conf. on Effect of Hydrogen on Behaviour of Materials, Jackson Lake Lodge, Moran, Wyoming. September, 1975, p. 150.
554. RANDALL, M.D., MONROE, R.D. and RIEPPEL, P.J. Causes of microcracking and microporosity in ultra high strength steel weld metal. Welding Journal, 1962, 41, (5), 193s - 206s.
555. RATH, B.B. and BERNSTEIN, I.M. The relation between grain boundary orientation and intergranular cracking. Metallurgical Transactions October 1971, 2, 2845 - 2851.
556. RAVI, K.V. and GIBALA, R. Low temperature strengthening in niobium-hydrogen single crystals. Metallurgical Transactions 1971, 2, (4), 1219 - 1225.
557. REEVE, L. Relation between the hydrogen content of weld metal and its oxygen content. Welding Journal, 1945, 24, (11), 618s - 623s.
558. REUTER, W.G. and HARTBOWER, C.E. Stress-corrosion and hydrogen-induced cracking in D6aC low-alloy steel. Proc. of an Int. Conf. on Effects of Hydrogen on Behaviour of Materials. Jackson Lake Lodge, Moran, Wyoming. September 1975. p. 159.
559. RICE, J.R. Mechanics aspects of stress corrosion cracking and hydrogen embrittlement. Proc. of Int. Conf. on Stress Corrosion Cracking and Hydrogen Embrittlement of Iron-Base Alloys. Unieux-Firminy, France, June 1973. p. 11.
560. RICE, J.R. Hydrogen and interfacial cohesion. Proc. of an Int. Conf. on Effect of Hydrogen on Behaviour of Materials. Jackson Lake Lodge, Moran, Wyoming, September 7 - 11, 1975, pp 455 - 466.
561. RIDLEY, N., CAULKIN, K.G. and LORIMER, G.W. Zirconium hydride precipitation in zircaloy. International Congress L'Hydrogene dans les Metaux. Paris, May - June, 1972. Editions Science et Industrie. p. 484.
562. RIPLING, E.J. Hydrogen embrittlement in a commercial alpha-beta titanium alloy. Transactions AIME, 1956, 206, 502 - 503. Journal of Metals, Vol. 8.
563. ROBINSON, J.L. The cracking of line pipe steels in environments containing wet hydrogen sulphide. Welding Institute Research Bulletin. 1977, 18, (5), 121 - 126.
564. ROGERS, H.C. The influence of hydrogen on the yield point in iron. Acta Metallurgica, 1956, 4, (3), 114 - 117.
565. ROGERS, H.C. Hydrogen embrittlement in engineering materials. Materials Protection, 1962, 1, (4), 26 - 33.
566. ROLLASON, E.C. Influence of hydrogen on weldability of high-tensile steels. Welding Journal. 1944, 23, (11), 604s - 605s.
567. ROLLASON, E.C. and MANCE, H.W. Estimation and influence of hydrogen in weld metal. Welding, 1945, 13, 436 - 461.
568. ROLLASON, E.C. and ROBERTS, R.R. Effect of cooling rate and composition on the embrittlement of weld metal. Journal of the Iron and Steel Institute, 1950, 166, (11), 105 - 112.
569. ROSIN, A.D., BLEWITT, T.H. and TROIANO, A.R. Hydrogen embrittlement in irradiated steels. Nuclear Engineering and Design, 1966, 4, p.446.

570. ROTHWEL, A.B. Weldability of HSLA structural steels. Metal Progress, 1977, 111, (6), 43 - 50.
571. SAGUES, A.A., ULITCHNY, M.G. and GIBALA, R. Hydrogen strengthening in niobium and niobium-base alloys. Proc. of an Int. Conf. on Effect of Hydrogen on Behaviour of Materials. Jackson Lake Lodge, Moran, Wyoming, September 1975. p. 390.
572. SAIBEL, E. Failure of a thick walled pressure vessel. Industrial and Engineering Chemicals, 1961, 53, p. 56A.
573. SALTER, G.R. Hydrogen absorption in arc welding. British Welding Journal, 1963, 10, 316 - 325.
574. SANDOZ, G. A unified theory for some effects of hydrogen source, alloying elements and potential in martensitic AISI 4340 steel. Metallurgical Transactions, 1972, 3, p. 1169.
575. SANDOZ, G. The interplay of hydrogen dissociation and composition in stress corrosion cracking of martensitic steel. International Congress L'Hydrogene dans les Metaux. Paris, May - June, 1972. Editions Science et Industrie. p. 335.
576. SAPIRO, L.S., MASLOV, V.A. The segregation of hydrogen in welds. Automatic Welding, 1965, 18, 5, 19 - 22.
577. SATOH, K., MATSUI, S. Reaction stress and weld cracking under hindered contraction. IIW-DOC-IX-574-68.
578. SATOH, K., TERA, K., YAMADA, S., NAGANO, T. and MATSUMURA, H. Study on weld cracking in multiple pass welds of high strength steel. IIW-DOC-IX-678-70.
579. SATOH, K. et al. Determination of preheating conditions to avoid weld cracking in steel constructions. IIW-DOC-IX-730-71.
580. SATOH, K., MATSUI, S., TERA, K., YAMADA, S., MATSUMURA, H. Weld cracking behaviour of 100 kg/mm² high strength steel by large-size restraint testing machine. IIW-DOC-IX-737-71.
581. SATOH, K. et al. JSSC guidance report on determination of safe preheating conditions without weld cracks in steel structures. IIW-DOC-IX-834-73.
582. SATOH, K., UEDA, Y., KIHARA, H. Recent trends of research into restraint stresses and strains in relation to weld cracking. IIW-DOC-425 - 73, Welding in the World, 1973, 11 (5 - 6), 133 - 156.
583. SAUNDERS, G.G. and KNOTT, J.F. The origins of zigzag fracture in high strength materials. The Welding Institute Research Bulletin, April 1975, pp. 106 - 109.
584. SAVAGE, W.F. and SZEKERES, E.S. A mechanism for crack formation in HY-80 steel weldments. Welding Journal, 1967, 46, (2), 94s - 96s.
585. SAVAGE, W.F., NIPPES, E.F. and SZEKERES, E.S. Hydrogen induced cold cracking in a low alloy steel. Welding Journal 1976, 55 (9), 276s - 283s.
586. SAVAGE, W.F., NIPPES, E.F. and HOMMA, H. Hydrogen induced cracking in HY-80 steel weldments. Welding Journal, 1976, 55, (11), 368s-376s.
587. SAVAGE, W.G., NIPPES, E.G. and SAWHILL, Jr. J.M. Hydrogen induced cracking during implant testing of alloy steels. Welding Journal 1976, 55, (12), 400s - 407s.

588. SAVAGE, W.F., NIPPES, E.F. and TOKUNAGA, Y. Hydrogen induced cracking in HY130 steel weldments. *Welding Journal*, 1978, 57, (4), 118s - 126s.
589. SAWHILL, J.M., DIX, A.W. and SAVAGE, W.F. Modified implant test for studying delayed cracking. *Welding Journal*, 1974, 53, (12), 554a - 560s.
590. SAWATZKY, A. Hydrogen distribution in zirconium sheathing of nuclear reactor fuels. *Proc. of an Int. Conf. on Hydrogen in Metals*. September 1973. Published by ASM. p. 361.
591. SAXTON, H.J., WEST, A.J. and THOMPSON, A.W. A new method for long-term slow crack growth testing in hydrogen. *Proc. of an Int. Conf. on Effect of Hydrogen on Behaviour of Materials*. Jackson Lake Lodge, Moran, Wyoming, September 1975. p. 631.
592. SCAMANS, G.M. and SWANN, G.M. Stress corrosion crack tip morphology. *Proc. of Int. Conf. on Stress Corrosion Cracking and Hydrogen Embrittlement of Iron Base Alloys*. Unieux-Firminy, France, June 1973. p. 166.
593. SCHAEFFLER, A.L., CAMPBELL, H.C. and THIELSCH, H. Hydrogen in mild steel weld metal. (A Review). *Welding Journal*, 1952, 31, (6), 283s - 309s.
594. SCHALLER, B., POIRIER, J., ROUX, C. and CLAUSS, A. Mechanical Behaviour of TA6V6EZ titanium alloy. Influence of hydrogen and oxygen embrittlement. *International Congress L'Hydrogene dans les Metaux*. Paris, May - June 1972. Editions Science et Industrie. p. 363.
595. SCHMIDT, P. Summarized results of joint programme. IIW-DOC-II-A-300-71.
596. SCHUETZ, A.E. and ROBERTSON. Hydrogen absorption, embrittlement and fracture of steel. *Corrosion*, 1957, 13, 437 - 458.
597. SCULLY, J.C. Models of stress corrosion cracking. *Proc. of Int. Conf. on Stress Corrosion Cracking and Hydrogen Embrittlement of Iron Base Alloys*. Unieux-Firminy, France. June 1973, p. 165.
598. SCULLY, J.C. Fractographic aspects of stress corrosion cracking and hydrogen embrittlement in iron base alloys. *Proc. of Int. Conf. on Stress Corrosion Cracking and Hydrogen Embrittlement of Iron Base Alloys*. Unieux-Firminy, France. June 1973, p. 496.
599. SCULLY, J.C. The role of hydrogen in stress corrosion cracking. *Proc. of an Int. Conf. on Effect of Hydrogen on Behaviour of Materials*. Jackson Lake Lodge, Moran, Wyoming, Sept. 1975. p. 129.
600. SCZERZENIE, F.E. and ROGERS, H.C. Hydrogen embrittlement of tungsten base heavy alloys. *Proc. of an Int. Conf. on Hydrogen in Metals*. September 1973. Published by ASM, p. 645.
601. SEABROOK, J.B., GRANT, N.J. and CARNEY, D. Hydrogen embrittlement of SAE 1020 steel. *Transactions of the AIME*, 188, (11), 1950, 1317 - 1321.
602. SEKIGUCHI, H., KOBAYASHI, T. and ANDO, S. Behaviour of hydrogen in steel welding. *IIW/IIS Annual Assembly, Public session, 1957 - Essen*.
603. SEWELL, F.D. Hydrogen embrittlement challenges tubular good performance. *ASME Paper 65-PET-13*, 1965.

604. SHAH, K.K. and JOHNSON, D.L. Effect of surface pre-oxidation of hydrogen permeation in alpha titanium. Proc. of an Int. Conf. on Hydrogen in Metals. September 1973. Published by ASM, p. 475.
605. SHEWMON, P.G. Hydrogen attack of carbon steel. Proc. of an Int. Conf. on Effects of Hydrogen on Behaviour of Materials. Jackson Lake Lodge, Moran, Wyoming, September, 1975, p. 59.
606. SIMPSON, C.J. and MOERMAN, J. Hydrogen embrittlement of zirconium 2.5 wt % niobium. Proc. of an Int. Conf. on Effect of Hydrogen on Behaviour of Materials. Jackson Lake Lodge, Moran, Wyoming. September 1975, p. 428.
607. SIMS, C.E. and BANTA, H.M. Development of weldable high strength steels. Welding Journal, 1949, 28, (4), 178s - 192s.
608. SIMS, C.E. and DAHLE, F.B. Welding aluminium containing steels. Welding Journal, 1941, 20, (10), 504s - 512s.
609. SIMS, C.E., Discussion of 'Crack sensitivity in aircraft steels'. Welding Journal, 1951, 30, (1), 52 - 53.
610. SIMS, C.E., The behaviour of gases in solid iron on steel. Gases in Metals, A.S.M., 1953.
611. SMALL, W.M., RADZILOWSKI, R.H. and PEHLKE, R.O. Kinetics of solution of hydrogen in liquid iron, nickel and copper containing dissolved oxygen and sulphur. Metallurgical Transactions, 1973, 4, 2045 - 2050.
612. SMIALOWSKI, M. Hydrogen in steel. Book published by Pergamon Press, Oxford/London 1962.
613. SMIALOWSKI, M. Effect of electrolytic charging conditions on hydrogen penetration and embrittlement of various steels. International Congress L'Hydrogene dans les Metaux. Paris, May - June 1972. Editions Science et Industrie. p. 300.
614. SMIALOWSKI, M. Hydrogen blistering and surface microcracks. Proc. of Int. Conf. on Stress Corrosion Cracking and Hydrogen Embrittlement of Iron Base Alloys. Unieux-Firminy, France, June 1973. p. 405.
615. SMITH, A.O., Horizontal butt weld fissure test. IIW-DOC-II-A-47-60.;
616. SMITH, D.C., RINEHART, W.G. and JOHANNES, K.P. Effect of moisture in the coatings of low hydrogen iron-powder electrodes. Welding Journal, 1956, 35, (7), 322s.
617. SMITH, D.C. Development, properties and usability of low hydrogen electrodes. Welding Journal, 1959, 38, (9), 377s - 392s.
618. SMITH, D.P. Hydrogen in metals. University Chicago Press, Chicago 1948.
619. SMITH, E.F., JACKO, R. and DUQUETTE. Hydrogen assisted fatigue cracking of high strength aluminium alloys. Proc. of an Int. Conf. on Effect of Hydrogen on Behaviour of Materials. Jackson Lake Lodge, Moran, Wyoming, Sept. 1975, p. 218.
620. SMITH, G.C. Effect of hydrogen on nickel and nickel-base alloys. Proc. of an Int. Conf. on Hydrogen in Metals, September 1973. Published by ASM. p. 485.
621. SMITH, J.H. and DAVIS, J.A. Stress corrosion and hydrogen embrittlement cracking behaviour of HY80 and HY130 weld metals. 89.021-024(4) (B-6304) 40.001-021(8) United States Steel Corp., Jan. 22, 1971.

622. SMITH, N. and BAGNALL, B.I. The influence of sulphur on heat affected zone cracking of carbon manganese steel welds. Autumn Meeting of the Welding Institute, 1968 - Cracking in Welds - published in Metal Construction and British Welding Journal, 1969, 1(2s), 17 - 23.
623. SMUGERESKY, J.E. Effect of hydrogen on the mechanical properties of iron-base superalloys. Metallurgical Transactions A, 1977, 6A, 1283 - 1289.
624. SPAHN, H., WAGNER, G.H. and STEINHOFF, U. Stress corrosion cracking and cathodic hydrogen embrittlement in the chemical industry. Proc. of Int. Conf. on Stress Corrosion Cracking and Hydrogen Embrittlement of Iron Base Alloys. Unieux-Firminy, France, June, 1973. p. 80.
625. SPEIDEL, M.O. Dynamic and static embrittlement of a high-strength steel in water. International Congress L'Hydrogene dans les Metaux. Paris, May - June, 1972. Editions Science et Industrie. p. 290.
626. SPEIDEL, M.O. Branching of subcritical cracks in metals. International Congress L'Hydrogene dans les Metaux. Paris, May - June 1972. Editions Science et Industrie. p. 358.
627. SPEIDEL, M.O. and FOURT, P.M. Stress corrosion cracking and hydrogen embrittlement in industrial circumstances. Proc. of Int. Conf. on Iron Base Alloys. Unieux-Firminy, France. June 1973. p. 57.
628. SPEIDEL, M.O. Hydrogen embrittlement of aluminium alloys. Proc. of an Int. Conf. on Hydrogen in Metals. 23 - 27 September 1973. Published by ASM, pp 249 - 273.;
629. SPEISER, R. Hydrogen in metals. Proc. of Int. Conf. on Stress Corrosion Cracking and Hydrogen Embrittlement of Iron Base Alloys. Unieux-Firminy, France, June 1973. p. 226.
630. SPRARAGEN, W. and CLAUSSEN, G.E. Weldability - weld metal cracks - a review of the literature to July 1st, 1939. Welding Journal, 1941, 20, 289s - 305s.
631. SRIKRISHNAN, V., LIU, H.W. and FICALORA, P.T. Selective chemisorption and hydrogen embrittlement - Scripta Metallurgica, 1975, 9, 663-666
632. SRIKRISHNAN, V., LIU, H.W., and FICALORA, P.J. Selective chemisorption and hydrogen embrittlement - the role of H₂S. Scripta Metallurgica, 1975, 9, 1341 - 1344.
633. STAEHLE, R.W. Predictions and experimental verification of the slip dissolution model for stress corrosion cracking of low strength alloys. Proc. of Int. Conf. on Stress Corrosion Cracking and Hydrogen Embrittlement of Iron Base Alloys. Unieux-Firminy, France, June, 1973, p. 180.
634. STEIGERWALD, E.A., SCHALLER, F.W. and TROIANO, A.R. Discontinuous crack growth in hydrogenated steel. Trans. Metallurgical Society of the AIME, December 1959.
635. STEIGERWALD, E.A., SCHALLER, F.W. and TROIANO, A.R. The role of stress in hydrogen induced delayed failure. Trans. Metallurgical Society of AIME. 1960, 218, 832 - 841.
636. STEIGERWALD, E.A. and BENJAMIN, W.D. Effect of composition on the environmentally induced delayed failure of precracked high strength steels. Metallurgical Transactions, 1971, 2, p. 606.

637. STEINBERGER, A.W., DE SIMONE, B.J. and STOOP, J. Crack sensitivity of aircraft steels. *Welding Journal*, September, 1950, 29(9), 752 - 764.
638. STEINBERGER, A.W. and STOOP, J. Studies of the crack sensitivity of aircraft steels. *Welding Journal*, 1952, 31(11), 527s - 542s.
639. STEINMAN, J.B., VAN NESS, H.C. and ANSELL, G.S. The effect of high pressure hydrogen upon the notch tensile strength and fracture more of 4130 steel. *Welding Journal*, 1965, 44, (5), 221s-224s.
640. STEPHENS, J.R. Role of Hf and Zr in the hydrogen embrittlement of Ta and Cb alloys. *Proc. of an Int. Conf. on Hydrogen in Metals*. September 1973. Published by ASM. p. 383.
641. STERN, I.L., KALINSKY and FENTON, E.A. Measurements of hydrogen in weld deposits. *Welding Journal*, 1949, 28, p. 405s.
642. STOLOFF, N.S. Effects of alloying on fracture characteristics. *Fracture*, Vol. VI, Edited by Liebowitz, H. Academic Press, New York, 1969, pp 1 - 81.
643. STOUT, R.D., TOR, S.S., McGEADY, L.J., DOAN, G.E. Quantitative measurements of the cracking tendency in welds. *Welding Journal*, 1946, 25, (9), 522s - 531s.
644. STOUT, R.D., TOR, S.S., McGEADY, L.J., DOAN, G.E. Some additional tests on the Lehigh restraint specimen. *Welding Journal*, 1947, 26, (11), 673s - 682s.
645. STOUT, R.D. The pre-heating and post heating of pressure vessel steels. *Welding Journal*, 1953, 32, (3), 14s - 21s.
646. STOUT, R.D., MACHMEIR, P.M. and QUATTRONE. Effect of impurities on properties of high-strength steel weld metal. *Welding Journal*, 1970, 49, (11), 521s - 530s.
647. STOUT, R.D. and DOTY, W.O. Weldability of steels. *Welding Research Council*, publication edited by Samuel Epstein and R.E. Somers. 2nd edition, 1971.
648. STOUT, R.D. Hardness as an index of weldability and service performance of steel weldments. *Welding Research Council Bulletin*, November 1973, No. 189.
649. STRAIN, R.L. and STOLOFF, N.S. Deformation and fracture of hydrided hafnium. *Proc. of an Int. Conf. on Hydrogen in Metals*. September 1973. Published by ASM. p. 371.
650. STROH, A.N. A theory of the fracture of metals. *Advances in Physics*, 1957, 6, 418 - 465.
651. STURGES, C.M. and MIODOWNIK, A.P. Interaction of hydrogen and dislocation in iron. *Acta Metallurgica*, 1969, 117, p. 1197.
652. SUGIYAMA, T., YAMAMOTO, S., YAMADA, M. and SUGINO, M. New techniques for hydrogen analysis and the development of ultra-low-hydrogen welding consumables. *Int. Conf. on Trends in Steels and Consumables for Welding*. The Welding Institute, Autumn Meeting, London, 13 - 16 November, 1978, Paper No. 30.
653. SUZUKI, H., INAGAKI, M. and NAKAMURA, H. Effects of restraining force on root cracking of high strength steel welds. *Transactions of National Research Institute for Metals*. 1963, 5, (3), 30 - 37.

654. SUZUKI, T., KUWABARA, M., MURAI, H. Hydrogen and root cracking in welding 80kg/mm² high strength steels. IIW-DOC-II-456-68.
655. SUZUKI, H et al. Effects of restraint intensity on delayed cracking in the welds of high strength steels. IIW-DOC-IX-846-73.
656. SWAN, D., LYTLE, A.R., McKINSEY, C.R. Hydrogen content and brittleness of weldments. Welding Journal, 1951, 30, p. 135s.
657. SWIFT, R.A. and RODGERS, H.C. A critical review of weld metal embrittlement. Welding Journal, 1971, 50, p. 357s.
658. SWISHER, J.H. Hydrogen compatibility of structural materials for energy-related applications. Proc. of an Int. Conf. on Effect of Hydrogen on Behaviour of Materials. Jackson Lake Lodge, Moran, Wyoming, September 1975, p. 558.
659. TADA, M., YAMAKAWA, K. and FUJITA, F.E. Behaviour of electrolytically charged hydrogen in pure iron. Scripta Metallurgica, 1975, 9, 5 - 8
660. TAMURA, H. A comparative study of cracking tests for high strength steel electrodes. Basic test results. IIW-DOC-II-222-62.
661. TAMURA, H. A comparative study of cracking tests for high strength steel electrodes. Reproducibility tests results. IIW-DOC-II-268-63.
662. TANIGUCHI, N. and TROIANO, A.R. Stress corrosion cracking of 4340 steel in different environments. Trans. Iron and Steel Institute of Japan. 1969, 9, p. 306.
663. TATRO, C.A., LIPTAI, R.G. and MOON, D.W. Acoustic emission from formation and advancement of cracks. Proc. of Int. Conf. on Stress Corrosion Cracking and Hydrogen Embrittlement of Iron Base Alloys. Unieux-Firminy, France, June 1973. p. 509.
664. TETELMAN, A.S.
Fracture of Solids, Interscience, New York, 1963, p. 671.
665. TETELMAN, A.S. and ROBERTSON, W.D. Direct observation and analysis of crack propagation in iron - 3% silicon single crystals. Acta Metallurgica, 1963, 11, 415 - 426.
666. TETELMAN, A.S. Fundamental aspects of fracture with reference to the cracking of steel weldments. Proceedings of a Symposium on Weld Imperfections at Lockheed Palo Alto Research Lab., Palo Alto, California 19 - 21 September 1966. pp 277 - 296.-
667. TETELMAN, A.S. The mechanism of hydrogen embrittlement in steel. Proc. of Conf. on Fundamental Aspects of Stress Corrosion Cracking. R.W. Staehle ed. Ohio State University, National Association of Corrosion Engineers, 1967, p. 446.
668. TETELMAN, A.S. and McEVILY, A.J. Fracture of structural metals. Wiley, New York, 1967.
669. TETELMAN, A.S. and KUNZ, S. A unified model for hydrogen embrittlement, liquid metal embrittlement and temper embrittlement due to weakening of atomic bonds. Proc. of Int. Conf. on Stress Corrosion Cracking and Hydrogen Embrittlement of Iron Base Alloys. Unieux-Firminy, France, June 1973. p. 359.
670. TETELMAN, A.S. Recent developments in classical (internal) hydrogen embrittlement. Proc. of an Int. Conf. on Hydrogen in Metals. 23 - 27 September 1973 - published by ASM, pp 17 - 34.

671. TETELMAN, A.S. Use of acoustic emission testing to monitor hydrogen embrittlement in steels. Tewksbury Symposium on Fracture, 3rd, University of Melbourne, Australia, June 4 - 6, 1974, p.78 - 97. Available from University of Melbourne, Faculty of Engineering.
672. THEUS, G.J. and STAEHLE, R.W. Review of stress corrosion cracking and hydrogen embrittlement in austenitic Fe-Cr-Ni alloys. Proc. of Int. Conf. on Stress Corrosion Cracking and Hydrogen Embrittlement of Iron Base Alloys. Unieux-Firminy, France, June 1973, p. 845.
673. THOMAS, D.E. Hydrogen isotopes in fusion reactors. Proc. of an Int. Conf. on Hydrogen in Metals, September 1973. Published by ASM. p. 691.
674. THOMAS, J.W. and KLECHKA, E.W. Refinery materials problems caused by hydrogen and industry remedy. Proc. of an Int. Conf. on Effect of Hydrogen on Behaviour of Materials. Jackson Lake Lodge, Moran, Wyoming, September 7 - 11, 1975, pp 542 - 557.
675. THOMAS, S.N.G. The implications of weld cracking in practice (colloquium, Discussion Session 6). Conference on Cracking in Welds. The Welding Institute Autumn Meeting, 1968. Published in Metal Construction and British Welding Journal. 1969, 1, (2s), 142.
676. THOMPSON, A.W. and WILCOX, B.A. Deformation and fracture of dispersion-strengthened nickel charged with hydrogen. Scripta Metallurgica 1972, 6, 689 - 696.
677. THOMPSON, A.W. Hydrogen embrittlement of stainless steels by lithium hydride. SLL-73-5004, Sandia Laboratories, Livermore, California, April 1973.
678. THOMPSON, A.W. and BROOKS, J.A. Hydrogen performance of precipitation strengthened stainless steels based on A-286. Metallurgical Transactions 1975, 6A, 1431 - 1442.
679. THOMPSON, A.W. Ductility losses in austenitic stainless steels caused by hydrogen. Proc. of an Int. Conf. on Hydrogen in Metals. September 1973. Published by ASM, p. 91.
680. THOMPSON, A.W. The mechanism of hydrogen participation in ductile fracture. Proc. of an Int. Conf. on Effect of Hydrogen on Behaviour of Materials. Jackson Lake Lodge, Moran, Wyoming, September 7 - 11, 1975. pp 467 - 477.
681. THOMPSON, R.B., THOMPSON, A.W. and THOMPSON, D.O. Transportation of hydrogen in pipelines : interaction of NDE and material requirements. Proc. of an Int. Conf. on Effect of Hydrogen on Behaviour of Materials. Jackson Lake Lodge, Moran, Wyoming. September 1975. p. 612.
682. TIEN, J.K. Diffusion and dislocation sweeping mechanism for hydrogen transport. Proc. of an Int. Conf. on Effect of Hydrogen on Behaviour of Materials. Jackson Lake Lodge, Moran, Wyoming, September, 1975. p. 309.
683. TIEN, J.K., THOMPSON, A.W., BERNSTEIN and RICHARDS, R.J. Hydrogen transport by dislocations. Metallurgical Transactions, 1976, 7A, 821 - 829.
684. TILLER, W.A. Thermodynamic-kinetic model of stress corrosion cracking. Proc. of Int. Conf. on Stress Corrosion Cracking and Hydrogen Embrittlement of Iron Base Alloys. Unieux-Firminy, France. June 1973. p. 332.

685. TOH, T., and BALDWIN, W.M. Ductility of steel with varying concentrations of hydrogen. Stress Corrosion, Cracking and Embrittlement, W.D. Robertson ed., John Wiley & Sons, New York, 1956, p. 176.
686. TOMASHOV, N.D., MODESTOVA, V.N., USOVA, V.V. and STROKOPYTOVA, T.I. Hydrogen absorption by titanium and its alloys in electrochemical processes. Int. Congress L'Hydrogene dans les Metaux. Paris, May - June 1972. Editions Science et Industrie, p. 226.
687. TOROK, T.E. and STOUT, R.D. Relation of dilatometric characteristics of steels to delayed cracking in welds. Welding Journal, 1965, 44, (12), 529s.
688. TOWSEND, Jr. -H.E., Effects of zinc coatings on the stress corrosion cracking and hydrogen embrittlement of low alloy steel. Proc. of an Int. Conf. on Hydrogen in Metals. September 1973. Published by ASM. p. 223.
689. TRAVIS, R.E., BARRY, J.M., MOFFATT, W.G. and ADAMS, C.M. Weld cracking under hindered contraction : comparison of welding processes. Welding Journal, 1964, 43, (11), 504s - 513s.
690. TRESEDER, R.S. Oil industry experience with hydrogen embrittlement and stress corrosion cracking. Proc. of Int. Conf. on Stress Corrosion Cracking and Hydrogen Embrittlement of Iron Base Alloys. Unieux-Firminy, France, June 1973. p. 147.
691. TROIANO, A.R. Delayed failure of high strength steels. Corrosion, National Association of Corrosion Engineers. 1959. 15, 207 - 212.
692. TROIANO, A.R. The role of hydrogen and other interstitials on the mechanical behaviour of metals. Transactions of the ASM - 1960, 52, (1), 54 - 80.
693. TROIANO, A.R. The influence of hydrogen on the mechanical behaviour of steel. Iron and Steel Institute Special Report No. 73 on the Harrogate Conference on Hydrogen in Steel, published 1962. p. 1.
694. TROIANO, A.R. HEHEMANN and SHIVELY, J.H. Hydrogen permeability and stress corrosion cracking. Colloque sur l'Hydrogen dans les Metaux, Valduc, 1967, p. 107.
695. TROIANO, A.R. and FIDELLE, J.P. Hydrogen embrittlement in stress corrosion cracking. International Congress L'Hydrogene dans les Metaux. Paris, May - June 1972, Editions Science et Industriale, p. 31.
696. TROIANO, A.R. General keynote lecture. Proc. of an Int. Conf. on Hydrogen in Metals. 23 - 27 September 1973. Published by ASM. pp 3 - 15.
697. TROPF, W.J. and KUHLMANN-WILSDORF, D. On degassing in the most economical manner. Proc. of an Int. Conf. on Hydrogen in Metals. September 1973. Published by ASM. p. 739.
698. TRUFFIER, J.L., BROUDEUR, R., TISON, R. and FIDELLE, J.P. Calculus and measurement of diffusivity and solubility of a gas in a solid, from permeability measurements on a sample only. International Congress L'Hydrogene dans les Metaux. Paris, May - June 1972. Editions Science et Industrie. p. 194.
699. TRUMAN, J.E. Tensile failure of carbon and stainless steel wires in the presence of water and hydrogen sulphide. Metallurgia, 1951, 43, p.8.

700. TRUMAN, J.E. Problems of stress corrosion cracking of steel in customer usage. Proc. of Int. Conf. on Stress Corrosion Cracking and Hydrogen Embrittlement of Iron Base Alloys. Unieux-Firminy, France, June 1973, p. 111.
701. TSUBOI, J., TERASHIMA, H. Crack and hydrogen in S.A.W. of H.T.-80 steel. IIW-DOC-II-614-72/IX-794-72.
702. TULIANI, S.S. A metallographic study of chevron cracks in submerged arc weld metals. Welding Research International 1976, 6, (6), 19 - 45.
703. UHLIG, H.H. An evaluation of stress corrosion cracking mechanisms. Proc. of a Conf. on Fundamental Aspects of Stress Corrosion Cracking. R.W. Staehle, ed. Ohio State University, National Association of Corrosion Engineers, 1967.
704. UHLIG, H.H. Stress sorption cracking and the critical potential. Proc. of Int. Conf. on Stress Corrosion Cracking and Hydrogen Embrittlement of Iron Base Alloys. Unieux-Firminy, France. June 1973. p. 174.
705. ULITCHNY, M.G. and GIBALA, R. Solute interactions involving hydrogen and their influence on mechanical behaviour of niobium single crystals. International Congress L'Hydrogene dans les Metaux. Paris, May - June 1972. Editions Science et Industrie. p. 128.
706. VALENTY, V.D. The formation of fish eyes in weld metal as a result of stressing. IIW-DOC-10-59.
707. GAUGHAN, H.G. and MORTON, M.E. de. Hydrogen embrittlement of steel and its relation to weld metal cracking. British Welding Journal, 1957, 4, (1), 40 - 61.
708. VENNETT, R.M. and ANSELL, G.S. The effect of high pressure hydrogen upon the tensile properties and fracture behaviour of 304L stainless steel. Trans. ASM, 1967, 60, (2), 242 - 251.
709. VENNETT, R.M. and ANSELL, G.S. A study of gaseous hydrogen damage in certain FCC materials. Trans. ASM, 1969, 62, (4), 1007 - 1012.
710. VERMILYEA, D.A. A film rupture model for stress corrosion cracking. Proc. of Int. Conf. on Stress Corrosion Cracking and Hydrogen Embrittlement of Iron Base Alloys. Unieux-Firminy, France, June 1973. p. 200.
711. VIBRANS, G. Fisheyes in rolled steel exposed to hydrogen at room temperature. Metallurgical Transactions A, 1977, 8A, pp 1318 - 1320.
712. VISWANATHAN, R. and HUDAK, S.J. The effect of impurities and strength level on hydrogen induced cracking in 4340 steels. Proc. of an Int. Conf. on Effect of Hydrogen on Behaviour of Materials. Jackson Lake Lodge, Moran, Wyoming, September 7 - 11, 1975. pp 262-272
713. VISWANATHAN, R. and HUDAK, Jr. S.J. The effect of impurities and strength level on hydrogen induced cracking in a low alloy turbine steel. Metallurgical Transactions A, 1977, 8A, 1633 - 1637.
714. VOLDRICH, C.B. Cold Cracking in the heat affected zone. Welding Journal, 1947, 26, (3), 153s - 169s.
715. VRABLE, J.B. Stress corrosion and hydrogen embrittlement of linepipe steel in underground environments. Materials Protection, 1972, 11, p. 23.

716. WACH, S. Diffusion of hydrogen through iron and steel membranes. Thesis, London SW11. 1966.
717. WALLNER, F., GIEGERL, E., and HASCHKA, G. Methods of hydrogen determination in the weld metal. International Congress L'Hydrogene dans les Metaux. Paris, May - June, 1972. Editions Science et Industrie. p. 506.
718. WALTER, R.J. and CHANDLER, W.T. Influence of hydrogen pressure and notch severity on hydrogen embrittlement at ambient temperatures. Materials Science and Engineering, 1971, 8, p. 90.
719. WALTER, R.J. and CHANDLER, W.T. Influence of gaseous hydrogen on inconel 718. Proc. of an Int. Conf. on Hydrogen in Metals. September 1973. Published by ASM. p. 515.
720. WALTER, R.J. and CHANDLER, W.T. Crack growth in ASME SA-105 Grade II steel in hydrogen at ambient temperature. Proc. of an Int. Conf. on Effect of Hydrogen on Behaviour of Materials. Jackson Lake Lodge, Moran, Wyoming, September 1975. p. 273.
721. WANG, M.T. and STAEHLE, R.W. Effect of heat treatment and stress intensity parameters on crack velocity and fractography of AISI 4340 steel. International Congress L'Hydrogene dans les Metaux. Paris, May - June 1972. Editions Science et Industrie. p. 342.
722. WARREN, W.G., VAUGHN, M.G. The initiation of brittle fracture at welded joints in steel structures. Trans. Welding Institute 1953, 16, (5), 127 - 135.
723. WATANABE, M., SATOH, K. and MATSUI, S. Effect of restraint on root cracking of steel welds. IIW-DOC-IX-409-64.
724. WATKINSON, F., BAKER, R.G. and TREMLETT, H.F. Hydrogen embrittlement in relation to the heat affected zone microstructure of steels. British Welding Journal, 1963, 10, 54 - 62.
725. WATKINSON, F. and BAKER, R.G. Welding of steel to BS 968 : 1952. British Welding Journal, 1967, 14, (11), 603 - 613.
726. WATKINSON, F. The practical implications of good weldability. Metals and Materials. 1968, 2, 217 - 222.
727. WATKINSON, F. Hydrogen cracking in high strength weld metals. Welding Journal 1969, 48, (9), 417s - 424s.
728. WATKINSON, F. Sulphur : double-agent. Welding Institute Research Bulletin, 1971, 12, (12), 341 - 342.
729. WATKINSON, F. The case for a subclassification of hydrogen controlled welding consumables. Welding Institute Research Bulletin, 1975, 16, (4), 109 - 112.
730. WATKINSON, F. and BODGER, Mrs. P. The advantages of low hydrogen welding (process and consumables) for high strength steels. Welding Research International, 1975, 5, (3), 34 - 62. Also in Welding Institute Members' Report, M81/74 Aug. 1974.
731. WEBB, W. An investigation into basic type agglomerated fluxes for submerged arc welding. MSc Thesis, Department of Materials, Cranfield Institute of Technology, 1969.
732. WEGRZYN, J. and APPS, R.L. Effect of nitrogen on fissuring in mild steel weld deposits. British Welding Journal, 1968, 15, (11), 532 - 540.

733. WEINER, L.C.
Corrosion, 1961, 17, 109.
734. WEISSHAUS, I. and KAUFMAN, A. Blistering in aluminium alloy 2618. Proc. of an Int. Conf. on Effect of Hydrogen on Behaviour of Materials. Jackson Lake Lodge, Moran, Wyomig, September 1975, p.623
735. WERNER, O. The cause of welding cracks in aircraft steels. Welding Journal, 1939, 18, p. 425s.
736. WEST, A.J., BROOKS, J.A. Hydrogen compatibility of 304L stainless steel welds. Proc. of an Int. Conf. on Effect of Hydrogen on Behaviour of Materials. Jackson Lake Lodge. Moran, Wyomig, September 1975, p.686.
737. WESTBROOK, J.H. Assessment of the roles of grain boundaries in stress corrosion cracking and hydrogen embrittlement in iron-base alloys. Proc. of Int. Conf. on Stress Corrosion Cracking and Hydrogen Embrittlement of Iron Base Alloys, Unieux-Firminy, France, June 1973. p. 26.
738. WESTLAKE, D.G. A generalised model for hydrogen embrittlement. Trans. ASM, 1969, 62, 1000 - 1006.
739. WESTPHAL, D.A. and WORZALA, F.J. Hydrogen attack of steel. Proc. of an Int. Conf. on Hydrogen in Metals. 23 - 27 September 1973, published by ASM, pp 79 - 89.
740. WIESTER, H.J., DAHL, W. and HENGSTENBERG, H. The influence of hydrogen on tensile properties of steel. Arch. Eisenhüttenwesen, 1963, 34, p. 915.
741. WILLI, A. and BAACH, H. (Oerlikon Switzerland). Water content in SAW fluxes and its influence upon weld cracking. Proc. of the 1st Int. Symposium on Cracking and Fracture in Welds. Japan Welding Society, Tokyo, Japan, November 1971. pp IIB2.1 - IIB2.10.
742. WILLIAMS, D.N., Report on hydrogen in titanium and titanium alloys. Report No. 100, Battelle Memorial Institute, Columbus, Ohio, May, 1958.
743. WILLIAMS, D.N., SCHWARTZBERG and JAFFEE, R.J. The effects of micro-structure and heat treatment on the hydrogen embrittlement of alpha-beta titanium alloys. Trans. ASM, 1959, 51, 802 - 819.
744. WILLIAMS, D.N., SCHWARTZBERG, F.R. and JAFFEE, R.I. Supersaturation as a factor in the hydrogen embrittlement of titanium alloys. Trans. of the ASM, 1960, 52, 182 - 190.
745. WILLIAMS, D.P. Comments on slow crack growth of steels in hydrogen and water environments.. Scripta Metallurgica, 1968, 2, p.385.
746. WILLIAMS, D.P. and NELSON, H.G. Embrittlement of 4130 steel by low pressure gaseous hydrogen. Metallurgical Transactions 1970, 1, 63 - 68.
747. WILLIAMS, D.P. and NELSON, H.G. Discussion of evaluation of hydrogen embrittlement mechanisms. Metallurgical Transactions 1971, 2, 1987 - 1989.
748. WILLIAMS, J.C. Hydride formation. Proc. of an Int. Conf. on Effect of Hydrogen on Behaviour of Materials. Jackson Lake Lodge, Moran, Wyomig, September 1975. p. 367.

749. WILLIAMS, R.D., ROACH, D.B., MARTIN, D.C. and VOLDRICH, C.B. Hydrogen content of weldments. *Welding Journal* 1949, 28, p. 311s.
750. WILSON, D.M. Weld metal behaviour in restrained fillet joints. Thesis submitted to the College of Aeronautics, Cranfield, for the Diploma of Advanced Engineering. 1966.
751. WILSON, F.H. Attribution of the embrittlement during anneals of aluminium brass to hydrogen. *Proc. of an Int. Conf. on Hydrogen in Metals*. September 1973. Published by ASM, p. 671.
752. WINN, W.H. Weldability of low alloy steels. *British Welding Journal*, 1964, 11, (8), 366 - 376.
753. WINTERTON, K. and COTTRELL, C.L.M. Evolution of hydrogen from weld metal. *Metallurgia*, 1954, 49, p.3.
754. WINTERTON, K. Some investigations of the causes of Halo formation. *British Welding Journal*. 1955, 2, (9), 385 - 392.
755. WINTERTON, K. and HINDS, E.G.P. Hydrogen content and tensile properties of welds. *British Welding Journal*, 1955, 2, p. 513.
756. WINTERTON, K. Fisheyes in weld metal test bars. *Metal Progress*, 1956, 69, (3), 120 - 122.
757. WINTERTON, K. Mechanism of microcracking in mild-steel welding. *Welding Journal*, 1957, 36, (10), 449s - 456s.
758. WINTERTON, K. Properties of mild steel weld metal not revealed by the all weld metal tensile test. *Welding Journal*, 1961, 40, (3), 106s - 109s.
759. WINTERTON, K. Weldability prediction from steel composition to avoid heat affected zone cracking. *Welding Journal*, 1961, 40, (6), 253s - 258s.
760. WISE, M.L.H., FARR, J.P.G., HARRIS, I.R. and HIRST, J.R. Transformation in palladium-hydrogen alloys. *International Congress L'Hydrogene dans les Metaux*. Paris, May - June, 1972, Editions Science et Industrie, p. 72.
761. WOODS, R.A. Hydrogen absorption and porosity formation during aluminium welding. *Proc. of an Int. Conf. on Hydrogen in Metals*. September 1973. Published by ASM. p. 713.
762. WRIEDT, H.A. and ORIANI, R.A. The effect of hydrogen on the Young Modulus of tantalum, niobium and vanadium. *Scripta Metallurgica*, 1974 8, (3), 203 - 208.
763. WRIGHT, V.S. and DAVISON, I.T. Chevron cracking in submerged arc welds. *Int. Conf. on Trends in Steels and Consumables for Welding*. Welding Institute Autumn Meeting. London 14 - 16 November 1978. Paper No. 38.
764. WRIGHT, V.S. and DAVISON, I.T. Chevron cracking in submerged arc welds. *Metal Construction*, 1979, 11, (3), 129 - 133.
765. YAMAKUA, K., TADA, M. and FUJITA, F.E. Recovery of pure iron quenched in liquid hydrogen. *Scripta Metallurgica*, 1975, 9, 1 - 4.
766. YAMAMOTO, S. and FUJITA, T. Delayed failure properties of high strength steels in water. *Proc. of the Int. Conf. on Fracture*, Brighton, England, 1969. P.L. Pratt, ed., Chapman and Hall, 1969, p. 425.

767. YOSHINO, K. and McMAHON, Jr. C.J. The cooperative relation between temper embrittlement and hydrogen embrittlement in a high strength steel. Metallurgical Transactions, 1974, 5, 363- 370.
768. YOUNG, K.B. and NICHOLS, H.J. Hydrogen embrittlement in oxyacetylene pressure welding? Welding Journal, 1948, 27, (1), 30s - 32s.
769. ZACKAY, V.F., GERBERICH, W.W. and McCOY, R.A. On the resistance of TRIP steel to hydrogen embrittlement. Metallurgical Transactions 1970, 1, p. 2031.
770. ZAKHAROV, A.P., SHARAPOV, V.M. and BABAD-ZAKHRYADIN, A.A. Permeation of hydrogen through molybdenum and tungsten at elevated temperatures. International Congress. L'Hydrogene dans les Metaux. Paris, May - June 1972. Editions Science et Industrie. p. 217.
771. ZAPFFE, C.A. and SIMS, C.E. Defects in weld metal and hydrogen in steel. Welding Journal, 1940, 19, 377s - 395s.
772. ZAPFFE, C.A. and SIMS, C.E. Hydrogen embrittlement, internal stress and defects in steel. Transactions of the AIME, 1941, 145, 225 - 259.
773. ZAPFFE, C.A. Fisheyes in steel welds caused by hydrogen. Metal Progress 1942, 42, p. 209.
774. ZAPFFE, C.A. and HASLAM, M.A. A test for hydrogen embrittlement and its application to 17% chromium, 1% carbon stainless steel wire. Transactions of the AIME, 1946, 167, 281 - 308.
775. ZAPFFE, C.A.
Transactions of the ASM, 1947, 39, 191 -
776. ZARELLA, W.J. Stress wave emission from non and irradiated hydrogen embrittled reactor steels. MSc Thesis, University of Idaho, May, 1969.
777. ZENER, C. The micro-mechanism of fracture. Fracturing of Metals, ASM, 1948, 3 - 31.
778. An example of blistering in a sulphuric acid tank due to hydrogen occlusion. Corrosion Technology, 1965, (December), p. 24.
779. Brittle Fracture of a thick walled pressure vessel - EWRA Bulletin, 1966, 7, (6).
780. Hydrogen embrittlement testing. A symposium presented at the 75th Annual Meeting of the ASTM, Los Angeles, June 1972, ASTM Special Technical Publication 543.
781. BS 5135 : 1974. British Standard Specification for Metal-Arc Welding of Carbon and Carbon-Manganese Steels.
782. Bibliography on 'Effects of restraint on heat affected zone cold cracking.' 29 References from 1969 - 1977. Welding Research International, 1978, 8, (2), 166 - 168.

APPENDIX II

APPENDIX II

TIME REQUIRED FOR HYDROGEN DIFFUSION FROM THE CENTRE OF THE JOINT IN THE CONTINUOUS WATER COOLING TEST

To avoid chevron cracking as well as other forms of weld metal hydrogen cracking one has :

- a) to prevent the introduction of hydrogen into the joint; or
- b) to allow hydrogen to diffuse before it becomes harmful.

Assuming that the hydrogen level in the joint is dangerously high a practical means of reducing it is by post heating, as the diffusivity of hydrogen increases rapidly with the temperature (see Figure 7).

For any calculation one has to know the initial hydrogen level, the level corresponding to the safe limit and the diffusion coefficient for the material under consideration. However, introducing a few assumptions and considering typical values for hydrogen level and diffusion coefficient (89) it is possible to evaluate the orders of magnitude of the times required for heat treatments at different temperatures. It was assumed that :

- (i) the diffusion model which is applicable is the one corresponding to a butt weld in 50mm thick plates with infinite dimensions;
- (ii) the initial hydrogen level was 10ml of hydrogen/100g of weld metal;
- (iii) the safe limit for the hydrogen level was 5ml of hydrogen/100g of weld metal;
- (iv) the diffusion coefficients adopted were the ones referred to by Coe (89), which are indicated in Figure 7;
- (v) the joint would be post heated at 150°, 200°, 400° and 650°C.

The assumption of a 50mm thick plate is based on the fact that hydrogen escapes through the surface of the weld and through the backing bar, in this case the distance that hydrogen has to diffuse is increased by an amount corresponding to the backing bar thickness (see Figures 16 to 18).

Once the diffusion coefficient and the diffusion model are known for a certain material and joint geometry, curves can be plotted relating the percentage of original hydrogen remaining at the centre of the joint after heat treating at a certain temperature. An example of such curves is presented below, after Coe (89).

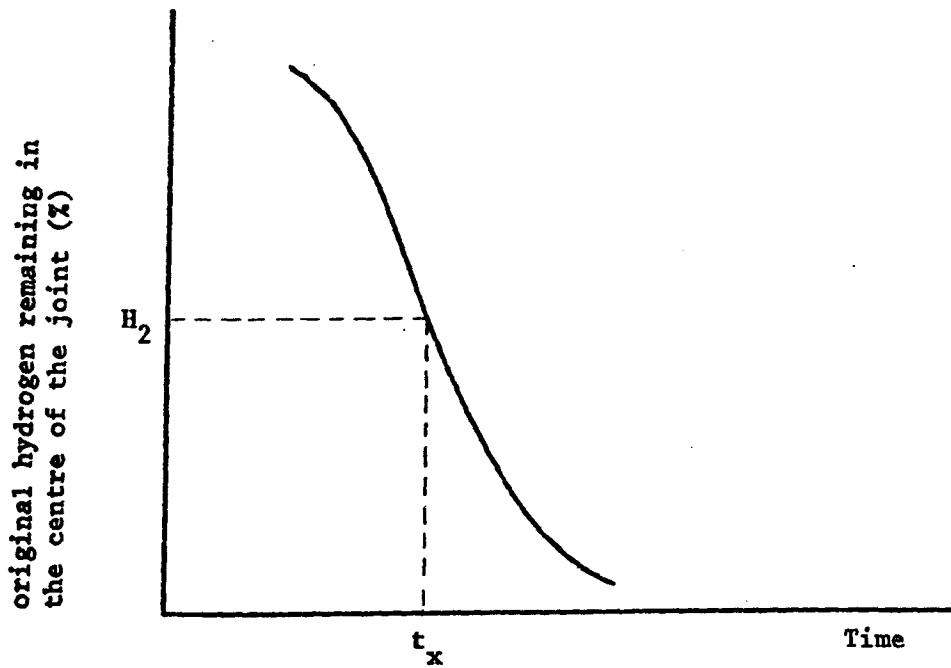


Figure II.1 Schematic illustration of the use of hydrogen removal curves. At time t_x the percentage of original hydrogen remaining at the centre of the material will be H_2 (after Coe).

Using the curves already plotted by Coe (89), Figure 5.19, the approximate times to remove 50% of original hydrogen, (i.e. to reduce the level from 10 to 5ml of hydrogen/100g of weld metal) after heat treatment at 150°, 200°, 400° and 650°C will be, respectively, 60, 30, 6 and 3 hours.